GEOCHIMICA ET COSMOCHIMICA ACTA

UNIVERSITY OF CALIFORNIA
LIBRARY
SEP 20 '57

JOURNAL OF THE GEOCHEMICAL SOCIETY

EDITORIAL ADVISORY BOARD

T. BARTH-OSLO · A. F. BUDDINGTON-PRINCETON, N.J. · L. CAPDECOMME-TOULOUSE
E. J. CONWAY-DUBLIN · P. ESKOLA-HELSINKI · P. GALLITELLI-MODENA
D. GUIMARÃES-BELO HORIZONTE · A. HADDING-LUND · O. HAHN-GÖTTINGEN
H. W. HARVEY-PLYMOUTH · F. HEIDE-JENA · A. HOLMES-EDINBURGH
G. E. HUTCHINSON-NEW HAVEN, CONN. · W. Q. KENNEDY-LEEDS · PH. H. KUENEN-GRONINGEN · S. LANDERGREN-STOCKHOLM · F. MACHATSCHKI-VIENNA
B. H. MASON-NEW YORK · A. MUIR-HARPENDEN · J. ORCEL-PARIS · E. RAGUIN-PARIS · K. RANKAMA-HELSINKI · E. REINHARD-BASLE · TH. G. SAHAMA-HELSINKI
C. E. TILLEY-CAMBRIDGE · T. VOGT-TRONDHEIM · W. WAHL-HELSINKI
T. WATANABE-TOKYO · F. WHIPPLE-CAMBRIDGE, MASS.
R. WILDT-NEW HAVEN, CONN.

EDITORS

L. H. AHRENS — CAPETOWN
C. W. CORRENS — GÖTTINGEN
E. INGERSON — WASHINGTON
S. R. NOCKOLDS — CAMBRIDGE
F. A. PANETH — MAINZ
H. C. UREY — CHICAGO
JOHN VERHOOGEN — BERKELEY, CALIF.
A. P. VINOGRADOV — MOSCOW
L. R. WAGER — OXFORD
F. E. WICKMAN — STOCKHOLM

VOLUME 12 Nos. 1/2

1957

PERGAMON PRESS LONDON · NEW YORK · PARIS

Geochim. et Cosmochim. Acta

QE 351

GEOCHIMICA ET COSMOCHIMICA ACTA

EDITORS

PROF. L. H. AHRENS, *Department of Chemistry, University of Capetown, Rondebosch, Cape Province, South Africa.*
PROF. C. W. CORRENS, *Sedimentpetrographisches Institut der Universitat, Lotzestr.* 13, *Göttingen, Germany.*
DR. E. INGERSON, *Geochemistry and Petrology Branch, U.S. Geological Survey, Washington* 25, *D.C., U.S.A.*
DR. S. R. NOCKOLDS, *Department of Mineralogy and Petrology, The University, Cambridge, England.*
PROF. F. A. PANETH, F.R.S., *Max-Planck-Institut für Chemie, Mainz, Saarstrasse* 23, *Germany.*
PROF. H. C. UREY, For. Mem. R.S., *The Enrico Fermi Institute for Nuclear Studies, University of Chicago, Illinois, U.S.A.*
DR. JOHN VERHOOGEN, *Department of Geology, University of California, Berkeley, California, U.S.A.*
PROF. A. P. VINOGRADOV, *The Academy of Sciences of the U.S.S.R., Moscow, U.S.S.R.*
PROF. L. R. WAGER, F.R.S., *Department of Geology and Mineralogy, The University, Oxford, England.*
PROF. F. E. WICKMAN, *Naturhistoriska Riksmuseets, Mineralogiska Avdelning, Stockholm* 50, *Sweden.*

VOLUME 12, NOS. 1/2 1957

CONTENTS

	PAGE
E. L. HORSTMAN: The distribution of lithium, rubidium, and caesium in igneous and sedimentary rocks	1
MORNA MATHIAS: The geochemistry of the Messum Igneous Complex, South-West Africa	29
E. HELLNER and R. EULER: Hydrothermale und röntgenographische Untersuchungen an gesteinsbilden Mineralen—I. Über ein geologisches Thermometer auf Grund von Untersuchungen an Biotiten	47
JOHN W. WINCHESTER and A. H. W. ATEN, JR: The content of tin in iron meteorites	57
KONRAD B. KRAUSKOPF: Separation of manganese from iron in sedimentary processes	61
ANTHONY P. MILLMAN: Biogeochemical investigations in areas of copper-tin mineralization in south-west England	85
G. DELEON and L. H. AHRENS: The distribution of Li, Rb, Cs, and Pb in some Yugoslav granites	94
THOMAS HOERING: The isotopic composition of the ammonia and the nitrate ion in rain	97
E-AN ZEN: Partial molar volumes of some salts in aqueous solutions	103
GO OKAMOTO, TAKESHI OKURA, and KATSUMI GOTO: Properties of silica in water	123
HARMON CRAIG: Isotopic standards for carbon and oxygen and correction factors for mass-spectrometric analysis of carbon dioxide	133
HITOSHI SAKAI: Fractionation of sulphur isotopes in nature	150
Geochemical Note:	
B. M. GORDON, L. FRIEDMAN, and G. EDWARDS: Caesium in stony meteorites	170
Some current papers in other journals	172
Book Review:	
"The Chemistry and Fertility of Sea Water" by H. W. HARVEY (reviewed by DAYTON E. CARRITT)	176

Publishing Offices: Pergamon Press Ltd., 4 & 5 Fitzroy Square, London W.1. (EUS 4455)

Subscription *per annum* (including postage) (A) £16. 10s. (U.S.A. $46.50); (B) For individual subscribers who are not members of the Geochemical Society and have not contributed papers to the Journal, and who certify that the Journal is for their private use, £10. 10s. (U.S.A. $30.00). Members of the Geochemical Society, or non members who occasionally publish papers in the Journal, £3. 10s. (U.S.A. $10.00) *per annum.*

Back numbers, £7 ($19.60) per volume

Distributors: I. R. Maxwell & Co., Ltd., 4 & 5 Fitzroy Square, London W.1.
and Pergamon Press, Inc., 22 East 55th Street, New York 22, N.Y.

PERGAMON PRESS
4 & 5 FITZROY SQUARE, LONDON W.1 122 EAST 55TH STREET, NEW YORK 22, N.Y.
24 RUE DES ÉCOLES, PARIS Ve

PRINTED IN NORTHERN IRELAND AT THE UNIVERSITIES PRESS, BELFAST

Geochimica et Cosmochimica Acta, 1957, Vol. 12, pp. 1 to 28. Pergamon Press Ltd., London

The distribution of lithium, rubidium, and caesium in igneous and sedimentary rocks

E. L. Horstman
Rock Analysis Laboratory, University of Minnesota, Minneapolis, Minnesota*

(*Received* 9 *August* 1956)

Abstract—Lithium, rubidium, and caesium have been determined on 186 samples, and rubidium and caesium on an additional 53 samples, representing sedimentary and igneous rocks from geographically diverse areas and ranging in age from Pre-Cambrian to recent. Determinations were made by a flame photometric method.

Lithium is closely related to magnesium and ferrous iron with a Mg/Li ratio varying from 2900 in ultramafic rocks to 120 in granites. Averages of 29 p.p.m. and 53 p.p.m. Li are reported for igneous and sedimentary rocks, respectively. Lithium is largely retained in the products of weathering because of concentration in clay minerals. This concentration is responsible for the high values obtained for shales. Impurities account for the greater part of the lithium content of carbonate rocks and sandstones.

The ratio K/Rb is statistically constant at 270 in igneous rocks. Averages of 120 p.p.m. for igneous rocks and of 110 p.p.m. Rb for sedimentary rocks are reported. These values are approximately a third of those previously accepted. Rubidium is retained in weathering largely by those clays having a structural position for the ion, although adsorption plays an important part in both clays and shales. The bulk of the rubidium present in igneous rocks is, however, lost in solution during weathering. Diagenetic recrystallization of illite to orthoclase results in exclusion of rubidium.

Like rubidium, caesium is related to potassium. Igneous rocks have an average ratio K/Cs of 7000. The average abundance of caesium in igneous rocks is less than 1 p.p.m. Cs. Sedimentary rocks average 4 p.p.m. Caesium reacts similarly to rubidium in the geochemical cycle.

Introduction

The classical studies of geochemistry and the bulk of the investigations in this field have been related to igneous petrology, and relatively little work has been done with the sedimentary rocks. This paper is concerned with the distribution of the trace-alkalis in some sedimentary materials and with their behaviour in the weathering cycle.

The development of a new method for the determination of the trace-alkali elements necessitated some work on igneous rocks to assure the validity of comparisons between igneous and sedimentary materials. These data also supply a check on the results obtained with the optical spectrograph, which until recently has been the principal tool for geochemical investigations of lithium, rubidium, and caesium.

In computing the average values for igneous and sedimentary rocks, the procedure of Strock (1936) was followed. For the average igneous rock, granite is weighted 39%, syenite 3%, diorite 39%, gabbro 18%, and ultramafic and others 1%. Extrusive igneous rocks are averaged with the intrusive rocks of similar composition. The average sedimentary rock is weighted shale 80%, sandstone 12%, and limestone 8%.

Analytical Method

All the determinations of lithium, rubidium, and caesium were made by a flame photometric method after removing interfering ions by a wet-chemical separation. Most of the separations were made by decomposing the finely ground sample in

* Present address: P.O. Box 510, Pensacola, Florida.

hydrofluoric acid and sulphuric acid. Cations with the exception of calcium, magnesium, and the alkali metals are removed from the solution resulting from the acid decomposition by precipitation with calcium carbonate. Calcium is removed from the filtrate by precipitation in alcohol solution. Alcohol is removed from this final filtrate by evaporation and the concentrated alkali salts and noninterfering magnesium salts are dissolved for the flame analysis. This procedure has been described in detail (Horstman, 1956). A number of the determinations of rubidium and caesium were made on the chloroplatinate residue of the J. Lawrence Smith alkali determination. Results from the two methods on the same sample proved comparable. The results given are expected to fall within 10% of the amount present. In general, the separation procedures used would tend to yield slightly low values, especially in the case of rubidium. The method is sensitive to 2 p.p.m. lithium and caesium and 5 p.p.m. rubidium, based on the original sample.

Geochemistry of Lithium

Previous work

Preliminary work on the geochemistry of lithium was carried out by Goldschmidt and others (1933), and a more thorough investigation was completed in Goldschmidt's laboratory by Strock (1936). Wager and Mitchell (1943), in their study of the geochemistry of the Skaergaard intrusion, determined lithium spectrographically. Lundegardh (1946) used a flame spectrograph rather than the arc for the determination of lithium in the rocks of the Central Roslagen area, Sweden. The occurrence of lithium in Caledonian rocks has been studied by Nockolds and Mitchell (1948); in an Irish lava series by Patterson (1951, 1955); in Ontario diabase by Fairbairn and others (1953); in pelitic sediments by Shaw (1954); and in ultramafics and chondrites by Pinson and others (1953). A comparison of lithium and other trace elements in a number of rock series has been made by Nockolds and Allen (1953, 1954). Swiss lavas have been studied by Amstutz (1953). Walker and Poldervaart (1949) investigated lithium in the Karroo dolerites; Sahama in the Rapakivi granites (1945b) and in the rocks of South Finnish Lapland (1945a). The occurrence of lithium in iron ores has been discussed by Landergren (1948). Higazy (1952) discusses the action of lithium in a metasomatic front, while the behaviour of lithium in weathering has been investigated by Butler (1953, 1954).

The abundance of lithium in minerals has been investigated by Strock (1936), Ahrens and Liebenberg (1945), Ahrens (1945a), Stevens and Schaller (1942), and Nockolds and Mitchell (1948). General problems relating to the geochemistry of lithium are discussed by Wickman (1943) and Rankama (1946), as well as the other workers mentioned. Summaries of the geochemistry of lithium are given by Goldschmidt (1954) and Rankama and Sahama (1950).

Igneous rocks

According to the rules outlined by Goldschmidt (1937), lithium will not substitute for sodium and potassium, but for magnesium, ferrous iron, aluminium, and titanium on the basis of similar ionic radii. The regular change in lithium content and in Li/Mg ratio occurring in differentiation (Table 3) has been observed

by STROCK (1936). A comparison of the lithium content of rock groups in different stages of differentiation with the results of other workers is given in Table 1. The problem of regional sampling enters into this comparison. STROCK's granite samples were essentially all from Germany, and probably included the composite used by WAGER and MITCHELL (1943). Because granites are weighted heavily in computing the average igneous rock, the use of granite samples from a lithium-rich province may have resulted in too high a value. The possible effect of regional sampling was studied by comparing the granitic rocks from several areas with the average of all granites analysed (Table 2), using the Student *t*-test outlined by SHAW and BANKIER (1954). It is shown that the West Texas granites and the Hong Kong granites are

Table 1. Comparison of average lithium values by different investigators

Investigator*	A	B	C	D	E	F	G	H	I	J
Rock type	(p.p.m. Li)									
Granitic	40	140		70		74		400	20	20
Syenite	28	12							3	35
Diorite	24	19								
Gabbro	17	10		75	7	10		20	2	30
Ultramafic	26	2					0·3		2	10
Shale	66	57	55							
Sandstone	15	17								
Limestone	5	28								
Laterite	56									
Av. igneous	29	65	20	60						
Av. sediment	53	52								
Chondrites	4	3·5					2·7			

* A. This paper—Worldwide.
B. STROCK (1936)—Worldwide.
C. SHAW (1954)—New England, Ontario, Skaergaard.
D. LUNDEGARDH (1946)—Sweden.
E. FAIRBAIRN and others (1953)—Ontario diabase.
F. PATTERSON (1951)—Irish lavas.
G. PINSON and others (1953).
H. WAGER and MITCHELL (1943)—German gabbro and granite.
I. WAGER and MITCHELL (1951)—Skaergaard, Greenland.
J. NOCKOLDS and MITCHELL (1948)—Caledonian intrusions.

significantly different from the average sampling. Fig. 1 compares the West Texas rocks to the average trend and the samples excluding West Texas to the average trend. The greater spread of points at the silicic end of the plot is evident in the West Texas area, and demonstrates the greater lithium content of these rocks. A true average for igneous rock would have to be properly weighted, not only for rock type, but also for geographic distribution. Lacking this ideal, as wide a sample distribution as is possible is desirable.

The granites show considerable variation in lithium content; syenites and diorites contain relatively less lithium, and although very few samples were analysed, the Student *t*-test shows a significant difference between these two groups and granite. Because of the large number of samples, the gabbro-basalt group is considered to be representative.

Table 2. Comparison of granite from different areas to the average granite by the Student t-test

Area	Number of samples	$\overline{Li}$ (p.p.m.)	σ Li (p.p.m.)	t value	Certainty level
Hong Kong	5	23	5	2·53	1·25%
West Texas	7	71	40	1·87	5·0%
Oklahoma	3	28	18	1·00	not significant
Average granite	23	40	30		

Table 3. Comparison of sample groups

	Number of samples	$\overline{Li}$ (p.p.m.)	σ Li (p.p.m.)	$\overline{Mg/Li}$	σ Mg/Li
Granitic rocks	23	40	30	120	210
Syenite	3	28	1	210	170
Diorite	3	24	7	330	220
Gabbro	10	17	17	2080	100
Ultramafic	2	26	17	2930	2820
Kaolinite	19	120	60	140	110
Montmorillonite	13	47	25	480	310
Mixed layer clay	5	47	14	450	270
Marine shale	26	72	40	310	170
Sandstone	4	15	13		
Limestone	7	5			
Laterite	14	56	30		
Recent sediments	13	54	10	320	25

Strock suggested that the ratio Li/Mg is a measure of the amount of differentiation. A comparison of the standard deviation of the ratios Mg/Li (reciprocal of Strock's ratio) and of $(FeO + MgO)/Li_2O$ shows that ferrous iron plays an important part in the distribution of lithium in the later differentiates. Although a plot of the average ratios against silica is similar for both ratios, the standard deviation of the ratio $(FeO + MgO)/Li_2O$ is low in the high-silica range. This suggests that when abundant magnesium is present, lithium is admitted into crystal structures according to the ratio Mg/Li, but as the amount of magnesium available for entry into the crystal structure decreases, ferrous iron also controls the admission of lithium. Triangular variation diagrams are used to plot the values Li_2O, $(MgO + FeO)$, and SiO_2. This plot reduces the spread of points normally occurring at the high-silica end of the diagram when magnesium alone is used.

Effect of an igneous intrusion on shale

The effect of an igneous intrusion on shale was studied on a suite of samples from the Boulder batholith, Dewey, Montana, collected by Grout (1937). The

results show that lithium is removed from the shale and from the recrystallized inclusions at the contact. Examination of the bulk analyses shows relative gains in sodium and slight losses in potassium, but not nearly so large as the loss of lithium. Magnesium shows a definite gain in the same series of samples. This would indicate that the small low-charged lithium ion is driven out of the heated

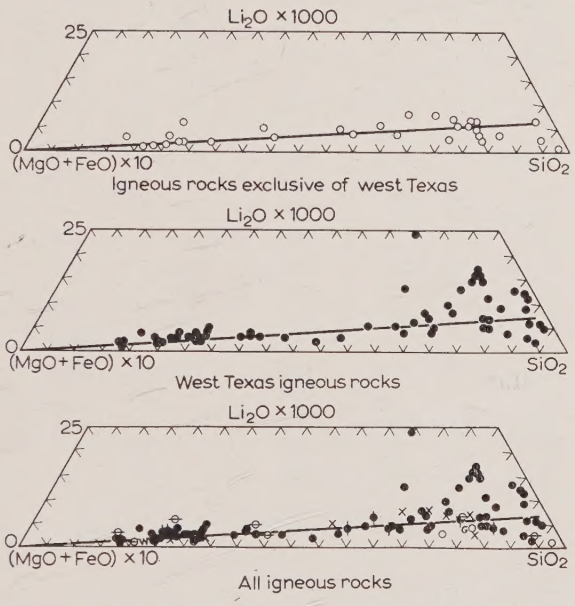

Fig. 1. Lithium enrichment: Variation of Li_2O with (FeO + MgO) and SiO_2 in igneous rocks.

● West Texas	X Composite
♦ Hong Kong	G Granite (G-1)
○ Oklahoma	W Diabase (W-1)
⊸ Minnesota	

crystal structure. The higher lithium value for the composite of inclusions near the centre of the batholith would tend to confirm STROCK's suggestion that basic inclusions soaked in the residual fluids of a magma are in position for lithium enrichment. Lithium is plotted against distance from the contact in Fig. 2.

Behaviour during weathering

The absolute amount of alkali metal present in rocks, in general, is reduced by weathering, but lithium shows no such trend. This is in general agreement with BUTLER's results (1953, 1954). The study of the distribution of lithium in the weathering cycle includes the samples used by GOLDICH (1938), BROCK (1943), and VAN HOUTEN (1953). Table 4 shows the change of lithium content and the ratio Mg/Li for each rock. The data show no definite trend; the lithium content is essentially constant, whereas the ratio Mg/Li shows erratic behaviour.

The lithium-rich minerals, particularly biotite, would be among the last minerals to weather, according to GOLDICH's weathering series. The decomposition of these minerals may correspond in time to the crystallization of the clay minerals which concentrate lithium. Lithium being a small ion with low valence, should not be

Table 4. Change in Li content (p.p.m.) and Mg/Li ratio with weathering

	Fresh rock ⟶ weathered rock							
Rhyolite*	Li	28	43	19				
	Mg/Li	40	40	100				
Granite*	Li	26	28	39	20	6	18	
	Mg/Li	190	180	80		220		
Granite*	Li	24	10	26				
	Mg/Li	110	30	20				
Rhyolite*	Li	23	26	35				
	Mg/Li	260	160	300				
Andesite*	Li	29	61					
	Mg/Li	230	180					
Granodiorite*	Li	16	26	14				
	Mg/Li	1000	500	1000				
Lamprophyre*	Li	35	48	46				
	Mg/Li	1350	570	60				
Granite gneiss†	Li	30	14	25	36	20	38	36
	Mg/Li	150	130	110	130	60	70	60
Diabase†	Li	23	21					
	Mg/Li	1120	360					
Amphibole†	Li	38	32					
	Mg/Li	870	390					
Siltstone‡	Li	74	98					
	Mg/Li	610	540					
Siltstone‡	Li	107	74					
	Mg/Li	390	340					
Sandstone‡	Li	150	67					
	Mg/Li	2	140					

* Brock (1943).
† Goldich (1938).
‡ Van Houten (1953).

adsorbed by the clays in an exchangeable position, but must enter the crystal structure for retention.

Clays

Lithium is concentrated in kaolinite, which on the average contains three times more lithium than granite. Montmorillonite has a greater average lithium content than granite, but cannot be differentiated from granite statistically. Because of difficulty in obtaining a pure illite sample, little information is available for this clay group. Four illitic clays from Minnesota (Riley, 1950) have lithium contents similar to that of montmorillonite and plot on a general trend with montmorillonite (Fig. 3). Major impurities in these clays are calcite and orthoclase. The crystallization of clay minerals takes place at low temperature and pressure, in contrast to conditions existing in a crystallizing magma. Under the more exacting conditions of crystallization in a low-energy state, lithium would not be expected to substitute for major elements unless ionic radii and electrostatic charge requirements are closely satisfied.

A possible explanation for the retention of lithium in kaolinite is that some magnesium is present in the octahedral layer in the place of aluminium,

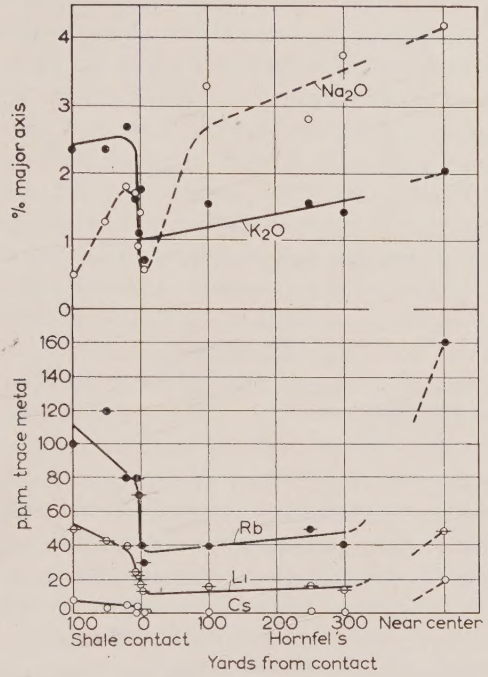

Fig. 2. Variations of the alkali metals in shale and shale inclusions with distance from a shale-igneous contact, Boulder batholith, Dewey, Montana.

resulting in a charge deficiency. In kaolinite only four of the six octahedral positions in the unit cell are occupied. A charge deficiency of one in addition to the vacant octahedral positions make it attractive for monovalent lithium to enter the

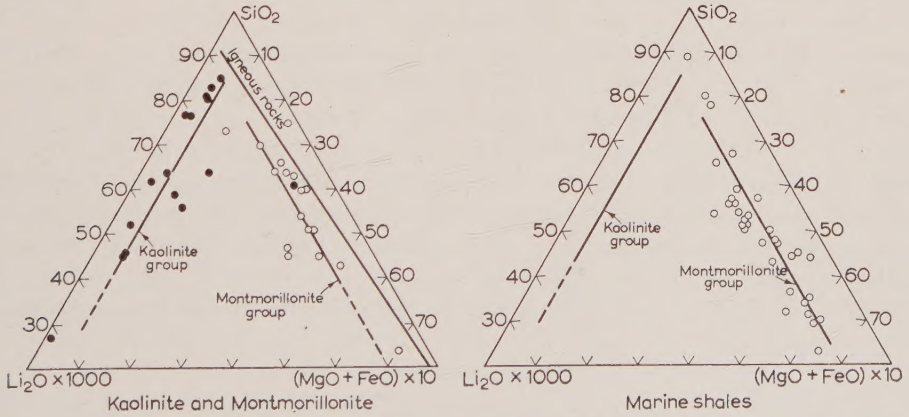

Fig. 3. Variations of Li_2O with (FeO + MgO) and SiO_2 in clay minerals and in marine shales.

structure. Ideally, one lithium ion might enter for each magnesium ion present, giving a Mg/Li ratio of 3·5. Some of the kaolinite samples analysed actually approach this value (ratio of 6). That none of the clays attains this theoretical

maximum is probably accounted for by some substitution of trivalent aluminium for quadrivalent silica in the tetrahedral layer and the paucity of lithium available at the time of crystallization. This may explain the potential demand for lithium in the crystallization of kaolinite and account for the retention of lithium in the products of weathering under conditions of kaolinization. The anauxite, halloysite, and dickite analysed show trends similar to kaolinite with the exception of one impure halloysite (20% montmorillonite) which shows a high Mg/Li ratio.

In montmorillonite the Mg/Li ratio and the average lithium content can also be explained structurally. Montmorillonites contain appreciable amounts of magnesium in the octahedral layer. Electroneutrality requirements can be met by the substitution of three magnesium ions for two aluminium ions and do not require a monovalent ion. Montmorillonites are observed to have Mg/Li ratios equivalent to intermediate igneous rocks, and lithium contents slightly higher (Table 3). This suggests enrichment of both magnesium and lithium in the montmorillonite. The illites are probably similar to the montmorillonite group.

In kaolinite only a small amount of magnesium might be acceptable to the structure, but magnesium may entirely replace aluminium in the montmorillonite structure (hectorite). Magnesium in the kaolinite structure requires a monovalent cation with a co-ordination number of 6 to provide electroneutrality, whereas montmorillonite contains sufficient magnesium to permit lithium to enter according to the ratio of Mg/Li probably present in the surrounding solutions. The extreme difference between the lithium content of kaolinite and of the other clay groups may reflect differences in chemical environment, which in turn are based on climate, topography, time, and parent rock. Further studies are needed to evaluate the relative importance of these factors, in particular the lithium content of the parent rock.

Laterites

Lithium occurs principally in the clay minerals present in the lateritic profile. The laterites examined are from the work of Goldich and Bergquist (1947, 1948) in the Dominican Republic and Haiti. The soil samples for which a magnesium value is available show a low Mg/Li ratio. The lithium content of any one sample may be a measure of the amount of clay mineral present. This is clearly shown by the analyses of several soil samples for which the clay content is given by Goldich and Bergquist (1947) (see Fig. 4). The low lithium value obtained for the iron-rich concretions (Appendix, sample 186), further suggests that the lithium is contained in the clay fraction of the samples. Landergren (1948), in studying the laterites of Ireland, found smaller amounts of lithium than are reported here. This may be the result of samples containing less clay or the effect of a basaltic parent material initially low in lithium.

Sedimentary rocks

Shale. Shales contain the bulk of the lithium in marine sediments. The data presented above suggest that the greater part of the available lithium enters the clay mineral at the weathering site. The sea, at present containing only 0·1 p.p.m. Li (Rankama and Sahama, 1950), has probably never contained large amounts of

lithium to be removed by adsorption, as suggested by Strock. All three clay mineral groups are present in marine sediments. Kaolinite is least abundant, illite most abundant. Grim (1953) explains this by the diagenetic change of kaolinite to illite or chlorite in the marine environment. The plot (Fig. 3) comparing shales to kaolinite and montmorillonite shows the similarity of shales to montmorillonite. It would seem to indicate that the formation of illite in the marine environment might be closely associated with the presence of montmorillonite in the fresh water entering the sea, rather than with the diagenetic recrystallization of kaolinite to illite, as suggested by Grim.

The shale samples show an appreciably higher lithium content than does montmorillonite, probably reflecting the higher lithium content of the small amounts of kaolinite present. Recent sediments, older sediments, and residual materials all show similar amounts of lithium, and it can be assumed that lithium is retained in the products of diagenesis.

Sandstone. The lithium content of sandstone will vary with the source of the quartz and with the clay impurities. Unpublished analyses of quartz using large samples show a range from 0·5 p.p.m. Li to 38 p.p.m. Li. Maxwell (1953) reported a maximum of 36 p.p.m. Li in chert samples. None of the sandstones analysed attains this high value. The glauconitic sandstone shows a greater lithium content than the other samples, indicating the concentration of lithium in the mica structure of glauconite, as shown by Strock.

Limestone. Seven limestone and dolomite samples studied by Goldich and Parmelee (1941) were analysed. These carbonate rocks are relatively pure, having insoluble residues of quartz, chalcedony, and chert ranging from 1 to 5%. Determinable amounts of lithium were not found in these samples, indicating that lithium does not occur as the carbonate or enter into the calcite or dolomite structure. The higher lithium content of limestone reported by Strock is probably the result of clay impurities.

Chondrites

Lithium is concentrated in the silicate phase of meteorites. Essential agreement among investigators is observed (Table 1).

Summary

Previous knowledge of the distribution of lithium is largely based on the work of Strock (1936). The distribution of lithium in igneous rocks is controlled by the concentration of lithium relative to ferrous iron and magnesium. In a magmatic melt, the ratio $(MgO + FeO)/Li_2O$ is large and early crystals contain little lithium. Magnesium and ferrous iron are removed in the crystallization process, enriching the residual liquid in lithium relative to the mafic constituents. At lower temperatures the lithium ion becomes sufficiently immobile to be admitted to suitable structures. Strock found lithium in monoclinic pyroxenes, amphiboles, and micas in amounts increasing in that order. This results in a concentration of lithium in the silicic rocks.

The present study gives an average of 40 p.p.m. Li for granites and of 17 p.p.m. for basalts, as compared to 140 p.p.m. and 10 p.p.m., respectively, reported by

Strock (1936). Strock reported an average value of 65 p.p.m. Li for the average igneous rock compared to only 29 p.p.m. Li in the present investigation. The writer's results are in good agreement with those of Shaw (1954), who estimated 20 p.p.m. Li. Samples of wide geographic distribution are essential to computations of an average.

Contrary to the behaviour of other alkali metals, lithium is largely retained in the products of weathering. Concentration or depletion of lithium in any one suite of weathering samples is relatively small. The retention of lithium may be related

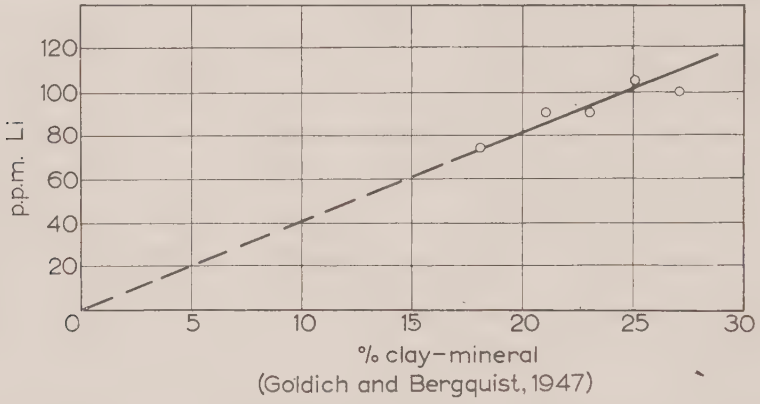

Fig. 4. Variation of Li with clay-mineral content of aluminous lateritic soil samples.

to the type of clay mineral formed. Lithium is concentrated in kaolinite, but montmorillonite and illite show only slightly larger amounts of lithium than the average for granite. The average amount of lithium in kaolinite is 120 p.p.m., as compared to 40 p.p.m. in granite. This increase cannot be wholly accounted for by concentration due to removal of other constituents during weathering. Lithium apparently is able to enter the crystal structure of kaolinite, but cannot be related to iron or magnesium contents.

The concentration of lithium in kaolinite is reflected in the low Mg/Li ratio of laterites and lateritic soil. The lithium content of lateritic materials averages 56 p.p.m., and is proportional to the amount of clay mineral present (Fig. 4).

Clay minerals in shales account for the bulk of the lithium in marine sediments. As a result of the entry of lithium into the clay minerals at the weathering site, lithium probably does not enter the sea in solution in any appreciable quantity. Shales contain an average of 66 p.p.m. Li. This value compares favourably with 57 p.p.m. found by Strock (1936) and with 55 p.p.m. reported by Shaw (1954). Sandstones contain small amounts of lithium, probably in clay impurities, but some quartz contains sufficient lithium to account for the amounts reported, 15 p.p.m. Li, compared to 17 p.p.m. Li by Strock. Limestone and dolomite free of clay contain little or no lithium.

The average sediment contains 53 p.p.m. Li, and this figure is in agreement with Strock's average of 52 p.p.m. An average of 4 p.p.m. Li is obtained for chondrites, compared to 3·5 p.p.m. reported by Strock (1936) and 2·7 p.p.m. reported by Pinson and others (1953).

Geochemistry of Rubidium

Previous work

Early work on the geochemistry of rubidium was carried out by Goldschmidt and others (1933). This investigation was later expanded to include sediments and minerals (1934), but an investigation comparable to that of lithium by Strock was not undertaken. Previously accepted averages of 310 p.p.m. for igneous rocks and 300 p.p.m. Rb for sediments were based on the results of Goldschmidt and others (1934). In addition to the work of Goldschmidt and his associates, regional studies have been carried out by Wager and Mitchell (1951), Erametsa and others

Table 5. Comparison of average rubidium values by different investigators

Investigator*	A	B	C	D	E	F	G	H	I	J
Rock type				(p.p.m. Rb)						
Granite	170	150	830	520	1200	400		700	600	930
Syenite	110							550		
Diorite	110									1000
Gabbro	30	<20	18				12(1)	0	20	25†
Ultramafic	10			2				0		
Shale	140		350					600		
Sandstone	60									
Limestone	<5									
Laterite	10						<10(2)			
Av. igneous	120		310	350						
Av. sediment	110		300				280(3)			
Chondrites	<5			9			5(4)			

* A. This paper—World-wide.
B. Wager and Mitchell (1951)—Skaergaard, Greenland.
C. Goldschmidt and others (1934)—Worldwide.
D. Ahrens and others (1952)—New England granites, world estimate.
E. Erametsa and others (1941)—Finland Rapakivi granites.
F. Nockolds and Mitchell (1953)—Caledonian intrusions.
G(1). Fairbairn and others (1953)—Ontario diabase.
G(2). Landergren (1948)—Irish laterite.
G(3). Canney (1952)—World sediment.
G(4). Noddack and Noddack (1930).
H. Sahama (1945a)—Finland.
I. Wager and Mitchell (1943)—German composites.
J. Patterson (1951)—Irish lavas.
† This value is too high on the basis of new work, Patterson (1955).

(1941), Nockolds and Mitchell (1948), Ahrens and others (1952), and Nockolds and Allen (1953, 1954). The work of Goldschmidt on minerals has been supplemented by Ahrens (1945a, 1945b), Stevens and Schaller (1942), and Nockolds and Mitchell (1948).

The distribution of rubidium in sediments has been investigated by Canney (1952). Butler (1953, 1954) considers the behaviour of rubidium during weathering. The results of this investigation are compared with those of previous investigators in Table 5.

Igneous rocks

The average igneous rock contains 120 p.p.m. Rb as opposed to the 310 p.p.m. reported by Goldschmidt and others (1934) and the 350 p.p.m. reported by

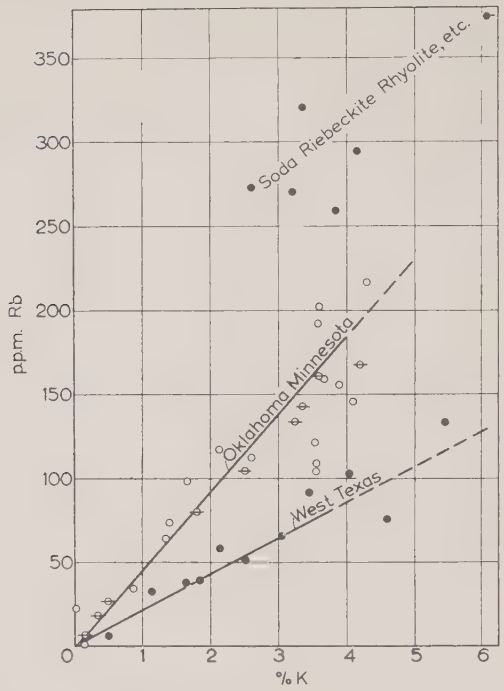

Fig. 5. Comparison of potassium-rubidium variations in West Texas, Minnesota, and Oklahoma igneous rock series.
⊹ Minnesota
○ Oklahoma
● West Texas

Ahrens and others (1952). Granitic rocks average 170 p.p.m.; intermediate rocks, 110 p.p.m.; and gabbro-basalt, 30 p.p.m. Rb. Ultramafic rocks show only 10 p.p.m. Rb (Table 6). Results for the gabbro-basalt group show fair agreement among all

Table 6. Comparison of sample groups

	Number of samples	$\overline{Rb}$ (p.p.m.)	σ Rb (p.p.m.)	$\overline{K}/Rb$	σ K/Rb
Granitic rocks	66	170	83	240	88
Syenite	3	110	41	410	70
Diorite	5	110	15	330	218
Gabbro	15	30	18	310	150
Ultramafic	5	10	10	350	335
Kaolinite	19	110	130	130	90
Montmorillonite	13	25	16	190	92
Mixed-layer clay	5	140	40	240	76
Marine shale	26	140	50	260	85
Sandstone	4	60	61	460	578
Limestone	7	<5			
Laterite	14	10	8	50	15
Recent sediment	13	120	40	320	25

workers (Table 5), but when greater amounts of rubidium are present, as in granitic rocks, only the work of WAGER and MITCHELL (1951) is in essential agreement with this report.

The trend of rubidium during differentiation is similar to that of lithium, increasing with the silica content. For rubidium, however, this relationship is subordinate to the control of rubidium by potassium. The ionic radii of the two ions are so close that rubidium almost exclusively follows potassium and occurs in potassium minerals. Rubidium, being slightly larger than potassium, is feebly enriched relative to potassium in the later differentiates (GOLDSCHMIDT and others, 1933; NOCKOLDS and MITCHELL, 1948). The sympathetic relationship of potassium and rubidium is shown in Fig. 7, in which rubidium is multiplied by 270, the average K/Rb ratio found in this investigation.

The ratio K/Rb has been accepted as being relatively constant for igneous rocks by AHRENS and others (1952), although they report variations from 75 to 150. NOCKOLDS and ALLEN (1953, 1954) report ratios from 125 to 360, but point out that ratios are constant only within a rock series, and this conclusion is confirmed by this investigation (Fig. 5). Table 7 shows varying ratios for different rock series. The West Texas series is reported with, and without, the abnormal rocks for comparison purposes. Two distinct K/Rb ratios result, the abnormal rocks averaging 120 and the remaining samples averaging 480.

Table 7. Comparison of ratios and rubidium content of different rock suites

Area	$\overline{\text{Rb}}$ (p.p.m.)	$\overline{\text{K/Rb}}$
Oklahoma	110	220
Minnesota	100	225
West Texas (excluding abnormal rocks)	60	480
West Texas (including abnormal rocks)	160	310
Average igneous rock	120	270

Ignoring regional differences and averaging K/Rb ratios for each igneous rock group, the ratios cannot be statistically differentiated with the Student *t*-test, with the exception of the syenite-granite comparison. The syenite average, however, is not representative. Groups of samples taken by themselves will show significant deviations from the average, as is shown by the wide spread of points in Fig. 6.

Effect on an igneous intrusion on shale

Fig. 2 shows the removal of rubidium from shale and the resultant hornfels at an igneous contact. The composite sample of inclusions from the centre of the Boulder batholith shows enrichment in rubidium. Rubidium is lost relative to potassium at the contact and immediately inside the intrusion. As in the case of lithium, the preferred ion, potassium, is retained and the trace ion is removed from the rock under a temperature gradient. The inclusions near the centre of the batholith are in position for enrichment in rubidium by the late-stage liquid. Rubidium is enriched in these xenoliths by a greater factor than lithium.

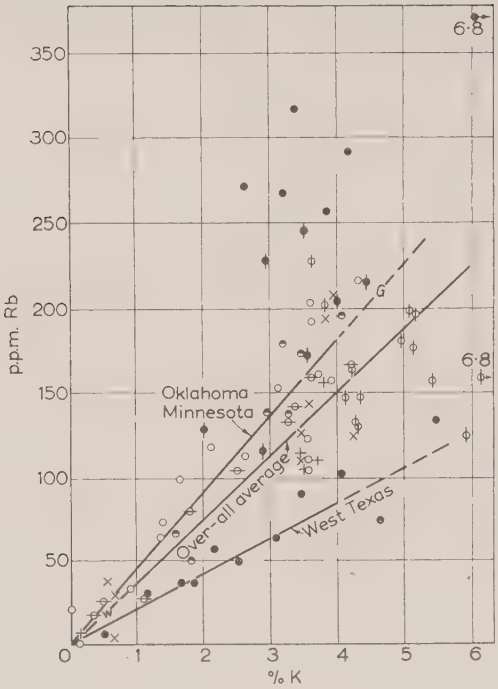

Fig. 6. Variations of Rb with K in igneous rocks.

- Hong Kong
- New England
- West Texas
- Peru
- Minnesota
- Oklahoma
- Alberta
- Composite

G Granite (G-1)
W Diabase (W-1)

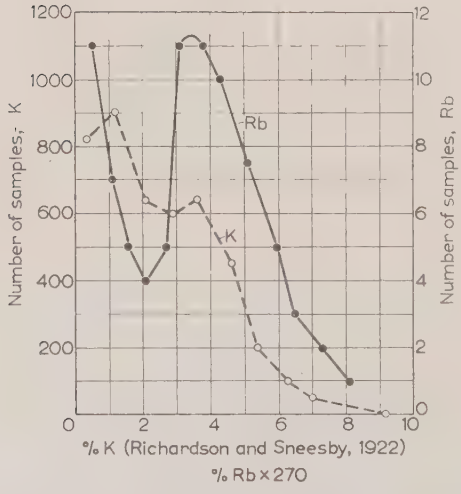

Fig. 7. Frequency distribution of rubidium and potassium in igneous rocks.

Behaviour during weathering

In weathering, as in igneous activity, rubidium is closely linked with potassium. Table 8 shows that the K/Rb ratio decreases during weathering, indicating a

Table 8. Change in rubidium content (p.p.m.) and K/Rb ratio with weathering

		Fresh rock ——→ weathered rock						
Rhyolite*	Rb	200	100	160				
	K/Rb	200	160	180				
Granite*	Rb	170	40	200	60	350	110	
	K/Rb	210	100	40	70	100	40	
Granite*	Rb	220	250	90				
	K/Rb	200	140	100				
Rhyolite*	Rb	250	210	40				
	K/Rb	140	150	70				
Andesite*	Rb	130	170					
	K/Rb	230	180					
Granodiorite*	Rb	230	90	60				
	K/Rb	130	140	80				
Lamprophyre*	Rb	120	160	80				
	K/Rb	250	230	110				
Granite gneiss†	Rb	130	200	140	150	60	10	10
	K/Rb	250	220	210	210	320	410	110
Diabase†	Rb	20	50					
	K/Rb	470	250					
Amphibolite†	Rb	10	20					
	K/Rb	210	140					
Siltstone‡	Rb	110	100					
	K/Rb	240	200					
Siltstone‡	Rb	150	150					
	K/Rb	250	220					
Sandstone‡	Rb	180	150					
	K/Rb	200	160					

* Brock (1943).
† Goldich (1938).
‡ Van Houten (1953).

relative concentration of rubidium. Disregarding intermediate stages of weathering, the trend is toward absolute loss of both potassium and rubidium, with potassium moving out of the weathering profile faster than rubidium. Many samples suggest that an early concentration of rubidium occurs prior to its eventual loss, corresponding to the early resistance of K-feldspar to weathering shown by Goldich (1938). Because orthoclase is relative high in rubidium, the two trends might be closely parallel.

Adsorption may play an important role in the concentration of rubidium relative to potassium in the late stages of weathering. As early as 1920 (Goldschmidt, 1954) it was found that rubidium is held in adsorption positions more firmly than is potassium. Butler (1954) reports that rubidium is concentrated relative to

potassium only when illite is formed from weathered mica and not when illite is formed from weathered feldspar. Butler saturated the clay-size fraction of his samples with calcium ion before determining rubidium. This technique may have removed the adsorbed rubidium, thus invalidating his conclusion that rubidium is lost relative to potassium during the process of weathering feldspar to clay.

The potassium and rubidium contents of clay minerals appear to be leached very slowly by weathering. The colloidal fractions of weathered siltstone and sandstone show only small reductions in rubidium content and a slight enrichment of rubidium relative to potassium compared to fresh material in the same sizes.

Clays

The structural and compositional differences of the major clay groups are reflected in their rubidium contents. The kaolinite group shows extreme variation, averaging 110 p.p.m. Rb, similar to intermediate rocks (Table 6). The montmorillonite group averages 25 p.p.m., compared to 30 p.p.m. for basalts and gabbros. Illitic clays from Minnesota (Appendix, No. 139–142) show an average of 190 p.p.m. Rb. Two of the mixed-layer clays (No. 132–133) are potassium bentonites composed of 80% illite layers (Weaver, 1953) and show an average rubidium content of 180 p.p.m. Kaolinite and montmorillonite show K/Rb ratios lower than igneous rocks, indicating enrichment of rubidium relative to potassium, but illitic shales and the mixed-layer clays show a ratio not significantly different from that of igneous rocks.

Rubidium is not controlled by potassium in kaolinite (Fig. 8). Because kaolinite has no suitable structural position for an ion as large as potassium or rubidium, both of these ions probably occur either in impurities or as adsorbed ions. The variations could result from either condition. There is, however, no correlation between impurities and rubidium content, or K/Rb ratio, suggesting that adsorption might be the important factor. The wide variation of rubidium might be the result of the different environments with respect to available trace-alkali elements in which the kaolinite crystallized.

The montmorillonite group shows closer control of rubidium by potassium (Fig. 8) than does kaolinite. According to some workers (Grim, 1953) potassium (and consequently rubidium) may be fixed in montmorillonite. Preferential adsorption of rubidium would then play a less important part in the K/Rb ratio, the K/Rb fixation ratio being more nearly that which is present in the surrounding environment.

The mixed-layer clays and illitic shales show K/Rb ratios similar to those of igneous rocks. These materials are crystallized in a marine environment. The average K/Rb ratio in sea-water is much higher than in igneous rocks (Rankama and Sahama, 1950). Illite, filling its interlayer ions, should remove rubidium preferentially to potassium, but the enrichment is too small to be shown statistically.

Laterites

The West Indies lateritic soils show an average rubidium content of 10 p.p.m. Rb. Landergren (1948) reported less than 10 p.p.m. Rb in Irish laterites. Rubidium probably has been adsorbed on these materials, because no correlation

between rubidium and potassium is observed (Appendix, No. 178–191). The amount of rubidium is too small to be determined accurately enough to show any relationship between clay and rubidium contents.

Sedimentary rocks

The average sedimentary rock contains 110 p.p.m. Rb. Earlier values of 300 p.p.m. and 280 p.p.m. were reported by Goldschmidt and others (1934) and by Canney (1952), respectively (Table 5).

Shale. An average of 140 p.p.m. Rb is reported for shale. This represents the bulk of the rubidium contained in sedimentary rock. Statistically there is no difference in the rubidium content of recent sediments and of older shales.

The rubidium content of shales is plotted against potassium in Fig. 8. Most of

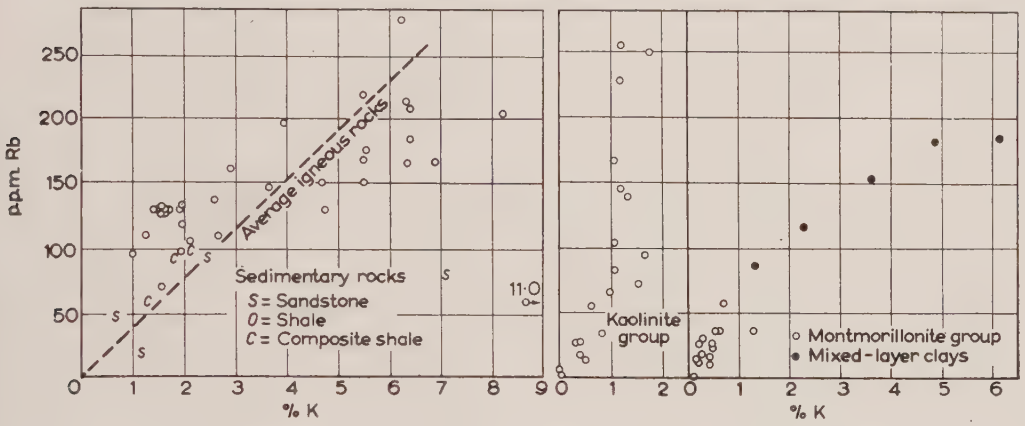

Fig. 8. Variations of Rb with K in clay minerals and in sedimentary rocks.

the samples show higher rubidium contents than do igneous rocks, but some high-potassium shales show low rubidium. This is probably due to diagenetic recrystallization of illite to orthoclase. A feldspathized shale (Appendix, No. 194) is an excellent example. During the low-temperature recrystallization, rubidium does not enter the feldspar structure. Of the samples falling below the trend of igneous rocks, the sandstone and five shale samples are identified as containing authigenic feldspar. The remaining samples have been exposed to hydrothermal activity, which may be responsible for recrystallization of some of the original clay minerals. As a group, shales show a close association with samples of illite, as should be expected from the abundance of this mineral in shale.

Sandstone. Sandstones contain little rubidium. The large rubidium ion does not enter the quartz structure in determinable amounts, and the rubidium present in sandstone must be accounted for by impurities. The glauconitic sandstone (Appendix, No. 164) shows a larger rubidium content than other sandstones, indicating enrichment of rubidium in glauconite. Samples 162 and 163 (Appendix) show high K/Rb ratios, indicative of authigenic feldspar.

Limestones. No determinable amount of rubidium was found in the seven limestone and dolomite samples investigated; this is in agreement with Sahama (1945a) (see Table 5).

Chondrites

The rubidium content of chondrites is less than 5 p.p.m. Rb, in essential agreement with other investigators (Table 5). The result of Ahrens and others (1952), if corrected for the spectrographic calibration error, would fall in the proper range.

Summary

Igneous rocks contain an average of 120 p.p.m. Rb. This value is significantly lower than earlier results, reflecting an error in the spectrographic determination of rubidium. In general, rubidium follows potassium in the geochemical cycle. This is shown by the bimodal distribution of the two elements (Fig. 7) and by the relative constancy of the K/Rb ratio. The ratio differs for different magmatic suites (Table 7), but shows little variation in a given rock series. An average ratio of 270 is reported for all igneous rocks.

Clays resulting from weathering contain much less rubidium than the unweathered rocks. In the early stages of weathering, rubidium may show a slight relative increase, because of the resistance of orthoclase to decomposition. In the late stages, rubidium is concentrated relative to potassium, possibly by preferential adsorption of rubidium on the clay particles. Clay-size material from marine sediments is relatively stable under weathering.

The rubidium content of the kaolinite group ranges from less than 5 p.p.m. to 580 p.p.m. Rb, probably reflecting the availability of rubidium in the weathering areas. The average value is 110 p.p.m. (Table 6). The erratic K/Rb ratios observed may be caused by adsorption, reflecting environmental conditions or by impurities. Montmorillonites contain an average of only 25 p.p.m. Rb, suggesting that subsilicic rocks are the parent material. In montmorillonite, the distribution of rubidium appears to be more closely controlled by potassium than in kaolinite. This may be accounted for by the partial fixation of potassium and of rubidium. In illitic clays and the related mixed-layer clays, potassium shows strong control over rubidium. The K/Rb ratio of the mixed-layer clays is 240 and is not statistically different from that for igneous rocks. The erratic distribution of rubidium in kaolinite is reflected in the rubidium distribution in lateritic soils. Laterites may have some rubidium adsorbed directly on the hydrolysates.

The average sedimentary rock contains 110 p.p.m. Rb. The bulk of the rubidium is found in illite, the most abundant mineral in shales. Some rubidium probably occurs adsorbed on the clay particles. Diagenetic recrystallization of illite to orthoclase results in the exclusion of rubidium from the orthoclase structure. The K/Rb ratio for shales is similar to that for igneous rocks. Quartz is not known to contain rubidium, and consequently the rubidium content of sandstones may be assigned to impurities. Pure carbonate rocks show no determinable rubidium. The abundance of rubidium in chondrites is less than 5 p.p.m. Rb.

Geochemistry of Caesium

Previous work

Knowledge of the distribution of caesium is based principally on the work of Goldschmidt and co-workers (1933, 1934), who reported an average of 7 p.p.m. Cs

for igneous rocks. This value was revised by GOLDSCHMIDT (1954) to 3 p.p.m. GOLDSCHMIDT and others (1934) reported 12 p.p.m. Cs as an average for sedimentary rocks, and CANNEY (1952) reported 8 p.p.m. A limited amount of work on caesium was carried out by SAHAMA (1945b) and ERAMETSA and others (1941).

Igneous rocks

The average igneous rock contains less than 1 p.p.m. Cs, and only in granitic rocks is caesium sufficiently concentrated to be determinable. Caesium is concentrated in potassium minerals, and probably follows potassium in the geochemical

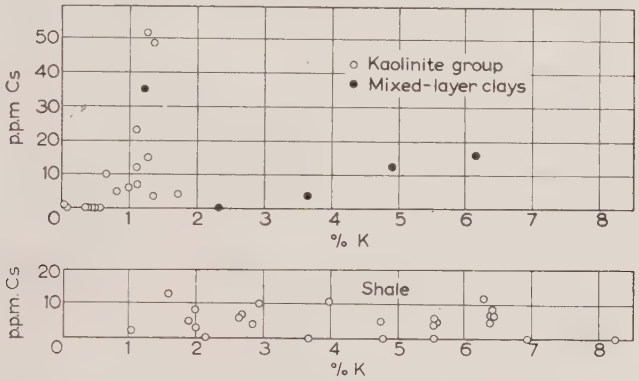

Fig. 9. Variations of Cs with K in clay minerals and in shales.

cycle. An average K/Cs ratio of 7000 is reported here, compared to 9000 reported by GOLDSMITH and others (1934) and 8000 reported by CANNEY (1952).

Effect of an igneous intrusion on shale

The data for caesium are too incomplete to show the sharp depletion at the shale-intrusion contact shown by lithium and rubidium (Fig. 2). Most of the hornfels inclusions do not contain determinable amounts of caesium, whereas the shale shows about 5 p.p.m. Cs. The composite sample of inclusions near the centre of the Boulder batholith shows extreme enrichment in caesium (21 p.p.m.), greater than the enrichment shown by either lithium or rubidium.

Clays

The analysed kaolinite samples average 14 p.p.m. Cs. Fig. 9 shows that, like rubidium, cesium in kaolinite does not appear to be controlled by potassium. Caesium probably varies with the availability of the element in the weathering areas, resulting in the wide range of observed values.

The mixed-layer clays show an average of 17 p.p.m. Cs. This average is raised by a sample (Appendix, No. 129) which is of hydrothermal rather than sedimentary origin. The K-bentonites have an average abundance of only 8 p.p.m. Cs. The four illitic clays from Minnesota (Appendix, No. 139–142) average 7 p.p.m. Cs. A high degree of control of caesium by potassium is shown in the K-bentonites (Fig. 9). The K/Cs ratio for the mixed layer clays is not significantly different from the other sample groups (Table 9).

Table 9. Comparison of average caesium values by different investigators

Investigator*	A	B	C	D	E	F
Rock type			(p.p.m. Cs)			
Granitic	1	40		10	3	
Syenite	<1			10		
Diorite	<1					
Gabbro	<1	0		10		
Ultrabasic	<1			10		
Shale	5	14				8
Sandstone	<1					7
Limestone	<1					8
Laterite	<1					
Av. igneous	<1	3				
Av. sedimentary	4	12				8
Chondrites	<1		0·1			

* A. This paper—World-wide.
B. Goldschmidt (1954)—Worldwide.
C. Noddack and Noddack (1930)
D. Sahama (1945b)—Finland.
E. Erametsa and others (1941)—Finland.
F. Canney (1952)—World sediment.

Table 10. Comparison of sample groups

	Number of Samples	$\overline{Cs}$ (p.p.m.)	σ Cs (p.p.m.)	$\overline{K}$/Cs	σ K/Cs
Granitic rocks	66	1	3	6700	3900
Syenite	3	<1			
Diorite	5	<1			
Gabbro	15	<1			
Ultramafic	5	<1			
Kaolinite	19	14	24	1300	1300
Montmorillonite	13	<1			
Mixed-layer clay	5	17	19	4200	3600
Marine shale	25	5	4	6800	3400
Sandstone	4	<1			
Limestone	7	<1			
Laterite	14	<1			
Recent sediments	13	6	3	2300	600

Sedimentary rocks

The average sedimentary rock is estimated to contain 4 p.p.m. Cs. Only in shale is the caesium present in determinable quantities, averaging 5 p.p.m. Both recent and older shales show similar amounts of caesium, but recent sediments have a much lower K/Cs ratio. This may indicate preferential adsorption of caesium early in sedimentation, with potassium being added later. The amount of caesium in shales is probably more dependent on potassium content than is indicated in Fig. 9. Canney reports an average K/Cs ratio of 2500 for shale opposed to the ratio of

6800 for shale and 2300 for recent sediments reported in this investigation. This difference can be partially explained by CANNEY's high spectrographic result for caesium. A sample of glauconitic sandstone contains 9 p.p.m. Cs, indicating the concentration of caesium by the mica structure of glauconite, as shown by GOLDSCHMIDT and others (1934).

Summary

The analytical method of this investigation is not sufficiently sensitive for the determination of caesium in most of the samples. In granites the average amount is only 1 p.p.m. Cs. Work by other investigators on minerals shows that caesium follows potassium in igneous rocks much as does rubidium. The ratio K/Cs is 7000, with reasonable agreement among all workers.

Caesium is greatly enriched in some kaolinites, but there is no apparent control by potassium in this group. The mixed-layer clays have an average of 17 p.p.m. Cs, compared to 14 p.p.m. for kaolinite. The few data available suggest control of caesium by potassium in the mixed-layer structure.

Shales average 5 p.p.m. Cs, with no apparent correlation between the caesium and potassium contents. In recent sediments, caesium is concentrated relative to potassium, resulting in a low K/Cs ratio.

Acknowledgements—The problem of the distribution of lithium, rubidium, and caesium in sediments was suggested by S. S. GOLDICH, and is a part of a programme of geochemical studies in progress at the University of Minnesota. Analytical work was done in the Rock Analysis Laboratory. Thanks are due to V. T. ALLEN, V. E. BARNES, R. R. BERG, M. P. BILLINGS, R. A. BURWASH, D. M. DAVIDSON, R. L. ERICKSON, S. S. GOLDICH, R. E. GRIM, F. F. GROUT, H. H. HESS, P. KAVANAGH, J. T. LONSDALE, C. M. RILEY, E. B. SANDELL, G. M. SCHWARTZ, R. B. TAYLOR, F. B. VAN HOUTEN, C. E. WEAVER, and M. P. WEISS; and the Oklahoma, Illinois, and Minnesota Geologic surveys for permission to use samples in the Rock Analysis Laboratory files. Special thanks are due to S. S. GOLDICH and E. B. SANDELL for reading and commenting on the manuscript.

The financial aid of the Gulf Oil Corporation Fellowship is gratefully acknowledged.

REFERENCES

AHRENS L. H. (1945a) Quantitative spectrochemical examination of the minor constituents in pollucite (Norway, Maine). *Amer. Min.* **30,** 616–622.

AHRENS L. H. (1945b) Geochemical studies on some of the rarer elements in South African rocks and minerals; II The geochemical relationship of thallium and rubidium in minerals of igneous origin. *Trans. Geol. Soc. S. Africa* **48,** 207.

AHRENS L. H. and LIEBENBERG W. R. (1945) Geochemical studies of some of the rarer elements in South African minerals and rocks; I Lithium in mica and feldspar. *Trans. Geol. Soc. S. Africa* **48,** 75.

AHRENS L. H., PINSON W. H., and KEARNS M. M. (1952) Association of rubidium and potassium and their abundance in common igneous rocks and meteorites. *Geochim. et Cosmochim. Acta* **2,** 229–242.

ALLEN V. T. (1941) Eocene anauxite clays and sands in the Coast Range of California. *Geol. Soc. Amer. Bull.* **52,** 271–294.

AMSTUTZ G. C. (1953) Geochemistry of Swiss lavas. *Geochim. et Cosmochim. Acta.* **3,** 157–168.

BARNES V. E., DAWSON R. F., and PARKINSON G. A. (1942) *Building stones of Central Texas* p. 198. University of Texas Publication 4246.

Berg R. R. (1952) Feldspathized sandstone. *J. Sed. Petrology* **22,** 221.

Brock R. W. (1943) Weathering of igneous rocks near Hong Kong. *Geol. Soc. Amer. Bull.* **54,** 717–738.

Burwash R. A. (1955) A reconnaissance of the subsurface Precambrian of the province of Alberta, Canada. Ph.D. thesis, University of Minnesota.

Butler J. R. (1953) The geochemistry and mineralogy of rock weathering, the Lizard area, Cornwall. *Geochim. et Cosmochim. Acta* **4,** 157–178.

Butler J. R. (1954) The geochemistry and mineralogy of rock weathering, the Nordmarka Area, Oslo. *Geochim. et Cosmochim. Acta* **6,** 268–281.

Canney F. C. (1952) Association of potassium, rubidium, cesium, and thallium in sediments. Ph.D. thesis, M.I.T.

Erametsa O., Sahama Th. G., and Kanula V. (1941) Spectrographic determination of rubidium and cesium in some Finnish minerals and rocks. *Bull. Comm. Geol. Finlande* **128,** 80.

Erickson R. L. (1953) Stratigraphy and petrology of the Tascotal Mesa Quadrangle, Texas. *Geol. Soc. Amer. Bull.* **64,** 1353–1386.

Fairbairn H. W. and others (1951) A co-operative investigation of precision and accuracy in chemical, spectrochemical and modal analysis of silicate rocks. *U.S. Geol. Surv. Bull.* **980,** 109.

Fairbairn H. W., Ahrens L. H., and Gorfunkle L. G. (1953) Minor element content of Ontario diabase. *Geochim. et Cosmochim. Acta* **3,** 34–46.

Goldich S. S. (1938) A study in rock weathering. *J. Geol.* **46,** 17–58.

Goldich S. S. (1941) Evolution of the Central Texas granites. *J. Geol.* **59,** 697–720.

Goldich S. S. and Bergquist H. R. (1947) Aluminous lateritic soil of the Sierra de Bahoruco area, Dominican Republic, W. I. *U.S. Geol. Surv. Bull.* **953–C,** 84.

Goldich S. S. and Bergquist H. R. (1948) Aluminous lateritic soil of the Republic of Haiti, W.I. *U.S. Geol. Surv. Bull.* **954–C,** 109.

Goldich S. S. and Parmelee E. B. (1947) Physical and chemical properties of Ellenberger rocks, Llano County, Texas. *Amer. Assoc. Petroleum Geol. Bull.* **31,** 1982–2020.

Goldschmidt V. M. (1954) *Geochemistry* Clarendon Press, Oxford.

Goldschmidt V. M. (1937) The principles of distribution of chemical elements in minerals and rocks. *J. Chem. Soc.* 655–693.

Goldschmidt V. M., Bauer H., and Witte H. (1934) Zur Geochemie der Alkalimetalle II. *Nach. Ges. Wiss. Göttingen, math-physik Klasse,* **IV,** N.F.1, No. 4, 39.

Goldschmidt V. M., Berman H., Hauptmann H., and Peters Cl. (1933) Zur Geochemie der Alkalimetalle I. *Nach. Ges. Wiss. Göttingen, math-physik Klasse,* **IV,** N.F.1.

Grim R. E. (1953) *Clay Mineralogy* p. 384. McGraw-Hill, New York.

Grout F. F. (1937) Criteria of origin of inclusions in plutonic rocks: *Geol. Soc. Amer. Bull.* **48,** 1521–1572.

Higazy R. A. (1952) Behaviour of the trace elements in a front of metosomatic metamorphism in the Dalradian of County Donegal. *Geochim. et Cosmochim. Acta* **2,** 170–184.

Horstman E. L. (1956) The determination of traces of lithium, rubidium and cesium in silicate rocks. *Anal. Chem.* **28,** 1417–1418.

Jenks W. F., and Goldich S. S. (1956) Rhyolitic tuff flows in southern Peru. *J. Geol.* **64,** 156–172.

Kavanagh P. (1954) The Hyland Lake area, New Quebec. Ph.D. thesis, Princeton University.

Kerr P. F. *et al.* (1950) Analytical data on reference clay materials. *Prelim. Rept.* 7, *Proj.* 49 American Petroleum Institute.

Kuroda P. K. and Sandell E. B. (1954) Geochemistry of molybdenum. *Geochim. et Cosmochim. Acta* **6,** 35–63.

Landergren S. (1948) On the geochemistry of Swedish iron ores and associated rocks: A study on iron formation. *Sveriges Geol. Undersokn,* Ser. C. Avhandl. och Uppsat, No. 496: Arsbok 42, No. 5.

Lonsdale J. T. (1940) Igneous rocks of Terlingua-Solitario region. *Geol. Soc. Amer. Bull.* **51,** 1539–1626.

Lundegardh P. H. (1946) Rock composition and development in Central Roslagen, Sweden. *Arkiv. Kemi Min. Geol.* **23A,** No. 9.

Maxwell J. A. (1953) Geochemical study of chert and related deposits. Ph.D. thesis, University of Minnesota.

Maxwell R. A., Lonsdale J. T., and Dickson K. O. (1949) The Big Bend Region: Guidebook, Field trip No. 1. *West Texas Geol. Soc.* 13–26.

Nockolds, S. R. and Allen R. (1953) The geochemistry of some igneous rock series; Part I, Calc-alkalic rocks. *Geochim. et Cosmochim. Acta* **4,** 105–142.

Nockolds S. R. and Allen R. (1954) The geochemistry of some igneous rock series; Part II, Alkali igneous rock series. *Geochim. et Cosmochim. Acta* **5,** 245–285.

Nockolds S. R. and Mitchell R. L. (1948) The geochemistry of some Caledonian plutonic rocks: A study in the relationship between major and trace elements of igneous rocks and their minerals. *Trans. Roy. Soc. Edinb.* **61,** 533–575.

Noddack I. and Noddack W. (1930) Die Häufigkeit der chemischen Elemente. *Naturwissenschaften* **18,** 757.

Onishi H. and Sandell E. B. (1955) Geochemistry of arsenic. *Geochim. et Cosmochim. Acta* **7,** 1–33.

Patterson E. M. (1951) A petrochemical study of the Tertiary lavas of Northeast Ireland. *Geochim. et Cosmochim. Acta* **2,** 283–299.

Patterson E. M. and Swaine D. J. (1955) A petrochemical study of the Tertiary tholeiitic basalts: Middle lavas of the Antrim Plateau. *Geochim. et Cosmochim. Acta* **8,** 173.

Pinson W. H., Ahrens L. H., and Franck M. L. (1953) The abundance of Li, Sc, Ba, and Zr in chondrites and some ultramafic rocks. *Geochim. et Cosmochim. Acta* **4,** 251–260.

Rankama K. (1946) On the geochemical differentiation in the Earth's crust. *Bull. Comm. Geol. Finlande* **137,** 40.

Rankama K. and Sahama Th. G. (1950) *Geochemistry* p. 911. University of Chicago Press.

Richardson W. A. and Sneesby G. (1922) The frequency-distribution of igneous rocks; I Frequency-distribution of the major oxides in analyses of igneous rocks. *Min. Mag.* **19,** 303–313.

Riley C. M. (1950) The possibility of bloating clays in Minnesota. *Summary Rept.* 5. Minnesota Geol. Survey.

Sahama Th. G. (1945a) Spurenelemente der Gesteine im Südlichen Finnish-Lappland. *Bull. Comm. Geol. Finlande* **135,** 85.

Sahama Th. G. (1945b) On the chemistry of the East Fennoscandian Rapakivi granites. *Bull. Comm. Geol. Finlande* **136,** 15–67.

Schwartz G. M. (1935) Silicification of shale in the Mogul mine. *J. Geol.* **43,** 524–529.

Shaw D. M. (1954) Trace elements in pelitic rocks; Part I, Variation during metamorphism; Part II, Geochemical relations. *Geol. Soc. Amer. Bull.* **65,** 1151–1182.

Shaw D. M. and Bankier J. D. (1954) Statistical methods applied to geochemistry. *Geochim. et Cosmochim. Acta* **5,** 111–123.

Stevens R. E. and Schaller W. T. (1942) The rare alkalies in micas. *Amer. Min.* **27,** 525–537.

Strock L. W. (1936) Geochemie des Lithiums. *Nach. Ges. Wiss. Göttingen,* math-physik Klasse, **IV,** N.F.1, No. 15, p. 171.

Taylor R. B. (1955) Petrology and petrography of the Duluth Gabbro Complex near Duluth, Minnesota. Ph.D. thesis, University of Minnesota.

Van Houten F. B. (1953) Clay minerals in sedimentary rocks and derived soils. *Amer. J. Sci.* **251,** 61–82.

Wager L. R. and Mitchell R. L. (1943) Preliminary observations on the distribution of trace elements in the rocks of the Skaergaard intrusion, Greenland. *Min. Mag.* **26,** 283.

Wager L. R. and Mitchell R. L. (1951) The distribution of trace elements during strong fractionation of basic magma; A further study of the Skaergaard intrusion, East Greenland. *Geochim. et Cosmochim. Acta* **1,** 129–208.

Walker F. and Poldervaart A. (1949) Karroo dolerites of the Union of South Africa. *Geol. Soc. Amer. Bull.* **60,** 591–706.

Weaver C. E. (1953), Mineralogy and petrology of some Ordovician K-bentonites and related limestones. *Geol. Soc. Amer. Bull.* **64,** 921–943.

Weiss M. P. (1954) Feldspathized shales from Minnesota. *Sed. Petrology* **24,** 270–274.

Wickman F. E. (1943) Some aspects of the geochemistry of igneous rocks and of the differentiation by crystallization. *Geol. Foren.* Stockholm, Förhandl. **65,** 371–396.

APPENDIX

Sample No.	Rock name	(p.p.m.) Li	Rb	Cs	Mg/Li (ratio)	K/Rb (ratio)	K/Cs (ratio)	Location and age	Reference	Page	Table	Sample
	Granitic crystalline rocks											
1	Granodiorite porphyry	16	230	—	1000	130	—	Hong Kong (K)	BROCK, 1943	733	8	10A
2	Granite	26	170	—	190	210	—	Hong Kong (K)	BROCK, 1943	727	4	4A
3	Rhyolite porphyry	23	250	4	260	140	8700	Hong Kong (K)	BROCK, 1943	731	6	6
4	Porphyritic granite	20	220	3	110	200	14700	Hong Kong (K)	BROCK, 1943	729	5	5
5	Rhyolite porphyry	28	200	—	40	200	—	Hong Kong (K)	BROCK, 1943	725	3	1
6	Granite (G-1)	23	210	—	90	220	—	Westerly, R.I.	FAIRBAIRN and others, 1951	8	1	
7	Granite gneiss	30	130	—	150	250	—	Morton, Minn. (PE)	GOLDICH, 1938	22	1	1
8	Riebeckite soda granite	93	320	—	4	110	—	Big Bend Area, Texas (T)	LONSDALE, 1940	1618	17	III
9	Riebeckite soda rhyolite	72	270	5	10	100	5200	Big Bend Area, Texas (T)	LONSDALE, 1940	1618	17	V
10	Riebeckite soda rhyolite	76	270	—	10	120	—	Big Bend Area, Texas (T)	LONSDALE, 1940	1618	17	I
11	Rhyolite	46	290	5	9	140	8300	Jordan Gap Quad., Texas (T)	S. S. GOLDICH, unpublished			
12	Riebeckite soda granite	143	650	3	3	60	12400	Big Bend Area, Texas (T)	MAXWELL, 1949	21	3	9
13	Riebeckite soda granite	51	260	—	1	150	—	Big Bend Area, Texas (T)	MAXWELL, 1949	21	3	6
14	Olivine aug. hb. granite	14	80	—	220	620	—	Big Bend Area, Texas (T)	MAXWELL, 1949	21	3	17
15	Rhyolite tuff flow		100	—		330	—	Tiabaya, Peru (Q)	JENKS and GOLDICH, 1956	168	3	1
16	Rhyolite tuff flow	30	200	—	30	210	—	Yarabamba, Peru (Q)	JENKS and GOLDICH, 1956	168	3	4
17	Rhyolite tuff flow		160	9		240	4600	Characato, Peru (Q)	JENKS and GOLDICH, 1956	168	3	3
18	Rhyolite tuff flow		120	—		300	—	Vitor, Peru (Q)	JENKS and GOLDICH, 1956	168	3	2
19	Rhyolite tuff flow		110	—		340	—	Rio de Torata, Peru (Q)	JENKS and GOLDICH, 1956	168	3	5
20	Leucogranite	45	110	—	6	320	—	Oklahoma (PE)	Oklahoma Geol. Survey, unpublished			
21	Leucogranite	10	220	—	10	200	—	T3N, R14W, Oklahoma (PE)	Oklahoma Geol. Survey, unpublished			
22	Leucogranite	29	120	—	80	290	—	T3N, R13W, Oklahoma (PE)	Oklahoma Geol. Survey, unpublished			
23	Leucorhyolite porphyry		160	—		240	—	T3N, R13W, Oklahoma (PE)	Oklahoma Geol. Survey, unpublished			
24	Leucorhyolite porphyry		160	10		230	3700	Oklahoma (PG)	Oklahoma Geol. Survey, unpublished			
25	Leucorhyolite porphyry		110	—		310	—	T5N, R16W, Oklahoma (PE)	Oklahoma Geol. Survey, unpublished			
26	Diorite-quartz monzonite		60	—		210	—	T4N, R17W, Oklahoma (PE)	Oklahoma Geol. Survey, unpublished			
27	Diorite-quartz monzonite		100	—		170	—	T4N, R17W, Oklahoma (PE)	Oklahoma Geol. Survey, unpublished			
28	Diorite-quartz monzonite		70	—		190	—	T4N, R17W, Oklahoma (PE)	Oklahoma Geol. Survey, unpublished			
29	Biotite granite	40	210	11		170	3300	T4N, R15W, Oklahoma (PE)	Oklahoma Geol. Survey, unpublished			
30	Biotite riebeckite granite		150	—		280	—	T3N, R13W, Oklahoma (PE)	Oklahoma Geol. Survey, unpublished			
31	Riebeckite granite		190	—		190	—	T3N, R14W, Oklahoma (PE)	Oklahoma Geol. Survey, unpublished			
32	Calc-alkali granite		180	—		280	—	Peace River Area, Canada (PE)	BURWASH, 1955			
33	Calc-alkali granite		120	—		480	—	McMurray, Alberta, Canada (PE)	BURWASH, 1955			
34	Muscovite alkali granite		200	—		260	—	Edmonton, Alberta, Canada (PE)	BURWASH, 1955			
35	Granodiorite		150	—		200	—	Edmonton, Alberta, Canada (PE)	BURWASH, 1955			
36	Biotite calc-alkali granite		180	—		290	—	McMurray, Alberta, Canada (PE)	BURWASH, 1955			
37	Garnet calc-alkali granite		160	—		340	—	McMurray, Alberta, Canada (PE)	BURWASH, 1955			
38	Alkali granite		130	—		320	—	N.W. Alberta, Canada (PE)	BURWASH, 1955			
39	Alkali granite		150	—		290	—	N.W. Alberta, Canada (PE)	BURWASH, 1955			
40	Alkali granite gneiss		160	—		430	—	Peace River, Alberta, Can. (PE)	BURWASH, 1955			
41	Calc-alkali granite		130	—		330	—	Peace River, Alberta, Can. (PE)	BURWASH, 1955			
42	Biotite adamellite gneiss		200	—		190	—	Peace River, Alberta, Can. (PE)	BURWASH, 1955			
43	Biotite adamellite gneiss		230	—		160	—	Peace River, Alberta, Can. (PE)	BURWASH, 1955			
44	Biotite adamellite gneiss		200	—		260	—	Edmonton, Alberta, Canada (PE)	BURWASH, 1955			
45	Calc-alkali granite		240	—		210	—	McMurray, Alberta, Canada (PE)	BURWASH, 1955			
46	Biotite adamellite		120	—		330	—	S.E. Alberta, Canada (PE)	BURWASH, 1955			
47	Calc-alkali granite		190	—		220	—	Marion River, N.W.T., Can. (PE)	BURWASH, 1955			
48	Calc-alkali granite		180	—		230	—	Marion River, N.W.T., Can. (PE)	BURWASH, 1955			
49	Muscovite alkali granite		110	—		170	—	Edmonton, Alberta, Canada (PE)	BURWASH, 1955			
50	Alkali rhyolite porphyry		160	—		260	—	S. Central Sask., Canada (PE)	BURWASH, 1955			
51	Gneiss		170	8		200	4300	Gorham Quad., N.H. (D)	M. P. BILLINGS, unpublished			
52	Gneiss		140	9		240	3600	Gorham Quad., N.H. (D)	M. P. BILLINGS, unpublished			
53	Gneiss		180	7		180	4600	Crawford Notch Quad., N.H. (D)	M. P. BILLINGS, unpublished			
54	Gneiss		140	—		210	—	Crawford Notch Quad., N.H. (D)	M. P. BILLINGS, unpublished			
55	Muscovite granite		50	—		350	—	Gorham Quad., N.H.	M. P. BILLINGS, unpublished			
56	Biotite granodiorite		70	—		230	—	Gorham Quad., N.H.	M. P. BILLINGS, unpublished			

57	Composite, 6 granites	39	210	—	50	190	—	Central Texas	GOLDICH, 1941			
58	Composite, 14 granite gneiss	40	110	—	150	310	—	Canada	ONISHI and SANDELL, 1955	4	1	8
59	Composite, 8 granites	30	140	—	110	250	—	Canada	ONISHI and SANDELL, 1955	4	1	6
60	Composite, 9 granitic rocks	29	190	—	90	200	—	California	ONISHI and SANDELL, 1955	4	1	3
61	Composite, 8 granites	14	130	—	130	280	—	U.S.A. and Canada	ONISHI and SANDELL, 1955	4	1	2
62	Granodiorite		80			220	—	Duluth, Minnesota (PE)	TAYLOR, 1955			
63	Granophyre		170			250	—	Duluth, Minnesota (PE)	TAYLOR, 1955			
64	Granophyre		100			240	—	Duluth, Minnesota (PE)	TAYLOR, 1955			
65	Granophyre		160			230	—	Duluth, Minnesota (PE)	TAYLOR, 1955			
66	Granophyre		140			240	—	Duluth, Minnesota (PE)	TAYLOR, 1955			
								Syenite, monzonite, and trachyte				
67	Syenite	29	130	—	80	410	—	Big Bend Area, Texas (T)	MAXWELL, 1949	21	3	20
68	Syenite	28	60	—	150	480	—	Tascotal Mesa Quad., Texas (T)	ERICKSON, 1954	1379	4	3
69	Composite, 6 syenites	28	130	—	400	340	—	New York and Minnesota	ONISHI and SANDELL, 1955	4	1	10
								Diorite and andesite				
70	Andesite	29	130	4	230	230	7500	Hong Kong (K?)	BROCK, 1943	732	7	9
71	Trachyandesite porphyry	26	100	—	180	400	—	Tascotal Mesa Quad., Texas (T)	ERICKSON, 1954	1378	3	4
72	Syenodiorite porphyry	16	90	—	580	380	—	Big Bend Area, Texas (T)	LONSDALE, 1940	1618	17	XII
73	Diorite		110	—		230	—	T4N, R17W, Oklahoma (PE)	Oklahoma Geol. Survey, unpublished			
74	Diorite		120	—		180	—	T4N, R17W, Oklahoma (PE)	Oklahoma Geol. Survey, unpublished			
								Gabbro and basalt				
75	Diabase (W-1)	14	20	—	2840	270	—	Fairfax Co., Virginia (Tr)	FAIRBAIRN and others, 1951	10	2	
76	Diabase	23	20	—	1120	470	—	Medford, Mass.	GOLDICH, 1938	40	8	8
77	Trachybasalt porphyry	29	60	—	680	380	—	Big Bend Area, Texas (T)	LONSDALE, 1940	1618	17	XV
78	Syenogabbro	14	50	—	1260	490	—	Big Bend Area, Texas (T)	LONSDALE, 1940	1618	17	XVI
79	Trachydolerite	20	40	—	1270	440	—	Big Bend Area, Texas (T)	LONSDALE, 1940	1618	17	XIX
80	Trachybasalt	14	30	—	2860	360	—	Big Bend Area, Texas (T)	MAXWELL, 1949	22	3	31
81	Syenogabbro	14	40	—	1850	480	—	Big Bend Area, Texas (T)	MAXWELL, 1949	22	3	30
82	Diallage gabbro		20	—		30	—	Oklahoma (PE)	Oklahoma Geol. Survey, unpublished			
83	Gabbro		30	—		260	—	Oklahoma (PE)	Oklahoma Geol. Survey, unpublished			
84	Gabbro		30	—		180	—	Duluth, Minnesota (PE)	TAYLOR 1955			
85	Troctolite		20	—		190	—	Duluth, Minnesota (PE)	TAYLOR, 1955			
86	Troctolite		—	—		—	—	Duluth, Minnesota (PE)	TAYLOR, 1955			
87	Composite, 24 basic rocks	13	40	—	4160	140	—	Worldwide	ONISHI and SANDELL, 1955	4	1	13
88	Composite, 4 gabbro-diorite	16	30	—	2390	230	—	California	ONISHI and SANDELL, 1955	4	1	12
89	Composite, 7 olivine basalt	13	Tr.	—	2380	—	—	Oregon	ONISHI and SANDELL, 1955	8	5	
								Ultramafic rocks				
90	Amphibolite	38	10	—	870	210	—	Black Hills, S.D.	GOLDICH, 1938	50	15	13
91	Picritic basalt	14	10	—	4990	850	—	Big Bend Area, Texas (T)	MAXWELL, 1949	22	3	41
92	Limburgitic basalt		20	—		150	—	Central Texas	BURWASH, 1955			
93	Serpentinized peridotite		—	—		—	—	Labrador (PE)	KAVANAGH, 1954			
94	Serpentinized peridotite		—	—		—	—	Labrador (PE)	KAVANAGH, 1954			
								Chondrites				
95	Composite, 7 chondrites	4	—	—		—	—		ONISHI and SANDELL, 1955	31	17	I
96	Composite, 7 chondrites	3	—	—		—	—		ONISHI and SANDELL, 1955	31	17	II
								Kaolinite group				
97	Kaolinite	133	60	6	180	150	1600	Brierley Hill, England (M)	KERR, 1950	45		100A
98	Kaolinite	233	30	5	6	240	1700	Chudleigh-Knighton, Eng. (T)	KERR, 1950	46		112A
99	Kaolinite	232	140	52	8	90	200	Newbridge, England (T)	KERR, 1950	46		113A
100	Kaolinite	108	250	15	10	50	800	St. Austell, England	KERR, 1950	46		114A
101	Kaolinite	52	160	23	30	60	500	Lee Moor, England	KERR, 1950	46		115A
102	Kaolinite	187	230	35	7	50	300	Hawkstor, England	KERR, 1950	47		116A
103	Kaolinite	117	100	7	20	100	1500	Holtzhausen, Germany (T)	KERR, 1950	47		123A

APPENDIX (*continued*)

Sample No.	Rock name	(p.p.m.) Li	Rb	Cs	Mg/Li (ratio)	K/Rb (ratio)	K/Cs (ratio)	Location and age	Reference	Page	Table	Sample
	Kaolinite group (*continued*)											
104	Kaolinite	28	140	4	50	100	3300	Tirschenreuth, Bavaria	KERR, 1950	47		126A
105	Kaolinite	35	90	4	40	180	4300	Hirshau, Bavaria (Tr)	KERR, 1950	47		127A
106	Kaolinite	144	60	10	9	120	700	Breitschied, Germany (T)	KERR, 1950	48		129A
107	Kaolinite	610	580	96	30	30	200	Echassieres, France	KERR, 1950	48		133D
108	Anauxite	42	30	—	30	140	—	Tesla, California (T)	ALLEN, 1941	277	2	2
109	Anauxite	43	30	—	40	130	—	Tesla, California (T)	ALLEN, 1941	277	2	3
110	Anauxite	78	80	12	80	210	900	Rio Vista, California (T)	ALLEN, 1941	284	6	1
111	Halloysite	40	20	—	30	230	—	Bedford, Indiana (C)	KERR, 1950	48		12B
112	Halloysite	30	—	—	490	—	—	Cadouin, France (T)	KERR, 1950	49		134A
113	Halloysite	55	—	—	20	—	—	Cadouin, France (T)	KERR, 1950	49		$135A_1$
114	Halloysite	43	10	—	110	50	—	Cadouin, France (T)	KERR, 1950	49		$135A_2$
115	Dickite	61	10	—	8	360	—	Anglesey, Wales (C)	KERR, 1950	51		102A
	Montmorillonite group											
116	Montmorillonite	75	40	—	210	350	—	Combe Hay, England (J)	KERR, 1950	55		107A
117	Montmorillonite	48	30	—	600	180	—	Nutfield, England (K)	KERR, 1950	54		105B
118	Montmorillonite	45	20	—	420	260	—	Nutfield, England (K)	KERR, 1950	54		104M
119	Bentonite	38	20	—	300	220	—	Wayne, Alberta, Canada (K)	R. E. GRIM, unpublished			
120	Bentonite	25	30	—	660	90	—	Rosedale, Alberta, Canada (K)	R. E. GRIM, unpublished			
121	Bentonite	46	40	—	230	150	—	Dorothy, Alberta, Canada (K)	R. E. GRIM, unpublished			
122	Bentonite	88	30	5	280	110	600	Marnia, Algeria (T)	R. E. GRIM, unpublished			
123	Bentonite	46	10	—	450	360	—	Belle Fourche, S.D. (K)	R. E. GRIM, unpublished			
124	Bentonite	34	20	—	520	110	—	Gonzales Co., Texas (K)	R. E. GRIM, unpublished			
125	Bentonite	31	60	5	500	130	1500	Gonzales Co., Texas (K)	R. E. GRIM, unpublished			
126	Bentonite	33	10	—	450	130	—	Gonzales Co., Texas (K)	R. E. GRIM, unpublished			
127	Bentonite	98	Tr.	—	270	—	—	Pembina, Manitoba, Canada (K)	R. E. GRIM, unpublished			
128	Bentonite	9	20	—	1370	170	—	Ponza, Italy (T?)	R. E. GRIM, unpublished			
	Other clay minerals											
129	Mixed layer	45	90	49	910	160	300	Pioche, Nevada	KERR, 1950	56		32A
130	K-Bentonite	49	120	—	190	200	—	Catawaba, Virginia (O)	KERR, 1950	57		38
131	K-Bentonite	25	150	4	380	240	9100	Tazewell, Virginia (O)	KERR, 1950	56		39
132	K-Bentonite	64	180	17	340	340	3600	Central Pennsylvania (O)	WEAVER, 1953	932	10	OH-2
133	K-Bentonite	52	180	13	430	270	3800	Central Pennsylvania (O)	WEAVER, 1953	932	10	$OH\text{-}N_1$
134	Attapulgite	29	40	—	1750	140	—	Attapulgus, Georgia (T)	KERR, 1950	58		45
	Shales											
135	Shale	50	100	8	290	200	2500	Dewey, Montana (K)	GROUT, 1937	1563	5	1
136	Shale	43	120	3		170	6500	Dewey, Montana (K)	GROUT, 1937	1562	4	2
137	Shale (Deadwood)	29	200	—	160	400	—	Black, Hills, S.D. (PE)	SCHWARTZ, 1935	528	1	1
138	Shale (Deadwood) (silicified)	23	150	—	80	370	—	Black, Hills, S.D. (PE)	SCHWARTZ, 1935	528	1	2
139	Shale (Decorah)	41	170	6	390	330	9200	Barr, Minnesota (O)	RILEY, 1950	14	III	$R8_2$
140	Shale (Decorah)	59	210	7	260	300	9100	Barr, Minnesota (O)	RILEY, 1950	14	III	$R8_3$
141	Shale (Decorah)	65	210	9	260	300	7100	Minneapolis, Minnesota (O)	RILEY, 1950	14	III	$R25_2$
142	Shale (Decorah)	42	180	5	410	320	11100	Minneapolis, Minnesota (O)	RILEY, 1950	14	III	$R25_3$
143	Colloid fraction, siltstone (Cimarron)	74	110	7	610	240	3800	Barber Co., Kansas (Pm)	VAN HOUTEN, 1953	74	3	aC
144	Colloid fraction, siltstone (Cimmaron)	107	150	—	390	250	—	Harper Co., Kansas (Pm)	VAN HOUTEN, 1953	74	3	bC
145	Colloid fraction, sandstone (Waubunsee)	150	180	—	2	200	—	Chautauqua Co., Kansas (Pm)	VAN HOUTEN, 1953	74	3	cC
146	Shale (Roan)	81	180	7	400	350	9000	N. Rhodesia, Africa (PE)	D. M. DAVIDSON, unpublished			
147	Shale (Roan)	65	160	5	550	380	12700	N. Rhodesia, Africa (PE)	D. M. DAVIDSON, unpublished			
148	Shale (Roan)	40	160	—	460	420	—	N. Rhodesia, Africa (PE)	D. M. DAVIDSON, unpublished			

149	Shale (Roan)	136	280	12	320	230	5200	N. Rhodesia, Africa (PE)	D. M. DAVIDSON, unpublished			
150	Shale (Roan)	92	220	4	440	250	13800	N. Rhodesia, Africa (PE)	D. M. DAVIDSON, unpublished			
151	Shale (Roan)	57	130	—	230	360	—	N. Rhodesia, Africa (PE)	D. M. DAVIDSON, unpublished			
152	Shale (Roan)	75	150	5	620	320	9400	N. Rhodesia, Africa (PE)	D. M. DAVIDSON, unpublished			
153	Shale (Tornillo)	33	100	2	340	100	5100	Near Castalon, Texas (K)	S. S. GOLDICH, unpublished			
154	Shale	212	70	13	20	220	1200	Morris, Illinois (P)	V. T. ALLEN, unpub. rept., Illinois Geol. Surv.			
155	Shale	38	120	4	280	220	7000	Chillicotte, Illinois (P)	V. T. ALLEN, unpub. rept., Illinois Geol. Surv.			
156	Shale	72	200	11	180	200	3600	Chillicotte, Illinois (P)	V. T. ALLEN, unpub. rept., Illinois Geol. Surv.			
157	Silty shale	110	140	6	430	180	4300	Tygart Dam	Rock Analysis Laboratory Files			
158	Shale	72	160	10	140	180	2900	Tygart Dam	Rock Analysis Laboratory Files			
159	Sandy shale	58	110	—	170	200	—	Tygart Dam	Rock Analysis Laboratory Files			
160	Composite, 7 shales	58	100	5		190	3700	U.S.A.	Rock Analysis Laboratory Files			
	Sandstone											
161	Sandstone	16	50	—	880	130	—	Minnesota	Rock Analysis Laboratory Files			
162	Sandstone	13	20	—	420	580	—	Minnesota	Rock Analysis Laboratory Files			
163	Sandstone (Franconia)	7	80	—	140	890	—	Franconia, Minnesota (E)	BERG, 1952	222	2	
164	Glauconitic sandstone (Lion Mt.)	25	100	9	100	260	2800	Mason Co., Texas	BARNES, 1942	122	50	
	Recent sediments											
165	Near shore sediment	63	130	9	310	140	2100	Galveston Bay, Texas (recent)	R. E. GRIM, unpublished			
166	Near shore sediment	58	130	—	350	150	—	Galveston Bay, Texas (recent)	R. E. GRIM, unpublished			
167	Near shore sediment	58	130	9	330	120	1800	Galveston Bay, Texas (recent)	R. E. GRIM, unpublished			
168	Near shore sediment	55	130	9	350	130	1800	Galveston Bay, Texas (recent)	R. E. GRIM, unpublished			
169	Near shore sediment	45	110	9	330	110	1400	Galveston Bay, Texas (recent)	R. E. GRIM, unpublished			
170	Near shore sediment	55	130	6	280	110	2400	Galveston Bay, Texas (recent)	R. E. GRIM, unpublished			
171	Near shore sediment	57	130	6	280	120	2500	Galveston Bay, Texas (recent)	R. E. GRIM, unpublished			
172	Near shore sediment	55	130	6	300	120	2600	Galveston Bay, Texas (recent)	R. E. GRIM, unpublished			
173	Near shore sediment	55	130	6	320	130	2800	Galveston Bay, Texas (recent)	R. E. GRIM, unpublished			
174	Near shore sediment	54	130	6	330	120	2600	Galveston Bay, Texas (recent)	R. E. GRIM, unpublished			
175	Composite, 4 red clays, deep sea	58	160	6		200	3400	Pacific Ocean (recent)	ONISHI and SANDELL, 1955	23	15	
176	Composite, 4 red clays, deep sea	55	60	6		210	2100	Pacific Ocean (recent)	ONISHI and SANDELL, 1955	23	15	
177	Composite, 6 globegerina ooze	29	10	—		340	—	Pacific Ocean (recent)	KURODA and SANDELL, 1954	57	14	
	Lateritic material											
178	Composite, aluminous lateritic soil	58	10	—		30	—	Haiti	GOLDICH and BERGQUIST, 1948	75	2	2
179	Composite, aluminous lateritic soil	33	10	—	6	40	—	Haiti	GOLDICH and BERGQUIST, 1948	75	2	6
180	Composite, aluminous lateritic soil	46	10			50	—	Haiti	GOLDICH and BERGQUIST, 1948	75	2	10
181	Aluminous lateritic soil	36	10	—		40	—	Haiti	GOLDICH and BERGQUIST, 1948	79	7	1–5
182	Aluminous lateritic soil	33	Tr.	—		—	—	Haiti	GOLDICH and BERGQUIST, 1948	79	7	10–15
183	Aluminous lateritic soil	33	10	—		80	—	Haiti	GOLDICH and BERGQUIST, 1948	79	7	20–25
184	Aluminous lateritic soil	43	Tr.	—		—	—	Haiti	GOLDICH and BERGQUIST, 1948	79	7	30–37
185	Aluminous lateritic soil	38	Tr.	—		—	—	Dominican Republic	GOLDICH and BERGQUIST, 1947	67	6	11
186	Aluminous lateritic soil (concretions)	8	Tr.	—		—	—	Dominican Republic	GOLDICH and BERGQUIST, 1947	67	6	12
187	Aluminous lateritic soil	101	20	—		50	—	Dominican Republic	GOLDICH and BERGQUIST, 1947	70	7	1
188	Aluminous lateritic soil	74	20	—		50	—	Dominican Republic	GOLDICH and BERGQUIST, 1947	70	7	2
189	Aluminous lateritic soil	89	10	—		50	—	Dominican Republic	GOLDICH and BERGQUIST, 1947	70	7	3
190	Aluminous lateritic soil	89	20	—		70	—	Dominican Republic	GOLDICH and BERGQUIST, 1947	70	7	4
191	Aluminous lateritic soil	104	Tr.	—		—	—	Dominican Republic	GOLDICH and BERGQUIST, 1947	70	7	5
	Miscellaneous samples											
192	Glacial clay	25	60	—	1170	240	—	Wrenshall, Minnesota	RILEY, 1950	14	III	W_1
193	Glacial clay	43	100	—	660	210	—	Carlton Co., Minnesota	RILEY, 1950	14	III	BH_2
194	Feldspathized shale (Dubuque)	28	60	—	230	1860	—	Fillmore Co., Minnesota (O)	WEISS, 1954	273	1	
195	Lamprophyre	35	120	—	1350	250	—	Hong Kong	BROCK, 1943	734	9	12

Appendix (*continued*)

Sample No.	Rock name	(p.p.m.) Li	Rb	Cs	Mg/Li (ratio)	K/Rb (ratio)	K/Cs (ratio)	Location and age	Reference	Page	Table	Sample
	Weathering series											
5	Rhyolite porphyry	28	200	—	40	200	—	Hong Kong	BROCK, 1943	725	3	1
5A	Weathered crust	43	100	—	40	160	—	Hong Kong	BROCK, 1943	725	3	1A
5B	Kaolinitic clay	19	160	3	100	180	9800	Hong Kong	BROCK, 1943	725	3	1X
2	Granite	26	170	—	190	210	—	Hong Kong	BROCK, 1943	727	4	4A
2A	Weathered granite	28	40	—	180	100	—	Hong Kong	BROCK, 1943	727	4	4B
2B	Weathered granite	39	200	—	80	40	—	Hong Kong	BROCK, 1943	727	4	4C
2C	Weathered granite	20	60	—		70	—	Hong Kong	BROCK, 1943	727	4	4D
2D	Weathered granite	6	350	—	220	100	-	Hong Kong	BROCK, 1943	727	4	4E
2E	Bauxitic clay	18	110	—		40	—	Hong Kong	BROCK, 1943	727	4	4F
4	Porphyritic granite	20	220	3	110	200	14700	Hong Kong	BROCK, 1943	729	5	5
4A	Weathered granite	10	250	7	30	140	5200	Hong Kong	BROCK, 1943	729	5	5A
4B	Weathered granite	26	90	7	20	100	1200	Hong Kong	BROCK, 1943	729	5	5B
3	Rhyolite porphyry	23	250	4	260	140	8700	Hong Kong	BROCK, 1943	731	6	6
3A	Weathered rhyolite	26	210	4	160	150	7800	Hong Kong	BROCK, 1943	731	6	6A
3B	Brown clay	35	40	—	300	70	—	Hong Kong	BROCK, 1943	731	6	7A
70	Andesite	29	130	4	230	230	7500	Hong Kong	BROCK, 1943	732	7	9
70A	Weathered andesite	61	170	2	180	180	15300	Hong Kong	BROCK, 1943	732	7	9A
1	Granodiorite porphyry	16	230	—	1000	130	—	Hong Kong	BROCK, 1943	733	8	10A
1A	Weathered granodiorite	26	90	—	500	140	—	Hong Kong	BROCK, 1943	733	8	10B
1B	Lateritic clay	14	60	-	1000	80	—	Hong Kong	BROCK, 1943	733	8	10C
200	Lamprophyre	35	120	-	1350	250	-	Hong Kong	BROCK, 1943	734	9	12
200A	Weathered lamprophyre	48	160	-	570	230	—	Hong Kong	BROCK, 1943	734	9	12A
200B	Weathered lamprophyre	46	80	—	60	110	—	Hong Kong	BROCK, 1943	734	9	12B
7	Granite gneiss	30	130	—	150	250	—	Morton, Minnesota	GOLDICH, 1938	22	1	1
7A	Weathered granite gneiss	14	200	—	130	220	—	Morton, Minnesota	GOLDICH, 1938	22	1	2
7B	Weathered granite gneiss	25	140	—	110	210	—	Morton, Minnesota	GOLDICH, 1938	22	1	3
7C	Weathered granite gneiss	36	150		130	210	—	Morton, Minnesota	GOLDICH, 1938	22	1	4
7D	Weathered granite gneiss	20	60		60	320	—	Morton, Minnesota	GOLDICH, 1938	22	1	5
7E	Weathered granite gneiss	38	10	—	70	410	—	Morton, Minnesota	GOLDICH, 1938	22	1	6
7F	Weathered granite gneiss	36	10	-	60	110	-	Morton, Minnesota	GOLDICH, 1938	22	1	7
76	Diabase	23	20	—	1120	470	-	Medford, Mass.	GOLDICH, 1938	40	8	8
76A	Weathered diabase	21	50	—	360	250	—	Medford, Mass.	GOLDICH, 1938	40	8	10
88	Amphibolite	38	10	—	870	210	—	Black Hills, S.D.	GOLDICH, 1938	50	15	13
88A	Weathered amphibolite	32	20	-	390	140	-	Black Hills, S.D.	GOLDICH, 1938	50	15	14
143	Colloid fraction, siltstone	74	110	7	610	240	3800	Barber Co., Kansas	VAN HOUTEN, 1953	74	3	aC
143A	Colloid fraction, soil	98	100	4	540	200	4800	Barber Co., Kansas	VAN HOUTEN, 1953	74	3	aA
144	Colloid fraction, siltstone	107	150	-	390	250	—	Harper Co., Kansas	VAN HOUTEN, 1953	74	3	bC
144A	Colloid fraction, soil	74	150	—	390	250	—	Harper Co., Kansas	VAN HOUTEN, 1953	74	3	bA
145	Colloid fraction, sandstone	150	180	—	2	200	—	Chautauqua Co., Kansas	VAN HOUTEN, 1953	74	3	cC
145A	Colloid fraction, soil	67	150	4	140	160	6000	Chautauqua Co., Kansas	VAN HOUTEN, 1953	74	3	cA
	Xenolith-intrusion series, Boulder batholith											
135	Shale	50	100	8	290	200	2500	Dewey, Montana	GROUT, 1937	1563	5	1
135A	Shale composite (136)	43	120	3		170	6500	Dewey, Montana	GROUT, 1937	1562	4	2
135B	Shale hornfels	40	80	5	260	260	4500	Dewey, Montana	GROUT, 1937	1563	5	3
135C	Hornfels breccia	25	80	—	640	160	—	Dewey, Montana	GROUT, 1937	1563	5	4
135D	Hornfels	23	70	4		200	3600	Dewey, Montana	GROUT, 1937	1562	4	5
135E	Hornfels inclusion	17	40	—	2000	250	—	Dewey, Montana	GROUT, 1937	1563	5	6
135F	Hornfels inclusion	14	30	—		180	—	Dewey, Montana	GROUT, 1937	1562	4	7
135G	Hornfels inclusion	16	40	—	1300	300	—	Dewey, Montana	GROUT, 1937	1563	5	8
135H	Composite, hornfels inclusions	17	50	—		240	—	Dewey, Montana	GROUT, 1937	1562	4	9
135I	Hornfels inclusion	14	40	—	2000	320	—	Dewey, Montana	GROUT, 1937	1563	5	10
135J	Composite, hornfels inclusions near the centre of the intrusion	49	160	21		110	800	Dewey, Montana	GROUT, 1937	1562	4	11

Geochimica et Cosmochimica Acta, 1957, Vol. 12, pp. 29 to 46. Pergamon Press Ltd., London

The geochemistry of the Messum Igneous Complex, South-West Africa

Morna Mathias
Department of Geology, University of Cape Town

(*Received* 7 *December* 1956)

Abstract—The distribution of major and trace elements in twenty-eight representative rocks from the Messum Igneous Complex of South-West Africa is discussed and illustrated by variation diagrams. Special attention is paid to three hybrid rock sequences: (a) basalt-granite, (b) dolerite-tinguaite, and (c) quartz-porphyry-tinguaite, in which the distribution is found to be essentially of the straight-line variation type. Brief geological descriptions are given where these are necessary for understanding the problems involved. Intrusive and cumulative rocks not represented in the hybrid series are also considered and comparisons drawn from other areas.

Introduction

A considerable body of information on the trace-element composition of rocks has been accumulating in the past ten years. This forms an essential standard for comparison. Of particular interest to the petrologist is the pioneer work by R. L. Mitchell, S. R. Nockolds, and L. R. Wager on rock series formed by fractional crystallization (Nockolds and Mitchell, 1948; Wager and Mitchell, 1951; Nockolds and Allen 1953, 1954, and 1955). Little, so far, has been published on the distribution of trace elements in rocks of hybrid origin. Nockolds and Allen give the subject brief mention, and consider that the trace-element distribution in four tholeiite-granite hybrids from Satakunta, Finland, may well be linear (Nockolds and Allen, 1955).

The rocks of the Messum Ring-Complex provide excellent material for the study of trace-element variation in hybrid rock series, as well as data for other igneous and cumulative rocks which show a wide range in composition. The spectrographic analysis of the trace elements was kindly carried out by Dr. S. R. Nockolds and Mr. R. S. Allen at the Department of Mineralogy and Petrology, Cambridge. The results have already been published, but without comment (Mathias, 1956). The technique employed is the same as that described by the former authors (Nockolds and Allen, 1953), and in order to make comparison as direct as possible, all results have been computed on the same basis and using the same methods of plotting.

The general geology and petrology of the Messum Igneous Complex have been described in separate papers (Korn and Martin, 1954; Mathias, 1956), but owing to the controversial nature of nearly all petrogenic theories and in particular those dealing with felspathoidal rocks, the salient facts concerning the origin of the presumed hybrid rocks will be reviewed briefly.

Basalt-granite Hybrid Series

(a) *Occurrence*

These hybrids, which range in composition from diorite to a rather mafic granite, resulted from the intrusive phase of the Ring-Complex when granite was intruded into the lavas and tuffs of the original volcanic cone, which lay

between the previously intruded sills of microeucrite and hypersthene microgabbro. The granite penetrated the tuff and lava rather than the gabbroic layers, owing to the fractured and more porous nature of the former. The tuffs were dominantly rhyolitic, and do not concern us here; the lavas were basaltic, and at least three types of basalt are distinguishable, viz. a tholeiite (W-3), a bronzite basalt (L-14), and a basalt akin to olivine basalt but richer in silica and poorer in alkalis than the average (L-11); also a felspar-phyric basalt (L-13) near L-11 in type. In the south-eastern part of the Complex all stages in the assimilation of basalt by granite are shown (see Martin, 1954, plate XIX), and there is a direct ratio between the amount of basalt assimilated and the contamination of the granite. Thus, where basalt fragments are sharp and angular, the surrounding granite is uncontaminated

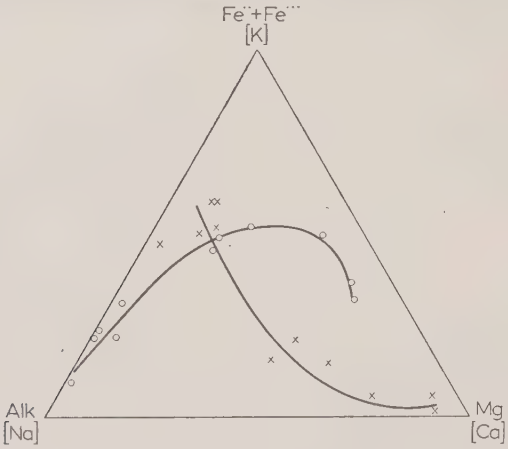

Fig. 1. Variation diagram for the coarse-grained calc-alkali rocks.
○ = Mg—Fe^{++} + Fe^{+++}—Alk.
× = (Ca)—(K)—(Na)

and leucocratic; conversely, the more diffuse and ill-defined the basalt fragments become, the darker and more basic is the matrix. There is no question here or possibility of separate intrusions of intermediate composition, and the dioritic and granodioritic rocks are undoubted hybrids. The only uncertainty concerns the basic end-member of the series. Even the least-altered basalt xenoliths have suffered too much metamorphism to enable one to recognize the variety of basalt originally present. Accordingly, all three varieties of basalt occurring in other parts of the Complex have been plotted, together with the average of their compositions.

(b) *Major elements* (*Table* 1*a*)

These show the expected straight-line variation (Fig. 3). It is interesting to note in this connection that if the field evidence had been misinterpreted, which could very easily have happened if the basalt xenoliths had been more completely digested, a sequence of "plutonic" rocks from eucrite to granite could be interpreted as an intrusive magmatic series. The variation diagrams might well be taken to support this erroneous conclusion, because they show smooth curves consistent with fractional crystallization (Fig. 2). Furthermore, when plotted

on a triangular diagram showing Mg—Fe·· + Fe···—Alk and Ca—K—Na (Fig. 1), the curves are not markedly different from those of the tholeiitic British (and Icelandic) Tertiary rocks (Nockolds and Allen, 1955, p. 38). It appears, therefore, that reasoning from the similarity of curves on variation diagrams to identity of origin is not always justified.

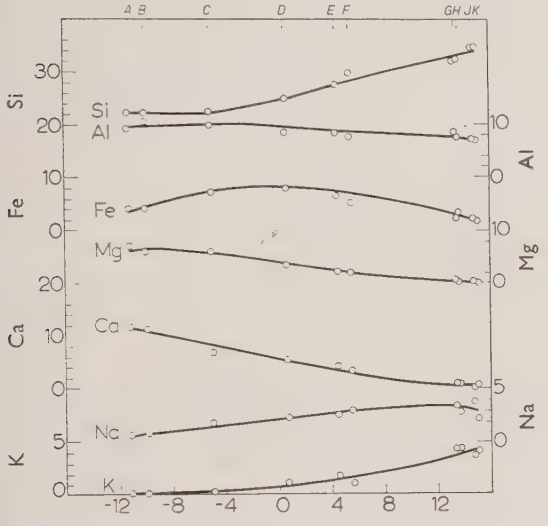

Fig. 2. Variation diagram showing principal cations plotted against [($\frac{1}{3}$Si + K)—(Ca +M g)] for the coarse-grained calc-alkali rocks.

A, Eucrite (T-50), B, Eucrite (3), C, Gabbro (T-58), D, Diorite hybrid (Y-9), E, Monzonite hybrid (P-10), F, Granodiorite hybrid (Y-20), G, Amphibole granite (P-17), Pyroxene granite (Y-15), J, Aplogranite, H, (K-47), K, Microgranite (Q-6).

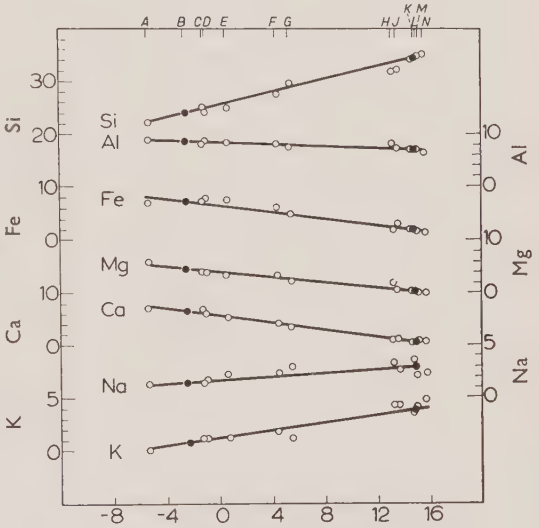

Fig. 3. Variation diagram showing principal cations plotted against [($\frac{1}{3}$Si + K)—(Ca + Mg)] for the basalt-granite hybrid series.

A, Basalt (L-11), B, Average basalt, C, Bronzite basalt (L-14), D, Basalt (W-3), E, Diorite hybrid (Y-9), F, Monzonite hybrid (P-10), G, Granodiorite hybrid (Y-20), H,Amphibole granite (P-17(, J, Pyroxene granite (Y-15), K, Aplogranite (K-47), L, Average granite, M, Microgranite (Q-6), N, Granophyre (O-12).

(c) *Minor elements* (*Tables* 1*a and* 1*b*)

The majority of trace elements also show straight-line variation, but there are one or two exceptions (Figs. 4, 5, and 6). The distribution of Cr and Ni is best represented by curves rising at the basic end and flattening towards the acid end. The curve for Li is anomalous. It is convex upwards, which indicates a concentration of Li in the hybrids greater than that in either the basaltic or granitic parent.

The explanation of these irregularities probably lies in (a) the variable distribution of trace elements within the group of basalts and the impossibility of telling which type of basalt has been assimilated by the intrusive granite to produce a particular hybrid; and (b), to a lesser extent, variations within the granite. Cr, Ni, Sr, and Ba all show variable concentration among the basalts. This variability is also shown in the ratios of trace elements to the major elements for which they generally substitute (Table 1b). Cr has been found to show the highest scatter of all trace elements studied. Ni follows, but to a lesser degree (Fairbairn,

Table 1a

	Volcanic phase					Intrusive phase								Hybrids				
	L-11	L-13	L-14	W-3	M-52	T-50	3	T-58	14	K-43	K-47	Q-6	O-12	Y-9	P-10	Y-20	P-17	Y-15
Si	234.10^3	235.10^3	251.10^3	240.10^3	355.10^3	223.10^3	221.10^3	223.10^3	216.10^3	219.10^3	342.10^3	347.10^3	353.10^3	249.10^3	277.10^3	297.10^3	319.10^3	323.10^3
Al	90.10^3	107.10^3	82.10^3	88.10^3	65.10^3	92.10^3	106.10^3	99.10^3	175.10^3	154.10^3	71.10^3	71.10^3	67.10^3	85.10^3	83.10^3	77.10^3	83.10^3	76.10^3
Ti	4.10^3	8.10^3	6.10^3	8.10^3	2.10^3	1.10^3	1.10^3	5.10^3	5.10^2	3.10^3	1.10^3	2.10^3	5.10^2	8.10^3	5.10^3	3.10^3	2.10^3	4.10^3
Fe···	32.10^3	21.10^3	16.10^3	40.10^3	16.10^3	12.10^3	8.10^3	19.10^3	7.10^3	12.10^3	8.10^3	2.10^3	4.10^3	24.10^3	19.10^3	20.10^3	14.10^3	23.10^3
Mg	60.10^3	27.10^3	39.10^3	39.10^3	2.10^3	70.10^3	59.10^3	60.10^3	4.10^3	14.10^3	1.10^3	1.10^3	2.10^3	35.10^3	23.10^3	20.10^3	6.10^3	3.10^3
Fe··	41.10^3	45.10^3	58.10^3	41.10^3	1.10^3	28.10^3	32.10^3	53.10^3	2.10^3	16.10^3	13.10^3	17.10^3	2.10^3	55.10^3	44.10^3	33.10^3	9.10^3	10.10^3
Na	14.10^3	19.10^3	16.10^3	18.10^3	21.10^3	7.10^3	9.10^3	18.10^3	12.10^3	16.10^3	38.10^3	22.10^3	25.10^3	24.10^3	26.10^3	31.10^3	34.10^3	28.10^3
Ca	72.10^3	77.10^3	68.10^3	64.10^3	3.10^3	118.10^3	114.10^3	70.10^3	120.10^3	105.10^3	3.10^3	8.10^3	8.10^3	55.10^3	43.10^3	36.10^3	11.10^3	12.10^3
K	1.10^3	10.10^3	12.10^3	12.10^3	5.10^3	7.10^2	5.10^2	4.10^3	6.10^2	3.10^3	37.10^3	42.10^3	48.10^3	13.10^3	18.10^3	12.10^3	44.10^3	44.10^3
P	(480)	(870)	(650)	(870)	(90)	(200)	(200)	(650)	(220)	(300)	—	—	—	(700)	—	—	—	—
B	—	5?	—	—	5	—	—	—	—	—	nd	nd	5	5	—	—	—	—
Ga	25	30	30	30	20	35	40	25	35	35	nd	nd	20	30	30	35	20	20
Cr	450	100	200	40	20	1500	575	40	20	25	nd	nd	2	40	5	15	—	—
V	250	200	200	275	—	125	125	200	50	100	nd	nd	—	200	100	100	55	20
Mo	—	—	—	—	—	—	—	—	—	—	nd	nd	—	—	—	—	—	—
Sn	100	25	—	35	—	—	—	—	100	—	nd	nd	—	30	—	—	—	—
Li	15	25	15	20	7	15	30	20	3	15	nd	nd	10	40	40	35	20	5
Ni	125	40	50	50	10	275	150	275	—	10	nd	nd	—	50	10	25	5	15
Co	40	25	30	20	—	45	40	55	—	10	nd	nd	—	25	10	15	5	—
Sc	30	15	40	—	—	60	60	15	—	—	nd	nd	—	15	—	—	—	—
Zr	70	125	100	150	400	—	—	70	—	10	nd	nd	125	150	125	300	200	1250
Mn	(930)	(1160)	(1400)	(1390)	(150)	(700)	(700)	(1200)	(150)	(460)	(300)	(400)	(100)	(1400)	(1200)	(1100)	(500)	(500)
Y	25	30	20	25	50	—	—	20	—	—	nd	nd	70	30	20	50	50	60
La	—	—	—	—	—	—	—	—	—	—	nd	nd	60	—	—	—	50	150
Sr	100	200	125	250	15	125	125	300	250	250	nd	nd	25	70	200	200	400	100
Pb	—	—	—	—	—	—	—	—	—	—	nd	nd	—	—	—	10	10	—
Ba	80	300	250	450	600	10	10	200	25	40	nd	nd	150	200	600	450	2250	1000
Rb	—	50	100	80	300	—	—	15	—	10	nd	nd	500	100	125	125	350	200
Cs	—	—	—	—	—	—	—	—	—	—	nd	nd	10?	—	—	—	10?	—
Fe	55	71	65	67	89	36	41	55	67	67	95	95	78	69	74	73	80	92
Mg	45	29	35	33	11	64	59	45	33	33	5	5	22	31	26	27	20	8
Fe	49	54	53	54	20	32	37	50	34	46	21	23	9	52	49	46	22	31
Mg	40	22	27	26	2	57	54	41	17	22	1	1	2	23	17	17	6	3
Alk	11	24	20	20	78	11	9	9	49	32	78	76	89	25	34	37	72	66
Ca	83	73	71	68	4	89	92	75	90	84	4	11	10	59	49	46	12	15
Na	16	18	16	19	30	6	7	20	9	13	49	30	31	26	30	39	38	33
K	1	9	13	13	66	5	1	5	1	3	47	59	59	15	21	15	50	52
Postn.	−5·3	−1·6	−1·1	−1·0	+15·9	−11·3	−9·9	−5·1	−5·2	−4·3	+14·7	+14·9	+15·7	+0·6	+4·4	+5·4	+13·3	+13·6

L-11 Basalt
L-13 Felspar-phyric basalt
L-14 Bronzite basalt
W-3 Tholeiitic basalt
M-52 Quartz-porphyry

T-50 Microeucrite
3 Microeucrite
T-58 Hypersthene microgabbro
14 Anorthosite

K-43 Anorthosite
K-47 Aplogranite
Q-6 Microgranite
O-12 Granophyre

Y-9 Diorite hybrid
P-10 Monzonite hybrid
Y-20 Granodiorite hybrid
P-17 Amphibole granite
Y-15 Pyroxene granite

Table 1b

	Volcanic phase					Intrusive phase					Hybrids				
	L-11	L-13	L-14	W3	M-52	T-50	3	T-58	14	K-43	O-12	Y-9	P-10	Y-20	P-17	Y-15
Ga × 1000/Al	0·3	0·3	0·4	0·3	0·3	0·4	0·4	0·2	0·2	0·2	0·3	0·3	0·4	0·4	0·2	0·3
Cr × 1000/Mg	7·5	3·7	5·1	1·0	10·0	21·4	9·7	0·7	5·0	1·8	1·0	1·1	0·2	0·7	—	—
V × 1000/Mg	4·2	7·4	5·1	7·0	—	1·8	2·1	3·3	12·5	7·1	—	5·7	4·3	5·0	9·2	6·7
Li × 1000/Mg	0·2	0·9	0·4	0·5	3·5	0·2	0·5	0·3	0·7	1·1	5·0	1·1	1·7	1·7	3·3	1·7
Ni × 1000/Mg	2·1	1·5	1·3	1·3	5·0	3·9	2·5	4·6	—	0·7	—	1·4	0·4	1·2	0·8	5·0
Co × 1000/Mg	0·7	0·9	0·8	0·5	—	0·6	0·7	0·9	—	0·7	—	0·7	0·4	0·7	0·8	—
Sc × 1000/Mg	0·5	0·5	1·0	—	—	0·9	1·0	0·2	—	—	—	0·4	—	—	—	—
Fe/Mg	1·2	2·4	1·9	2·1	8·5	0·6	0·7	1·2	2·0	2·1	4·1	2·3	2·8	2·6	4·0	11·0
Cr × 1000/Fe	6·2	1·5	2·7	0·5	1·2	37·5	14·0	0·5	2·2	0·9	0·3	0·5	0·1	0·3	—	—
V × 1000/Fe	3·4	3·0	2·7	3·4	—	3·1	3·0	2·8	5·5	3·6	—	2·5	1·6	1·9	2·3	0·6
Co × 1000/Fe	0·5	0·4	0·4	0·2	—	1·1	1·0	0·8	—	0·4	—	0·3	0·2	0·3	0·2	—
Sc × 1000/Fe	0·4	0·2	0·5	—	—	1·5	1·5	0·2	—	—	—	0·2	—	—	—	—
Y × 1000/Ca	0·3	0·4	0·3	0·4	16·7	—	—	0·3	—	—	8·7	0·5	0·5	1·4	4·5	5·0
Sr × 100/Ca	0·1	0·3	0·2	0·4	0·5	0·1	0·1	0·4	0·2	0·2	0·3	0·1	0·5	0·5	3·6	0·8
Sr × 100/Ca + K	0·1	0·2	0·2	0·3	0·03	0·1	0·1	0·4	0·2	0·2	0·04	0·1	0·3	0·4	0·7	0·2
Ba × 100/K	8·0	3·0	2·1	3·7	1·3	1·4	2·0	5·0	4·2	1·1	0·3	1·5	3·3	3·7	5·1	2·3
Rb × 100/K	—	0·5	0·8	0·7	0·6	—	—	0·4	—	0·3	1·0	0·7	0·7	1·0	0·8	0·4

Ahrens, and Gorfinkle, 1953, p. 45). This scatter, characteristically present within the basalt group, is due to the high sensitivity of these elements to fractionation and is to be expected amongst the Messum basalts. Li shows quite considerable variation within granites, having a range greater than that of other alkali

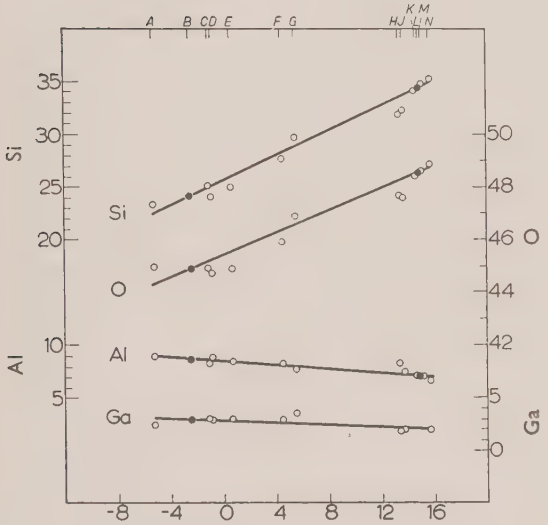

Fig. 4. Variation in silicon, oxygen, aluminium, and gallium for the basalt-granite hybrid series. Values in weight per cent, with Ga × 1000.

A, Basalt (L-11), B, Average basalt, C, Bronzite basalt (L-14), D, Basalt (W-3), E, Diorite hybrid (Y-9), F, Monzonite hybrid (P-10), G, Granodiorite hybrid (Y-20), H, Amphibole granite (P-17), J, Pyroxene granite (Y-15), K, Aplogranite (K-47), L, Average granite, M, Microgranite (Q-6), N, Granophyre (O-12).

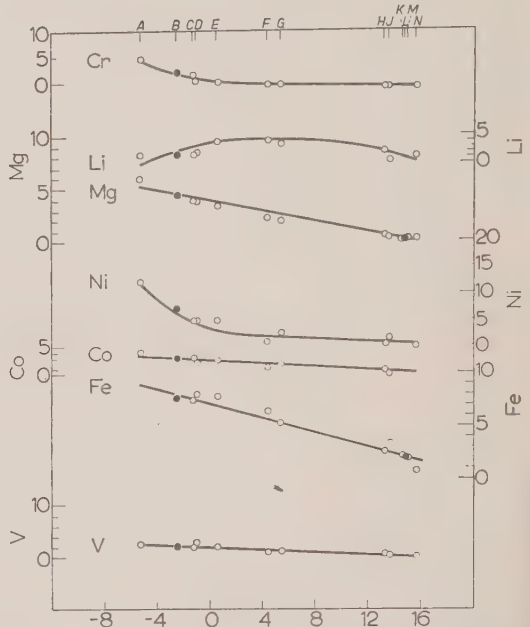

Fig. 5. Variation in chromium, lithium, magnesium, nickel, cobalt, iron, and vanadium for the basalt-granite hybrid series. Values in weight per cent, with Li, Ni, and Co × 1000; Cr and V × 100

A, Basalt (L-11), B, Average basalt, C, Bronzite basalt (L-14), D, Basalt (W-3), E, Diorite hybrid (Y-9), F, Monzonite hybrid (P-10), G, Granodiorite hybrid (Y-20), H, Amphibole granite (P-17), J, Pyroxene granite (Y-15), K, Aplogranite (K-47), L, Average granite, M, Microgranite (Q-6), N, Granophyre (O-12).

metals (Ahrens—private communication), and it is just possible that the hybrids were assimilation products of a later, Li-enriched, fraction. If not, the anomaly must remain unexplained at present.

Zr is abnormally concentrated in the pyroxene granite (Y-15), in which it is present in an amount of 0·125% as compared to 0·0125% in the normal granophyre (O-12) and a maximum of 0·03% in the other hybrids. Zr determinations on twenty-six Canadian granites showed a much lower variation of from 0·008% to 0·041% (Ahrens, 1954), but abnormal fluctuations in Zr content have been recorded as in the case of pyroxene-mica diorites from the Garabal Hill-Glen Fyne Complex and the Carn Chois intrusion (Nockolds and Mitchell, 1948, pp. 539 and 543, Nos. 12 and 26). Zr differs from the majority of trace elements in occurring mainly as crystals of zircon and only proxying for other cations to a very limited extent. It is thus more susceptible to sampling error than other trace

elements which are diadochic with the major elements and so better distributed through the rock.

The remaining trace elements show a perfectly normal and predictable distribution.

Calc-alkaline Intrusives and Cumulative Rocks

Into this group fall the gabbroic rocks, i.e. the microeucrites (T-50 and 3) and the hypersthene microgabbros (T-58) together with the anorthosites (14 and

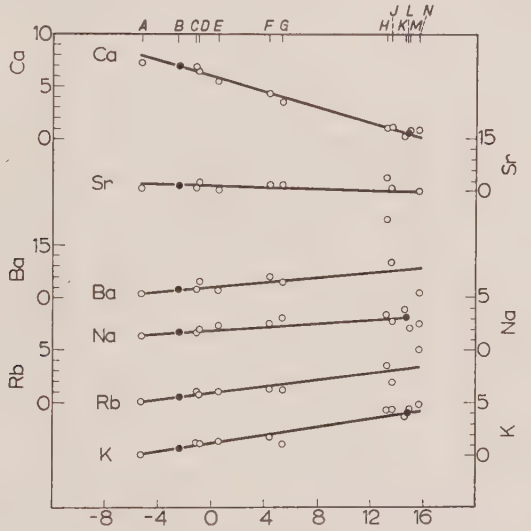

Fig. 6. Variation in calcium, strontium, barium, sodium, rubidium, and potassium for the basalt-granite hybrid series. Values in weight per cent, with Sr, Ba, and Rb × 100. A, Basalt (L-11). B, Average Basalt, C, Bronzite basalt (L-14), D, Basalt (W-3), E, Diorite hybrid (Y-9), F, Monzonite (P-10), G, Granodiorite (Y-20), H. Amphibole granite (P-17), J, Pyroxene granite (Y-15), K, Aplogranite (K-47), L, Average granite, M, Microgranite (Q-6), N, Granophyre (O-12).

K-43). All these rocks are intrusive into the original volcanics of the cone against which they are chilled. They represent the oldest rocks of the intrusive phase.

(a) *Major elements* (*Table* 1*a*)

Compared to the earlier Messum basalts, the eucrites are lower in Si, Ti, Na, K, and total Fe; higher in Al and Ca; and slightly higher in Mg. The eucrites also differ from the calc-alkali basalts, normal tholeiites, and alkali basalts listed by Nockolds (1953, 1954, 1956) in being lower in Ti, Na, K, and total Fe, and higher in Mg and Ca. They are also lower in Si than the calc-alkali basalts and tholeiites and higher in Al than the tholeiites. This chemical characteristic of low iron and alkalis and high lime and moderately high magnesium in the eucrites has already been commented upon (Mathias, 1956). It is thought to be due to assimilation of argillaceous material with consequent early precipitation of bytownite and to upward transfusion of alkalis. A simple cumulative origin without assimilation is unlikely as this would not account for the abnormally low alkalis.

The hypersthene microgabbro (T-58) is somewhat lower in Si and higher in Al than the early basalts, but otherwise fairly similar to them, particularly L-11. It shows slight differences in composition to both the calc-alkali and tholeiitic basalts, having lower Si and higher Mg than either, and lower alkalis than the calc-alkali basalts and higher Fe^{2+}, whereas it has lower Fe^{2+} and higher Al than the tholeiites. The composition is best explained in conjunction with the field relationships as due to normal processes of crystal fractionation of the eucritic magma, viz. iron and alkali enrichment. It is interesting to note that biotite appears at such an early stage of fractionation. This supports the view that the eucritic magma had been contaminated by assimilation of argillaceous rocks, as the latter are rich in K, and this would be likely to result in the early formation of biotite.

The anorthosites (14 and K-43) are representative respectively of unaltered and metasomatically altered types. The evidence for their cumulative origin by a process of gas-flotation has been considered already in some detail (Mathias, 1956). Anorthosite-14 is an exceptionally pure rock which contains over 97% by weight of bytownite. K-43 has the following modal composition:

Plagioclase 72·5%, pyroxene 2·6%, biotite + chlorite 9·6%, clinozoisite 13·3%, sphene 0·5%, and iron ore 1·5%.

(b) *Minor elements* (*Tables* 1*a and* 1*b*)

Ga is practically constant in the eucrites, gabbros, and anorthosites, where it substitutes for Al in the plagioclase felspar lattice. The Cr content of rocks is apt to be very variable, but even so the high content in the eucrite T-50 is difficult to explain, as T-50 is ore-free and is not particularly high in Fe or Mg. V shows little variation, except that it is low in the pure anorthosite, which is to be expected. The somewhat high V content of the hypersthene gabbro is doubtless due to its higher Fe content. Li, Ni, and Co substitute for Fe and Mg and are normally distributed, being absent or in low concentration in the anorthosites. Mn shows a maximum concentration in the hypersthene gabbro which has the highest Fe^{2+} content. Y is absent from the eucrites and anorthosites and only occurs in very small amounts in the basalts and the hypersthene gabbro. Its occurrence in the hypersthene gabbro rather than the other rocks which have a higher Ca content may possibly be due to the refractory nature of the Al bead in the arc (Ahrens, 1950). Sr is highest in the hypersthene gabbro, which is relatively low in Ca, but this anomaly may be partially accounted for by the higher K content of this rock. Ba and Rb show a normal distribution, substituting for K.

Dolerite-tinguaite Hybrid Series

(a) *Occurrence*

Within the inner ring-faulting at Messum, foyaites have been intruded near the centre of the Complex and their hypabyssal counterparts, tinguaites, occur as ring and radial dykes. These intrusions penetrate the down-faulted agglomerates and lavas, both basic and acid, and in places react with doleritic or basaltic material to produce a series of melanocratic fenitized rocks. The evidence for fenitization as opposed to magmatic intrusion of a series of alkaline rocks is that in the theralite, which is the only type which could possibly be interpreted as magmatic on the field evidence, there is clear proof of the replacement origin of the

nepheline, viz. plagioclase crystals are embayed and in places have the two ends completely separated by nepheline. Theralite outcrops as older ring-shaped screens in the central foyaite and probably represents former eucritic or hypersthene gabbroic sheets, fenitized, but otherwise similar to those occurring outside the inner ring-dyke system. The other melanocratic hybrids occur as marginal modifications of older basic dykes, as flows or as xenoliths caught up by the tinguaites.

The chief difficulty encountered in considering the chemistry of this series is the uncertainty as to the composition of the basic end-member. It is not always possible to tell what was the original composition of a hybrid, particularly a xenolithic hybrid, and even relict texture such as ophitic does not indicate the composition of the, presumably doleritic, parent. The analysed hybrids were taken from a variety of localities, and were almost certainly derived from different types of basaltic, doleritic, and gabbroic or eucritic parent material, all of these being readily available in the Complex. In the diagrams all the different mafic parental types have been plotted.

The intrusive material responsible for the fenitization was probably foyaite but as no analyses of uncontaminated foyaite are available, tinguaite analyses have been used instead, as being the hypabyssal counterpart of foyaite and chemically indistinguishable from it.

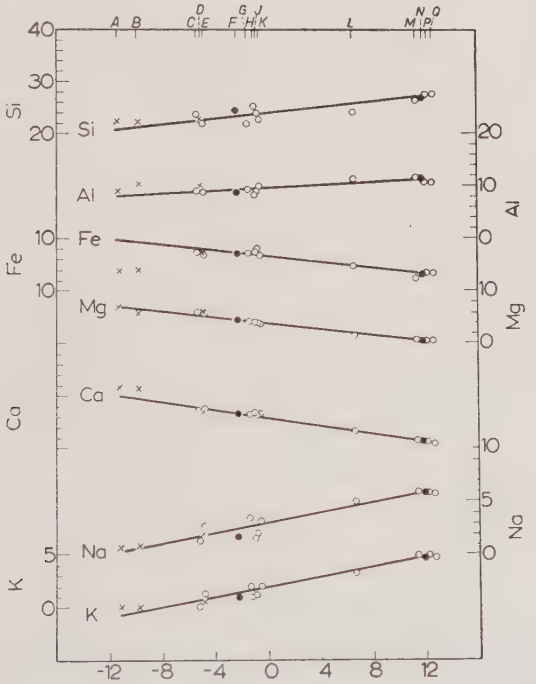

Fig. 7. Variation diagram showing principal cations plotted against [(⅛Si + K)—(Ca + Mg)] for the dolerite-tinguaite hybrid series.
A, Eucrite (T-50), B, Eucrite (3), C, Basalt (L-11), D, Gabbro (T-58), E, Theralite hybrid (G-9), F, Average basalt, G, Basalt hybrid (V-20), H, Bronzite basalt (L-14), J, Basalt (W-3), K, Basalt hybrid (G-11), L, Foyaite hybrid (E-17), M, Sodalite tinguaite (G-4), N, Average tinguaite, P, Ring-dyke tinguaite (E-1), Q, Ring-dyke tinguaite (G-23).

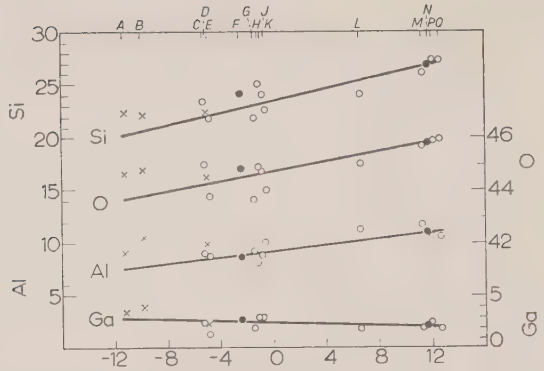

Fig. 8. Variation in silicon, oxygen, aluminium, and gallium for the dolerite-tinguaite hybrid series. Values in weight per cent, with Ga × 1000.

A, Eucrite (T-50), B, Eucrite (3), C, Basalt (L-11), D, Gabbro (T-58), E, Theralite hybrid (G-9), F, Average basalt, G, Basalt hybrid (V-20), H, Bronzite basalt (L-14), J, Basalt (W-3), K, Basalt hybrid (G-11), L, Foyaite hybrid (E-17), M, Sodalite tinguaite (G-4), N, Average tinguaite, P, Ring-dyke tinguaite (E-1), Q, Ring-dyke tinguaite (G-23).

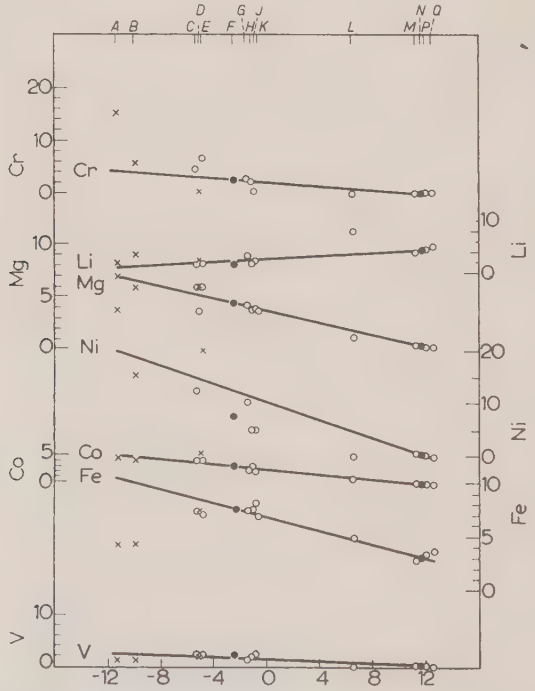

Fig. 9. Variation in chromium, lithium, magnesium, nickel, cobalt, iron, and vanadium for the dolerite-tinguaite hybrid series. Values in weight per cent, with Li, Ni, and Co × 1000, Cr and V × 100.

A, Eucrite (T-50), B, Eucrite (3), C, Basalt (L-11), D, Gabbro (T-58), E, Theralite hybrid (G-9), F, Average basalt, G, Basalt hybrid (V-20), H, Bronzite basalt (L-14), J, Basalt (W-3), K, Basalt hybrid (G-11), L, Foyaite hybrid (E-17), M, Sodalite tinguaite (G-4), N, Average tinguaite, P, Ring-dyke tinguaite (E-1), Q, Ring-dyke tinguaite (G-23).

(b) *Major elements* (*Tables* 1*a and* 2*a*)

The variation of the major elements when plotted against ($\frac{1}{3}$Si + K)—(Ca + Mg) is shown on Fig. 7. Considering the uncertainty regarding the composition of the basic parent, the deviation from straight-line variation is slight. Apart from the coarser-grained rocks (T-50, 3, and T-58) which show scattering, straight-line linkage is the most satisfactory representation.

In Fig. 7 points for the average tinguaite and the average basalt have been

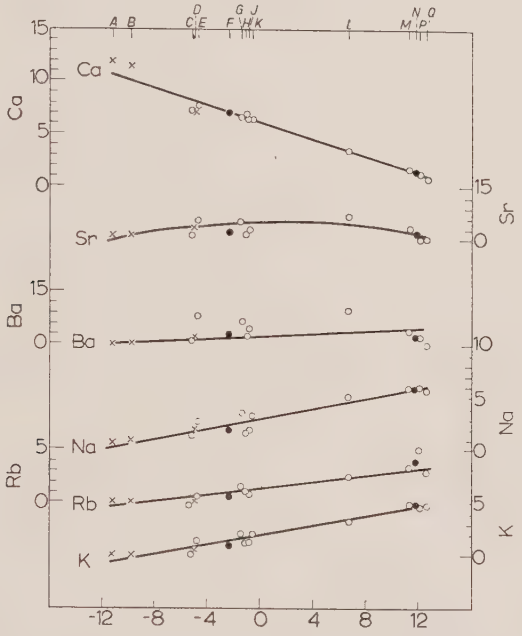

Fig. 10. Variation in calcium, strontium, barium, sodium, rubidium, and potassium for the dolerite-tinguaite hybrid series. Values in weight per cent, with Sr, Ba, and Rb × 100.
A, Eucrite (T-50), B, Eucrite (3), C, Basalt (L-11), D, Gabbro (T-58), E, Theralite hybrid (G-9), F, Average basalt, G, Basalt hybrid (V-20), H, Bronzite basalt (L-14), J, Basalt (W-3), K, Basalt hybrid (G-11), L, Foyaite hybrid (E-17), M, Sodalite tinguaite (G-4), N, Average tinguaite, P, Ring-dyke tinguaite (E-1), Q, Ring-dyke tinguaite (G-23).

joined, and it will be seen that the most scatter is shown by Si and the alkalis. Now, it is quite possible that some differential transfusion of alkalis has taken place whereby not the tinguaite magma only, but also alkaline solutions, were involved in the hybridization of the mafic rocks. This would account for the departures from straight-line variation and is in harmony with the known high solubility of alkaline silicates (Kennedy, 1955).

(c) *Minor elements* (*Tables* 1*a*, 2*a and* 2*b*)

The variation of these elements is generally of the straight-line type, but here again the early eucrites are nearly always aberrant. The values for Ni show considerable scatter and the distribution of Sr and Ba is best indicated by curves which are slightly convex upward. Sr and Ba are below the limit of sensitivity in the tinguaite G-23, whereas they are present in both the other tinguaites (Figs. 8, 9, and 10).

Table 2a

	Alkaline phase						Fenites and rheomorphic rocks								
	G-23	E-1	G-4	M-30	H-13	P-5	G-9	V-20	G-11	E-17	G-27	H-15	M-13	K-5	M-28
Si	274.10^3	273.10^3	262.10^3	292.10^3	209.10^3	214.10^3	219.10^3	219.10^3	225.10^3	242.10^3	271.10^3	305.10^3	330.10^3	353.10^3	349.10^3
Al	107.10^3	107.10^3	118.10^3	86.10^3	102.10^3	98.10^3	88.10^3	93.10^3	99.10^3	114.10^3	114.10^3	85.10^3	77.10^3	66.10^3	71.10^3
Ti	3.10^3	3.10^3	2.10^3	3.10^3	8.10^3	8.10^3	7.10^3	10.10^3	7.10^3	6.10^3	3.10^3	3.10^3	2.10^3	1.10^3	1.10^3
$Fe^{...}$	17.10^3	15.10^3	13.10^3	38.10^3	29.10^3	26.10^3	16.10^3	16.10^3	11.10^3	18.10^3	10.10^3	15.10^3	16.10^3	21.10^3	14.10^3
Mg	5.10^3	5.10^3	6.10^3	4.10^3	38.10^3	48.10^3	60.10^3	43.10^3	38.10^3	14.10^3	4.10^3	3.10^3	2.10^3	1.10^3	2.10^3
$Fe^{..}$	19.10^3	18.10^3	14.10^3	13.10^3	38.10^3	43.10^3	54.10^3	57.10^3	57.10^3	32.10^3	14.10^3	22.10^3	4.10^3	1.10^3	1.10^3
Na	57.10^3	58.10^3	60.10^3	41.10^3	52.10^3	38.10^3	27.10^3	35.10^3	33.10^3	50.10^3	58.10^3	42.10^3	41.10^3	29.10^3	28.10^3
Ca	8.10^3	13.10^3	17.10^3	19.10^3	66.10^3	66.10^3	76.10^3	65.10^3	64.10^3	35.10^3	18.10^3	9.10^3	8.10^3	1.10^3	2.10^3
K	47.10^3	46.10^3	49.10^3	36.10^3	22.10^3	18.10^3	13.10^3	21.10^3	20.10^3	33.10^3	46.10^3	45.10^3	40.10^3	38.10^3	42.10^3
P	(500)	—	—	(400)	(900)	(1100)	(400)	(2100)	(1900)	(2400)	—	(500)	—	(100)	(200)
B	—	5	—	nd	—	—	—	—	nd	—	—	nd	5	5	5
Ga	20	25	20	nd	10	15	15	20	nd	20	20	nd	10	25	20
Cr	7	—	15	nd	300	500	650	275	nd	10	—	nd	—	—	—
V	—	5?	15	nd	150	100	225	150	nd	50	5	nd	—	5	5
Mo	3	10	10	nd	—	3	—	3	nd	—	5	nd	—	—	—
Sn	—	80	—	nd	—	—	40	—	nd	—	—	nd	30	75	—
Li	50	45	40	nd	25	30	15	30	nd	80	25	nd	45	50	15
Ni	—	3	5	nd	100	150	200	100	nd	—	—	nd	5	5	—
Co	—	—	—	nd	30	30	40	25	nd	10	—	nd	—	—	—
Se	—	—	—	nd	—	—	20	—	nd	—	—	nd	—	—	—
Zr	200	350	175	nd	100	70	125	150	nd	150	150	nd	500	650	150
Mn	(2000)	(1600)	(1000)	(1900)	(1600)	(1700)	(1400)	(1500)	(1900)	(1800)	(1100)	(2000)	(200)	(200)	(200)
Y	35	60	20	nd	25	20	25	20	nd	30	30	nd	60	35	30
La	60	100	50?	nd	—	—	—	—	nd	50?	60	nd	150	—	100
Sr	—	30	350	nd	1500	1500	500	500	nd	700	350	nd	5	5	30
Pb	—	—	20	nd	—	—	—	—	nd	—	—	nd	—	—	—
Ba	—	200	400	nd	1000	800	800	650	nd	1000	1200	nd	100	20	400
Rb	300	500	350	nd	100	100	50	150	nd	250	300	nd	450	600	300
Cs	—	—	10?	nd	—	—	—	—	nd	—	—	nd	—	—	—
Fe	88	87	81	93	63	59	54	63	65	78	86	92	91	96	88
Mg	12	13	19	7	37	41	46	37	35	22	14	8	9	4	12
Fe	25	23	19	39	37	40	41	43	43	34	19	29	19	25	17
Mg	3	4	4	3	22	28	35	25	24	9	3	2	2	1	2
Alk	72	73	77	58	41	32	24	32	33	57	78	69	79	74	81
Ca	7	11	14	20	48	54	65	54	55	30	15	9	9	1	3
Na	51	50	47	43	37	31	23	29	28	42	47	44	46	43	39
K	42	39	39	37	15	15	12	17	17	28	38	47	45	56	58
Postn.	+12·5	+11·9	+11·2	+11·0	−1·4	−2·5	−5·0	−1·5	−0·7	+6·5	+11·3	+13·5	+13·9	+15·3	+15·4

G-23 Ring-dyke tinguaite
E-1 Ring-dyke tinguaite
G-4 Sodalite tinguaite
M-30 Syenite-porphyry
H-13 Olivine nephelinite
P-5 Olivine tephrite
G-9 Gabbro hybrid
V-20 Basalt hybrid
G-11 Basalt hybrid
E-17 Foyaite hybrid
G-27 Leucocratic foyaite hybrid
H-15 Syenite hybrid
M-13 Rheomorphic nordmarkite
K-5 Rheomorphic granite
M-28 Rheomorphic granite

Table 2b

	Alkaline phase					Fenites and rheomorphic rocks						
	G-23	E-1	G-4	H-13	P-5	G-9	V-20	E-17	G-27	M-13	K-5	M-28
Ga × 1000/Al	0·2	0·2	0·2	0·1	0·1	0·2	0·2	0·2	0·2	0·1	0·4	0·3
Cr × 1000/Mg	1·4	—	2·3	7·8	10·4	10·8	6·4	0·7	—	—	—	—
V × 1000/Mg	—	1·0	2·3	3·9	2·1	3·7	3·5	3·6	1·2	—	5·0	2·5
Li × 1000/Mg	10·0	9·0	6·1	0·6	0·6	0·2	0·7	5·7	6·2	22·5	50·0	7·5
Ni × 1000/Mg	—	0·6	0·8	2·6	3·1	3·3	2·3	—	—	2·5	5·0	—
Co × 1000/Mg	—	—	—	0·8	0·6	0·7	0·6	0·7	—	—	—	—
Sc × 1000/Mg	—	—	—	—	—	0·3	—	—	—	—	—	—
Fe/Mg	7·2	6·7	4·5	1·8	1·4	1·2	1·7	3·6	6·0	10·0	22·0	7·5
Cr × 1000/Fe	0·2	—	0·5	4·5	7·2	9·3	3·8	0·2	—	—	—	—
V × 1000/Fe	—	0·1	0·5	2·2	1·4	3·2	2·0	1·0	0·2	—	0·2	0·3
Co × 1000/Fe	—	—	—	0·4	0·4	0·6	0·3	0·2	—	—	—	—
Sc × 1000/Fe	—	—	—	—	—	0·3	—	—	—	—	—	—
Y × 1000/Ca	4·4	4·6	1·1	0·4	0·3	0·3	0·3	0·9	1·7	7·5	35·0	15·0
Sr × 100/Ca	—	0·2	2·0	2·3	2·3	0·7	0·8	2·0	1·9	0·1	0·5	1·5
Sr × 100/Ca + K	—	0·05	0·5	1·7	1·8	0·6	0·6	1·0	0·5	0·01	0·01	0·1
Ba × 100/K	—	0·4	0·8	4·5	4·4	6·1	3·1	2·9	2·6	0·2	0·1	0·9
Rb × 100/K	0·6	1·1	0·7	0·4	0·5	0·4	0·7	0·7	0·6	1·1	1·6	0·7

The trace-element composition of the Messum basalts is quite normal. All the elements fall within the range set by the Ontario diabases (Fairbairn, Ahrens, and Gorfinkle, 1953).

Comparisons for the tinguaites are less easy to find. Certain phonolites from Polynesia are reasonably close in composition, but have higher Al and Na and lower Fe^{2+}, Ca, and Mg (Nockolds and Allen, 1954, p. 270). The trace-element compositions of the Messum tinguaites are similar to the Polynesian phonolites except in the case of Li, Zr, La, Sr, Ba, and Rb, all of which are lower in the Messum tinguaites except Sr and Ba, which are erratic. Li and La apparently do not follow Fe, Mg, and Ca respectively, as the former are lower and the latter are higher in the tinguaites. Rb has a value approximately half that of the Polynesian phonolites, although the values for K are higher in two of the three phonolites. Sr varies from <10 to 350 p.p.m. and Ba from <10 to 400 p.p.m. in the tinguaites. In both cases the highest values are found in the sodalite tinguaite (G-4), which is also highest in Ca and K. Ba is considerably higher (400 p.p.m.) in the sodalite tinguaite compared to the highest value (30 p.p.m.) for the phonolites.

Quartz-porphyry-tinguaite Hybrid Series

(a) *Occurrence*

This series also occurs within the inner ring-dyke system of the core. In this case the intrusive foyaite or tinguaite has altered and metasomatized the original oversaturated lavas and tuffs of the Messum volcano, producing hybrid rocks of composition ranging from nordmarkite through syenite to leucocratic foyaite. This constitutes a variation of the well-known fenitization process, whereby granites are metasomatically altered *in situ* to rocks of syenitic composition; the altered rocks in this case being the volcanic equivalents of granite. The evidence for fenitization at Messum is of the same kind as that invoked for such classic districts as Alnö (von Eckermann, 1950) and Spitskop (Strauss and Truter, 1950), viz. relict structures in the fenites, shown by the continuation of the leucocratic and melanocratic facies of the migmatites with unaltered strike into the fenite zone at Alnö and a similar continuation of the textural characteristics of the Bushveld granite and granophyre into the red and white umptekite zone at Spitskop. The syenite fenite at Messum shows relict agglomerate structure and also old "resister" dykes of dolerite which have been altered and embayed but which still preserve their attitude virtually intact.

Petrologists differ in their ideas regarding the agent of fenitization. Alkaline emanations in one form or another are favoured by most, but von Eckermann (1950) believes that fenitization was accomplished by a carbonatite magma. Foyaitic magma was available at Messum, as is shown by the foyaite and tinguaite intrusions, but whether this magma or its residue was the fenitizing agent is a point which a study of the variation of the elements may help in deciding.

(b) *Major elements* (*Tables* 1*a and* 1*b; 2a and* 2*b*)

Fig. 11 shows the excellent straight-line variation in this series, which consists of the three tinguaites, together with their average, then a leucocratic foyaite hybrid, a syenite hybrid (or fenite), and finally the quartz-porphyry, M-52.

Three rheomorphic oversaturated veins, developed from the lavas at a late stage of the metamorphism, are included for comparison. They represent the silica-rich material expelled as a result of the fenitization and are of nordmarkitic and granitic composition. The evidence from the variation diagrams favours the view that fenitization was brought about by the foyaite magma rather than alkaline emanations, although alkaline solutions may well have acted as forerunners.

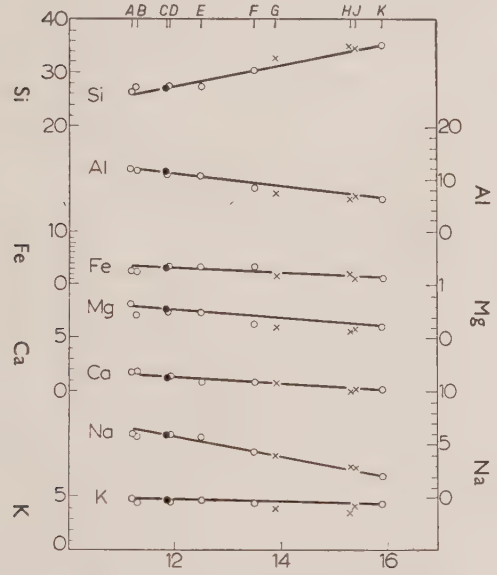

Fig. 11. Variation diagram showing the principal cations plotted against [(⅓Si + K)—(Ca + Mg)] for the quartz-porphyry-tinguaite hybrid series.

A, Sodalite tinguaite (G-4), B, Leucocratic foyaite hybrid (G-27), C, Average tinguaite, D, Ring-dyke tinguaite (E-1), E, Ring-dyke tinguaite (G-23), F, Syenite hybrid (H-15), G, Rheomorphic nordmarkite (M-13), H, Rheomorphic granite (K-5), J, Rheomorphic granite (M-28), K, Quartz-porphyry (M-52).

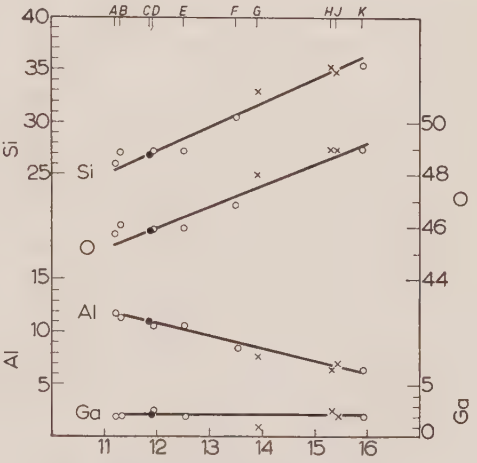

Fig. 12. Variation in silicon, oxygen, aluminium, and gallium for the quartz-porphyry tinguaite hybrid series. Values in weight per cent, with Ga × 1000.

A, Sodalite tinguaite (G-4), B, Leucocratic foyaite hybrid (G-27), C, Average tinguaite, D, Ring-dyke tinguaite (E-1), E, Ring-dyke tinguaite (G-23), F, Syenite hybrid (H-15), G, Rheomorphic nordmarkite (M-13), H, Rheomorphic granite (K-5), J, Rheomorphic granite) M-28), K, Quartz-porphyry (M-52).

(c) *Minor elements* (*Tables* 1*a and* 1*b; 2a and 2b*)

Ba and Li are the only minor elements which depart at all notably from straight-line variation, and in these the departure is not great (Figs. 13 and 14). Zr is very variable in the rheomorphic veins, but as these were probably emplaced in a partly solid condition, the amount of zircon present is likely to be erratic (Fig. 15).

Tinguaites from the neighbouring Complex of Okonjeje, which are very similar in mineralogy and geological setting, have a trace-element composition which closely parallels the Messum tinguaites, except that Sr is abnormally high in the Messum sodalite tinguaite (350 p.p.m.) compared to the tinguaites from Okonjeje,

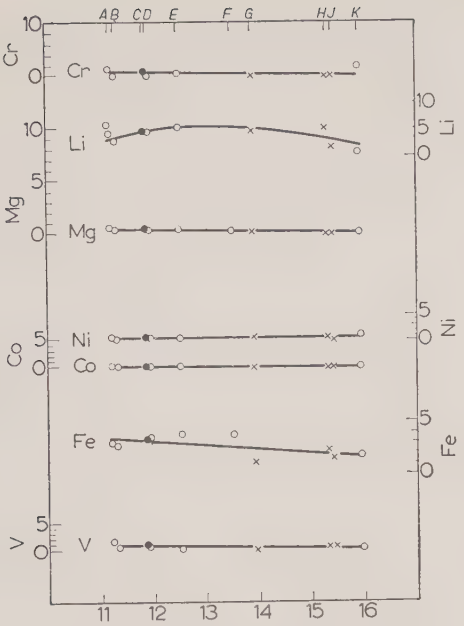

Fig. 13. Variation in chromium, lithium, magnesium, nickel, cobalt, iron, and vanadium for the quartz-porphyry-tinguaite series. Values in weight per cent, with Li, Ni, and Co × 1000, Cr and V × 100.

A, Sodalite tinguaite (G-4), B, Leucocratic foyaite hybrid (G-27), C, Average tinguaite, D, Ring-dyke tinguaite (E-1), E, Ring-dyke tinguaite (G-23), F, Syenite hybrid (H-15), G, Rheomorphic nordmarkite (M-13), H, Rheomorphic granite (K-5), J, Rheomorphic granite (M-28), K, Quartz-porphyry (M-52).

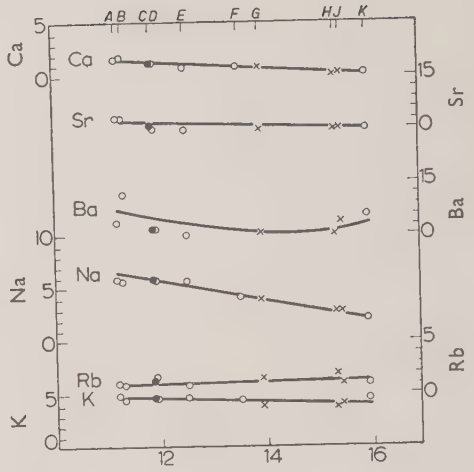

Fig. 14. Variation in calcium, strontium, barium, sodium, rubidium, and potassium for the quartz-porphyry-tinguaite hybrid series. Values in weight per cent, with Sr, Ba, and Rb × 100.

A, Sodalite tinguaite (G-4), B, Leucocratic foyte hybrid (G-27), C, Average tinguaite, D, Ring-dyke tinguaite (E-1), E, Ring-dyke tinguaite (G-23), F, Syenite hybrid (H-15), G, Rheomorphic nordmarkite (M-13), H, Rheomorphic granite (K-5), J, Rheomorphic granite (M-28), K, Quartz-porphyry (M-52).

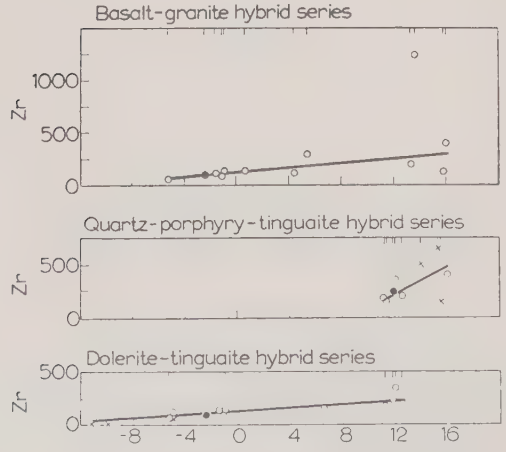

Fig. 15. Variation in zirconium in the basalt-granite series, the quartz-porphyry-tinguaite series, and the dolerite-tinguaite series. Values in p.p.m. (Lettering as in previous diagrams.)

which have a maximum of 25 p.p.m. (Simpson, 1954). Ba shows the same order of fluctuation in the two South-West African tinguaites and Rb the same rather low values compared to the Polynesian phonolites.

Late Alkaline Intrusives

The final phase of activity at Messum resulted in the emplacement of dykes of olivine nephelinite, olivine tephrite, and nephelinite. The two former types have been analysed and their trace-element composition determined (Table 2).

It is instructive to compare these rocks with the melanocratic hybrid G-9, which is theralitic in composition, as rocks rather similar to the theralite (andesine essexites) occur in the neighbouring complex of Okonjeje and are there considered to be of magmatic origin (Simpson, 1955). Trace-element composition is not likely to be conclusive in determining the origin of these rocks, but it may afford valuable contributory evidence. The position is that at Messum there occur two rock types, the theralite and the olivine tephrite, which are of closely related composition but which are thought to have different modes of origin. If this is a correct postulate, they might be expected to have a somewhat different trace-element content, whereas if the theralite were actually of magmatic origin it should show a close similarity to the olivine tephrite, as it would presumably have been derived from the same magma chamber. In comparing the trace-element composition of the two rock types, allowance must be made for a modal difference. The tephrite has a higher proportion of felspar and felspathoid and consequently higher alkalis and alumina and lower Si, Mg, and Ca than the theralite, which is a more melanocratic rock. It also has a higher ratio Fe^{3+}/Fe^{2+}, although total Fe is approximately the same.

The trace elements which show a significant difference in amount for the two rock types are Cr, V, Li, Ni, Co, Zr, Mn, Sr, and Rb. Of these, Li, Mn, Sr, and Rb are higher in the tephrite and the remainder lower. The lower values for V, Ni, Co, and Cr may perhaps be attributed to the lower Mg and Fe^{3+}, and the higher Rb to the higher K content, but this still leaves anomalous values for Li, Mn, and Sr. The latter, which is three times as abundant in the tephrite, is particularly hard to explain on a theory of similar magmatic source, and this high Sr content favours the view that the theralite had a different origin. In this respect it is interesting to note that the Okonjeje andesine essexite also shows a high Sr value (1350 p.p.m., compared to 1500 p.p.m. for the Messum theralite), but at Okonjeje the assumed parental rock type, the core gabbro, also shows a high Sr content, whereas the gabbroic rocks at Messum are all comparatively low in Sr, having a maximum value of 300 p.p.m.

References

Ahrens L. H. (1954) The lognormal distribution of the elements. *Geochim. et Cosmochim. Acta* **5,** 49–73.

Fairbairn H. W., Ahrens L. H., and Gorfinkle L. G. (1953) Minor element content of Ontario diabase. *Geochim. et Cosmochim. Acta* **3,** 34–46.

Kennedy G. C. (1955) Some aspects of the role of water in rock melts. *Geol. Soc. Amer.* Special Paper 62, 489–503

Korn H. and Martin H. (1954) The Messum Igneous Complex in South-West Africa. *Trans. Geol. Soc. S. Afr.* **57,** 83–124.

Mathias M. (1956) The petrology of the Messum Igneous Complex, South-West Africa. *Trans. Geol. Soc. S. Afr.* 59.

Nockolds S. R. and Mitchell R. L. (1948) The geochemistry of some Caledonian plutonic rocks: A study in the relationship between the major and trace elements of igneous rocks and their minerals. *Trans. Roy. Soc. Edin.* **61,** 533–575.

Nockolds S. R. and Allen R. S. (1953) The geochemistry of some igneous rock series: Pt. 1. *Geochim. et Cosmochim. Acta* **4,** 105–142.

Nockolds S. R. and Allen R. S. (1954) The geochemistry of some igneous rock series: Pt. 2. *Geochim. et Cosmochim. Acta* **5,** 245–285.

Nockolds S. R. and Allen R. S. (1955) The geochemistry of some igneous rock series: Pt. 3. *Geochim. et Cosmochim. Acta* **8,** 34–77.

Simpson E. S. W. (1954) The Okonjeje Igneous Complex, South-West Africa. *Trans. Geol. Soc. S. Afr.* **57,** 125–172.

Strauss C. A. and Truter F. C. (1950) The alkali complex at Spitskop, Sekukuniland, Eastern Transvaal. *Trans. Geol. Soc. S. Afr.* **53,** 81–130.

von Eckermann H. (1950) The genesis of the Alnö alkaline rocks, Rep. 18th Session Intern. Geol. Congress, Gt. Brit. **3,** 94–101.

Wager L. R. and Mitchell R. L. (1951) The distribution of trace elements during strong fractionation of basic magma –a further study of the Skaergaard intrusion, East Greenland. *Geochim. et Cosmochim. Acta* **1,** 129–208.

Geochimica et Cosmochimica Acta, 1957, Vol. 12, pp. 47 to 56. Pergamon Press Ltd., London

Hydrothermale und röntgenographische Untersuchungen an gesteinsbildenden Mineralen—I

Über ein geologisches Thermometer auf Grund von Untersuchungen an Biotiten

E. Hellner and R. Euler
Mineralogisches Institut der Universität, Marburg/Lahn

(*Received* 2 *August* 1956)

Abstract—Hydrothermal experiments (350°–800°C and 500–1000 bars) with natural biotites of the Albtal-granit (Schwarzwald, Germany) show, that from 500° upwards n_β and n_γ rise continuously; at 650° 2 V begins to enlarge.

The oriented growth of hematite in biotite is observed about 400°C and above.

Biotites of the paragneiss of the Gelbachtal (Schwarzwald) show a one-dimensional disordered stage of a three-layer type; these biotites order to a six-layer polymorph at the temperature of 600°C.

Cordierite appears in this paragneiss first at about 500°C. It seems that these experimental results could be useful in geologic thermometry.

In zahlreichen Publikationen der letzten Jahre wird von verschiedenen Autoren über Versuche mit dem Ziel berichtet, Kriterien für ein geologisches Thermometer zu finden. Eine zusammenfassende kritische Stellungnahme zu den einzelnen Methoden ist vor kurzem von Ingerson (1955) gegeben. In neuester Zeit sind weitere Arbeiten bekannt geworden, die weiter unten erwähnt werden.

Zwei Gesichtspunkte waren maßgebend dafür, das hydrothermale und röntgenographische Verhalten des Biotits zu untersuchen:

(1) Der Biotit ist Hauptgemengteil vieler Gesteine.

(2) Es wurde vermutet, daß die bei tiefer Temperatur entstandenen Biotite —entsprechend der Blattstruktur—eindimensionale Fehlordnung im Röntgendiagramm erkennen lassen würden, während die bei höherer Temperatur gebildeten Biotite einen geordneten Typ ausbilden würden.

(a) Ergebnisse der optischen Untersuchungen an hydrothermal behandelten Biotiten

Hydrothermale Untersuchungen an Biotiten sind von Roy (1949) durchgeführt worden. Roy teilte mit, daß bei hydrothermalen Versuchen bis zu 400°C die Biotite grün und gefleckt werden. Zwischen 400°C und 500°C bei 27 bis 70 bar sollen alle Glimmer zu amorphen hydratisierten Oxyden abgebaut werden. Temperaturen über 500°C und Drucke von 35 bis 700 bar "begünstigen die Stabilität der Glimmer."

Bei den hydrothermalen Versuchen, über deren Ergebnisse hier berichtet werden soll, wurden nur gesteinsbildende Biotite sowohl als isolierte Kristalle als auch im Gesteinsverband verwandt. Die Untersuchungen wurden in geschlossenen Bomben (Kennedy, 1954) bei 250–1000 bar und Temperaturen von 300–800° durchgeführt. Der Bombenraum hatte einen Durchmesser von 12 mm und war 24 mm lang. Die Versuchsdauer betrug 3–30 Tage. Mit Hilfe des von Kennedy (1950)

* Zum größten Teil auf der Tagung der Deutschen Mineralogischen Gesellschaft (DMG) in Aachen am 29.8.55 vorgetragen. (Fortschritte der Mineralogie, Bd. 34, (1956), 43).

berechneten spezifischen H_2O-Volumens wurden bei den jeweiligen Temperaturen die gewünschten Drucke eingestellt. H_2O war immer im Überschuß vorhanden (mehr als 50 Gew.-% bezogen auf die Probe).

Hydrothermal untersucht wurden isolierte Biotite, die aus dem Albtalgranit (Schwarzwald) herauspräpariert wurden, ferner Biotite im Gesteinsverband des

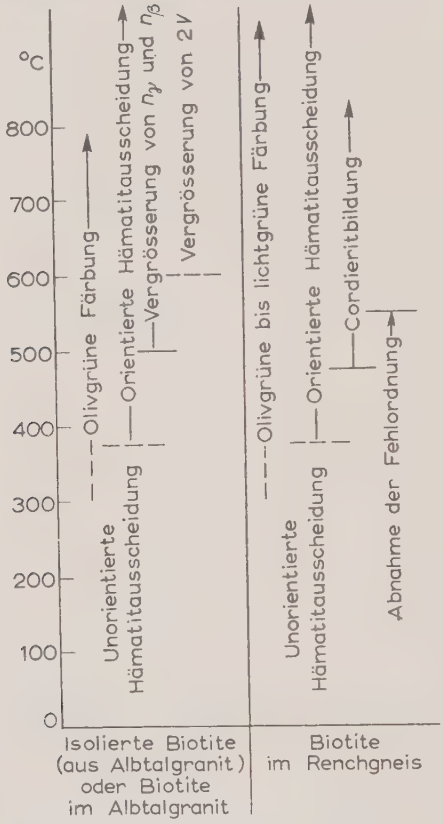

Abb. 1. Ergebnisse hydrothermaler Versuche an Biotiten.

Albtalgranits und Biotite im Gesteinsverband des Paragneises vom Gelbachtal bzw. Frohnbachtal (Blatt Oberwolfach, Schwarzwald). Die Paragneise enthalten als Hauptbestandteil neben Biotit auch Quarz und Plagioklas (etwa An_{40}). In Abb. 1 und Tab. 1 und 2 sind die erhaltenen Ergebnisse dargestellt.

Bis zu 500°C verhalten sich alle hier untersuchten Biotite gleich: Mit steigender Temperatur tritt zunehmend eine olivgrüne Verfärbung der Biotite auf. In einem Versuch bei 350°C wurde unorientierte Hämatitausscheidung beobachtet. Biotite, die bei 400°C oder bei höheren Temperaturen untersucht wurden, zeigen orientierte blättchenförmige Hämatitausscheidung; die Blättchennormale entspricht der [001]-Richtung des Hämatits, was durch röntgenographische Einkristallaufnahmen festgestellt wurde. Die Hämatitausscheidung wird zu höheren Temperaturen—auch über 500°C hinaus—stärker; dabei überwiegt bei höheren Temperaturen im Gesteinsverband des Albtalgranits (etwa bei 700°C und höher)

Tabelle 1. Hydrothermale Versuche mit isolierten Biotiten aus dem Albtalgranit (Schwarzwald), sowie Biotiten im Gesteinsverband des Albtalgranits

Versuch-Nr.	Temperatur in °C	Druck in bar	Zeit in Tagen	$n_\gamma \simeq n_\beta$	2 V	Weitere Beobachtungen
Ausgangsmaterial				$1{,}65_2$	0–15°	
TB V 2	350	500	3	$1{,}65_2$	0–15°	unorientierte Hämatitausscheidung
TB V 3	400	500	3	$1{,}65_2$	0–15°	Beginn der orientierten Hämatitausscheidung, rötlich durchscheinend. Größe der Blättchen bis $\sim 3\,\mu$, daneben noch unorientierte Hämatitausscheidung
TB V 4	450	500	3	$1{,}65_2$	0–15°	nur noch orientierte Hämatitausscheidung, Blättchen rötlich durchscheinend, Biotite z.T. schwach olivgrü verfärbt
TB V 5	500	500	3	$1{,}65_4$	bis 15°	orientiert ausgeschiedene Hämatitblättchen bis $5\,\mu$ groß; Biotite schwach olivgrün gefärbt
TB V 6	550	500	4	$1{,}65_8$	bis 15°	Hämatitblättchen bis zu $7\,\mu$ groß; Biotite etwas stärker zum Olivgrün verfärbt
TB V 7	600	500	4	$1{,}66_0$	bis 15°	Hämatitblättchen bis zu $15\,\mu$ groß; Biotite stärker zum Olivgrün verfärbt
TB V 8b	650	800	3	$1{,}66_4$	16–24°	Hämatitausscheidung auffallend größer, bis zu $15\,\mu$ groß; Biotite olivgrün
TB V 8a	600	500	4			
	+650	800	3	$1{,}66_4$	15–24°	wie 8b
TB V 9b	650	500	11	$1{,}66_4$	18–23°	Hämatitausscheidung stärker als in 8b und bis etwa $20\,\mu$ groß; Biotite olivgrün
TB V 9a	650	800	3			
	+650	500	11	$1{,}66_4$	16–24°	wie 9b
TB V 10b	700	800	4	$1{,}67_1$	18–33°	Dispersion der optischen Achsen, z.B. bei einem Biotit mit 2 V = 32° ergibt $2\,V_{rot} = 28°$, $2\,V_{blau} = 36°$, bei einem Biotit mit 2 V = 30° ergibt $2\,V_{rot}$ 26°, $2\,V_{blau}$ – 34°, sehr starke Hämatitausscheidung, bis $20\,\mu$ groß und undurchsichtig; Biotite olivgrün
TB V 24a	700	1000	7	$1{,}67_1$	30–33°	wie 10 b
TB V 10a	650	500	11			
	+700	800	4	$1{,}67_1$	29–34°	wie 10 b
TBgV 3	800	1000	12	$n_\gamma = 1{,}68_4$ $n_\beta = 1{,}68_0$	40–42°	Hämatitblättchen meist undurchsichtig und rhombenförmig, bis $150\,\mu$ groß, Biotite olivgrün

die Ausbildung des Hämatits als rhombenförmiges Blättchen mit den Winkeln 60° bzw. 120°, während bei tieferen Temperaturen die Hämatite meist als sechsseitige und dreiseitige Blättchen vorliegnn. Auf Abbildungen wird hier verzichtet, da eine ausführliche Beschreibung mit Abbildung in Rosenbusch-Mügge (1927, Seite 579 und Tafel XVII, Fig. 4) enthalten ist. Identisch mit diesen Beobachtungdn sind die Angaben von Roy (1949), daß die Biotite grünlich und gefleckt

Tabelle 2. Hydrothermale Versuche mit dem Renchgneis des Gelbachtales und des Frohnbachtales (Schwarzwald). Untersuchungsergebnisse an Biotiten

Versuch-Nr.	Temperatur in °C	Druck in bar	Zeit in Tagen	$n_\gamma \simeq n_\beta$	2 V	weitere Beobachtungen
Ausgangsmaterial				$1{,}64_0$	0°	braune Biotitblättchen
TBgV 6a	400	1000	30	$1{,}64_0$	0°	Hämatitblättchen bis zu 4 μ groß; Biotite schmutzig grün
TB V 15	500	1000	13	$1{,}64_5$	0°	Hämatitblättchen und Cordierit im Biotit; Biotit schmutzig grün
TB V 23	500	1000	15	$1{,}64_6$	0–3°	Hämatitblättchen wenig; Cordierit idiomorph; Biotit schmutzig grünlich-bräunlich
TB V 26	500	1000	21	$1{,}64_6$	0°	Hämatitblättchen, Cordierit idiomorph auch in Biotiten, Biotit schmutzig grün
TB V 22	550	1000	10	$1{,}64_6$	0–10°	Hämatitblättchen etwas größer. Cordierit, Biotite schmutzig grün
TB V 16	550	1000	30	$1{,}64_6$	0–15°	Hämatitblättchen; Cordierit; Biotite schmutzig grünlich
TB V 14	600	1000	10	$1{,}64_6$	0–10°	Hämatit; Cordierit; Biotite grünlich-bräunlich bis hell gelblich; hell gelbliche Biotite zeigen z.T. starke und feinkörnige Hämatitausscheidung
TB V 19	600	1000	13	$1{,}64_6$	0–15°	wie TB V 14
TBgV 6c	600	1000	30	$1{,}64_6$	0–10°	Hämatitblättchen bis 10 μ groß; Cordieritleisten gut im Biotit zu erkennen, Biotit schmutzig grünlich-bräunlich
TB V 13	700	1000	10	$1{,}64_6$	0–10°	olivgrüne Biotite mit wenig Hämatit, grünlich-gelbliche Biotite mit reichlich Hämatitausscheidung, außerdem graue Biotite.

(spotted) werden. Allerdings konnte von uns nicht beobachtet werden, daß zwischen 400° und 500°C ein Instabilitätsgebiet für Biotite unter den in Tab. 1 und 2 aufgeführten hydrothermalen Versuchsbedingungen besteht.

Oberhalb 500° wird ein unterschiedliches Verhalten einerseits bei isolierten Biotiten und Biotiten im Gesteinsverband des Albtalgranits und andererseits bei Biotiten im Gesteinsverband des Paragneises beobachtet.

Isolierte Biotite und solche im Gesteinsverband des Albtalgranits zeigen ab 600°C eine Vergrößerung des Winkels der optischen Achsen 2V; die Messungen

wurden mit dem U-Tisch durchgeführt und differierten für die einzelnen Temperaturen um $\pm 4°$:

unbehandelte Biotite aus dem Albtalgranit		2 V = 0–15°
650°C	800 bar	2 V = 20°
700°C	800 bar	2 V = 31°
800°C	1000 bar	2 V = 41°.

Ferner ist zu beobachten, daß die Brechzahlen n_γ und n_β ab 500° größer werden. Ein Unterschied zwischen n_γ und n_β konnte an Biotiten, die bis einschließlich 700°C getempert waren, nicht gemessen werden. Bei 800°C hydrothermal behandelte Biotite zeigen eine Differenz zwishen $n_\gamma = 1{,}68_4$ und $n_\beta = 1{,}68_0$.

Gessen wurden:

Temperatur	n_γ
Ausgangsmaterial aus Albtalgranit	$1{,}65_2$
500°C	$1{,}65_4$
550°C	$1{,}65_8$
600°C	$1{,}66_0$
650°C	$1{,}66_4$
700°C	$1{,}67_1$
800°C	$1{,}68_4$

Anders ist das Verhalten der Biotite, die im Gesteinsverband des Paragneises (Gelbachtal. Frohnbachtal) hydrothermal behandelt wurden. Im Ausgangsmaterial findet man nur einachsige Biotite. Diese Eigenschaft bleibt bei hydrothermaler Behandlung bis ungefähr 500° erhalten. Versuche bei 550°C zeigen, daß ein Teil der Biotite unverändert einachsig bleibt, während ein anderer Teil seinen Achsenwinkel bis auf 15° vergrößert. Biotite aus Paragneisproben, die bei 600° und 700°C hydrothermal getempert wurden, zeigen keine Vergrößerung des Achsenwinkels, im Gegensatz zu Biotiten des Albtalgranits.

Ein schwaches Ansteigen der Brechzahlen n_γ und n_β ist von 400° auf 500°C festzustellen; für Biotite im Ausgangsmaterial und aus Proben von 400°C ist $n_\gamma = 1{,}64_0$, für Biotite aus Proben von 500° ist $n_\gamma = 1{,}64_6$. Diese letztere Brechzahl haben auch Biotite, die bei höherer Temperatur im Paragneis hydrothermal behandelt wurden; sie zeigen also nicht ein Ansteigen der Brechzahl, wie es für Biotite des Albtalgranits ab 500°C gefunden wurde.

Von 450–500°C an aufwärts entsteht in den hydrothermal behandelten Proben des Paragneises Cordierit, der teils in Leisten im Biotit zu erkennen, teils in idiomorphen wasserklaren pseudohexagonalen Prismen auf den Biotiten ausgebildet ist. Die Cordieritleisten in den Biotiten sind so orientiert, daß die Richtung [001] des Cordierits in der Blättchenebene des Biotits liegt. Unter dem Mikroskop erkennt man an den aufgewachsenen Kriställchen, daß jedes dieser Prismen mit der Basis (001) ausgebildet ist und einen für Cordierit charakteristischen Durchkreuzungsdrilling darstellt, $n_\alpha = 1{,}546$–$1{,}549$, $n_\gamma = 1{,}555$–$1{,}558$. Auch röntgenographisch konnte der Cordierit durch Einkristallaufnahmen nachgewiesen werden (Größe des Kristalls 0,04 mm Länge). Im System $MgO—Al_2O_3—SiO_2—H_2O$

fanden Roy und Roy (1955) ebenfalls Cordierit ab 500°; Winkler gelang es 1955 bei hydrothermaler Metamorphose von illitischen Tonen, Cordierit nachzuweisen.

(b) Ergebnisse der röntgenographischen Untersuchungen

Röntgenographische Untersuchungen wurden nur an Biotiteinkristallen mit kristallreflektierter monochromatischer MoK_α- und FeK_α-Strahlung durchgeführt. Für die Herstellung der Aufnahmen standen Dreh-, Schwenk-, und Weissenbergkameras zur Verfügung.

Vollständig eindimensional fehlgeordnete Glimmer zeigen in Schwenk- und Drehaufnahmen um die Blättchennormale neben scharfen auch diffuse Gitterstäbe II. Art. Die scharfen Gitterstäbe sind bei hexagonaler Aufstellung mit $h-k \equiv 0$ (mod. 3) zu indizieren, haben also z.B. die Indizes (11.l) und (30.l), die diffusen Gitterstäbe haben Indizes der Form $h - k \not\equiv 0$ (mod. 3). Auf dem (30.l)-Stab entsprechen die Abstände der Schichtlinien I. Art für fast alle polytypen Glimmer einer Translationsperiode von $\sim$10 Å.* Alle hier untersuchten Biotite, deren Ergebnisse in Tabelle 3 zusammengestellt sind, zeigen für Reflexe auf dem (11.l)-Stab einen Schichtlinienabstand von 30 Å. Dabei ist as gleichgültig, ob der Biotit einen fehlgeordneten 3-Schichttyp, einen geordneten 3-Schicht- oder einen geordneten 6-Schichttyp ausbildet.†

Außer den beiden extremen Fällen, der vollständigen Ordnung und der vollständigen Fehlordnung sind beim Biotit Übergänge bekannt (z.B. Hendricks und Jefferson, 1939). Bei beginnender Ordnung treten Maxima auf den diffusen Stäben entsprechend dem Schichttyp auf, der angenähert wird; allerdings liegen bei beginnender Ordnung die schwach zu erkennenden Maxima auf den diffusen Gitterstäben noch nicht exakt auf den Schichtlinien I. Art, die für den anzunähernden Typ charakteristisch sind. Diese Verschiebung der sich neubildenden Maxima auf den diffusen Stäben ist aus der statistischen Theorie der Berechnung der eindimensionalen Fehlordnung abzuleiten [siehe Jagodzinski (1949) oder Hellner (1956)]. Bei beginnender Ordnung ist es daher oft schwierig, aus den schwach auftretenden Maxima auf den diffusen Stäben den Gittertyp zu bestimmen, der bei vollständiger Ordnung eingenommen wird. Mit zunehmender Ordnung werden die sich bildenden Maxima auf den diffusen Gitterstäben stärker und ordnen sich schließlich den Gitterstäben I. Art entsprechend dem sich ausbildenden Schichttyp exakt ein.

---

* Auf eine Ausnahme beim monoklinen 2-Schichttyp des Muskovits haben Hendricks und Jefferson (1939) hingewiesen, jedoch ohne die auftretenden Zwischenreflexe aus der Intensitätsberechnung erklären zu können.

† Die hier gegebene Definition für fehlgeordnete Glimmer unterscheidet sich von der von Yoder und Eugster (1954 und 1955) gegebenen Auffassung über den sogenannten 1 Md-Typ (disordered one-layer, monoclinic polymorph). Während der Drucklegung erschien außerdem eine Arbeit von Smith und Yoder (1956) über "Experimental and theoretical studies of the mica polymorphs." In unserer Arbeit ist nur zwischen 3-Schichttypen, 6-Schichttypen und Vielschichttypen unterschieden worden. Die Theorie zur statistischen Berechnung eindimensionaler Lagenfehlordnung fordert, daß der Vektor in Richtung der Fehlordnung *senkrecht* auf den beiden anderen Vektoren steht, die in der Ebene der geordneten Schichten liegen. Die Diskussion von fehlgeordneten und teilweise fehlgeordneten Glimmern erfordert daher die Einführung von polymorphen Typen, deren c-Achsen senkrecht auf der a- und b-Achse stehen. Es erscheint vom Standpunkt der Fehlordnung zweckmäßig, die von Hendricks und Jefferson (1939) sowie von Smith und Yoder (1956) aufgestellten polymorphen Formen auf Typen mit rechtwinkligen Achsen zu beziehen. In unserer Arbeit sind z.B. der 1M-, $2M_1$- und 3T-Typ als 3-Schichttypen zusammengefaßt; ihre Unterscheidung muß durch Intensitätsdiskussionen vorgenommen werden, worüber in einer weiteren Arbeit berichtet wird.

Es wurde erwartet, daß Biotite in Gesteinen, die bei tiefer Temperatur gebildet wurden, eindimensionale Fehlordnung im Röntgendiagramm erkennen lassen. In Tabelle 3 sind die Ergebnisse dieser röntgenographischen Untersuchungen für Biotite aus verschiedenen Gesteinen mitgeteilt.

Tabelle 3. Ergebnisse der röntgenographischen Untersuchungen an Biotiten aus verschiedenen Gesteinen

Name des untersuchten Gesteins	Fundpunkt	Beobachtungen aus Einkristallaufnahmen an den Gitterstäben $h - k \not\equiv 0$ (mod. 3) bezogen auf eine hexagonale Aufstellung
Para-Biotitgneis	Gelbachtal/Schwarzwald	Gitterstäbe nur diffus
Para-Biotitgneis	Schlehdornbruch/ Schwarzwald	diffuse Gitterstäbe mit ganz schwach angedeuteten Maxima
Granat-Disthen-Glimmerschiefer	Schiehallion/Schottland	z.T. stark diffuse Gitterstäbe mit schwach angedeuteten Maxima, die sich einem Vielschichttyp annähern; z.T. weniger stark diffuse Gitterstäbe mit Maxima, die sich einem 3-Schichttyp annähern
Granat-Glimmerschiefer	Loch Tummel/Schottland	Fehlordnung mit schwach erkennbaren Maxima, Bestimmung des Schichttyps nicht eindeutig (vielschichtiger Typ), z.T. Zuordnung zu einem 3-Schichttyp möglich
Para-Biotitgneis	Hauenstein/Schwarzwald	diffuse Gitterstäbe zeigen z.T. Maxima eines vielschichtigen Typs, der noch nicht eindeutig bestimmt werden kann, z.T. Maxima, die einem 6-Schichttyp zugeordnet werden können
Mischgneis	Hechtsberg/Schwarzwald	stark und weniger stark diffuse Gitterstäbe, Zuordnung zu einem Typ nicht immer eindeutig möglich, z.T. Zuordnung zu einem 6-Schichttyp
"Orthogneis" (Schapbachgneis)	Vogelsberg/Schwarzwald	z.T. diffuse Gitterstäbe mit ganz schwach erkennbaren Maxima, z.T. weniger diffuse Gitterstäbe mit Maxima, die einem 6-Schichttyp angehören
Albtalgranit	Tiefenstein/Albtal, Schwarzwald	geordneter 3-Schichttyp
Mambacher Hybridgranit	Kleines Wiesental/ Schwarzwald	geordneter 3-Schichttyp
Orthogneis	Dazio Grande-Schlucht, Antigoriotal, Tessin/ Schweiz	geordneter 6-Schichttyp
Metatexit	Straße Muggenbrunn-Todtnauberg, Punkt 955,0 O/Schwarzwald	geordneter 6-Schichttyp
Metatexit (biotitreicher Restbestand)	Schlehdornbruch am Urenkopf/Schwarzwald	geordneter 6-Schichttyp

Die (11.l)-Reflexe der Biotite aus sämtlichen in der Tabelle aufgeführten Gesteinen zeigen die Intensitätsabfolge eines 3-Schichttyps.

Biotite, die aus dem Para-Biotitgneis des Gelbachtales und des Schlehdornbruches (beide Schwarzwald) herauspräpariert wurden, zeigen auf Einkristallaufnahmen um die Blättchennormale scharfe Interferenzen für die Gitterstäbe II.

Art, die mit $h - k = 0$ (mod. 3) in hexagonaler Aufstellung zu indizieren sind. Die Intensitätsabfolge der (11.l)-Reflexe entspricht der eines 3-Schichttyps, wie es auch bei allen anderen hier untersuchten Biotiten der Fall ist. Die Gitterstäbe $h - k \neq 0$ (mod. 3) sind diffus, z.T. mit ganz schwach angedeuteten Maxima, die keinem Schichttyp zugeordnet werden können.

Die Biotite aus dem Granat-Disthen-Glimmerschiefer von Schiehallion und dem Granat-Glimmerschiefer von Loch Tummel (beide Schottland) zeigen z.T. stark diffuse Gitterstäbe mit schwach angedeuteten Maxima, z.T. weniger stark diffuse Gitterstäbe mit Maxima, die sich einem 3-Schichttyp annähern.

Biotite aus dem Para-Biotitgneis Hauenstein, dem Mischgneis Hechtsberg und dem Schapbachgneis Vogelsberg (alle Schwarzwald) zeigen z.T. stark diffuse, z.T. weniger stark diffuse Gitterstäbe. Auf den weniger stark diffusen Gitterstäben erkennt man in allen drei Fällen Maxima, die einem 6-Schichttyp zugeordnet werden können.

Biotite aus dem Albtalgranit, dem Mambacher Granit (beide Schwarzwald) ergaben auch für die Stäbe $h - k \neq 0$ (mod. 3) nur scharfe Interferenzen, die einem geordneten 3-Schichttyp entsprechen.

Biotite aus den Metatexiten von Todtnauberg und Schlehdornbruch (Schwarzwald) und aus dem Antigoriogneis (Tessin, Schweiz) zeigen einen geordneten 6-Schichttyp.

Auffallend ist, daß die Biotite des Antigoriogneises einen geordneten 6-Schichttyp ausbilden, während die Biotite des Schapbachgneises vom Vogelsberg (Schwarzwald), der ebenfalls als Orthogneis angesprochen wird, teilweise diffuse Gitterstäbe zeigen.

In diesem Zusammenhang schien es interessant, die hydrothermal behandelten Biotite röntgenographisch zu untersuchen. Die unbehandelten Biotite des Albtalgranits zeigen einen geordneten 3-Schichttyp im Röntgendiagramm; die zwischen 350° und 800°C in Druckbomben behandelten Biotite desselben Gesteins lassen keine Änderung bezüglich des geordneten Zustands und des Schichttyps erkennen.

Anders ist das röntgenographische Verhalten der hydrothermal behandelten Biotite des Paragneises vom Gelbachtal und Frohnbachtal. Aus Tabelle 3 geht hervor, daß die unbehandelten Biotite dieses Paragneises diffuse Gitterstäbe II. Art ohne zusätzliche Maxima zeigen. Bei einer Versuchsdauer von 7–10 Tagen erkennt man bei Temperaturen zwischen 500° und 600°C sowie 1000 bar Maxima auf den noch diffusen Gitterstäben, die auf Ausbildung eines 6-Schichttyps hindeuten. Nach einer Versuchsdauer von 30 Tagen bei 600° zeigen die Biotite nur noch scharfe Interferenzen, die einem 6-Schichttyp zugeordnet werden müssen. Bei 550° und 500°C 30 Tage lang getemperte Biotite sind noch schwach fehlgeordnet, weil auf den Stäben $h - k \neq 0$ (mod. 3) neben den Reflexen des 6-Schichttyps noch diffuser Untergrund zu erkennen ist. Um den Einfluß des Druckes untersuchen zu können, wurden Versuche bei 500° bzw. 600° und 250 bar durchgeführt. Die entnommenen Biotite sind in ihrem röntgenographischen Verhalten denen bei gleicher Temperatur und 1000 bar untersuchten gleich. Es besteht daher kein Einfluß des Druckes innerhalb des untersuchten Bereichs von 250–1000 bar.

Hieraus darf man folgern, daß Biotite mit einem fehlgeordneten 3-Schichttyp und ähnlicher chemischer Zusammensetzung bei 600°C einen geordneten 6-Schichttyp ausbilden und keine Fehlordnung mehr zeigen. Auffallend ist, daß der hier ausgebildete 6-Schichttyp auch in Biotiten der untersuchten Metatexite des Schwarzwaldes auftritt. Ob bei mehrmonatigen Versuchen und tieferen Temperaturen andere Typen außer dem hier ausgebildeten 6-Schichttyp angenähert werden —wie etwa ein 3-Schichttyp—soll in weiteren Versuchen geprüft werden.

Aus diesen Untersuchungsergebnissen zeigt sich, daß Biotite aus Orthogneisen keine Fehlordnung im Röntgendiagramm erkennen lassen dürfen. Unter Orthogneis wird hier ein Gestein verstanden, das durch Überprägung von Eruptivgesteinen granitischer bis dioritischer Zusammensetzung entstanden ist. Zeigen Biotite eines sogenannten "Orthogneises" jedoch Fehlordnung, so ist die Ortho-Natur dieses Gesteins im Sinne obiger Definition abzulehnen. Umgekehrt darf jedoch nicht geschlossen werden, daß, wenn im Röntgendiagramm keine eindimensionale Fehlordnung der Biotite erkennbar ist, der Gneis ein Orthogneis sein muß. Vielmehr kann es sich auch um einen Paragneis handeln, der auf 600°C oder darüber "aufgeheizt" wurde. Diese Aussagen gelten unter der Voraussetzung, daß sich eine Schmelze granitischer bis dioritischer Zusammensetzung erst oberhalb 600°C bildet, was auf Grund der Untersuchungen von Bowen (1954) und Tuttle (1955) gerechtfertigt erscheint.

Da die Biotite des "Orthogneises" vom Vogelsberg (Orginalfundpunkt des Schapbachgneises) teilweise eindimensionale Fehlordnung zeigen, muß geschlossen werden, daß die Bildungstemperatur unter 600°C gelegen hat; deshalb solltes sich hier nicht um einen Orthogneis im Sinne obiger Definition handeln. Weitere Untersuchungen über die Ortho-Natur der Schapbachgneise sind geplant. Interessant ist, daß auch Hoenes (1940, S. 246/47) bei einem Vergleich der Modalbestände von Schapbachgneisen, Granuliten und Graniten gezwungen ist, Zweifel an der Orthonatur des Schapbachgneises zu äußern.

Zur Natur des Antigoriogneises kann gesagt werden, daß die röntgenographische Untersuchung an Biotiteinkristallen (geordneter 6-Schichttyp) nicht gegen die Orthonatur des Gneises spricht.

Die Bildungstemperatur einiger Gneise kann schon verhältnismäßig gut aus vorliegenden Untersuchungen bestimmt werden. Z.B. zeigen Biotite aus dem Cordierit-Gneis von Gutach (Elzachtal, Schwarzwald) Hämatitausscheidung und gut erkennbare eindimensionale Fehlordnung. (Die 11.*l*-Reflexe lassen einen fehlgeordneten 3-Schichttyp erkennen.) Daraus darf man schießen, daß dieser Gneis sich bei Temperaturen zwischen 450° und 600° gebildet haben muß, denn erst bei 450–500°C beginnt der Stabilitätsbereich des Cordierits und ab 600°C verschwindet die Fehlordnung der Biotite.

Die Bildungstemperatur der untersuchten Metatexite dürfte bei 600°C oder höher gelegen haben, weil die Biotite keine Fehlordnung zeigen.

Zusammenfassung—Auf Grund der bisherigen Beobachtungen können folgende Kriterien für ein mögliches geologisches Thermometer herangezogen werden:

(1) Beginn der orientierten Hämatitausscheidung ab 350°C.
(2) Abnahme der eindimensionalen Fehlordnung des 3-Schichttyps mit steigender Temperatur; bei 600°C und 30-tägiger hydrothermaler

Temperung wurde keine Fehlordnung mehr nachgewiesen. Auseinem fehlgeordneten 3-Schichttyp bildet sich ein geordneter 6-Schichttyp.

(3) Bei 450–500°C und höher zeigt der hydrothermal behandelte Renchgneis aus dem Gelbachtal und Frohnbachtal Cordieritbildung. Daraus ist zu schließen, daß die Bildungstemperatur eines Gneises 450–500°C überschritten haben muß, wenn Cordierit vorliegt.

Isolierte Biotite und Biotite im Gesteinsverband des Albtalgranits zeigen ab 600°C eine Vergrößerung von 2 V und ab 500°C eine Vergrößerung von n_γ und n_β.

Wegen der Beobachtungen unter 1 und 2 kann der Schapbachgneis vom Vogelsberg(Schwarzwald) auf Grund der bisher durchgeführten Untersuchungen nicht als Orthogneis angesprochen werden. Die Beobachtungen unter (1), (2), und (3) gestatten, den Bildungsbereich des Cordieritgneises von Gutach (Schwarzwald) auf 450°–600°C festzulegen.

Herrn Prof. Dr. H. G. F. Winkler, Direktor des Instituts, danken wir für sein förderndes Interesse und anregende Diskussionen. Auch Herrn Prof. Dr. C. W. Correns, Göttingen, danken wir für wertvolle Anregungen. Die Deutsche Forschungsgemeinschaft unterstützte diese Arbeiten durch Bereitstellung von Personalmitteln für den einen von uns (R. E.) und durch eine Sachbeihilfe, wofür auch an dieser Stelle gedankt sei.

Literatur

Bowen N. L. (1954) Experiment as an aid to the understanding of the natural world. *Proc. Acad. Natural Sciences Philadelphia* **56,** 1–12.

Hellner E. (1956) Flußspat-Misch-Typen. *Z. Krist.* **107,** 99–123.

Hendricks S. B. und Jefferson M. E. (1939) Polymorphism of the micas. *Amer. Mineral.* **24,** 729–771.

Hoenes D. (1940) Magmatische Tätigkeit, Metamorphose und Migmatitbildung im Grundgebirge des südwestlichen Schwarzwaldes. *Neues Jb. Mineral. etc. Beil.-Bd.* **76,** *Abt. A.* 153–256.

Ingerson E. (1955) *Geologic thermometry in the crust of the earth.* Geological Society of America, Special Paper Nr. 62, 465–488.

Jagodzinski H. (1949) Eindimensionale Fehlordnung in Kristallen und ihr Einfluß auf die Röntgeninterferenzen. I. Berechnung des Fehlordnungsgrades aus den Röntgenintensitäten. II. Berechnung der fehlgeordneten dichtesten Kugelpackungen mit Wechselwirkungen der Reichweite 3. *Acta Cryst.* **2,** 201–207, 208–214.

Kennedy G. C. (1954) A note on the hydrothermal synthesis of single crystals of silicates and other rockforming minerals. *Amer. Min.* **39,** 654–660.

Rosenbusch-Mügge (1927) Mikroskopische Physiographie der petrographisch wichtigen Mineralien. I, 2 Stuttgart 1927.

Roy D. M. und Roy R. (1955) Synthesis and stability of minerals in the system $MgO—Al_2O_3—SiO_2—H_2O$. *Amer. Min.* **40,** 147–178.

Roy R. (1949) Decomposition and resynthesis of micas. *J. Amer. Ceram. Soc.* **32,** 202–209.

Smith J. V. und Yoder H. S. (195) Experimental and theoretical studies of the mica polymorphs. *Min. Mag.* **31,** 209–235.

Tuttle O. F. (1955) The origin of granite. *Scientific American* April 1955.

Winkler H. G. F. (1955) Hydrothermale Metamorphose von Tonen, I. *Naturwiss.* **42,** 460.

Yoder H. S. und Eugster H. P. (1954) Phlogopite synthesis and stability range. *Geochim. et Cosmochim. Acta* **6,** 157–185.

Yoder H. S. und Eugster H. P. (1955) Synthetic and natural muscovites. *Geochim. et Cosmochim. Acta* **8,** 225–280.

Geochimica et Cosmochimica Acta, 1957, Vol. 12, pp. 57 to 60. Pergamon Press Ltd., London

The content of tin in iron meteorites

John W. Winchester* and A. H. W. Aten Jr.
Institute for Nuclear Research, Amsterdam, Netherlands

(*Received* 10 *August* 1956; in revised form 27 *October* 1956)

Abstract—The tin contents of eight iron meteorites have been determined by colorimetric chemical analysis to be 20·2, 10·7, 8, 7·6, 6·3, 5, <1·0 and <0·8 p.p.m., giving an average of 6·7 p.p.m. tin in iron meteorites. Comparison with the palladium contents of iron meteorites indicates that the cosmic abundance of tin isotopes is not abnormally high because of the 50-proton closed nuclear shell.

Experimental

The tin content of eight iron meteorites† has been determined. Chemical analysis was colorimetric with chemical yield corrections by radioactive isotope dilution.

Samples of between 1 and 5 g were sawed from the meteorites with a steel saw, cleaned by etching in 12 M HCl, weighed, and dissolved in 12 M HCl. A small residue was dissolved in H_2SO_4 and HNO_3, HNO_3 was destroyed by adding HCl and fuming, and the two meteorite solutions were combined. Nearly carrier-free 9·5 day Sn^{125} tracer (Winchester, to be published) was added and tin was separated and determined by the procedure of Farnsworth and Pekola (1954) consisting of (a) distillation of volatile chlorides other than tin from H_2SO_4 at 155°–170°C in the presence of H_3PO_4 and hydrazine while slowly adding 12 M HCl, (b) distillation of tin at 140°C while adding 1:2 HCl-HBr mixture; and (c) destruction of HBr with H_2O_2 and determination of tin colorimetrically by measuring the absorption at 530 mμ of the tin(II) dithiol complex in sulphuric-acid solution containing thioglycolic acid and Teepol detergent. Finally, (d) the chemical yield of the analysis was determined by counting β-radiation in a solid source prepared from an aliquot of the colorimetric solution (Farnsworth and Pekola, 1954).

Colorimetry was performed with a Kipp colorimeter (type Engel) using a 530 mμ maximum filter and 4 cm path length cells. Beer's and Lambert's laws were found to be obeyed up to 16 γ/ml and 4 cm path length, and colour intensity was found to be independent of H_2SO_4 concentration within a factor of 2 of that used. Because quantitative distillation from the mixture containing precipitated meteoritic iron is difficult, chemical yields were usually between 80% and 90%. Transmissions usually lay between 60% and 90%, and a reagent blank was subtracted from all readings. Test analysis of a solution containg 32·0 γ of Sn gave 32·8 $\pm$ 1·5 γ, and of a standard-steel sample NBS 51A rated at 0·011% Sn gave 0·0114 $\pm$ 0·0004%.

The elements Se, Te, Ge, Tl, Au, and Re, not considered by Farnsworth and Pekola, were tested for possible interference and were found not to interfere. Se, the most serious offender, if ten times as abundant as Sn, will make the apparent

* Present Address: Department of Geology and Geophysics, Massachusetts Institute of Technology, Cambridge, Mass., U.S.A.

† The meteorites were obtained from Rheinisches Mineralien-Kontor Dr. F. Krantz, Bonn, Germany.

tin concentration 10% high, and cause a green discoloration in the red dithiol complex solution; this discoloration was never observed in the meteorite analysis.

Discussion

The measured tin concentrations are listed in Table 1. It is noteworthy that the nickel-poor ataxite and coarsest octahedrite (hexahedrite breccia) analyses

Table 1. Tin contents of iron meteorites

Meteorite[1]	Sn (p.p.m.) individual analyses	Selected value
1. Tocopilla (Cerros de Buey Muerto), H.	20·6 ± 1·5 19·9 ± 1·5	20·2
2. Locust grove, D(Ni-poor)	13·2 ± 0·6 7·3 ± 0·3 2·70 ± 0·15	8
3. Sao Juliao de Moreira, Ogg (Hb[2])	5·7 ± 0·2 3·9 ± 1·0	5
4. Cañon Diablo, Og	8·0 ± 0·4 6·1 ± 0·2 6·3 ± 0·3	6·3
5. Tamarugal (El Inca), Om	< 0·6 < 0·8	< 0·8
6. Henbury, Om	< 2·6 < 1·0	< 1·0
7. Toluca, Om	7·8 ± 0·3 7·3 ± 0·5	7·6
8. Muonionalusta, Of	9·1 ± 1·5 11·1 ± 0·4	10·7
		weighted average 6·7 p.p.m.[3]

(1) Classification by Prior (1953).
(2) Classified by Krantz as hexahedrite breccia.
(3) The frequencies of occurrence of meteorites of each class which have been used in computing the weighted average are: H 7·7%, D(Ni-poor) 4·4%, Ogg 3·9%, Og 15·8%, Om 33·2%, Of 10·8%. Other classes not represented include Off 4·0%, D(Ni-rich) 6·1%, brecciated octahedrites 2·6% and unclassified 11·7%. Almost the same value (7·2 p.p.m.) is found for the average tin content if all figures in the last column are given equal weight.

suggest nonuniformity. The medium octahedrites are singular in having either a medium concentration or no tin at all. Goldberg *et al.* (1951) find the gallium, palladium, and gold contents in six hexahedrites to be rather uniform, and also find that the gallium contents of medium octahedrites fall roughly into two groups, Toluca being high and Henbury low. There is, however, no general

correlation between gallium and tin concentration in the other meteorites. X-ray powder photographs were taken on test samples of meteorites 1, 4, 6, 7, 8 of Table 1, and taenite lines were found in the Of and both Om samples. No correlation between tin and taenite content is evident, however.

The average tin content of iron meteorites has been computed as shown in Table 1. PRIOR (1953) lists the 545 known iron meteorites according to class, and the frequency of occurrence of specimens of each class has been used to weight the individual tin values in computing the weighted average.

For comparison, reliable data are available for palladium and gold in 45 iron meteorites (GOLDBERG *et al.*, 1951), and a frequency weighted average gives 4·0 p.p.m. Pd and 1·5 p.p.m. Au. If we assume that tin, palladium, and gold reside exclusively in the metal phase,* then these relative concentrations should be the same as in average meteoritic matter, regardless of the silicate-metal ratio. In Table 2 are listed the abundances of separate nuclides (in arbitrary units)

Table 2. Relative nuclear mass abundances

Nuclide	Relative Abundances
Pd-105	0·85
Pd-106	1·02
Pd-108	1·01
Sn-117	0·43
Sn-118	1·36
Sn-119	0·48
Sn-120	1·86
Au-197	0·76

computed assuming terrestrial isotopic abundances and atomic weights, and as there are no other appreciably abundant nuclides of these mass numbers, they also represent mass abundances. The probable error in the tin abundances due to the spread of values in the meteorites analysed is about 30%.

The abundance difference between odd- and even-neutron nuclei is variable, being 20% in palladium and a factor of 3 in tin, but generally among middle-weight nuclides it is a factor of 2. The isotope abundance ratio of tin to palladium amounts to 1·6 for even-mass isotopes and to 0·5 for odd-mass isotopes. Therefore, it seems unlikely that tin isotopes have abnormally high cosmic abundances in spite of their magic proton number, which supports the conclusions of SUESS and UREY (1956).

Acknowledgements—This investigation is part of the research programme of the Foundation for Fundamental Research of Matter (F.O.M.), and was carried out with

* Considering the large probable error in the averages, the figure of 1·0 p.p.m. Sn in chondrites, as recently determined by Sandell (quoted by SUESS and UREY, 1956), does not seem to be inconsistent with this assumption, if chrondites contain about 9% free metal, as suggested by UREY (1952).

the financial support of the Organization for Pure Scientific Research (Z.W.O.). The authors are grateful to the crew of the Philips synchrocyclotron for deuteron irradiations and to Professor W. P. de Roever and Dr. H. Koning of Leiden University for the X-ray analyses. One of us (J. W. W.) wishes to give special thanks to the U.S. Educational Foundation in the Netherlands for a Fulbright grant.

References

Farnsworth M. and Pekola J. (1954) *Anal. Chem.* **26,** 735.
Goldberg E., Uchiyama A., and Brown H. (1951) *Geochim. et Cosmochim. Acta* **2,** 1.
Prior G. T. (1953) *Catalogue of Meteorites* (2nd ed). British Museum, London.
Suess H. E. and Urey H. C. (1956) *Rev. Mod. Phys.* **28,** 53.
Urey H. C. (1952) *The Planets* p. 204. Yale University Press, New Haven, Conn.

Geochimica et Cosmochimica Acta, 1957, Vol. 12, pp. 61 to 84. Pergamon Press Ltd., London

Separation of manganese from iron in sedimentary processes

Konrad B. Krauskopf
Stanford University, California

(*Received* 8 *June* 1956)

Abstract—Thermochemical data on compounds of manganese and iron are in general agreement with reported mineral associations, provided that the more complex mineral compounds, for which data do not exist, be assumed to have somewhat larger stability fields than their nearest simple chemical equivalents. The data show that the iron compounds to be expected in nature are uniformly less soluble than the corresponding manganese compounds, and that ferrous ion is more easily oxidized than manganous ion under any naturally occurring pH-*Eh* conditions. Thus, inorganic processes should always lead to precipitation of iron before manganese from a solution containing both metals, unless the Mn/Fe ratio is very high.

The oxidation of manganous and ferrous ions by atmospheric oxygen takes place by slow reactions which can be utilized as an energy source by bacteria. Selective oxidation and precipitation by different species of bacteria can lead to partial separation of the metals, but this is probably not a major factor in the formation of large, nearly pure deposits of manganese or iron compounds.

Selective dissolution of the metals from igneous rocks, a mechanism of separation often postulated in the literature, was tested by treating basaltic andesite with a number of solvents at temperatures ranging from 25 to 300°C. The ratios of Mn to Fe in the resulting solutions were all approximately the same as in the original rock, showing that this assumed process of separation is ineffective.

Isolation of manganese in solution can be accomplished by precipitating the iron first. This is most effectively done by adding alkali gradually to a solution containing both metals, keeping the solution in contact with atmospheric oxygen. The reaction can be demonstrated in the laboratory under conditions similar to those in nature by letting dilute acid percolate through crushed lava and then through limestone: iron dissolved from the lava is precipitated in the limestone, and the solution is left with a high Mn/Fe ratio. This suggests a possible explanation for the origin of many manganese deposits, especially those associated with lavas and tuffs, but it requires that iron oxide in amounts many times that of the manganese be deposited in the rocks through which the solutions have passed.

The close chemical similarity between manganese and iron is reflected geologically in their common association in rocks of all kinds. The association is especially marked in igneous rocks, where the ratio Mn/Fe seldom strays outside the limits 1/100 and 1/10, except in rare pegmatites. Sedimentary processes, where oxidation plays a larger role, lead to more effective separation of the two elements. The chemistry of iron and manganese during sedimentation is relatively simple and in its broad outlines is well understood, but the precise mechanism by which the two metals become separated remains mysterious. It is easy to see how manganese in solution may be deposited as carbonate or silicate where the environment is reducing, or as one of the several oxide minerals if oxygen is present, but why iron is not always deposited at the same time is much less clear. This is the essential puzzle in the geochemistry of manganese.

An explanation for the deposition of nearly iron-free manganese minerals can obviously be sought in two directions: either the original solution may have contained no iron, or some precipitation process may remove manganese alone from a solution containing both metals. The stumbling-block in precipitation processes has always been that iron should be more readily deposited than manganese; its carbonate, sulphide, silicate, and hydroxide are all less soluble than the corresponding manganese compounds, and it reacts with oxygen more readily, so that a solution containing both metals should give precipitates of both, either in the same deposit or in close proximity. This difficulty has led most geological writers to

assume solutions containing only manganese, generally derived from volcanic rocks, because manganese deposits are commonly found with such rocks and because springs in volcanic areas have been observed to deposit manganese compounds. This assumption is hardly an explanation, however; it does no more than push the essential process of separation underground, where direct observation is no longer possible.

Such questions about the origin of manganese deposits have been the subject of a voluminous literature. The essential chemistry and the chief problems were outlined in a paper by VOGT (1906) half a century ago; since that time much descriptive information has accumulated and the possible roles of bacteria and colloids in manganese deposition have been explored, but the separation of manganese from iron is still a troublesome question. The object of the present paper is less to solve the problem than to dress it up in modern language and to summarize pertinent work of the past fifty years. A possible hypothesis will be suggested, but its application to field occurrences must remain speculative pending the collection of more data.

The author is indebted to his colleagues, GEORGE A. THOMPSON and CHARLES F. PARK, for critical reading of the manuscript.

Eh-pH RELATIONS

It is common knowledge that neutral and acid solutions can hold large concentrations of Fe^{++} and Mn^{++};* that in alkaline solution these ions can be precipitated as hydroxides, carbonates, silicates, or sulphides, depending on what anions are present; that the divalent ions can be oxidized by moderately powerful oxidizing agents; that the oxidation by atmospheric oxygen is slow; that the oxidation is more complete in alkaline solution than in acid, and at any given acidity more complete for iron than for manganese; and that the products of oxidation are very insoluble oxides and hydroxides which can be represented by such formulas as Fe_3O_4, $Fe(OH)_3$, Fe_2O_3, Mn_3O_4, $Mn(OH)_3$, Mn_2O_3, and MnO_2.

These facts (except the slowness of the oxidation reactions) may be conveniently and quantitatively summarized by means of diagrams showing stability fields of possible compounds at different values of *Eh* and pH. Such diagrams have been extensively used by GARRELS and his co-workers (GARRELS, 1953; HUBER and GARRELS, 1953), and GARRELS' description of the method of constructing the diagrams makes a detailed explanation unnecessary here (see Appendix). For each metal, two diagrams are given, one showing stability fields for anhydrous oxides and the other showing fields for hydroxides; on each diagram stability fields for the simple sulphides, carbonates, and silicates are also indicated. Each line on a diagram is a boundary between the fields for a relatively more oxidized compound above and a more reduced compound below, the two compounds being named at

* Perhaps it should be pointed out that this statement is merely a generalization of the common assertion in geological literature that "manganese may be transported as the bicarbonate, sulphate, or chloride." To say that manganese (or iron) is present *as* such-and-such a compound puts the emphasis in the wrong place. It is immaterial what particular anions a solution contains—whether chloride, sulphate, bicarbonate, or rarer ones like nitrate, phosphate, or bromide—so long as none of the anions form insoluble compounds with the metal. The essential point is that the ions Fe^{++} and Mn^{++} are not precipitated by any of the anions commonly met with in natural solutions as long as the solution is not alkaline.

the ends of the lines. For example, from Fig, 1, at a pH of 7 and an *Eh* of 0·7 V, MnO_2 is the stable manganese oxide; at a pH of 9 and an *Eh* of 0·3 V, Mn_2O_3 is more stable.

Stabilities of the carbonates, sulphides, and silicates are of course dependent on assumed concentrations of the corresponding anions. Lines on the diagrams are

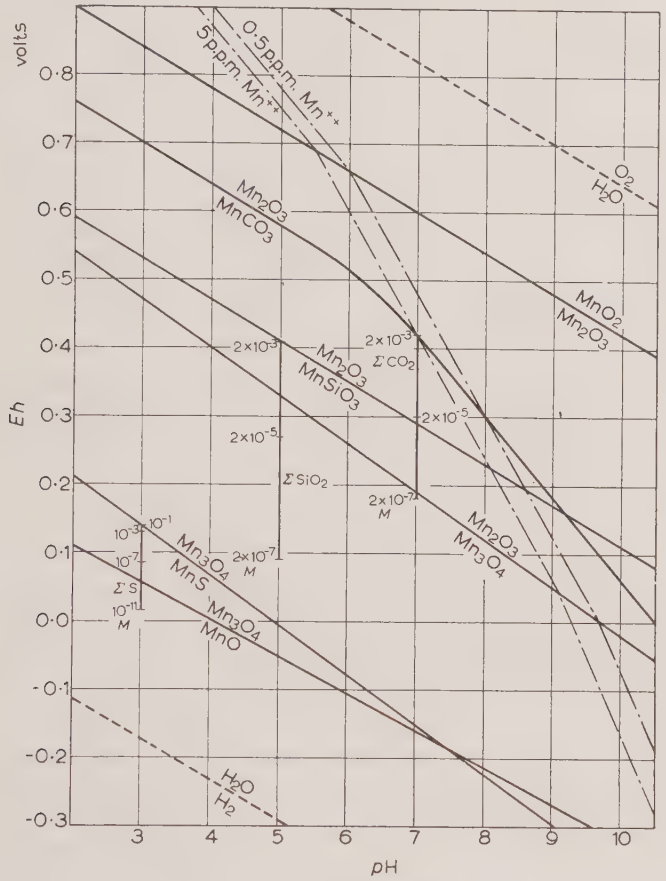

Fig. 1. *Eh*-pH diagram for anhydrous manganese compounds. Solid lines are boundaries of stability fields; each line separates the field of an oxidized form (above) from that of a reduced form (below). Cross-bars on vertical lines show positions of field boundaries at lower concentrations of carbonate, sulphide, and silica. Dashed lines are limits of possible redox potentials in water solution. Dash-dot lines are "isoconcentration" lines, drawn through points where the concentration of Mn^{++} in equilibrium with the oxides is 5 p.p.m. and 0·5 p.p.m. respectively.

drawn for (a) total carbonate = $CO_2 + HCO_3^- + CO_3^{--} = 0{\cdot}002$ M (equilibrium with atmospheric CO_2 at pH 8), (b) total sulphur = $H_2S + HS^- + S^{--} + SO_4^{--} = 0{\cdot}1$ M, and (c) total silica = chiefly $H_4SiO_4 = 0{\cdot}002$ M (amount soluble at 25°). Amounts by which these lines would be shifted by a decrease in concentration are indicated by the vertical lines with crossbars. For example, at pH 5·0 and *Eh* 0·5 V, $MnCO_3$ is the stable Mn compound if total dissolved carbonate is 0·0002 M, but Mn_2O_3 is stable if carbonate is much less than this. Note that the stability of

the sulphides is surprisingly little affected by changes in total dissolved sulphur unless the total is less than about 10^{-5} M. At a point like pH 7, *Eh* 0·0, below the lines for $MnCO_3$, $MnSiO_3$, and Mn_3O_4, the compound or compounds formed would depend on what anions are present: $MnCO_3$ if carbonate is in excess of silica, $MnSiO_3$ if silica is in excess, and Mn_3O_4 if both carbonate and silica are minor.

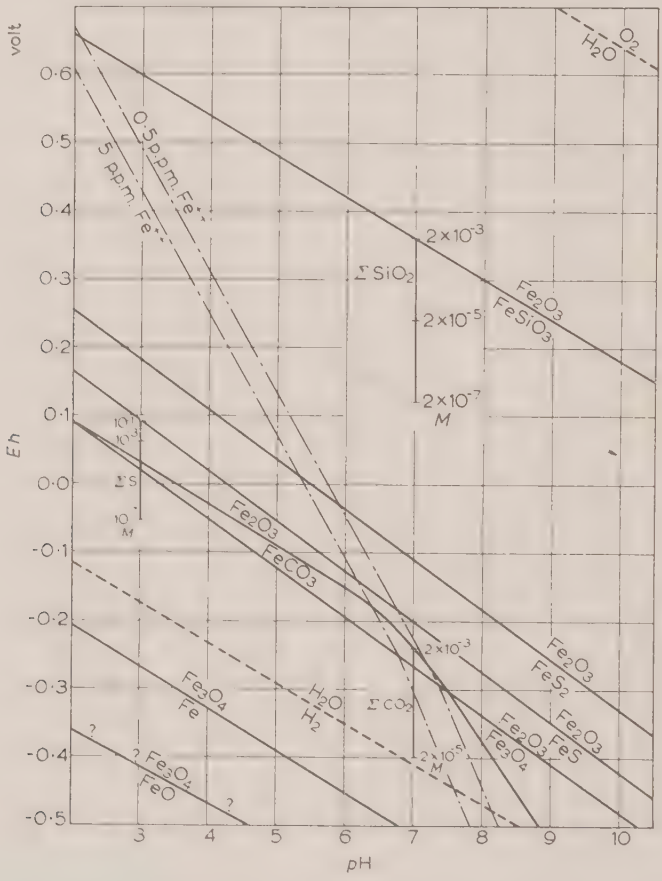

Fig. 2. *Eh*-pH diagram for anhydrous iron compounds. Symbols same as in Fig. 1. Question marks along Fe_3O_4-FeO boundary indicate that under these conditions FeO is unstable with respect to Fe and Fe_3O_4.

Also on the diagrams are shown (dashed lines) the theoretical limits of pH and Eh for natural aqueous solutions imposed by the oxidation of H_2O to O_2 and the reduction of H_2O to H_2. No oxidizing or reducing agent outside these limits can exist in contact with water, because the water would thereby be decomposed.

Theoretically, the equilibrium *Eh* of a solution in contact with atmospheric oxygen should be given by the upper dashed line. The "effective" *Eh*, however, appears to be somewhat less, because one of the steps in oxidation reactions involving O_2 is very slow. Measured *Eh* values in aerated water, both fresh and marine, cluster in the range 0·35–0·45 V for near-neutral solutions, instead of the theoretical 0·75–0·85 V (COOPER, 1937; ZOBELL, 1946; GARRELS, 1953; HUBER

and Garrels, 1953). Probably, as Cooper suggests, the effective *Eh* for slow geologic processes is somewhere between these ranges, but assigning a specific value for a given reaction is not feasible.

The diagrams become more useful if maximum concentrations of Mn^{++} are shown as well as the solid phases with which the Mn^{++} is in equilibrium. Two "iso-concentration lines" are shown on each diagram, one for 5 p.p.m. and one for 0·5 p.p.m. of each metal ion. These are plotted only for the oxides or hydroxides, in other words on the assumption that concentrations of sulphide, carbonate, and silicate are negligible. Manganese in natural solutions seldom has a concentration greater than 5 p.p.m., so that the diagrams actually have their major geologic interest only to the right of the 5 p.p.m. line.

The question inevitably arises with regard to such diagrams: How closely do the artificial compounds for which data are plotted correspond to natural minerals? In other words, are the diagrams only abstractions, of interest chiefly to a theoretical chemist, or can they be usefully applied to the more complicated substances and environments with which a geologist must deal? There is no simple answer, but a few predictions from the diagrams can be tested against natural occurrences, as explained below. It should be emphasized first, however, just how far the diagrams are from actual geologic situations. Figs. 3 and 4, showing stability fields for hydroxides, should be fairly accurate representations of precipitates from laboratory solutions. Figs. 1 and 2 include compounds closer to mineral formulas, but for several the resemblance is rather strained: MnO_2 can perhaps stand for pyrolusite, but hardly for psilomelane or wad; Mn_2O_3 is a poor substitute for braunite or manganite, as is Fe_2O_3 for limonite and $FeSiO_3$ for chamosite. The simple fact that the more complex substances exist in nature suggests that they are more stable than the artificial compounds on the diagrams, hence that their fields of stability would be larger than those shown. One other difficulty in applying this kind of diagram is that the stability fields are strictly accurate only at 25° and 1-atm pressure.

Mineral Associations

Despite the serious limitations just discussed, the diagrams show qualitative agreement with observations on the occurrence of manganese and iron minerals. The greater susceptibility of ferrous compounds to oxidation, the effect of increasing pH in making oxidation of both metals more complete, the fact that MnO is stable in natural environments while FeO is not, are all shown clearly by the diagrams. The iron diagram (Fig. 2) shows that any combination of the minerals hematite (or limonite), siderite, pyrite, magnetite, and iron silicate (e.g. chamosite) should be capable of stable coexistance at certain conditions of pH, *Eh*, and anion concentrations, or that any one should be capable of changing to another if conditions are altered. The manganese diagram, on the other hand, suggests that some mineral combinations should be impossible as *primary* associations: pyrolusite can form with no other mineral than braunite or manganite (if these have stability fields like that of Mn_2O_3); braunite and manganite should be able to coexist with hausmannite, rhodochrosite, or rhodonite (or some other manganese silicate), but not with alabandite or manganosite; alabandite and manganosite should not form at all except locally where solutions contain abnormal concentrations of Mn^{++}, and

should be accompanied by no primary oxide mineral except possibly hausmannite. A survey of the literature shows that these predictions are generally fulfilled, except that the relations of pyrolusite are uncertain because it is so commonly of secondary origin. (Two articles with especially complete descriptions of manganese mineral associations are THIEL (1924) and LEE (1955).) If psilomelane is considered as a

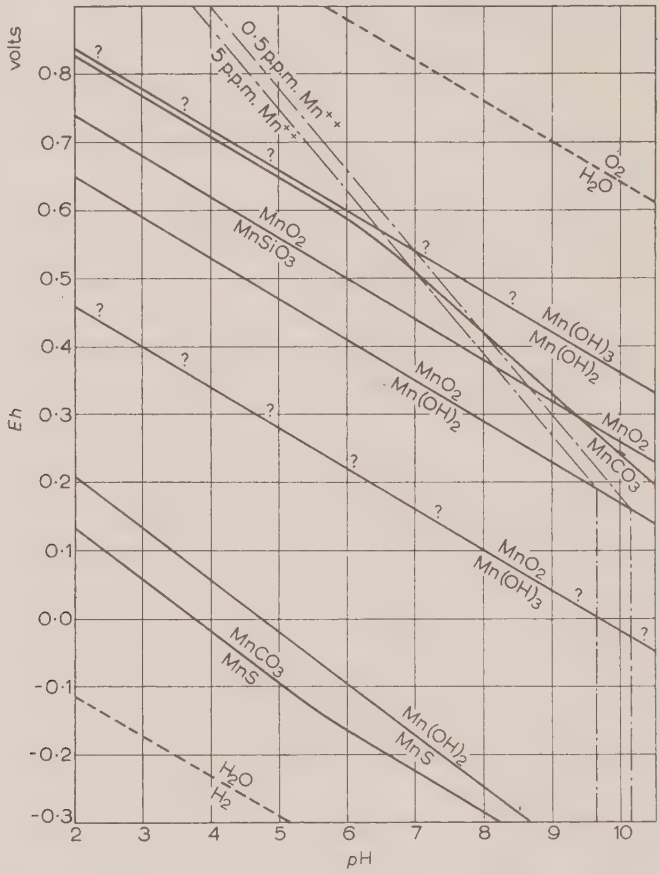

Fig. 3. *Eh*-pH diagram for manganese hydroxides. Symbols same as in Fig. 1. Question marks along stability boundaries for $Mn(OH)_3$ indicate that under these conditions $Mn(OH)_3$ is metastable.

variety of MnO_2, it appears to constitute an exception to the predictions in that the forbidden association psilomelane-hausmannite is well established, although not common; the best-documented example is that described by MISER (1922) at Batesville, Arkansas, where intimate mixtures of the two appear to be unquestionably primary. The anomaly is explainable by assuming that the relatively complicated structure of psilomelane is more stable in mildly oxidizing environments than is pyrolusite, so that its stability field extends well below that of plain MnO_2 and grazes the field of Mn_3O_4.

If the diagrams for manganese and iron are superimposed, the broad Fe_2O_3 field overlaps all the manganese fields down to hausmannite. In other words,

where iron and manganese occur together, hematite or limonite should be stable in the presence of any of the manganese oxides except manganosite (and even with this one if the concentration of sulphur is low). The field of pyrite partly overlaps the field of hausmannite, but is far below those of Mn_2O_3 and MnO_2. This does not support PARK's (1942) statement that pyrolusite and pyrite apparently formed

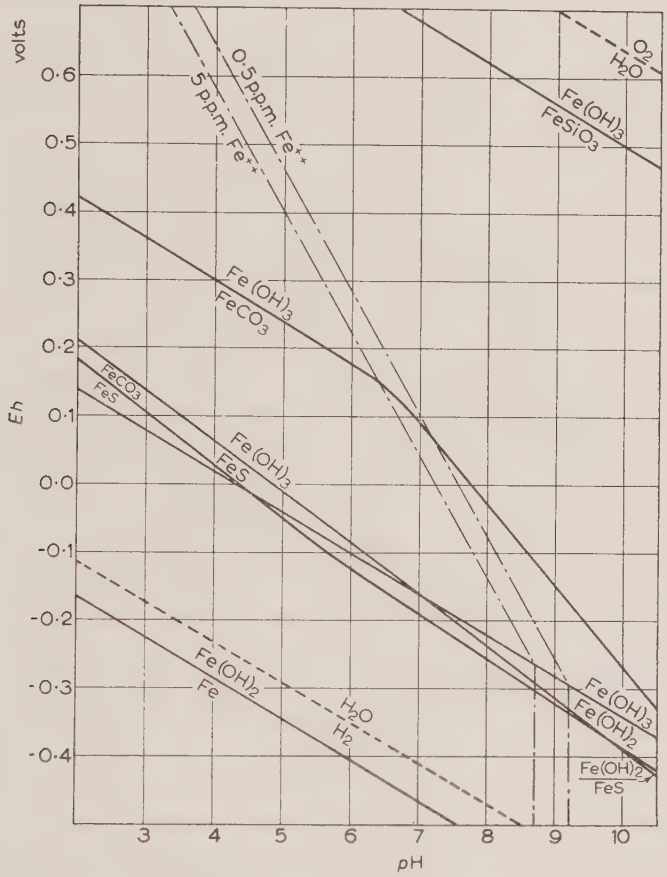

Fig. 4. *Eh*-pH diagram for iron hydroxides. Symbols same as in Fig. 1.

under the same conditions in a Cuban deposit; perhaps the discrepancy means that the stability fields for one or both minerals are broader at temperatures somewhat above 25°.

One other deduction from the diagrams can be checked with the known distribution of iron and manganese minerals. On Fig. 1 the iso-concentration line for 5 p.p.m. Mn^{++} crosses the pH range for normal sea-water at an *Eh* of about 0·2 V. and the line for 5 p.p.b. (or 0·005 p.p.m.) would cross at about 0·4 V. A concentration of 5 p.p.b. is only barely within the normal range for sea-water: THOMPSON and WILSON (1935) give for the normal range 0·7–10 p.p.b. Mn, and HARVEY (1949) suggests that the greater part of this is in filtrable particles rather than true solution. Hence, manganese cannot precipitate as an oxide in the sea

except where conditions are strongly oxidizing: ZOBELL (1946) gives −0·5 to 0·35 V as the usual range of *Eh* in marine sediments, and only in the extreme upper part of this range can manganese oxide form (except, of course, locally where manganese may be introduced in exceptionally large concentrations). Even the silicate and carbonate can precipitate from normal sea-water only where the concentrations of the anions or of Mn^{++} are abnormally high, and the precipitation of MnS is completely impossible. Fig. 2, on the other hand, shows the line for 5 p.p.m. Fe^{++} crossing the pH range of sea-water at an *Eh* of about −0·6 V, well below any *Eh* recorded or to be expected in the most reducing of marine environments. Hence, any of the possible iron compounds should be stable in contact with sea-water, Fe_2O_3 wherever conditions are at least mildly oxidizing, and the other compounds where conditions are reducing. In agreement with these predictions, the only manganese compound reported from present-day marine sediments is the dioxide, and this only from oxidizing environments, whereas iron is well known in the form of ferric oxide, pyrite, and glauconite, and less certainly as magnetite and siderite also.

Thus, Figs. 1 and 2, with reasonable modifications for compounds regarding which data are lacking, can be shown to fit most of the observed facts of occurrence and association of manganese and iron minerals. On the other hand, boundaries of the stability fields are so uncertain because of complex mineral compositions and possible temperature effects that the diagrams cannot be regarded as suitable for quantitative predictions.

It should be emphasized again that there is nothing original here in the diagrams or their interpretation. KRUMBEIN and GARRELS (1952) have published an iron diagram including Fe_2O_3, $FeCO_3$, and FeS, and this diagram has been discussed and used by several authors, notably HUBER and GARRELS (1953) and JAMES (1954). The demonstration that magnetite has a field of stability at ordinary temperatures is due to DELTOMBE and POURBAIX (1954) and to HUBER (1956). Manganese diagrams have been published by CHARLOT (1949), BLUMER (1950), and MOUSSARD, BRENET, JOLAS, POURBAIX, and VAN MUYLDER (1954). The diagrams in these papers differ from the ones presented here in that they show the particular compounds that would exist at equilibrium under specific conditions of *Eh*, pH, and concentrations of various anions. The intention here, in Figs. 1–4, is to present the relationships in more general fashion, outlining only the maximum extent of the stability fields under natural conditions and showing alternative precipitates that may form in response to various anion concentrations.

DISSOLUTION OF MANGANESE

The difficulty of precipitating manganese unaccompanied by the more insoluble compounds of iron is clearly shown by the data of Figs. 1 and 2. A possible way of circumventing the difficulty is to suppose that the original solution contained manganese with little or no iron, in other words that the process of dissolution by which the metals were leached out of the original rock was somehow extraordinarily favourable to manganese. Theoretically there is little reason to expect such differential dissolution from the primary minerals of igneous rocks, since the ions Mn^{++} and Fe^{++} have similar sizes and occupy similar positions in the structures of

ferromagnesian silicates. Nevertheless, it is widely accepted that manganese is dissolved more readily than iron (e.g. LINDGREN, 1933, p. 280; RANKAMA and SAHAMA, 1950, p. 647; GOLDSCHMIDT, 1954, p. 633). This idea needs examination.

For the faster dissolution of manganese, two authorities are often cited, VOGT (1906) and EMMONS (1911, p. 39). VOGT urges as a proof of preferential dissolution the common observation that the Mn/Fe ratio in soil-water is higher than in igneous rocks. He goes on to explain the more rapid dissolution as due to the fact that iron in igneous rocks occurs both in the difficultly soluble accessory oxides and in the ferromagnesian minerals, whereas manganese occurs only in the latter. VOGT may be right in assuming such a difference in susceptibility to weathering and a difference in Mn/Fe ratios between oxides and silicates, but only in extreme cases could these differences account for more than a few per cent difference in over-all solubility. The observation that soil-water has a higher Mn/Fe ratio than adjacent rock is more plausibly explained (LJUNGGREN, 1953) by early precipitation of iron in soil-forming processes than by differential solubility of original minerals.

EMMONS' statement has an apparently sounder basis. He quotes experiments by E. C. SULLIVAN in which samples of "white porphyry" from Leadville, Colorado, were subjected to the action of carbonic and dilute sulphuric acids; in two of the experiments iron and manganese were dissolved in roughly the same amounts, and in the others manganese was dissolved in excess of iron. The rock is not described except for the statement that it contained 0·8% Fe and 0·033% Mn, but the general description of the "white porphyry" given by EMMONS, IRVING, and LOUGHLIN (1927, pp. 43–46) leaves no doubt that it is an unusual petrographic type. Dark minerals are almost completely absent except for "very scarce" magnetite and an occasional trace of biotite; most of the rock is evidently much altered; scattered pyrite is abundant near ore bodies. Such a rock might well give an anomalous Mn/Fe ratio in a dilute acid solution, and is certainly not representative of the kind of igneous rocks commonly supposed to furnish manganese to ore deposits.

Thus the notion that manganese dissolves more readily than iron from igneous rocks rests on extremely flimsy evidence. To test the idea with a rock of composition closer to the andesites and basalts which are often found with manganese ores, a series of experiments was tried using a sample of Parícutin lava. This rock is a basaltic andesite collected from a flow active in late 1945, for which WILCOX gives (1954, p. 294, analyses 6–10) an average of 56·4% SiO_2, 5·23% Fe, and 0·09% Mn. Experiments were tried not only at room temperature, but at temperatures up to 220°: the solvents used include H_2CO_3, H_2SO_4, HCl, and sea-water; times of standing ranged from 1 to 8 days. The experiments with sea-water and HCl were tried in an effort to simulate conditions of alteration of basalt when moving lava enters the sea—conditions which have been suggested as peculiarly favourable for the formation of manganese ores (PARK, 1946; TALIAFERRO and HUDSON, 1943). Further experiments with the same end in view consisted of pouring molten basalt into sea-water and into sea-water plus HCl, and of passing vapours from boiling HCl through a mixture of basalt fragments and sea-salt at a temperature near 300°. Results of these various experiments are shown in Table 1.

The table shows that iron and manganese are extracted from basalt by all the

solvents tried, and that the combination sea-water plus HCl is particularly effective, but in no case was the ratio Fe/Mn in the resulting solution notably different from that in the rock. Extreme values obtained were 25 and 93, whereas the ratio in the rock itself is 58. Certainly nothing in these experiments gives any hint of a possible process whereby manganese can be dissolved out of a mafic rock to the exclusion of iron.

This discussion has been concerned only with the feasibility of separating the

Table 1. Extraction of manganese, iron, and silica from lava
Composition of lava: SiO_2 56·41%, Fe 5·23%, Mn 0·09%; ratio Fe/Mn = 58

	pH	Temp (°C)	Time (days)	Amount of lava (g)	Vol. of solution (ml)	Mn extracted (mg)	Mn extracted (% of total)	Fe extracted (mg)	Fe extracted (% of total)	Ratio Fe/Mn	SiO_2 (mg)
H_2CO_3 alone	5·5	23	1	20	40	0·016	0·09	0·41	0·04	26	
H_2SO_4 alone	0	23	1	20	40	0·44	2·4	28	2·7	63	
HCl alone	3·0–5·3	210	8	10	50	0·5	5·5	24	4·6	48	9·3
HCl alone	1·0–2·8	210	4	5	50	0·27	6·0	25	9·6	93	20
Sea-water alone	7·2	210	5	10	50	0·2	2·2	5	1·0	25	9·2
Sea-water + HCl	0·9–5·0	210	8	7	50	1·2	19	65	17·5	54	16
Sea-water + HCl	1·0–4·4	210	4	5	50	0·38	8·5	30	11·5	79	15
Sea-water + HCl	1·0–1·2	100	2	30	750	5·9	22	280	18	49	870
HCl + steam + sea salt		300	0·04	64		4·0	7·0	243	7·3	61	
Molten lava + dist'd H_2O	6·7				1000	<0·01		0·04		>4	1
Molten lava + sea-water	8·4				1000	<0·01		0·04		>4	2
Molten lava + sea-water + HCl	1·3				1000	0·01		0·6		60	2

two metals by simple dissolution in dilute acids. A further possibility suggests itself, that the dissolution process might be accompanied by oxidation. Before exploring this lead, we turn to a consideration of the oxidation process by itself. Specifically, if a solution contains both metals, can some mechanism of precipitation-by-oxidation give a deposit of pure or nearly pure manganese oxides?

Oxidation and Precipitation of Manganese

When a solution containing a few p.p.m. of Mn^{++} is gradually made alkaline, the colour turns pale yellow-brown and deepens as the pH increases. No precipitation occurs over a period of several hours, but at pH's of 7 and over a precipitate can be brought down by boiling. The amount of manganese left in solution is on the order of 1 p.p.m. at pH 7·5–8 and 0·1 p.p.m. at 8·5. These are approximately the amounts that would be predicted from Fig. 3, if the effective or short-term value of *Eh* is near 0·4 V. If air is bubbled through the solutions for several days, the concentration of Mn^{++} gradually diminishes, probably as a result of slow oxidation of the remaining dissolved manganese. Murray and Irvine (1895) report a similar slow oxidation when manganese bicarbonate is added to sea-water, the reaction requiring several months for completion. These results indicate that manganese precipitates under these conditions directly as MnO_2 (or a hydrate of

MnO_2) rather than as $Mn(OH)_3$; if $Mn(OH)_3$ forms at all, it is metastable, as is shown by the position of the $MnO_2/Mn(OH)_3$ boundary below the $MnO_2/Mn(OH)_2$ boundary on Fig. 3. Ferrous solutions in contact with air behave similarly to manganese solutions when a base is slowly added, except that a precipitate of $Fe(OH)_3$ begins to appear at a much lower pH and settles without boiling. Unlike manganese, iron forms no compounds with a valence higher than 3, which would be stable in geologic environments.

The fact that $Fe(OH)_3$ is much more insoluble than MnO_2 means that addition of base to a solution containing both metals will precipitate the iron almost quantitatively before precipitation of manganese starts. If a solution containing 10^{-4} mole/litre of each metal, for example, is kept at an *Eh* of 0·2 V and is made progressively alkaline, iron starts precipitating at pH 6·1; manganese is not affected until the pH has reached 9·5 and the iron concentration has dropped to 10^{-15} M. Similarly, if the pH is kept at 6·0 and the redox potential is raised (say by dissolving O_2), iron starts to precipitate at a potential of +0·2 V and manganese only at +0·6 V, when the iron in solution again has been reduced to 10^{-15} M. Both reactions are slow, but the rates are not sufficiently different to give any possibility of precipitating manganese before iron; if anything, the experiments suggest that the difference in rate would favour still earlier precipitation of iron. Similar experiments demonstrating that iron oxide is precipitated before manganese oxide have been reported many times (e.g. Vogt, 1906; Zapffe, 1931; Otto, 1936).

Although straight inorganic precipitation thus offers no hope for early separation of manganese, the fact that the two oxidation reactions are slow, leaves open the chance that bacteria or a catalytic agent might have some effect in changing the reaction rates and thereby in reversing the normal precipitation order.

Bacteria are known to aid the oxidation of both metals, the organisms apparently using the energy of the reactions for their life processes (Baier, 1937). Some bacteria thrive on iron exclusively; at least two species are known which can use either metal, but which favour manganese (Zapffe, 1931). This obviously gives us a possible means for precipitating manganese in larger amounts than iron; that the process actually works is demonstrated by the deposits of manganese oxide in water pipes (precipitated out of water containing roughly equal amounts of the two metals) which first led Zapffe to investigate the problem. Bacterial action is also strongly suggested in experiments by Junner (reported by Service, 1943), in which oxides with a fairly high Mn/Fe ratio accumulated on algal coatings on quartz boulders placed in stream-water containing at least twenty-five times as much iron as manganese. Bacteria likewise furnish a reasonable explanation for the curious fact observed by Ljunggren (1955) that some Swedish lakes have iron-rich deposits in one part and manganese-rich deposits in another, apparently produced from a single kind of inflowing water. That bacteria can serve as a general solution to the manganese problem, however, is hardly likely. To suppose that the manganese-precipitating bacteria were present in all the various environments where manganese deposits are found, and to suppose further that they were present to the exclusion of iron bacteria, is the sort of *ad hoc* hypothesis that cannot be completely eliminated but that seems too improbable for serious consideration. Baier (1937) points out also that manganese oxide deposits forming

today by bacterial action on mixed solutions are never as iron-poor as are many manganese ores.

Besides showing that bacteria aid in the precipitation of manganese, Zapffe demonstrated that the precipitation is catalysed by MnO_2 itself, and pointed out in a review of the literature that this catalytic property had been noted by several investigators before him. Zapffe showed further that catalysis by MnO_2 could be utilized for removing manganese from water on a large scale, by passing well-aerated water over pyrolusite and then over charcoal; in this way the concentration of manganese could be reduced from 0·8 p.p.m. to 0·02–0·04 p.p.m. in a routine operation. Zapffe's experiments leave no room for doubt that catalytic precipitation must play a role in the geochemistry of manganese, but it can hardly be a major factor in localizing large ore deposits. Catalysis is effective only where a solution is well aerated, where contact with the solid is intimate and prolonged, and where the pH is at least 7.

In summary, manganese can be removed from solution in preference to iron by at least two species of bacteria, and the precipitation once started is aided by the catalytic activity of MnO_2. These processes furnish a reasonable explanation for the partial separation of iron and manganese in certain small deposits, for example bog-ores and deposits from lakes and streams. Localization of large deposits, however, particularly deposits associated with volcanic rocks, requires additional means of concentrating manganese.

Colloidal Oxides

Ferric oxide and manganese dioxide are known to form fairly stable sols, and this property is often cited as a possible means of transporting the metals in solutions containing oxygen. The colloids as usually prepared have opposite signs, positive for iron and negative for manganese—a circumstance possibly accountable for the reported contrast in kinds of adsorbed ions associated with iron and manganese deposits (e.g. Behrend, 1924; Goldberg, 1954). The colloids furthermore differ in their stability toward coagulation by electrolytes and by other colloids, and such differences have often been suggested as an important factor in separation of the two metals (e.g. Berg and Friedensburg, 1942; Ödman, 1947).

Data on behaviour of the colloids are fragmentary and conflicting. Behrend (1924), for example, reports that manganese sols are much less stable than iron sols; Berg and Friedensburg (1942) claim that iron sols are more stable at pH 6 and manganese sols at pH 7; Knaust (1930) failed to find any significant difference in stability. Organic colloids are reported to help stabilize iron sols (Moore and Maynard, 1929, p. 371) but not manganese sols (Savage, 1936). Dilute silica sols (30–60 p.p.m. SiO_2), according to Moore and Maynard (pp. 512–517), aid in the coagulation of iron sols, although coagulation can be prevented by a little organic matter; Knaust (1930), on the contrary, reports that coagulation of both iron and manganese sols is delayed by the addition of a little silica. Hazel (1940) notes a protective action of silica on manganese sols, and Pieruccini (1951) finds that silica precipitates manganese sols only when Ca^{++} is present.

Exploratory experiments in connection with the present work indicated that iron sols are generally more stable than manganese sols, although the difference is not great and is dependent on concentrations and on methods of preparing the sols. Small amounts of silica had little effect on coagulation of either sol, but large concentrations (160–500 p.p.m. SiO_2) prevented precipitation of the oxides (concentrations 50 p.p.m. Fe and Mn), even at a pH of 9, for at least several months.

These scanty experimental results do not indicate differences between the colloids sufficiently marked and sufficiently consistent to serve as a means of large-scale separation of the two elements. The possibility cannot be excluded that stability differences may be responsible for partial separation locally.

Dissolution Accompanied by Oxidation*

Introduction

Up to this point we have considered the possibility of dissolving manganese in preference to iron from rocks containing both metals, and of precipitating manganese preferentially from solution. An alternative way of isolating manganese has been suggested tentatively or implicitly by many authors (e.g. Vogt, 1906; Hewett, 1932; Ljunggren, 1953): iron may precipitate first, leaving manganese free to be transported and precipitated by itself. This hypothesis requires that the explanation for any given manganese deposit also account for the disposal of large quantities of iron; but such a requirement may not be out of reason, inasmuch as many manganese-ore bodies are associated with rocks containing abundant hematite, limonite, or other iron minerals.

Theoretically the prior precipitation of iron could be accomplished as carbonate, silicate, sulphide, or oxide, since the iron compounds of all these anions are more insoluble than the manganese compounds. The difference in solubility is greatest for the oxides, and separation by this means is easy to demonstrate experimentally.

Experiments

In one experiment, summarized in Table 2, finely pulverized basalt was allowed to stand for an hour in 1 N H_2SO_4, giving a solution with 5 p.p.m. Mn^{++} and 230 p.p.m. Fe^{++}. The excess acid was neutralized with NaOH, and enough of the base was added to bring the pH into the range 6–7. In this range the iron slowly oxidizes and precipitates according to the reaction

$$2Fe^{++} + \tfrac{1}{2}O_2 + 5H_2O = 2Fe(OH)_3 + 4H^+$$

The H^+ liberated in the reaction tends to lower the pH, so that successive additions of base are necessary to bring the pH back to the range 6–7 (Table 2). Too much base must be avoided, for an excess would precipitate all the iron at once and the manganese with it. As long as the pH remains just under 7 the iron is progressively removed, its concentration dropping below the limit of detectability after 2 days, while the manganese is practically unaffected. This forms, then, a solution containing manganese as the only heavy metal, exactly the sort of solution needed to account for the origin of manganese deposits. The manganese once isolated can precipitate in any of the various compounds found in nature, depending on the subsequent history of the solution. One obvious means of precipitation is illustrated by the last two lines

* The hypothesis developed in this section, as it applies specifically to the origin of manganese deposits in volcanic associations, has been described more fully elsewhere (Krauskopf, 1957).

of Table 2: the conditions need be changed only by raising the pH above 8, and most of the manganese precipitates as MnO_2.

Note that the requirements of the experiment are not at all stringent, and could be readily duplicated in nature. We start with a slightly acid solution—just how acid is immaterial—percolating through rocks containing ferromagnesian minerals. We suppose that the solution is exposed to air, or at least contains some dissolved oxygen; the precise value of *Eh* does not matter, since Figs. 3 and 4 show that for any *Eh* there should be a range of at least three

Table 2. Dissolution and oxidation of iron and manganese

Procedure: 20 g of finely powdered Parícutin basalt placed in 200 ml of distilled water kept in a water-bath at 55° and stirred continuously. Water replenished from time to time to make up evaporation losses, but volume allowed to fluctuate between 100 and 200 ml.

Time	pH	Dissolved Mn (p.p.m.)	Dissolved Fe (p.p.m.)	Approx vol. of solution (ml)	Substance added	Resulting pH
1 day	7·5	< 0·1		150	CO_2 bubbled through very slowly	5·2
2 days	6·1	0·1		100	H_2SO_4 to make sol'n ca. 1 N H^+	0
2 days + 1 hr		5·0		120	NaOH sol'n	6·1
3 days	4·4	5·5	220	120	NaOH sol'n	6·8
3 days + 4 hr	5·4				NaOH sol'n	7·1
4 days	6·1				NaOH sol'n	6·9
4 days + 10 hr	6·5	3·0	< 0·1	200	NaOH sol'n	8·0
5 days	7·4	3·0		100	NaOH sol'n	8·5
6 days	8·0	0·6		150	NaOH sol'n	8·9
7 days	8·4	0·1		100		

pH units in which the equilibrium concentration of Fe^{++} is less than 0·01 p.p.m., while the Mn^{++} concentration is greater than 1 p.p.m. The only specific requirement is that the alkalinity must *gradually* increase, so that iron is oxidized before manganese.

The temperature of the experiment just described was kept at 55°C in order to speed up the reactions. That a similar result could be obtained at room temperature is shown by a less elaborate experiment: a vertical glass tube 1 cm in diameter and 160 cm long was filled with coarsely ground basalt, the lower half of the tube containing powdered $CaCO_3$ also, and 0·1 N H_2SO_4 was allowed to percolate downward through the tube at a rate of 3 drops (ca. 0·15 ml) per hour. The upper part of the $CaCO_3$ gradually turned brown, and a brown precipitate formed in the liquid as it dripped from the bottom of the tube. After 3 days the solution that had collected was filtered and analysed; it showed a pH of 5·5, an Mn content of 55 p.p.m., and an Fe content of 200 p.p.m. Thus the Mn/Fe ratio was about 1/4, in contrast to 1/60 in the rock; if the experiment were arranged so that better aeration and longer contact of the solution with the carbonate were possible, the iron could be eliminated almost completely.

In this manner, then, if opportunity is provided for thorough oxidation and gradual neutralization, acid solutions percolating through igneous rocks can be made to precipitate most of the iron as ferric oxide and to dissolve most of the manganese.

Evidence of separation in nature

Direct evidence that iron and manganese are being separated in nature by the gradual neutralization of acid solutions under oxidizing conditions is furnished by

observations of Vogt (1906) and Hanson (1932). Both of these authors, one in Norway and one in Canada, describe an increase in the Mn/Fe ratio downward from the surface in veins altered by supergene solutions and a similar increase in bog-ore deposits on gentle slopes away from the springs that supply the two metals. Ljunggren (1953) also finds evidence for this process of separation in the fact that ground-water in south-western Sweden has a higher Mn/Fe ratio than does bedrock; evidently acid surface waters percolating through soils deposit much of their iron as ferric oxide in the *B* horizon, thereby becoming enriched in manganese.

Origin of manganese deposits associated with volcanic rocks

This process of separation is particularly attractive as an explanation for the many manganese deposits intimately associated with mafic to intermediate lavas which have flowed into shallow sea-water (for example, Park, 1942 and 1946; Wurm, 1953; and Taliaferro and Hudson, 1943). Gases accompanying such lavas would form acid solutions in sea-water, and these solutions in contact with the lava would extract much of its iron and manganese. Sea-water normally contains dissolved oxygen, so that the iron would be gradually oxidized as the original acids are neutralized by mixing with more and more water. (Visible precipitation of iron oxide where acid volcanic waters mix with sea-water is described by Fouqué (1879, pp. 175–176) at Santorin, where the precipitated oxide discolours the Mediterranean for several kilometres from the warm springs that supply the iron.) The manganese would remain in solution until the pH had climbed to nearly its normal value in the sea, 8·0–8·4, which would probably be reached only in water above or adjacent to the lava. Hence the iron oxide should be distributed widely through the lava and accompanying sediments, while most of the manganese would be concentrated in layers and pockets between the flows. The chert that normally accompanies this kind of deposit presumably represents silica extracted from the lava along with the two metals (Table 1). The fact that limestone is also commonly associated with these manganese ores may mean that calcium is dissolved from the lava along with manganese and iron, or else that a sea bottom on which limy mud is accumulating forms a particularly favourable environment for precipitating iron and manganese because the carbonate helps in neutralizing the original acid solutions.

This explanation is not greatly different from that given by Park (1946), except that he ascribes to hot sea-water a special ability to extract manganese from the lava. Experiments suggest rather that the function of sea-water is to provide a medium for dissolving acid gases and then for gradually neutralizing the acids, the isolation of manganese being due to prior precipitation of iron. This explanation carries with it the proviso that much iron oxide must be present at no great distance from the manganese deposits; the total quantity of iron oxide, in fact, must amount to some fifty times the total amount of manganese. It is well known that this kind of manganese-ore body is associated with red shale, red limestone, red chert, partly oxidized volcanic debris, and even small deposits of hematite itself; but whether the amount of iron oxide in such materials would add up to the necessary large quantity remains an open question. A crucial test of the hypothesis would be the analysis of many rocks in an area containing manganese

deposits of this kind, and an attempt at quantitative estimates of the over-all amounts of iron and manganese oxides present.

For the extraction of iron and manganese from volcanic rocks, the strongly-acid solutions resulting from dissolution of volcanic gases are convenient but not essential. Ordinary meteoric waters, with no more acidity than that produced by atmospheric CO_2 and the products of organic decay in the soil, are capable of effecting the same extraction, albeit much more slowly. Again, the two metals may be separated by early oxidation and precipitation of iron, provided that the acidity of the solutions is gradually neutralized; or possibly in some places the iron is precipitated as carbonate, sulphide, or silicate rather than as oxide. The manganese, remaining in solution longer than the iron, could be deposited in any of several environments: where the solutions become more alkaline than pH 8, where evaporation concentrates the metal, or where the solutions encounter excess silicate or carbonate ion in a reducing environment. Such a sequence of events could account for the layers rich in manganese minerals associated with Pre-Cambrian iron ores (for example, Grout and Wolff, 1955, pp. 27–36), and also for manganese deposits interbedded with tuffs (for example, Hewett and Webber, 1931). Again, a large amount of iron oxide or other secondary iron minerals should be present, although the association need not be as close as in the deposits with submarine lavas; in the Pre-Cambrian ores the iron minerals are obvious, but in the later tuff deposits the iron must be assumed disseminated through the tuff or perhaps concentrated beneath the surface.

One other type of manganese deposit probably associated with volcanic activity or volcanic rocks is represented by accumulations of manganese oxide at hot springs (e.g. Uncia, Bolivia, described by Lindgren, 1922; Juab County, Utah, described by Callaghan and Thomas, 1939; possibly Golconda, Nevada, described by Kerr, 1940; and several others mentioned by White, 1955). Here the water is probably largely of meteoric origin, heated by lava beneath the surface and perhaps acquiring slight acidity from gases still escaping out of the lava. Such deposits always have at least a little associated iron oxide, but the bulk of the iron required by the hypothesis must be assumed to be deposited underground as the warm water makes its way to the surface.

Origin of other manganese deposits

Volcanic rocks are a likely source for manganese because they contain an abundance of fresh ferromagnesian minerals readily accessible to circulating waters. They are, of course, not the only possible source. Glacial debris, containing fresh minerals and readily permeable to oxygen-rich meteoric water, is another obvious suggestion for material which could supply manganese in considerable quantity. The ground-water described by Zapffe (1931), containing an average of 0·8 p.p.m. Mn^{++} and only 1 p.p.m. Fe^{++}, is a good example of the sort of solution that might be expected from the water percolating through glacial material. It is perhaps no accident (D. F. Hewett, personal communication) that bog-ores of manganese, both in North America and in Scandinavia, are concentrated in areas underlain by the latest Pleistocene till. Other rocks and sediments furnish manganese in smaller amounts to ground and surface waters, and the processes of soil formation (by

selective precipitation of iron oxide as surface water becomes more alkaline in the *B* horizon) effect some increase in the Mn/Fe ratio.

Whether or not manganese minerals accumulate must depend on the concentration of manganese in solution and on the changes in pH and *Eh* which the solution undergoes. If the concentration is as low as it is in most surface waters (1–40 parts per billion, according to HARVEY, 1949), precipitation is impossible unless the pH is well above 8, higher than in most natural waters; this follows from Figs. 1 and 3 if the effective *Eh* of surface waters is assumed to be 0·35–0·4 V. Hence, the manganese in large part remains in solution and is carried to the sea. One can readily imagine local conditions, however, that might lead to precipitation even from such very dilute solutions. The manganese might become more concentrated by evaporation in an arid region; the solution might become gradually alkaline, so that all iron would be eliminated, and then might ultimately reach an alkalinity at which very small concentrations of manganese would precipitate; the precipitation might be accelerated by bacteria, by catalytic action of MnO_2, or by unusual concentrations of silicate or carbonate. If the original concentration of manganese were even slightly greater than normal, the precipitation would of course be aided. Probably the most essential requirement for accumulation of manganese from ordinary surface waters is that the necessary slightly unusual conditions persist for a geologically long time. Otherwise the manganese would precipitate only locally and in very minor amounts, as it does in the cracks and cavities of nearly all rocks.

These considerations make possible an explanation for the most puzzling of manganese deposits—those interbedded with and replacing sedimentary rocks, and showing no obvious association with source materials that might have supplied unusual amounts of the metal. Ores in the Batesville district, Arkansas (MISER, 1922), and the enormous deposits at Chiatura and Nikopol in southern Russia (DRAKE, 1898) are examples of this type. Unfortunately, the explanation is exceedingly general: one may postulate that the manganese was deposited slowly from ordinary surface waters in an environment that remained slightly more alkaline than normal for a long period, or one may speculate that the manganese was a bit more concentrated than usual despite the lack of an obvious source, but neither of these assumptions helps to reconstruct details of the environment that led to accumulation of so much metal in these particular places.

Another factor that may play a role in sedimentary deposits is the possibility of re-solution and redistribution of earlier disseminated manganese minerals. Manganese carbonate and silicate are slowly soluble in weakly acid solutions; the oxides are immune to attack as long as conditions are oxidizing, but go into solution readily when the environment becomes reducing (MURRAY and IRVINE, 1895; MURATA, 1939). Once dissolved, the manganese is readily precipitated again by a slight change of conditions. Thus manganese should be mobile on a small scale, and should ultimately concentrate from a disseminated deposit into the part of a bed or sequence of beds having *Eh* and pH conditions which will make manganese minerals most insoluble. The commonly observed concentrations of oxides in the near-surface parts of manganese carbonate and silicate deposits are good illustrations of the dissolution and small-scale migration of the metal. HEWETT (1916) has

suggested a similar process in explaining small manganese accumulations in residual clay, stream channel deposits, and fault zones in Virginia and Maryland. It should be noted that each cycle of re-solution and re-precipitation leads to further separation from iron, for manganese minerals are both more easily dissolved and less easily precipitated than the corresponding iron compounds; hence it should be possible for manganese to accumulate while iron remains widely disseminated.

One other long-standing question about the geochemistry of manganese is the reason for the high content of manganese in the red clay of the deep sea. The general explanation suggested by Murray and Irvine (1895) still seems satisfactory: manganese oxide precipitated in shallow-water sediments is unstable because of reduction by organic matter, and all of the possible compounds of divalent manganese are too soluble to remain in contact with sea-water except in local areas where the supply of manganese is abnormally large or the pH is abnormally high. Hence, manganese supplied to the sea by streams gradually migrates to deeper water where the sediments contain too little organic matter to keep the dioxide reduced. Iron is less effectively concentrated in deep-sea sediments, because its oxide at the pH of sea-water is much less readily reduced, or if reduced is fixed in the form of stable and insoluble pyrite. (Analyses made by Correns (1937) show the contrast in Mn/Fe ratios between shallow-water and deep-water marine sediments.) The general relations seem clear enough, but several questions of detail remain, particularly the reasons for the accumulation of manganese in the form of nodules. These questions have been examined recently by Pettersson (1945), Goldberg (1954), and Dietz (1955), but are outside the area of the present report.

Summary

Manganese and iron are readily dissolved from igneous rocks as the divalent ions by dilute acid solutions, their ratio in solution being initially about the same as that in the rock. The ions are oxidized by atmospheric oxygen, iron to a valence of +3 and manganese to a valence of +4. In these higher valences the metals form insoluble oxides and hydroxides, the iron compounds being more insoluble than those of manganese. The divalent ions may be precipitated also without oxidation as hydroxides, carbonates, silicates, and sulphides; again, the iron compounds are less soluble, the contrast being especially notable for the sulphides. Data on electrode potentials permit the outlining of fields of stability on *Eh*-pH diagrams, the stabilities corresponding qualitatively to the known facts of mineral association.

Reactions of the divalent ions with dissolved oxygen are slow, but may be speeded up by bacteria. Some species of bacteria utilize the iron reaction exclusively, and others favour the manganese reaction. Bacterial activity, therefore, provides a means by which one element or the other may be precipitated from a mixture in relatively pure form. Catalytic speeding up of manganese oxidation by already-precipitated MnO_2 also helps to isolate manganese. These processes provide at least a partial explanation for the separation of the two metals in bog-ores and in lake and stream deposits. They doubtless also play a role, although probably not a major one, in the localization of larger manganese deposits.

Another means of separating the two metals is provided by the greater insolubility of ferric oxide and hydroxide. Over a pH range of at least 3 units, at any

value of *Eh*, Fe^{++} in equilibrium with ferric oxide has a concentration of less than 0·01 p.p.m., while Mn^{++} in equilibrium with Mn_2O_3 or MnO_2 has a concentration greater than 1 p.p.m. If the alkalinity is gradually increased through this range, manganese will be left by itself in the solution and will precipitate only when the pH becomes still higher. The manganese may precipitate as oxide, carbonate, or silicate, depending on the *Eh* and on the concentration of carbonate and silicate ions. This mechanism requires that formation of a manganese deposit be preceded by the precipitation of iron in amounts many times that of the manganese. Rocks adjacent to manganese deposits are commonly rich in iron oxide, but whether the quantity is sufficient to establish the hypothesis remains to be tested by analysis.

The hypothesis of isolation of manganese by prior precipitation of iron oxide is particularly suited to explaining manganese deposits associated with submarine lava flows. Here the volcanic rocks are a convenient source of acid, and sea-water serves both as a solvent for the acid gases and as a means of gradually neutralizing them. Other kinds of manganese deposits can be accounted for by the same mechanism, but in much more general terms; the solvent of the two metals may be postulated as meteoric water containing carbonic acid, and its neutralization can be ascribed to mixing with sea-water, ground-water of arid regions, or water in contact with limestone. Such a process would be most effective where manganese is supplied to meteoric water in amounts slightly greater than normal, say by the weathering of volcanic material or glacial debris, but abnormality of supply is probably not essential if the necessary pH gradient is maintained for a long time. Manganese minerals once deposited can be concentrated by redissolving and reprecipitation; even the oxide minerals are readily dissolved in a reducing environment. The formation of a large deposit may require several cycles of deposition and redistribution, each step leading to further separation of manganese from iron.

This explanation of manganese deposition as due in part to bacterial activity and in part to differential oxidation of iron and manganese has the merit of invoking no processes other than well-known ones of weathering and sedimentation, processes, furthermore, which can be duplicated step by step in the laboratory. No submarine springs or hydrothermal solutions mysteriously deprived of all metals except manganese need be imagined. This is not to deny the existence of hydrothermal manganese ores, of course, but simply to point out that hydrothermal solutions are not necessary to explain most deposits.

Against the hypothesis can be urged the facts that visible iron oxide is notably lacking near some manganese deposits, and that the quantitative sufficiency of the iron oxide near other deposits has nowhere been demonstrated. A test of the hypothesis based on relative amounts of associated iron and manganese oxides should be possible at some deposits, but for others even this sort of rough check is impossible because the postulated iron-containing material has either been eroded, or is too deeply buried, or is too far distant to be recognizable.

A more serious difficulty with the hypothesis is its elasticity. If the expected iron oxide is not found, it can be explained away as eroded, deeply buried, or widely disseminated. If manganese deposits are not found in apparently favourable spots, their absence can be shrugged off as a minor aberration of pH or dissolved

oxygen. Whether or not a given sedimentary sequence contains a second Chiatura deposit depends on a nice adjustment of many factors in the sedimentary environment regarding which no independent evidence is available. Expressed in another way, the hypothesis has little *predictive* value: it is satisfying in that it requires no unusual geologic processes, but it is not sufficiently definite in its conclusions to specify that new deposits of manganese should be looked for in particular geologic environments.

APPENDIX

The calculations are so similar to those described by GARRELS (1953) that the briefest summary should suffice.

Take first the MnO_2-Mn_2O_3 boundary on Fig. 1. For the two electrode reactions we write

$$Mn^{++} + 2H_2O = MnO_2 + 4H^+ + 2e^-; \quad \Delta F^\circ = 56{\cdot}7 \text{ kcal}, \; E^\circ = 1{\cdot}23 \text{ V}$$

$$2Mn^{++} + 3H_2O = Mn_2O_3 + 6H^+ + 2e^-; \quad \Delta F^\circ = 66{\cdot}6 \text{ kcal}, \; E^\circ = 1{\cdot}44 \text{ V}$$

The ΔF° values are calculated by adding free energies given by LATIMER (1952), and the E° values are found from the relation $E^\circ = \Delta F^\circ/nf$, where n is the coefficient of e^- in the electrode reaction and f is the Faraday constant, 23·1 kcal/volt-coulomb. For the sign of E° the European convention is used (opposite to LATIMER's). The redox potential for the first equation as a function of concentrations is

$$Eh = 1{\cdot}23 + \frac{0{\cdot}06}{2} \log (H^+)^4 - \frac{0{\cdot}06}{2} \log (Mn^{++})$$

$$= 1{\cdot}23 - 0{\cdot}12 \text{ pH} - 0{\cdot}03 \log (Mn^{++})$$

Here the parentheses indicate concentrations; the factor 0·06 is the gas constant multiplied by the absolute temperature and by the conversion factor from natural to decimal logarithms, and divided by the Faraday constant; and the 2 is the coefficient of e^-. A similar equation for the second reaction is

$$Eh = 1{\cdot}44 - 0{\cdot}18 \text{ pH} - 0{\cdot}06 \log (Mn^{++})$$

Rearrangement gives two equations for (Mn^{++}) in terms of Eh and pH:

$$\text{for equilibrium with } MnO_2\text{:} \quad \log (Mn^{++}) = 41 - 4 \text{ pH} - 33{\cdot}3 \, Eh$$

$$\text{for equilibrium with } Mn_2O_3\text{:} \quad \log (Mn^{++}) = 24 - 3 \text{ pH} - 16{\cdot}7 \, Eh$$

For strongly oxidizing solutions (high Eh) the first of these gives a lower figure for (Mn^{++}) than the second, indicating that MnO_2 is the more stable compound; for less oxidizing solutions the second gives a lower (Mn^{++}), meaning that Mn_2O_3 is more stable. Along the boundary both oxides are equally stable, and (Mn^{++}) in equilibrium with them must be the same. Hence we obtain an equation for the boundary by equating the two expressions for $\log (Mn^{++})$:

$$41 - 4 \text{ pH} - 33{\cdot}3 \, Eh = 24 - 3 \text{ pH} - 16{\cdot}7 \, Eh$$

$$Eh = 1{\cdot}02 - 0{\cdot}06 \text{ pH}$$

This gives the upper solid line on Fig. 1. All other boundaries between oxides and hydroxides are found similarly.

For $MnCO_3$ no oxidation is involved, but only the simple equilibrium:

$$MnCO_3 = Mn^{++} + CO_3^{--}; \; K = 8{\cdot}8 \times 10^{-11} \text{ (LATIMER)}$$

We assume that the total carbonate, $(CO_3^{--}) + (HCO_3^-) + (H_2CO_3)$, is 0·002 M. The (CO_3^{--}) itself is then given by

$$(CO_3^{--}) = \frac{0{\cdot}002}{1 + \dfrac{(H^+)}{4{\cdot}8 \times 10^{-11}} + \dfrac{(H^+)^2}{2{\cdot}0 \times 10^{-17}}}$$

where $4{\cdot}8 \times 10^{-11}$ is the second ionization constant of H_2CO_3 and $2{\cdot}0 \times 10^{-17}$ is the product of the two ionization constants. The concentration of Mn^{++} is then $8{\cdot}8 \times 10^{-11}$ divided by this quantity; taking logarithms and simplifying exponents, we obtain

$$\log (Mn^{++}) = -7{\cdot}4 + \log \left(1 + \frac{(H^+)}{10^{-10{\cdot}3}} + \frac{(H^+)^2}{10^{-16{\cdot}7}}\right)$$

For pH's less than 5 the (H^+) term is small compared with the $(H^+)^2$ term, so that

$$\log (Mn^{++}) = -7{\cdot}4 + \log (H^+)^2 + 16{\cdot}7 = 9{\cdot}3 - 2\,\text{pH}$$

For pH's greater than 7 the (H^+) term is the larger, so that

$$\log (Mn^{++}) = -7{\cdot}4 + \log (H^+) + 10{\cdot}3 = 2{\cdot}9 - \text{pH}$$

The boundary $MnCO_3$–Mn_2O_3 consists of two lines obtained by combining these with the equation for Mn_2O_3 above:

$$\text{for pH} < 5;\ 24 - 3\,\text{pH} - 16{\cdot}7\,Eh = 7{\cdot}4 - 2\,\text{pH, or } Eh = 0{\cdot}88 - 0{\cdot}06\,\text{pH}$$

$$\text{for pH} > 7:\ 24 - 3\,\text{pH} - 16{\cdot}7\,Eh = 2{\cdot}9 - \text{pH, or } Eh = 1{\cdot}26 - 0{\cdot}12\,\text{pH}$$

All other oxide-carbonate and oxide-silicate boundaries are found by a similar calculation.

Boundaries between MnS and the two lower oxides are found similarly by using the solubility product $(Mn^{++})(S^{--}) = 7 \times 10^{-16}$, except that here an added complication arises because S^{--} depends not only on pH and total dissolved sulphur but also on the oxidation equilibrium with SO_4^{--}. For the electrode reaction

$$S^{--} + 4H_2O = SO_4^{--} + 8H^+ + 8e^-$$

Latimer gives $E^\circ = 0{\cdot}14$ V. The redox potential may then be expressed as a function of concentrations

$$Eh = 0{\cdot}14 + \frac{0{\cdot}06}{8}\left(\log \frac{(SO_4^{--})}{(S^{--})} + \log (H^+)^8\right)$$

$$= 0{\cdot}14 - 0{\cdot}06\,\text{pH} + 0{\cdot}0075 \log \frac{(SO_4^{--})}{(S^{--})}$$

or, by rearranging,

$$\log \frac{(SO_4^{--})}{(S^{--})} = 133{\cdot}3\,Eh + 8\,\text{pH} - 18{\cdot}7$$

Now, if total dissolved sulphur is assumed to be 0·1 M,

$$(SO_4^{--}) + (S^{--}) + (HS^-) + H_2S = 0{\cdot}1$$

or

$$(S^{--})\left(\frac{(SO_4^{--})}{(S^{--})} + 1 + \frac{(H^+)}{10^{-15}} + \frac{(H^+)^2}{10^{-22}}\right) = 0{\cdot}1$$

where 10^{-15} is the second dissociation constant of H_2S and 10^{-22} is the product of the two dissociation constants. The term $(SO_4^{--})/(S^{--})$ for any Eh,pH pair may be found from the preceding equation, and (S^{--}) may be found by substituting this value and the corresponding (H^+); then (Mn^{++}) is obtained from the relation $(Mn^{++}) = 7 \times 10^{-16}/(S^{--})$. Values so obtained may be compared with concentrations of (Mn^{++}) in equilibrium with the oxides (MnO and Mn_3O_4) to find the Eh,pH combinations where these values become equal.

It would be possible to derive an analytical expression for (Mn^{++}) in terms of Eh and pH, as was done in the other calculations, but the expression would be too unwieldy for easy use. The simplest procedure is to set up an array of values of (Mn^{++}) for different Eh's and pH's, and then to compare this array mechanically with similar ones for the oxides. The boundary so obtained is not quite as accurate as the others, but the accuracy is more than sufficient for the purpose.

Lines on the other diagrams require no further comment except for the boundary between pyrite and ferric oxide on Fig. 2. This boundary is drawn on the assumption that Fe^{++} in equilibrium with pyrite is fixed by the equilibrium

$$FeS_2 = Fe^{++} + S^{--} + S$$

for which LATIMER gives the necessary free-energy figures. The boundary would be practically identical if the equilibrium were assumed to be

$$FeS_2 = Fe^{++} + S_2^{--}$$

The actual equilibrium that determines Fe^{++} is not known, so that this boundary is the least certain of those shown.

REFERENCES

BAIER C. R. (1937) Die Bedeutung der Bacterien für die Bildung oxydischen Eisen- und Manganerze. *Geologie der Meere und Binnengewässer* **1,** 325–348.

BEHREND F. (1924) Über die Bildung von Eisen und Manganerzen durch deren Hydroxydsole auf Verwitterungslagerstätten. *Zt. Prakt. Geol.* **32,** 102–108.

BERG G. und FRIEDENSBURG F. (1942) Mangan. *Die metallischen Rohstoffe* Vol. V. p. 232 (esp. pages 2–11) F. Enke, Stuttgart.

BLUMER M. (1950) Die Existenzgrenzen anorganischer Ionen bei der Bildung von Sedimentgesteinen. Geochemische Untersuchungen IV. *Helv. Chim. Acta* **33,** 1568–81.

CALLAGHAN E. and THOMAS H. E. (1939) Manganese in a thermal spring in west-central Utah. *Econ. Geol.* **34,** 905–920.

CHARLOT G. (1949) *Théorie et méthode nouvelles d'analyse qualitative* (3rd edition) Paris.

COOPER L. H. N. (1937) Oxidation-reduction potential in sea water. *J. Mar. Biol. Ass.* N.S. **22,** 167–76.

CORRENS C. W. (1937) *Deutsche Atlantische Expedition* 1925–27 Band 3. Teil 3. Lieferung 2. 219–233.

DELTOMBE E. and POURBAIX M. (1954) Comportement électrochimique du fer en solution carbonique. *Rapport Technique, No.* **8,** p. 5. Centre Belge d'Étude de la Corrosion.

DIETZ R. S. (1955) Manganese nodules on the northeast Pacific sea floor. *Calif. J. Min. Geol.* **51,** 209–20.

DRAKE C. F. (1898) The manganese industry of the Caucasus. *Amer. Inst. Min. Engrs.* **28,** 191.

EMMONS W. H. (1911) The agency of manganese in the superficial alteration and secondary enrichment of gold deposits in the United States. *Amer. Inst. Min. Engrs.* **42,** 3–73.

EMMONS S. F., IRVING J. D., and LOUGHLIN G. F. (1927) Geology and ore deposits of the Leadville mining district. *U.S. Geol. Surv.*, Prof. Paper 148, p. 368.

FOUQUÉ F. (1879) *Santorin et ses Éruptions* Paris.

GARRELS R. M. (1953) Mineral species as functions of pH and oxidation-reduction potentials. *Geochim. et Cosmochim. Acta* **5,** 153–168.

GOLDBERG E. D. (1954) Marine geochemistry I. Chemical scavengers of the sea. *J. Geol.* **62,** 249–265.

GOLDSCHMIDT V. M. (1954) *Geochemistry* Oxford University Press.

GROUT F. F. and WOLFF J. F. (1955) Geology of the Cuyuna district, Minnesota. *Minn. Geol. Surv. Bull.* **36,** 144.

HANSON G. (1932) Manganese deposits of Canada. *Canada Dept. Mines, Geol. Surv. Econ. Geol.* Series No. 12 p. 120

HARVEY H. W. (1949) On manganese in sea and fresh water. *J. Mar. Biol. Ass. U.K* **28,** 155–164.

HAZEL F. J. (1940) Silicic acid as a protective colloid for MnO_2 sols. *J. Phys. Chem.* **44,** 422–427.

HEWETT D. F. (1916) Some manganese mines in Virginia and Maryland. *U.S. Geol. Surv. Bull.* **640,** 37–71.

HEWETT D. F. and WEBBER B. N. (1931) Bedded deposits of manganese oxides near Las Vegas, Nevada. *Univ. Nevada Bull.* **25,** No. 6, 17.

Hewett D. F. (1932) Manganese in sediments. In *Treatise on Sedimentation* (Edited by W. H. Twenhofel) p 562–581. Williams and Wilkins, Baltimore.

Huber N. K. and Garrels R. M. (1953) Relation of pH and oxidation potential to sedimentary iron mineral formation. *Econ. Geol.* **48,** 447–457.

Huber N. K. (1956) Environmental control of sedimentary iron minerals and its relation to the origin of the Ironwood iron-formation. Ph.D. dissertation, Northwestern University.

James H. L. (1954) Sedimentary facies of iron formation. *Econ. Geol.* **49,** 235–293.

Kerr P. F. (1940) Tungsten-bearing manganese deposit at Golconda, Nevada. *Geol. Soc. Amer. Bull.* **51,** 1359–1390.

Knaust W. Über Sole von Eisenhydroxid und Manganhydroxid. *Chemie der Erde* **4,** 529–548.

Krauskopf K. B. (1957) Separation of manganese from iron in the formation of manganese deposits in volcanic associations. *Rpts. of 20th Int. Geol. Cong. Mexico.* In press.

Krumbein W. C. and Garrels R. M. (1952) Origin and classification of chemical sediments in terms of pH and oxidation-reduction potentials. *J. Geol.* **60,** 1–33.

Latimer W. M. (1952) *Oxidation potentials* Prentice-Hall, New York.

Lee D. E. (1955) Mineralogy of some Japanese manganese ores. *Stanford Univ. Publ., Geol. Sciences* **5,** 1–64.

Lindgren W. (1922) Recent deposits of a thermal spring in Bolivia. *Econ. Geol.* **17,** 201–206.

Lindgren W. (1933) *Mineral deposits* McGraw-Hill, New York.

Ljunggren P. (1953) Some data concerning the formation of manganiferous and ferriferous bog ores. *Geol. Fören. Stockholm Förh.* **75,** 277–297.

Ljunggren P. (1955) Geochemistry and radioactivity of some manganese and iron bog ores. *Geol. Fören. Stockholm Förh.* **77,** 33–44.

Miser H. D. (1922) Manganese ore in the Batesville district, Arkansas. *U.S. Geol. Surv. Bull.* **734,** 273.

Moore E. S. and Maynard J. E. (1929) Solution, transportation and precipitation of iron and silica. *Econ. Geol.* **24,** 272–303, 365–402, 506–527.

Moussard A. M., Brenet J., Jolas F., Pourbaix M., Van Muylder J. (1954) Comportement électrochimique du manganèse. *Centre Belge d'Étude de la Corrosion, Rapport Technique* No. 18. p. 7.

Murata K. J. (1939) Exchangeable manganese in river and ocean muds. *Amer. J. Sci.* **237,** 725–733.

Murray J. and Irvine R. (1895) On the manganese oxide and manganese nodules in marine deposits. *Trans. Roy. Soc. Edin.* **37,** 721–742.

Ödman O. H. (1947) Manganese mineralization in the Ultevis district, Jokkmokk, Sweden. *Sverig. Geol. Undersökn. Årsbok* **41,** No. 6, 90 p.

Otto H. (1936) Die Rolle des Mangans in den Mineralien. *Min. Petrog. Mitt.* **47,** 89–140.

Park C. F. (1942) Manganese deposits of Cuba. *U.S. Geol. Surv. Bull.* **935—B,** 75–97.

Park C. F. (1946) Spilite and manganese problems of the Olympic peninsula, Washington. *Amer. J. Sci.* **244,** 305–323.

Pettersson H. (1945) Manganese nodules and the chronology of the ocean floor. *Göteborgs Kungl. Vetenskaps- och vitterhets samhälle, Handlingar* 6F, series B. Vol. II No. 8.

Pieruccini R. (1951) Diffusion of manganese in limestone and chert sediments of the northern Toscana Appenines. *Atti. soc. toscana sci. nat., Pisa, Mem.* Series A **58,** 6–59.

Rankama K. and Sahama T. G. (1950) *Geochemistry* Univ. Chicago Press.

Savage W. S. (1936) Transportation and precipitation of manganese. *Econ. Geol.* **31,** 278–298.

Service H. (1943) Geology of the Nsuta manganese ore deposits. *Gold Coast Geol. Surv. Mem.* **5,** 32 p.

Taliaferro N. L. and Hudson F. S. (1943) Genesis of the manganese deposits of the Coast Ranges of California. *Calif. Div. Mines Bull.* **125,** 217–275.

Thiel G. A. (1924) The manganese minerals: their identification and paragenesis. *Econ. Geol.* **19,** 107–145.

Thompson T. G. and Wilson T. L. (1935) The occurrence and determination of manganese in sea water. *J. Amer. Chem. Soc.* **57,** 233.

Vogt J. H. L. (1906) Über Manganwiesenerz. *Z. prakt. Geol.* **14,** 217–233.

White D. E. (1955) Thermal springs and epithermal ore deposits. *Econ. Geol. 50th Anniversary Vol.* 99–154.

Wilcox R. E. (1954) Petrology of Parícutin Volcano. *U.S. Geol. Surv. Bull.* **965–C,** 281–349.

Wurm A. (1953) Über Manganerzvorkommen in den Anden Südamerikas. *Ns. Jb. Abh.* **96,** 173–9.

Zapffe C. (1931) Deposition of manganese. *Econ. Geol.* **26,** 799–832.

Zobell C. E. (1946) Studies on redox potential of marine sediments. *Amer. Assoc. Petroleum Geol. Bull.* **30,** 477–513.

Geochimica et Cosmochimica Acta, 1957, Vol. 12, pp. 85 to 93. Pergamon Press Ltd., London

Biogeochemical investigations in areas of copper-tin mineralization in south-west England

Anthony P. Millman
Department of Mining Geology, Imperial College of Science and Technology, London

(*Received* 3 *January* 1957)

Abstract—Semi-quantitative methods of spectrographic analysis have been employed for the determination of Cu, Sn, Zn, Pb, and Ag in the leaves and twigs of a variety of trees growing in an area of copper-tin mineralization on the borders of Cornwall and Devon. The distribution of these ore metals in the soil profiles was also determined. Ore-negative (background) values have been derived for the trees and the soils, and these are compared with the results of earlier work in Southern Nigeria and Northern Rhodesia.

1. Introduction

As part of the research programme of the Department of Mining Geology, investigations were initiated in 1949 into the possibility of testing and establishing new methods of mineral exploration based on the detection of abnormal quantities of ore metals in natural waters, vegetation, and soils. A preliminary reconnaissance was carried out in Nigeria, West Africa, in 1949, in an area of lead-zinc mineralization. The results showed that lode-springs and mine-seepage waters contained large amounts of heavy metals and that the entry of these waters into the local drainage pattern caused significant increases in the metal content of streams and rivers for considerable distances from the area of mineralization (Webb and Millman, 1950). Similarly numerous samples of several species of savannah trees growing at varying distances from known lead-zinc lodes showed a wide range in the content of lead, zinc, and silver in both twigs and leaves. For example, dried twig samples of *Afzelia africana* showed a maximum of 2000 p.p.m. Zn, 140 p.p.m. Pb, and 0·31 p.p.m. Ag in proximity to mineralization, as compared with <100 p.p.m. Zn, 0·8 p.p.m. Pb, and 0·05 p.p.m. Ag background values in ore-negative areas (Webb and Millman, 1951). The investigation in Africa revealed the complex nature of plant reaction to ore metals and an area of Cu-Sn-Pb-Zn mineralization on the borders of Cornwall and Devon was selected in 1950 for the particular study of some of the problems.

2. Secondary Dispersion of Ore Metals in Vegetation

Plants may be said to sample the soil in their immediate environment, since they absorb from the nutrient solution entering their roots, elements in either true solution or the colloidal state. This solution may contain material liberated from adjacent mineralization. The metallic salts and complexes entering the roots will then be carried to the leaves and twigs, where they are concentrated by evaporation. The reactions of different plants to varying concentrations of ore metals in soils is, however, more complicated than this. The simplest and broadest subdivision of plants, for the purposes of geochemical prospecting, is into those displaying (i) overt or (ii) covert reactions to abnormal concentrations of ore metals (Webb and Millman, 1951). Plants displaying overt reactions are termed

indicator plants, and many of these have been described (Linstow, 1929; Dorn, 1937); in brief, this group has been further subdivided into specific indicator plants and symptomatic indicator plants. The criteria in the above are, however, entirely botanical, since they require an expert knowledge of plant recognition and growth characteristics, and do not involve actual chemical analysis, and they thus constitute the basis for *geobotanical* prospecting. However, plants which react covertly are those which will absorb and concentrate elements to varying degrees without betraying the fact that they have done so by a display of peculiarities in either growth symptoms or selective distribution. Thus, plants of this group may betray, in their trace-element content, the geological setting of their environment and may reveal the presence of high concentrations of ore metals. This covert storage of elements can only be detected by specially sensitive methods of chemical analysis, and techniques involving the analytical determination of ore metals in covert reactor plants constitute *biogeochemical* prospecting.

Systematic methods of sampling and analysis of plants of wide distribution were first applied by the Swedish Prospecting Company in Scandinavia in 1937 (Dorn, 1939), and methods employing spectrographic techniques of analysis were patented (Brundin, 1939). Among subsequent investigations of the biogeochemical methods are the following: (a) copper and zinc (Warren and one or more coworkers, 1947–1952; White, 1950; Vogt *et al.*, 1943; Robinson *et al.*, 1947; Lovering *et al.*, 1950), (b) lead and zinc (Rankama, 1940; Hedstrom and Nordstrom, 1945; Harbaugh, 1950), (c) nickel (Rankama, 1940; Maliuga, 1947), (d) gold (Warren *et al.*, 1950), (e) uranium (Cannon, 1952).

3. Area of Investigation

The biogeochemical studies described in this paper were carried out in the Hingston Down and Gunnislake area of eastern Cornwall, about 4 miles to the south-west of Tavistock. The climate is temperate and the annual rainfall about 48 in. Hingston Down itself forms a conspicuous ridge, trending roughly east–west, surrounded by low-lying areas composed mostly of farmland. The River Tamar, which divides Cornwall from Devon, has cut a steep-sided valley round the eastern margin of the ridge, and along the slopes of this valley there are several large reafforestation areas of pine trees. Hingston Down is almost barren of vegetation, except for patchy development of bracken and heather. However, some residual areas of natural wood remain, composed mostly of oak, birch, willow, and beech, and it is in these woods that the biogeochemical traverses were carried out. Weathering of the rocks does not appear to have produced any extensive development of residual clay soil, which is nowhere thicker than 2 ft.

The area examined falls within the zone of copper-tin mineralization of south-west England, which is about 10 miles wide and 100 miles in length, extending from Land's End to north-east Cornwall, and into western Devon. This mineralized area follows roughly the axis of a belt of granitic intrusions from which the ores have emanated. The granite invades dominantly slatey rocks and appears in the form of several large bosses. The mineral lodes occur in both the slates and the underlying granite and have a general east-west strike, dipping steeply to the north or south. Zoning of the minerals in the lodes is a conspicuous feature, both

laterally and in depth; the ore minerals in the area examined include cassiterite, chalcopyrite, bornite, pyrite, arsenopyrite, wolframite, galena, and sphalerite, and these are associated with gangue quartz, chlorite, and tourmaline. Oxidation and secondary enrichment of the copper minerals have taken place, sometimes to considerable depths.

Both plant and soil traverses were carried out near the sub-outcropping positions of lodes in the neighbourhood of three disused mines—Hingston Down Consols, West Drakewalls, and Russell United, all of which have been worked for both tin and copper. Traverses were also made in areas known to be free of mineralization.

4. Analytical Procedure

The technique employed for the semi-quantitative spectrographic analysis of plant ashes and soil samples is a modified version of the procedure described by Mitchell (1948), the samples being analysed on a large Hilger quartz spectrograph (E492), employing cathode excitation, the cathode portion of the arc being recorded. The details of the procedure are described elsewhere (Webb and Millman, 1951). The wavelengths of the lines used and their sensitivity in the plant ash and soil bases are shown in Table 1. The plant ashes were prepared by incineration at 435°C ± 5° of a 1 g representative sample of oven-dried plant material. The resulting ash was then weighed on a torsion balance.

Table 1. Spectral wavelengths and sensitivities of ore metals in plant ash and soil bases

Element	Wavelength (Å)	Sensitivity limit in p.p.m.		Example of equivalent concentration in oven-dried plant material in p.p.m. with ash yield of 3%
		Soil base	Plant base	
Pb	2833·1	10	10	0·3
Zn	3282·3	300	3000	90
Ag	3280·7	1	1	0·03
Cu	3274·0	1	1	0·03
Sn	2840·0	10	10	0·3
Mn	2801·1	—	1	0·03
Cd	3261·1	—	300	9
Bi	3067·7	—	30	0·9

(—) = not included in base

5. Results of Investigations

A qualitative spectrographic examination of the plant samples showed that increased concentrations of Pb, Zn, Ag, Sn, and Cu were to be found in the leaves and twigs of trees growing in proximity to the tin-copper lodes. These elements therefore were the ones selected for semi-quantitative spectrographic determination. Emphasis throughout the investigations was centred on (i) the determination of background or ore-negative concentrations of ore metal in different species, (ii) the widths of the biogeochemical anomalies, and (iii) the relationships between plant and soil-metal concentrations for various species. The special problem of variation

in ore metal content throughout leaves and twigs of the same tree was also studied with a view to determining which was more suitable for sampling purposes.

(a) *Comparison of metal content of leaves and twigs*

An oak and a birch tree, both about 20 ft in height, growing 8 ft apart in the wooded area to the east of Hingston Down Consols mine, were examined for variation in metal content in the leaves and twigs. Three 15–25 g sample pairs of leaves and twigs were collected from the two trees, particular care being taken to avoid contamination. The detailed procedure of sampling, drying, ashing, and analysis is described elsewhere (Webb and Millman, 1951). A composite sample

Table 2. Replicate analyses of the leaves and twigs of two adjacent trees (birch and oak), and the underlying soil (*B* horizon). South-west England

		p.p.m. metal in dried sample				
		Pb	Ag	Zn	Sn	Cu
Betula sp. (birch) Height, 25 ft. Bed-rock, hornfels	Leaves (average for 3 samples, each in duplicate)	5·9	0·41	520	1·2	12
	Twigs (average for 3 samples, each in duplicate)	16	0·16	290	0·36	7·8
	Soil (average for composite)	20	<1	<300	250	100
Quercus sp. (oak) Height, 20 ft. Bed-rock, hornfels	Leaves (average for 3 samples, each in duplicate)	3	0·43	<130	1·4	23
	Twigs (average for 3 samples, each in duplicate)	9·3	0·07	44	0·9	12
	Soil (average for composite)	10	<1	<300	250	75

of the soil underlying both trees was also collected. All of the samples, after preparation, were analysed spectrographically in duplicate. The results shown in abbreviated form in Table 2 indicate that in both *Betula sp.* and *Quercus sp.* Sn Cu, Zn, and Ag are preferentially concentrated in the leaves—Sn, Cu, and Zn showing a twofold concentration, and Ag a threefold. Lead, however, shows a threefold concentration in the twigs. This latter fact is of considerable importance, since previous workers have believed that lead entering a plant was concentrated in the roots and variation of the lead content in both twigs and leaves was therefore considered unlikely.

The maximum deviation of individual samples from the average value for the particular organ is of the order of 30–50%, and hence is not greater than the normal error for semi-quantitative spectrography. The magnitude of the deviation emphasises, however, the desirability of collecting representative twig or leaf samples.

(b) *Content of ore metals in samples of trees in mineralized and non-mineralized areas*

The analytical results of sixty-two samples of *Quercus sp.*, twenty-eight of *Betula sp.*, and nineteen of *Fagus sp.*, plotted on the basis of frequency diagrams, show that the range of values presented in Table 3 are characteristic of background or "ore-negative" contents of ore metals in the Gunnislake area. The data for fifteen different species in Nigeria and Rhodesia also shown in Table 3 fall within a comparable range of values for Cu, Sn, and Zn, but the background content of Pb is generally higher in the trees from south-west England, and the Ag content is also slightly higher.

Table 3. Normal or background concentration of ore metals in twig samples of trees from south-west England, Southern Nigeria, and Northern Rhodesia

p.p.m. metal in oven-dried twig samples

	South-west England			Southern Nigeria Northern Rhodesia
Metal	*Quercus sp.*	*Betula sp.*	*Fagus sp.*	Average for 15* species.
Lead	<1–6	1–9	<1–6	*c.* 1
Zinc	<100	<100	<100	<100
Silver	Up to 0·15	Up to 0·2	Up to 0·1	*c.* 0·05
Copper	<1–6	<1–6	<1–6	*c.* 6
Tin	Up to 0·2	Up to 0·2	Up to 0·2	*c.* 0·2

* (Webb and Millman, 1951). Savannah vegetation including *Afzelia africana; Rubiaceae sp.; Baphia nitida; Parinari curatellifolia; Albizzia zygia; Lophira alata; Vitex cuneata; Parkia oliveri; Millettia sp.; Newbouldia laevis; Trichilia prieuriana; Anacardiaceae sp.; Brachystegia boehmii; Acacia sp.; Isoberlinia globiflora.*

In proximity to mineralized bed-rock, the peak values of ore metal concentrations, expressed as p.p.m. of dried plant material, may be remarkably high without inducing peculiar growth characteristics such as chlorosis; for example, in some of the Nigerian trees (Webb and Millman, 1951), 550 p.p.m. Pb and 2000 p.p.m. Zn was detected, as compared with normal background values of *c.* 1 p.p.m. Pb and <100 p.p.m. Zn. In Cornwall, however, the maximum anomalies are much less spectacular; to some extent this is probably due to the lower tenor of mineralization. A maximum of 1 p.p.m. Sn was found in *Quercus sp.* growing on soil containing 250 p.p.m. Sn, up to 360 p.p.m. Zn in *Salix sp.* on soil containing <300 p.p.m. Zn, and 12 p.p.m. Cu in *Quercus sp.* on soil containing 200 p.p.m. Cu.

(c) *Comparison of ore-metal content of trees and their underlying soils*

The analytical results of fourteen representative twig samples of *Quercus sp.*, *Salix sp.*, *Fagus sp.*, and *Betula sp.*, and the corresponding soil sample for each, are shown in Table 4. It is apparent that the Pb and Cu contents of the twigs are comparable in magnitude. Over the range of 20–100 p.p.m. Cu and up to 10 p.p.m.

Pb in the soils, the metal content of the plants was 1·6–12 p.p.m. Cu and 1·1–13 p.p.m. Pb, thus showing a tendency for a larger proportion of lead to enter the plant. The results for silver show that up to 0·2 p.p.m. Ag may be found in plants growing on soils containing less than 1 p.p.m. Ag, the limit of sensitivity. The results for tin are particularly interesting. They illustrate the relative immobility

Table 4. Ore-metal content of trees and underlying soils (*B* horizon). South-west England

Sample No.	p.p.m. metal in dried twig sample or soil				
	Pb	Ag	Zn	Sn	Cu
Quercus sp. 334	1·1	0·02	*	*	2·1
Soil 531	<10	<1	<300	30	100
Quercus sp. 335	3·2	0·05	*	*	3·2
Soil 546	<10	<1	<300	30	100
Quercus sp. 336	8·5	0·09	85	0·17	5·1
Soil 555	<10	<1	<300	30	30
Quercus sp. 297	9·3	0·07	44	0·9	12
Soil 517	10	<1	<300	250	75
Quercus sp. 300	13	0·19	42	0·42	6·3
Soil 518	10	<1	<300	100	50
Quercus sp. 301	9	0·18	54	0·54	9·0
Soil 519	<10	<1	<300	<10	75
Betula sp. 393	1·6	0·04	160	0·08	1·6
Soil 554	20	<1	<300	100	30
Betula sp. 364	16	0·16	290	0·36	7·8
Soil 516	20	<1	<300	250	100
Fagus sp. 397	2·1	0·03	*	0·14	5·3
Soil 533	<10	<1	<300	10	50
Fagus sp. 399	1·4	0·04	21	*	2·1
Soil 540	10	<1	<300	30	30
Fagus sp. 400	1·6	0·02	*	*	1·6
Soil 553	10	<1	<300	30	20
Salix sp. 417	1·3	0·04	130	0·13	3·9
Soil 536	<10	<1	<300	50	30
Salix sp. 418	1·8	0·05	360	*	5·4
Soil 540	10	<1	<300	30	30
Salix sp. 419	3	0·05	300	*	9
soil 546	<10	<1	<300	30	100

* Signifies content below sensitivity level of 3000 p.p.m. Zn or 10 p.p.m. Sn in plant ash base.

of tin (due to the stability of eluvial cassiterite in soils), since the plant uptake reaches a maximum of only 1 p.p.m. in soils containing as much as 250 p.p.m. Sn, whereas for concentrations in soil of less than 300 p.p.m. of the more soluble Zn, up to 360 p.p.m. Zn could be detected in trees growing on that soil. The uptake

of tin by plants, however, would probably be much greater in those areas where stannite, $2(Cu_2FeSnS_4)$, is present in the ore, since it is much more easily oxidized than cassiterite and would probably liberate quantities of "available" tin in the form of a colloidal stannate.

Normal or "ore-negative" contents of ore metals in the *B* soil horizon have been derived from analyses of 132 residual soil samples collected over granite and slatey rocks in the Gunnislake area. The range of normal values recorded is as follows: for Pb, <10–30 p.p.m., for Cu, 10–100 p.p.m., for Sn, <10–100 p.p.m. The range of 50–100 p.p.m. for Sn is more frequently found in soils derived from granitic rocks. Some of the peak values of the ore-positive anomalies in the soils at Gunnislake are extremely high, contents of 0·5% Sn (5000 p.p.m.) and 0·1% Cu (1000 p.p.m.) being not uncommon. Sampling was carried out below the A_0 horizon (0–$\frac{1}{2}$ in.) at depths of 6–9 in. (*A*), and 9–18 in. (*B*). Fifteen soil profiles were analysed for selective distribution of ore metals in the upper (*A*) and lower (*B*) horizons. In eight cases of the fifteen, the tin content was found to be greater in the lower horizon by factors of between 2 and 7, and in four cases equal. In the remaining three cases, the tin content was higher in the upper horizon by a maximum factor of 2. Copper was also found to be enriched in the lower horizon by factors of between 2 and 5 in eleven of the fifteen sections, but was equal in three, and higher by a factor of 2 in the upper horizon of one section only. The background lead values, all between <10–30 p.p.m. and unrelated to mineralization, were found to be equal in the two horizons in eleven of the fifteen sample sections. The optimum depth of soil sampling for the successful detection of concealed copper-tin veins therefore appears to be the *B* horizon.

(d) *Comparison between individual species growing on similar ground*

Thirty-nine pairs of tree species growing in proximity to each other were sampled with the object of determining whether particular species exhibited any preference for the accumulation of certain ore metals. From detailed examination of the results, it is evident that for the species examined. *Betula sp.* is the best accumulator plant for lead, *Salix sp.* and *Betula sp.* the best for zinc, and *Quercus sp.* the best for copper. *Fagus sp.* was found to be inferior to the other three species in its ability to concentrate lead and zinc. No preference for tin accumulation was observed in any of the species examined.

6. Conclusions

(a) The investigations concerning the determination of traces of ore metals in a variety of plants growing in both tropical and temperate environments have shown that anomalous concentrations of ore metals in plants may be associated with the presence of concealed mineralization below the soil cover, or to dispersed phases liberated from a more distant ore-body.

(b) Previous investigators have demonstrated that lead is concentrated in the roots of trees and lesser plants, and have postulated that the determination of lead in leaves and twigs as an index of mineralization is not feasible. However, the results of the studies in the west of England and West Africa have shown conclusively that anomalous lead concentrations, sometimes of considerable

magnitude, occur in both leaves and twigs of trees growing in proximity to areas of sub-outcropping lead-zinc deposits. Studies of the variation of metal content throughout a tree show that in the west of England, lead is concentrated preferentially in the twigs of several species as compared with their leaves, and that copper, tin, zinc, and silver are concentrated in the leaves.

(c) Replicate analyses of several samples of leaves or twigs from the same tree show deviations of up to 50% from the average content of leaves or twigs from the particular tree.

(d) Within the classification of normal accumulator plants, it has been found that certain species are more favourable for the detection of specific metals. For lead, *Betula sp.* appears to be favourable; for copper, *Quercus sp.*; and for zinc, *Salix sp.* and *Betula sp.* *Fagus sp.* was found to be inferior to the other species examined in its capacity to accumulate lead and zinc. No common species was found to show preferential concentration of tin.

(e) Comparison of the analyses of plants with those of the underlying soils shows that although the biogeochemical method of prospecting is suitable for detecting lead, zinc, and copper mineralization, the method is unsatisfactory for tin in view of the low-ratio uptake of that metal by plants even with substantial quantities of cassiterite present in the soil.

(f) The profiles of the biogeochemical anomalies are rarely smooth and frequently have erratic values, high and low, whereas those in soils show a much smoother trend. In Nigeria, the minimum width of the biogeochemical anomaly for interesting lead-zinc veins is about 50 ft. In the Gunnislake area of Cornwall, the copper-tin anomaly widths in soil profiles are as narrow as 10 ft.

(g) The correct evaluation of the significance of "ore-positive" results, as compared with negative or background values, is dependent on an intimate knowledge of the particular area based on well-founded data of the background concentration of metals in a wide variety of species in the different soils forming on the several types of bed-rock. This data should be obtained from orientation surveys which should include traverses over known lodes, especially those which have been little disturbed by mining.

(h) One of the more frustrating aspects of the plant method of prospecting is the limitation imposed by inadequate distribution of trees, which precludes the maintenance of satisfactory sampling patterns. Although the plant investigations in Cornwall have contributed new geochemical data, it is evident that the method is unsuitable for prospecting in this area in view of the sparse vegetation and relatively narrow width of anomalies. Moreover, for tin, analysis of soils would be much more satisfactory, since the uptake of this metal by plants is so small. In tropical areas, however, where wide secondary dispersion of ore metals may be expected, the plant method may be more usefully employed, particularly for detecting lead, zinc, and copper mineralization.

Acknowledgements—I should like to thank the Geology Department of Imperial College for provision of spectrographic materials, and also the Central Research Fund Committee of the University of London for the finances for this research. I should also like to thank Dr. J. Butler of Imperial College for his helpful

criticism of the manuscript. The results appearing in this paper constituted part of a thesis for the University of London degree of Doctor of Philosophy, entitled "The Theory and Practice of Geochemical Prospecting," April 1953.

References

Brundin N. (1939) U.S. Patent No. 2,158,980.
Cannon H. L. (1952) *Amer. J. Sci.* **250,** 755–770.
Dorn v. P. (1937) *Der Biologe* (Munich) **6,** 11–13.
Dorn v. P. (1939) *Svenska Prospekterings Aktiebolaget* p. 11 Malmo.
Harbaugh J. W. (1950) *Econ. Geol.* **45,** 706–712.
Hedstrom H. and Nordstrom A. (1945) *Jernkontor. Ann.* **39,** 6–10.
Linstow O. v. (1929) *Abh. preuss. Geol. Land.-Aust.* N.F.H. **114,** 1–246.
Lovering T. S., Huff L., and Almond H. (1950) *Econ. Geol.* **45,** 493–514.
Maliuga D. P. (1947) *Akad. Nauk. Izv. Ser. Geol.* **3,** 135–138.
Mitchell R. L. (1948) Tech. Comm. 44, Commonwealth Bureau of Soil Science.
Rankama K. (1940) *Bull. Comm. Géol. Finlande* **126,** 90–106.
Robinson W. O., Lakin H., and Reichen L. E. (1947) *Econ. Geol.* **42,** 572–582.
Vogt T., Braadlie O., and Bergh H. (1943) *K. norske vidensk. Selsk.* **16,** 55–58.
Warren H. V. and Howatson C. H. (1947) *Bull. Geol. Soc. Amer.* **58,** 803–820.
Warren H. V. and Delavault R. E. (1948) *Geophys. J.* **13,** 609–624; (1949) *Bull. Geol. Soc. Amer.* **60,** 531–560.
Warren H. V., Delavault R. E., and Irish R. I. (1949) *Trans. Roy. Soc. Can.* **43,** 119–137.
Warren H. V. and Delavault R. E. (1950) *Bull. Geol. Soc. Amer.* **61,** 123–128.
Warren H. V., Delavault R. E., and Irish R. I. (1952) *Bull. Geol. Soc. Amer.* **63,** 435–484.
Webb J. S. and Millman A. P. (1950) *Bull. Instn. Min. Metall., Lond.* **518,** 3–16; (1951) *Bull. Instn. Min. Metall., Lond.* **537,** 473–504.
White W. H. (1950) *Canad. Min. Metall. Bull.* **43,** 368–371.

Geochimica et Cosmochimica Acta, 1957, Vol. 12, pp. 94 to 96. Pergamon Press Ltd., London

The distribution of Li, Rb, Cs, and Pb in some Yugoslav granites

G. Deleon
Savezni Geološki Zavod, Belgrade

and

L. H. Ahrens
Department of Geology and Mineralogy, Oxford

(*Received* 10 *August* 1956)

Abstract—Authors discuss the results of twelve spectrochemical analyses of granites and granodiorites. It is shown that Li content varies between 10 and 72 p.p.m., but most of the specimens lie in the range of 20 p.p.m. The K/Rb ratios agree well with already published data. An interesting Cs enrichment is reported. The Pb × 1000/K ratio values show some tendency to cluster around 0·4, 0·7–0·8, and 1·0.

A recent spectrochemical investigation of some granites and granodiorites from Serbia and Macedonia, Yugoslavia, has shown some interesting features. The number of specimens analysed is not sufficient to be representative of the acid igneous rocks of Yugoslavia, but the data are reported because they are the first quantitative trace element results from these rocks and are additional data for use in statistical studies.

In this paper, only the alkali elements and lead are considered, and discussion of the remaining trace elements will be reported elsewhere. Most of the results are of the same order of magnitude as published analyses of acid igneous rocks and agree with established regularities (Ahrens, 1952).

All analyses were performed spectrographically, using indium as internal standard for lead and the variable internal standard method for the alkalies (Ahrens, 1954a). These methods enable comparisons to be made with previously published analyses, particularly as G-1 and W-1 were used as standards (the

Table 1. Alkali and lead content

	%		p.p.m.						
Locality	K	Na	Li	Rb	Cs	Pb	Na/K	K/Rb	1000 × K/Pb
1. Lojane	6·67	1·69	10 ± 1	303 ± 5	5·0	31 ± 1	0·25	220	0·47
2. Kopaonik	3·22	2·72	20 ± 1	163 ± 3	9·2	26 ± 2	0·84	198	0·80
3. Željin	2·22	2·59	23 ± 0	115 ± 2	18·4 ± 0	22 ± 3	1·17	193	1·0
4. Tanda	3·66	2·52	19 ± 2	215 ± 15	21 ± 0.5	17 ± 1·5	0·69	170	0·46
5. Crnajka	2·84	2·56	22 ± 0	302 ± 1	14 ± 1	12 ± 2	0·90	94	0·42
6. Vagan	3·18	2·23	50 ± 1	181 ± 0	10·4 ± 1	25 ± 1	0·70	175	0·79
7. Darosava	3·44	2·52	72 ± 2	235 ± 2	115 ± 3	32 ± 0·5	0·73	146	0·93
8. Surdulica	2·05	2·58	24 ± 0	122 ± 0	3·7	16 ± 1	1·26	170	0·46
9. Kumgur	2·20	2·86	24 ± 1	110 ± 10	12 ± 2	15 ± 0·5	1·30	200	0·70
10. Ravno Bucje	1·72	3·03	17 ± 1	123 ± 3	5 ± 0·2	17·5 ± 2	1·76	140	1·02
11. Cer	2·39	2·62	58 ± 4	184 ± 5	23.5 ± 1·5	28 ± 1	1·09	130	1·17
12. Starevina	2·59	2·94	19 ± 0·5	110 ± 5	<1	19 ± 1	1·13	235	0·73

(1) granite
(2) grandiorite
(3) grandiorite
(4) granite
(5) granite
(6) granite
(7) granite
(8) grandiorite
(9) granite
(10) granite
(11) granite
(12) gneiss-granite

Rb values used were those reported by Herzog and Pinson, 1956). All analyses were made in duplicate except for unusual and controversial cases where four to six runs were made.

Alkali Elements

Table 1 shows that cesium has a much larger variation than Li or Rb. The same relationship has been observed for Rb and Cs in New England granites: see, for example, Ahrens (1954b), particularly Fig. 21.

The lithium values are more comparable with the average of 44 p.p.m. for North American granites (Ahrens, personal communication) than of the higher figures of 180 p.p.m. reported by Strock (1936) for German granites.

The Rb content is normal for these rock types. Only the Crnajka granite shows a K/Rb ratio different from that established by Ahrens (1952). (For corrected value of this ratio, see Taylor *et al.*, 1956.)

The amount of cesium reported in these rocks is of unusual interest. The Darosava granite (Fig. 1) shows extreme enrichment of Cs (115 p.p.m.) compared with the average of about 6–7 p.p.m. for granites (Ahrens, personal communication).

Of particular interest is the fact that the Darosava granite and the Vagan granite (10 p.p.m. Cs) form parts of the same intrusion (Mt. Bukulja), the localities being a few hundred yards apart. They show only minor differences in mineral composition. It is unlikely that small differences in the biotite content would affect the Cs content so markedly. Differential leaching of alkalies is improbable, for the rocks are very fresh and the Na/K ratio is similar.

A detailed study of the problem is now being carried out. Similar Cs enrichment has been noted in metamorphic aureoles in South-West England (C. Bowler, personal communication).

Lead

The Pb content varies between 12 and 32 p.p.m., corresponding to results from other granites. While K^{+} (1·33 Å) and Pb^{2+} (1·20 Å) have similar ionic radii, the K/Pb ratio is not constant.

Attention is drawn to the tendency of values of the Pb × 1000/K ratio to cluster around 0·4, 0·7, 0·8, and 1·0. This feature can be seen in other areas, but the number of analyses is too small to draw conclusions.

Acknowledgements—Grateful acknowledgement is made by one of us (G. D.) to the Director of Savezni Geološki Zavod, Belgrade, Yugoslavia, for a grant to work in the spectrographic laboratory of the Department of Geology and Mineralogy, Oxford, where facilities for research were kindly placed at his disposal by Professor L. R. Wager, D. L. H. Ahrens, and Dr. E. A. Vincent. Dr. S. R. Taylor kindly helped in the preparation of the manuscript and in carrying out the analyses.

References

Ahrens L. H. *et al.* (1952) Association of Rb and K and their abundance in common igneous rocks and meteorites. *Geochim. et Cosmochim. Acta* **2**, 229.

Ahrens L. H. (1954a) *Quantitative Spectrochemical Analysis of Silicates* Pergamon Press, London.

Ahrens L. H. (1954b) The lognormal distribution of the elements. *Geochim. et Cosmochim. Acta* **5,** 49.

Herzog L. F. and Pinson W. H. Jr. (1956) The Sr and Rb content of the granite G-1 and diabase W-1. *Geochim. et Cosmochim. Acta* **8,** 295.

Strock L. (1936) Zur geochemie des Lithiums. *Nachr. Ges. Wiss. Göttingen* IV, N.F. 1 No. 15 p. 171.

Taylor S. R. *et al.* (1956) Some anomalous K/Rb ratios in igneous rocks and their petrological significance. *Geochim. et Cosmochim. Acta* (in press).

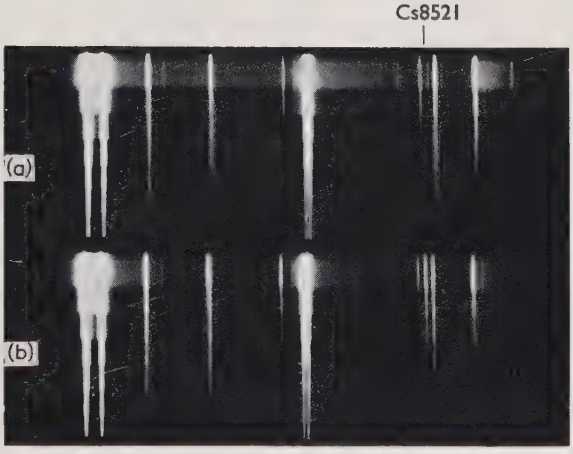

Fig. 1. Alkali-metal spectra of Bukulja mountain granites. (a) Vagan, (b) Darasova. Cesium enrichment in (b) is very marked.

Geochimica et Cosmochimica Acta, 1957, Vol. 12, pp. 97 to 102. Pergamon Press Ltd., London

The isotopic composition of the ammonia and the nitrate ion in rain

Thomas Hoering
Department of Chemistry, University of Arkansas, Fayetteville, Arkansas, U.S.A.

(*Received* 24 *October* 1956)

Abstract—The ammonia and the nitrate ions in rain-water have been quantitatively isolated with the use of ion exchange resins. The nitrogen isotope ratio of each fraction has been measured relative to atmospheric nitrogen. A kinetic isotope effect has been calculated on the basis of the formation of nitrate from atmospheric ammonia. The nitrogen-15 content of the two ions vary from rain to rain with respect to the nitrogen-15 content of atmospheric nitrogen. There is a constant kinetic isotope effect between the ammonia and nitrate ion of $1{\cdot}004_3 \pm 0{\cdot}001_4$. This result is in agreement with the postulate that the nitrate arises from the oxidation of ammonia. The isotope effect during the laboratory fixation of nitrogen with electric sparks was measured.

Introduction

It has long been assumed that electrical fixation of atmospheric N_2 is responsible for the nitrate ions in rain. This hypothesis appears reasonable by analogy with the industrial process for nitrogen fixation. The theories of the origin of nitrogen compounds in the atmosphere have been critically discussed by Hutchinson (1954). He concludes that atmospheric NH_3 arises from decomposition of organic matter and exists as NH_3 adsorbed on dust particles. He also concludes that little atmospheric nitrogen is fixed by lightning, but rather that the oxidation of ammonia is responsible for the presence of nitrate ions in rain.

This paper reports on the study of the amounts and the nitrogen isotope ratios of the nitrate ions and the ammonia in rain. The data has been examined on the basis that the nitrate is formed either by the reactions

$$N_2{}^{14} \xrightarrow{\text{oxidation}} 2N^{14}O \tag{1}$$

$$N_2{}^{15} \xrightarrow{\text{oxidation}} 2N^{15}O \tag{2}$$

or by a series of reactions

$$N^{14}H_3 \xrightarrow{\text{oxidation}} N^{14}O_3{}^- \tag{3}$$

$$N^{15}H_3 \xrightarrow{\text{oxidation}} N^{15}O_3{}^- \tag{4}$$

A kinetic isotope effect, β, is defined as follows. In the increment of time d the fractional decrease of heavy and light isotopic molecules is given by

$$\frac{d(A)}{(A)} = \beta \frac{d(A^*)}{(A^*)} \tag{5}$$

where A and A^* are the concentrations of the light and heavy isotopic molecules respectively. It has been shown that the expression for the isotope effect which

is obtained on partial conversion of reactants to products in processes of this kind may be put in the convenient form (NAIR, 1956; BIGELEISEN, 1949a, 1949b)

$$\beta = \frac{\ln (1 - f)}{\ln \left(1 - f \frac{r_p}{r_a{}^0}\right)} \tag{6}$$

where f is the fraction of the initial reactant which has been converted to nitrate, r_p is the N^{15}/N^{14} ratio in the nitrate fraction, $r_a{}^0$ is the initial N^{15}/N^{14} ratio in the reactant before oxidation has occurred.

If the nitrate in rain is formed by reactions (1) and (2), caused by electrical fixation, a comparison of the fractionation of nitrogen-15 between N_2 and NO_3 should give a constant value for β, the kinetic isotope effect. One may also examine the isotope effect in the electrical fixation of nitrogen in laboratory experiments and see if this fractionation has any relation to that observed in nature.

If the nitrate is formed by reactions (3) and (4), the fractionation of nitrogen-15 between the ammonia and the nitrate should give a constant value of β.

EXPERIMENTAL

Approximately 20 litre samples of rain were collected in clean enamelled containers placed on the roof of the chemistry laboratory. The samples were filtered through filter paper and stored in Pyrex glass containers. Tests with Nessler's reagent and with diphenyl amine reagent on the filter paper showed that no ammonia or nitrate was lost in this process. Processing of the sample usually began within a day after the end of the rain. It is assumed that any nitrite has been oxidized to nitrate in this time. Chemical operations were planned to minimize the danger of contamination of the samples with fumes of NH_3 and NH_4Cl found in a chemistry laboratory.

The ions were isolated by ion exchange chromatography. Dowex-50 × 8, 40-mesh in the lithium form was used to exchange ammonia from rain. Saturated $BaCl_2$ was used to elute the ions from the resin. Dowex-1 × 8, 40-mesh in the chloride form was used to exchange nitrate ions from rain. Saturated potassium chloride was used to elute the ions from the resin. Two columns, 100 mm long and 20 mm i.d., were placed in series and the filtered rain passed through at a rate of 1 to 2 litres per hour. The adsorbed ions were eluted completely in volumes of 100 ml. The nitrate ions were reduced quantitatively to ammonia by the zinc-iron method (GRIFFIN, 1927), and the ammonia from each fraction was distilled into an excess of standard acid and back-titrated with standard base.

During the separation, the filtered rain was siphoned through the ion exchange columns in a continuous stream without being exposed to the laboratory atmosphere. Attempts were made to isolate NH_3 from the air of the laboratory by drawing it through a wash-bottle containing dilute acid. In 24 hours, the amount of NH_3 which could be collected in this manner under normal conditions was not detectable with Nessler's reagent. A large volume of the redistilled water used in the experiments was carried through the separation procedure. A very low ammonia and nitrate blank was measured. All reagents used were tested for ammonia and nitrate impurities and found to be free from them. The isotopic composition of a number of commercial ammonium and nitrate compounds has been measured in this laboratory. With few exceptions, the nitrogen isotope ratios in these samples were very close to that of atmospheric nitrogen. Therefore, the results of these experiments would not be sensitive to small amounts of contamination from this source.

After the nitrogen analysis, the isolated ammonia was converted to N_2 by oxidation with sodium hypobromite (RITTENBERG, 1947). The resulting N_2 was purified (HOERING, 1955) and analyzed for the nitrogen isotope ratio, relative to atmospheric nitrogen, in a mass spectrometer designed for measurement of small differences in isotope content (MCKINNEY *et al.*, 1950).

The nitrogen isotope content of atmospheric N_2 is constant (Dole, 1954; Hoering, 1956). Samples of our standard were compared with the Bureau of Standards Isotope Reference Standard, and found to be identical to within 0·2 parts per thousand. Known amounts of reagent-grade ammonium chloride and sodium nitrate of known isotope ratios were put through the separation procedure. The nitrogen was completely recovered from each compound with little isotope fractionation. The results of the control experiments with reagent ammonia and nitrate indicate that the precision of the measurements is better than 0·6 parts per thousand difference in the ratio N^{15}/N^{14} relative to atmospheric N_2.

Laboratory experiments to maesure isotope fractionation during electrical fixation of nitrogen were performed. Electrodes of Pt and of W were sealed through a Pyrex tube. The gap between the points was about $\frac{1}{4}$ in. A spark was produced by a 10,000-V transformer. Air was pulled slowly through the spark and through a gas-washing bottle containing 0·1 M sodium hydroxide. The ozone produced during the discharge insured oxidation of all oxides of nitrogen to nitrate ion in the alkaline solution. Portions of this fixed nitrogen were reduced to NH_3, oxidized to N_2, and analyzed for the N^{15}/N^{14} ratio.

Experimental Results

Table 1 shows the experimental results of the quantitative analysis of rain for nitrate ions and ammonia and shows the results of the isotopic analysis of the two fractions. There is no apparent relation between the isotopic composition

Table 1. The quantitative analysis and the isotopic analysis of the ammonium and nitrate ions in rain

Date	n_{NH_3} (millimoles)	$n_{NO_3^-}$ (millimoles)	δ_{NH_3}	$\delta_{NO_3^-}$	f (calculated)	δ_{NH_3} (calculated)	β
June 12	0·511	0·362	+2·3	−2·7	0.415	+0·21	$1{\cdot}002_7$
June 12	0·274	0·388	+6·2	+3·4	0·549	+5·61	$1{\cdot}004_3$
June 16	0·699	0·582	−0·1	−7·2	0·431	−3·14	$1{\cdot}005_4$
June 19	0·149	0·608	+3·6	−4·0	0·803	−2·50	$1{\cdot}003_7$
June 28	0·220	0·540	+4·9	−4·7	0·711	−0·95	$1{\cdot}008_4$
August 10	0·350	0·580	+2·7	−3·1	0·624	−0·91	$1{\cdot}003_8$
August 14	0·245	0·570	+7·9	0·0	0·699	+2·38	$1{\cdot}005_4$
August 19	0·250	0·450	+9·0	+0·2	0·643	+3·34	$1{\cdot}002_7$
August 19	0·248	0·190	+4·5	+2·6	0·434	+3·69	$1{\cdot}002_0$
							$1{\cdot}004_3 \pm 0{\cdot}001_4$

of the nitrate ion and atmospheric nitrogen. (Atmospheric N_2 is defined equal to zero on this scale.) The data is then treated on the basis of reactions (3) and (4) and an isotope effect is calculated by equation (6). The following quantities are defined:

n_{NH_3} and $n_{NO_3^-}$ are the millimoles of each species isolated from the same sample of rain.

δ is defined as the parts per thousand difference in the N^{15}/N^{14} ratio compared to atmospheric nitrogen as the standard

$$\delta = \frac{(N^{15}/N^{14})_x - (N^{15}/N^{14})_{std}}{(N^{15}/N^{14})_{std}} \times 1000 \qquad (7)$$

f is the fraction of the initial ammonia which has been oxidized to NO_3^-, and is given by

$$f = \frac{n_{NO_3^-}}{n_{NH_3} + n_{NO_3^-}} \tag{8}$$

$\delta^0_{HN_3}$ is the calculated initial value of the N^{15}/N^{14} per mil difference in the ammonia fraction before oxidation has occurred.

$$\delta^0_{NH_3} = \frac{\delta_{NH_3} n_{NH_3} + \delta_{NO_3^-} n_{NO_3^-}}{n_{NH_3} + n_{NO_3}} \tag{9}$$

The value of the fraction $r_p/r_a{}^0$ in equation (3) is given by

$$r_p/r_a{}^0 = \frac{1 + \frac{\delta_{NO_3^-}}{1000}}{1 + \frac{\delta^0_{NH_3}}{1000}} \tag{10}$$

Small isotope effects were observed in the laboratory fixation of nitrogen with electric sparks. The nitrogen fixed between platinum points measured +1·4 parts per thousand higher than atmospheric nitrogen. Nitrogen fixed between tungsten points measured —0·5 parts per thousand lower than atmospheric nitrogen.

DISCUSSION

The data of Table 1 shows that although the N^{15}/N^{14} ratios of the two nitrogen-containing fractions vary from rain to rain relative to atmospheric N_2, they are related to each other by equations (3) and (4) with a kinetic isotope effect of $1{\cdot}004_3 \pm 0{\cdot}001_4$. The reasonably constant value of the isotope effect is evidence that reactions (3) and (4) are satisfactory explanations for the presence of nitrate ions in rain.

The data in Table 1 can be used to calculate an apparent equilibrium fractionation factor of $1{\cdot}007_7 \pm 0{\cdot}001_2$ for the exchange

$$N^{14}H_3 + N^{15}O_3^- = N^{15}H_3 + N^{14}O_3^- \tag{11}$$

However, from a consideration of the chemistry of ammonia and nitrate ion, it seems very unlikely that they enter into any equilibrium, as in equation (11). The rate of nitrogen between ammonia and nitric acid is undoubtedly very slow under the conditions in rain-water. Ratio of partition functions for isotopic species of nitrate ion are not known and an equilibrium fractionation factor for (11) cannot be calculated. From the general trends of fractionation factors, one might expect this factor for (11) to be less than 1. Examination of calculated and measured equilibrium fractionation factors show that in general the heavy isotope concentrates in the more oxidized form of the element (UREY, 1947).* Therefore, equilibrium processes such as (11) have not played any part in the observed fractionation and the apparent constant value of the equilibrium fractionation factor is fortuitous.

* Only three exceptions to this are known to the author. They are carbon monoxide, nitric oxide, and ammonium ion.

The average deviation of the isotope effect, β, calculated in Table 1 is two to three times the error expected from chemical manipulation and mass spectrometer analysis. This may be due to the fact that some difficulty was experienced in getting a clean separation of the nitrate ion from the organic matter in rain. The ratio of nitrate to ammonia measured in these experiments is somewhat higher than has been reported (Hutchinson, 1954). The value of β calculated by equation (3) is insensitive to the value of f used for such small isotope effects noted in these experiments.

Ingerson (1953) has suggested that nitrates fixed by lightning should be depleted in N^{15} with respect to atmospheric nitrogen if the N_2 and NO are in equilibrium at a low enough temperature:

$$N_2^{14} + 2N^{15}O = N_2^{15} + 2N^{14}O \qquad (12)$$

The calculated enrichment factor for this reaction is 1·015 at 25°C. (It should be noted that this equilibrium is one of the few exceptions to the rule that the heavy isotope concentrates in the more oxidized form.) The laboratory experiments on electrical fixation indicate that either N_2 and NO are not in equilibrium during the process or else that the effective temperature is too high and the fractionation small. As the nitrate isolated from rain is sometimes higher, sometimes lower in nitrogen-15, than atmospheric nitrogen, reaction (12) probably has not been important in the production of nitrate.

One may examine the possibility that the nitrate arose from electrical fixation of N_2 and that the ammonia has been produced from the nitrate. If this were the case, one would expect the ammonia to be depleted in nitrogen-15 relative to the nitrate since the lighter isotope would react faster. The data in Table 1 show the opposite to be true.

The observed value for the kinetic isotope effect, $1{\cdot}004_3$, is small compared to that expected for the breaking or the formation of a bond to nitrogen (Bigeleisen, 1949a). A mechanism in which the rate of the reaction is controlled by diffusion of a reactant may have an isotope effect of this magnitude. Hutchinson (1954) suggests that photochemical oxidation of ammonia to nitrate ion may be important. The exact value of the expected isotope effect in either case is not known.

Acknowledgements—This work was supported by funds of the U.S. Atomic Energy Commission through Contract AT-(40-1)-1313 with the University of Arkansas. The assistance of Forrest Carter in performing the chromatographic separations is acknowledged.

References

Bigeleisen J. (1949a) Isotope reaction velocities. *J. Chem. Phys.* **17,** 675.

Bigeleisen J. (1949b) The validity of the use of tracers to follow chemical reactions. *Science* **110,** 14.

Dole M. (1954) Isotopic composition of atmospheric oxygen and nitrogen. *Geochim. et Cosmochim. Acta* **6,** 65.

Griffin R. C. (1927) *Technical Methods of Analysis,* McGraw-Hill, New York.

Hoering T. C. (1955) Variations of nitrogen-fifteen abundance in naturally occurring substances. *Science* **122,** 1233.

HOERING T. C. (1956) *Nuclear Processes in Geological Settings* Proceedings of the Second Conference of the Subcommittee on Nuclear Geophysics of the National Research Council, Pennsylvania State University, September 1955.

HUTCHINSON G. E. (1954) *The Earth as a Planet* Vol. II. *The Solar System* Chapter 8. *The Biochemistry of the Terrestrial Atmosphere* (Ed. G. P. KUIPER) University of Chicago Press.

INGERSON E. (1953) Nonradiogenic isotopes in geology. *Bull. Geol. Soc. Amer.* **64,** 301.

MCKINNEY C. R., MCCREA J. M., EPSTEIN S., ALLEN H. A., and UREY H. C. (1950) Improvements in mass spectrometers for the measurement of small differences in isotope abundance ratios. *Rev. Sci. Instrum.* **21,** 724.

NAIR P. M. (1956) Ph.D. thesis, University of Arkansas.

RITTENBERG D. (1947) *Preparation and Measurement of Isotopic Tracers* p. 31. Edwards Bros., Ann Arbor, Michigan.

UREY H. C. (1947) Thermodynamic properties of isotopic substances. *J. Chem. Soc.* 562.

Geochimica et Cosmochimica Acta, 1957, Vol. 12, pp. 103 to 122. Pergamon Press Ltd., London

Partial molar volumes of some salts in aqueous solutions*

E-an Zen

(*Received* 18 *June* 1956)

Abstract—A considerable body of information exists on the densities of aqueous solutions of simple electrolytes at different temperatures. From these data the partial molar volumes of these salts in solution have been computed as functions of concentration and temperature. Knowledge of these volumes has further enabled a calculation of the partial molar volumes of water in the corresponding solutions through the use of the Gibbs-Duhem equation.

Many difficulties arise as one attempts to extrapolate the volume data to infinite dilution. One common problem is the lack of sufficiently accurate density data at low concentrations. Another major difficulty is the lack of a reliable theory of electrolytic solutions at high concentrations; for the Debye-Hückel theory is valid only for very dilute solutions, and cannot be used in many cases of geologic interest.

It is found that at low concentrations the partial molar volumes of the ions are approximately additive. These "ionic partial molar volumes" are tabulated; from these the partial molar volumes of salts for which no direct data exist may be estimated. The additive relation is best obeyed by univalent salts, and becomes progressively less satisfactory as the ionic charges increase.

The partial molar volumes of most of the studied salts are less than their molar volumes in the solid state; and so their pressure coefficients of solubility are positive. Such information is useful in many geochemical problems. Some possible applications are suggested and summarized, and examples given.

Introduction

A considerable proportion of the minerals in chemically precipitated sediments are relatively simple salts which in aqueous solutions form electrolytes. As geologists, we are interested in the solubilities of these salts in natural waters, as functions of the physical and chemical variables which are operative.

The variables that affect the solubility of a given salt in water are: composition of the water, temperature, and pressure. The effect of temperature depends on the difference between the partial molar entropies of the salt in the two phases, solid and solution; and the effect of pressure, the corresponding difference in the partial molar volumes. The present study is concerned with the latter effect, and is devoted principally to a compilation of data from numerous sources.

Theoretical Considerations

The effect of changing pressure on the solubility of a given simple salt under isothermal conditions is given by the requirement that the chemical potentials of that salt in the solid state and in solution shall remain equal. Now, if G denotes the total Gibbs free energy of a given phase, T the absolute temperature, P the hydrostatic pressure, and n_i^α the number of moles of the ith salt in a given phase α, then the chemical potential is defined by the differential equation

$$\mu_i^\alpha = \left(\frac{\partial G}{\partial n_i}\right)^\alpha_{T,P,n_i} \tag{1}$$

where the subscripts outside of the parentheses indicate quantities held constant.

* Contribution no. 368, Department of Mineralogy and Petrology, Harvard University.

The condition of chemical equilibrium under changing pressures then leads to the relation (see, for instance, PRIGOGINE and DEFAY, 1954, p. 366)

$$\left(\frac{\partial N_i}{\partial P}\right)^{\beta}_{T} = \frac{V_i^{\alpha} - \bar{V}_i^{\beta}}{(\partial \mu_i / \partial N_i)^{\beta}_{T,P}} \tag{2}$$

where:

$$\left(\frac{\partial \mu_i}{\partial P}\right)_{T,N} = \bar{V}_i \equiv \left(\frac{V_{(n)}}{\partial n_i}\right)_{T,P,n_j} \tag{3}$$

and where phase α is also assumed to be pure, so that $\bar{V}_i^{\alpha} = V_i^{\alpha}$, the molar volume.

Numerical evaluation of the pressure coefficient of solubility $(\partial N_i/\partial P)_T$ requires knowledge of the volumes and also the factor $(\partial \mu_i/\partial N_i)_{T,P}$. Unfortunately, the latter quantity can be explicitly calculated only for very dilute solutions, for which the Debye-Hückel theory is valid. However, for a thermodynamically stable phase, this quantity must remain positive for all i's (GIBBS, 1878, p. 113; PRIGOGINE and DEFAY, 1954, p. 221); hence, if we can evaluate the volume terms, the qualitative effect of pressure on solubility for a given salt can still be stated. This information is helpful in many sedimentological and geochemical problems.

The molar volumes of most simple salts are known, to varying degrees of accuracy, through crystallographic studies. The partial molar volumes of these same salts in aqueous solutions can be derived from density data of the solutions; a number of these in fact have already appeared in the chemical literature.

PARTIAL MOLAR VOLUMES

Volume data on aqueous solutions of electrolytes are usually tabulated in terms of weights per cent of the salt versus densities of the solutions at specified temperatures and 1-atm pressure. In the present study, the data are first converted to the formula or mole fractions of the salt, N_2, and the mean molar volume of the solution, $\tilde{V}$, where

$$\tilde{V} = V/n = (1 - N_2)\bar{V}_1 + N_2\bar{V}_2 \tag{4}$$

for a binary system.

Several methods of handling the data are available. A graphical method, due to ROOZEBOOM (LEWIS and RANDALL, 1923, p. 38), requires the determination of the tangents to a plot of $\tilde{V}$ versus N. The intercepts of this tangent at $N_2 = 0$ and $N_2 = 1$ give the corresponding values of $\bar{V}_1$ and $\bar{V}_2$, respectively. In practice, however, this method is unsuitable, since very slight misfits of an analytical expression or graph to the data may result in large errors in the derivative values. Accordingly, this method was abandoned in favour of the method of the apparent molar volumes.

The apparent molar volume of a solute is defined as the total volume change upon addition of n moles of the salt, assuming the partial molar volume of the solvent to be equal to its molar volume, V_1^0:

$$\phi_2 = \frac{V - n_1 V_1^0}{n_2} \tag{5}$$

where, and hereafter, the subscript "1" shall denote the solvent, "2" the solute, and the superscript "0" the pure state. In terms of mole fractions,

$$\phi_2 = \frac{\tilde{V} - N_1 V_1^0}{N_2} \tag{6}$$

To use the method of apparent volumes, we observe that, if the mean molar volume is expanded in a Taylor series in terms of N_2 and equated with (4), we obtain, for the first three terms of the expansion corresponding to a moderately dilute solution,

$$\bar{V}_1 = V_1^0 + \frac{N_2^2}{2}\left(\frac{\partial \bar{V}_2}{\partial N_2}\right)_{T,P;N_2=0} \tag{7}$$

where use is made of the relation (Guggenheim, 1950, p. 174)

$$\left(\frac{\partial \tilde{V}}{\partial N_2}\right)_{T,P} = \bar{V}_2 - \bar{V}_1 \tag{8}$$

Substituting (7) and (6) into (5), we get

$$\bar{V}_2 = \phi_2 - \frac{N_1 N_2}{2}\left(\frac{\partial \bar{V}_2}{\partial N_2}\right)_{T,P;N_2=0} \tag{9}$$

Now, empirically it has been found (Masson, 1929; Scott, 1931; Geffcken, 1931) that over wide ranges of concentrations the apparent molar volumes of many electrolytes are linear functions of the square root of the molar concentrations,

$$\phi_2 = \phi_2(0) + ac^{1/2} \tag{10}$$

where a is a constant and c is the volume molarity. Since

$$C_2 = N_2/\tilde{V} \tag{11}$$

and $\tilde{V}$ is only a slowly-varying function of N_2, we have, very nearly,

$$\phi_2 = \phi_2(0) + \left(\frac{\partial \phi_2}{\partial N_2^{1/2}}\right)_{T,P} N_2^{1/2} \tag{12}$$

where $(\partial \phi_2/\partial N_2^{1/2})_{T,P}$ is a constant (equation 12 may be taken as the first two terms of a Taylor expansion). Substitution of (12) into (9) leads to the result

$$\bar{V}_2 = \phi_2(0) + \tfrac{1}{2} N_2^{1/2}\left(\frac{\partial \phi_2}{\partial N_2^{1/2}}\right)_{T,P}(3 - N_2) \tag{13}$$

where we have made use of the relations

$$\frac{\partial}{\partial X} = \frac{1}{2X^{1/2}} \cdot \frac{\partial}{\partial X^{1/2}} \tag{14}$$

and

$$\frac{\partial \bar{V}_2}{\partial N_2} = -2\frac{\partial \phi_2}{\partial N_2} \tag{15}$$

to the indicated order of approximation. Equation (13) is the basis for all subsequent calculations.

In practice, the adapted procedure is as follows. The values of $\phi(N_2)$ are first calculated, and plotted against $N_2^{1/2}$ to determine the range of approximate validity of relation (12). The data are next fitted by least-squares method to a straight line and substituted into equation (13) to yield the values of $\bar{V}_2$. The range of validity of (12) is severely limited by the quality of the data, a factor which will be discussed next. Tables 1–4 give the results, in terms of the coefficients $\partial\phi_2/\partial N_2^{1/2}$ and the limiting values $\bar{V}_2(0) = \phi(0)$, for twenty-one salts and for four temperatures. The values are given only to the first decimal place, since it is felt that the accuracy of the data does not justify another. For salts other than uni-univalent, even this figure is probably unreliable.

Partial Molar Volume of H_2O

The partial molar volume of H_2O in a solution can be obtained from a knowledge of the partial molar volume of the solute through the Gibbs-Duhem relation:

$$\frac{\partial\bar{V}_1/\partial N_2}{\partial\bar{V}_2/\partial N_2} = -N_2/N_1 \tag{16}$$

with $\bar{V}_2$ given by (13), we have

$$\frac{\partial\bar{V}_2}{\partial N_2} = \frac{3}{4}\frac{\partial\phi_2}{\partial N_2^{1/2}}[N_2^{-1/2} - N_2^{1/2}] \tag{17}$$

and so

$$\bar{V}_1(N_2) - V_1^0 = -\frac{3}{4}\frac{\partial\phi_2}{\partial N_2^{1/2}}\int_0^{N_2}\frac{N_2^{1/2} - N_2^{3/2}}{1 - N_2}\,dN_2 \approx -\frac{1}{2}\frac{\partial\phi_2}{\partial N_2^{1/2}}N_2^{3/2} \tag{18}$$

for moderately dilute solutions. We can estimate the magnitude of this correction term as follows. For uni-univalent salt the coefficient is at most around 25. For $N_2 = 0{\cdot}01$, the correction is $2{\cdot}5 \times 10^{-2}$ c.c. For a bi-bivalent salt, the coefficient is no more than 50; hence for $N_2 = 0{\cdot}005$ (which gives a solution of comparable normality) the correction is no more than 0·02 c.c. For our purposes these are completely negligible.

Evaluation of the Data

The data used in the compilation came from a variety of sources, and therefore their reliability should be examined.

Most of the density data were taken from the International Critical Tables, which are already compilations, sometimes composite, of experimental results. In general, the actual density determinations were carried out at temperatures and concentrations different from the tabulated values, and obviously interpolations of the data have been carried out. Uncertainties introduced by these interpolations are not stated. It is thus impossible to estimate their effect on the partial molar volumes.

If the densities were determined on moderately concentrated solutions and the results extrapolated to lower concentrations, gross errors may be introduced. As

Table 1. Partial molar volumes, in c.c./mole, of selected salts at 25°C

Salt	$\phi(0)$	$\frac{\partial \phi_2}{\partial N_2^{1/2}}$	Ref.	Other authorities	
				$\phi(0)$	Ref.
CsCl	39·3	14·07	1	39·2	5
				39·02	18
				39·15	19
KCl	26·4	17·63	1	26·742	8
	26·4	18·34	3	26·74	6
				26·27	12
				26·8	5
				26·81	9
				26·36	18
				26·52	19
NaCl	16·8	13·16	1	16·67	6
	15·9	19·81	2	17·03	7
				16·6	5
				16·538	8
				16·28	18
				16·40	19
HCl	18·0	6·34	1	17·755	8
	17·4	12·74	2	18·1	5
				18·07	6
				17·83	10
				17·98	11
				18·20	18
CsBr	45·8	16·75	1	46·1	5
				46·20	18
				46·19	19
KBr	33·4	18·77	3	33·97	6
				33·7	5
				33·54	18
				33·73	19
NaBr	23·4	12·62	1	23·48	9
				23·45	18
				23·51	19
HBr	24·2	7·13	1		
KNO_3	38·2	14·60	1	38·0	5
$NaNO_3$	27·8	17·33	1	27·48	12
HNO_3	29·0	6·67	1		
KOH				3·4	5
NaOH				−6·8	5
$CaCl_2$	18·4	42·74	1	16·86	6
				18·5	5
				18·26	13
$MgCl_2$	15·6	44·77	1	14·50	6
				15·3	5
K_2CO_3	12·2	82·17	1		
Na_2CO_3	−6·0	87·96	1	−6·7	5
K_2SO_4	30·1	122·51	3	32·28	6
				31·9	5
Na_2SO_4	10·9	95·21	1	11·5	5
				11·52	9
H_2SO_4	14·9	537·76	4		
	29·4	65·45*	1		
$MgSO_4$	−3·9	78·24	1		

* The better value to use at N_2 greater than 0·002.

Table 2. Partial molar volumes, in c.c./mole, of selected salts at 20°C

Salt	$\phi(0)$	$\frac{\partial \phi_2}{\partial N_2^{1/2}}$	Ref.	Other authorities	
				$\phi(0)$	Ref.
CsCl	38·7	16·22	1	39·03	14*
KCl	26·0	17·90	1	26·07	15
				26·97	14
NaCl	16·1	14·89	1	15·98	15
				17·03	14
HCl	17·8	6·24	1	17·75	11
CsBr	45·1	18·64	1	45·32	14
NaBr	22·8	13·43	1	23·27	14
HBr	23·4	10·56	1		
KNO_3	37·3	18·09	1		
$NaNO_3$	27·0	18·95	1		
HNO_3	28·6	5·90	1		
KOH				3·48	15
NaOH	−6·4	23·64	1	−6·52	16
				−5·57	14
$CaCl_2$	17·6	45·37	1		
$MgCl_2$	15·5	43·28	1		
K_2CO_3	10·2	93·79	1		
Na_2CO_3	−7·6	94·88	1		
Na_2SO_4	10·3	88·40	1		
$MgSO_4$	−4·8	81·66	1		

* BERNAL and FOWLER give their data in terms of cubic angstroms per ion. In converting the data, their value of Avogadro's number, $N = 6{\cdot}06 \times 10^{23}$, has been used (BERNAL and FOWLER, 1933, p. 525).

Table 3. Partial molar volumes, in c.c./mole, of selected salts at 10°C

Salt	$\phi(0)$	$\frac{\partial \phi_2}{\partial N_2^{1/2}}$	Ref.	Other authorities	
				$\phi(0)$	Ref.
CsCl	37·3	18·10	1		
KCl	25·0	19·27	1	24·78	15
NaCl	14·7	17·17	1	14·45	15
HCl	17·2	6·37	1	17·16	11
CsBr	43·7	20·11	1		
NaBr	21·0	17·70	1		
KNO_3	35·3	21·67	1		
$NaNO_3$	25·5	17·71	1		
HNO_3	27·3	6·64	1		
KOH				1·86	15
NaOH	−9·1	36·19	1	−8·16	16
$CaCl_2$	15·7	51·13	1		
$MgCl_2$	14·6	45·16	1		
K_2CO_3	7·8	96·85	1		
Na_2CO_3	−10·1	99·65	1		
Na_2SO_4	8·6	86·18	1		
$MgSO_4$	−6·7	88·29	1		

an example, the partial molar volume of sulphuric acid at 25°C is found to be 29·4 c.c./mole when the International Critical Tables data are used. However, the lowest concentration of the actually measured solution was 5 wt. per cent (Domke

Table 4. Partial molar volumes, in c.c./mole, of selected salts at 0°C

Salt	$\phi(0)$	$\frac{\partial \phi_2}{\partial N_2^{1/2}}$	Ref.	Other authorities	
				$\phi(0)$	Ref.
CsCl	35·7	20·85	1	35·40	18
				35·23	19
KCl	23·4	20·29	1	23·05	15
				23·97	17
				23·00	18
				23·00	19
NaCl	13·1	19·08	1	12·57	15
				13·45	17
				12·4	18
				12·36	19
HCl	16·5	5·98	1	16·40	11
CsBr	41·7	24·35	1	41·95	18
				41·95	19
NaBr	18·9	21·74	1	18·95	18
				18·86	19
KNO_3	32·5	28·42	1		
$NaNO_3$	22·4	26·34	1		
HNO_3	25·6	7·92	1		
KOH				−0·50	15
NaOH	−12·9	50·36	1	−10·58	16
$CaCl_2$	13·8	50·64	1		
$MgCl_2$	12·7	49·37	1		
K_2CO_3	2·7	117·19	1		
Na_2CO_3	−15·1	115·58	1		
Na_2SO_4	3·7	104·30	1		
$MgSO_4$	−10·0	99·79	1		

KEY TO TABLES 1–4

1. *International Critical Tables* Vol. III.
2. Wirth, 1940b.
3. Wirth, 1937.
4. Klotz and Eckert, 1942.
5. Owen and Brinkley, 1941.
6. Wirth, 1940a.
7. Adams, 1931.
8. Owen and Brinkley, 1949.
9. Geffcken and Price, 1934.
10. Redlich and Bigeleisen, 1942.
11. Akerlof and Teare, 1938.
12. Drucker, 1941.
13. Gucker, 1934.
14. Bernal and Fowler, 1933.
15. Akerlöf and Bender, 1941.
16. Akerlöf and Kegeles, 1939.
17. Batuecus, 1946.
18. Geffcken, 1931.
19. Scott, 1931.

and Bein, 1905, p. 132), which is fairly concentrated; although in the International Critical Tables compilation of the original data densities are given for all integral percentages of sulphuric acid between zero and 5%. On the other hand, when the dilute-solution data of Klotz and Eckert (1942) were used, a value of 14·9

c.c./mole was obtained. At higher concentrations ($N_2 > 0{\cdot}002$) the values of ϕ computed from the two sets of data agree closely, as they should.†

High-dilution data, on the other hand, are subject to large errors of a different kind, since in this range the actual concentrations of the solutions are subject to large experimental uncertainties. Such errors may or may not be removed by statistical treatment of the results (for example, see Owen and Brinkley, 1949, p. 763).

A number of other sources of experimental errors may be cited. Unfortunately, due to incomplete specification of experimental details accompanying the data, the importance of these contributions cannot be evaluated.

(1) *Temperature control.* Most of the determinations were made in thermostated baths. Although high precision and sharp controls are commonly claimed, the possibility of systematic errors remains. Since, however, the thermal expansivities of the solutions are not large, as a rule, the errors due to this source are probably negligible.

(2) *Purity of the chemical reagents used.* It is impossible to evaluate this source of error, since only in a few instances is special attention given to the purity of the reagents. The accepted density and actual purity of water add further, though likely small, possible errors to the results.

Conversion of the data into partial molar volumes bring in additional sources of error. Some of these follow.

(1) Using the linear relation, equation (12), in extrapolating the data. This source of error is most serious for salts involving polyvalent ions, however even for uni-univalent salts at N_2 less than 0·01, plots of $N_2^{\frac{1}{2}}$ against ϕ_2 often show decided curvatures. In fitting the least-squares straight line to the data, we have tacitly taken the "scatter" of the data to be random.

(2) The empirical rule of Masson and Geffcken is given in terms of the volume molarity. In this paper, on the other hand, the mole fraction has been used. This introduces a systematic error which increases with concentration and becomes zero at zero concentration. It can be readily verified, however, that for salts whose values of $\partial\phi_2/\partial N_2^{\frac{1}{2}}$ are as large as 100, the error due to this approximation, for N_2 as large as 0·01, is only about 0·01 c.c.; for our purposes this is acceptable. Because the mole fraction is a more convenient thermodynamic variable than the molarity in many applications, the former is chosen despite the aforementioned approximation.

(3) Errors due to extrapolation of data are minimized by the least-squares method only in so far as these are truly random. The method is in no wise capable of detecting systematic errors.

Other possible sources of error have been reviewed by Scott (1931).

Comparison with Data in the Literature

Column 5 of Tables 1–4 gives the values of $\phi(0)$ for a number of salts as computed by other workers. These data require only a few comments. Firstly, there is a discrepancy between the results of Adams and the present writer (ref. 1) on NaCl at 25°C. Since the International Critical Tables, as well as Adams, derived the numerical values essentially from Hall's data (1924), the discrepancy represents a minimum measure of the sensitivity of the results to

† It should be pointed out that sulphuric acid presents an extreme case due to incomplete ionization at moderate concentrations. For most uni-univalent salts the concentration dependence will not be so critical.

methods of treatment of the original data. The present results, however, agree closely with those of WIRTH (1940b) based on an independent set of measurements. It is also close to the critical data of OWEN and BRINKLEY (1941). Secondly, the results of AKERLÖF *et al.* are deduced from solutions of moderate to high concentrations; thus the close agreement suggests the extent of validity of the rule of MASSON and GEFFCKEN, verifying the conclusions of SCOTT. Finally, we notice that the agreement between different authors on uni-bi, bi-uni, and bi-bivalent salts are generally poor. Solutions of such salts commonly behave nonlinearly except at high dilutions, and the volume data presented here must be used only as crude first approximations.

PARTIAL MOLAR VOLUMES OF IONS

In solutions at infinite dilution, the interactions between solute ions vanish; it then becomes possible to regard the partial molar volume of an electrolyte as the sum of ionic contributions. In fact, even at finite concentrations, as long as the linear relationship (12) holds, we might expect the approximation to be valid:

$$\bar{V}_2(N_2) \approx \sum_r \nu_r \bar{V}_r(0) + \sum_r \nu_r \left(\frac{\partial \bar{V}_r}{\partial N_2}\right)_{N_2=0} N_2 \tag{19}$$

where ν_r is the stoichiometric coefficient of ionic species r, and $\bar{V}_r$ is the ionic partial molar volume. This additive property has been found to be valid at infinite dilution by a number of workers. Thus, AKERLOF and BENDER (1941) find that it is obeyed by simple alkali halides and hydroxides; and WIRTH (1940a) arrives at a similar conclusion for a number of electrolytes important in sea-water. FAJANS and JOHNSON (1942) produce a similar table of $\phi(0)$ for a large number of uni-, bi-, and trivalent ions. The most satisfactory table published to date, however, seems to be that of BERNAL and FOWLER (1933).

Since experimentally one always deals with neutral salts whose volume represents the sum of all participating ionic contributions, these latter values can be obtained only by making additional stipulations. WIRTH assumes that

$$\bar{V}_{K^+} = \bar{V}_{F^-}$$

and obtains his series of ionic partial molar volumes. FAJANS and JOHNSON assume, on the other hand, that at infinite dilution

$$\bar{V}_{NH_4^+} = \bar{V}_{Cl^-} = V_{H_2O}$$

and thereby obtain a similar series of values which are numerically different from those given by WIRTH.

The assumption made by BERNAL and FOWLER, and used also by DARMOIS (1941), amounts to the statement that for cesium chloride the ratio of the ionic partial molar volumes in an infinitely dilute solution is equal to the same ratio in crystalline CsCl:

$$\bar{V}_{Cs^+}/\bar{V}_{Cl^-} = V_{Cs}^{x}/V_{Cl}^{x} \tag{20}$$

This assumption appears less stringent than the others, in that it demands only the equality of certain ratios and not the actual sizes. Furthermore, since on an atomic scale the partial molar volume of an ion is doubtless intimately related to its hydration characteristics, which depend on the size and charge of the ion, the use of cesium and chloride ions with their large and roughly comparable

sizes makes assumption (20) seem plausible. On the other hand, this assumption, which we adapt for this discussion, depends on the presumption of a knowledge of the ionic radii in solid CsCl. Experimentally, however, only the sums of the radii are measurable quantities, and their breakdown into ionic contributions are rather arbitrary. The same arbitrariness is carried into the ionic partial molar volumes. It is fortunate that in any application of the data we always deal with neutral salts, and so the errors due to the assumption will cancel out exactly.

In Tables 5–8 the results of calculations, using assumption (20), are presented. The scheme of computation is indicated below.

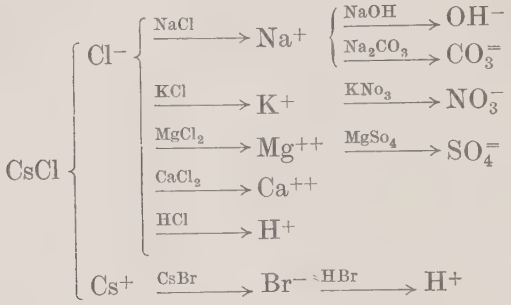

The data are given to one more significant figure than in Tables 1–4 to expedite rounding-off of the figures in any application.

The additive property can be checked by comparison of the results of Tables 5–8 with directly determined values of the partial molar volumes. A few typical results are given in Table 9; the agreements are satisfactory in view of all the experimental and computational uncertainties.

In examining Table 9, notice that for the weak electrolytic radicle CO_3^{--} the process of hydrolysis is ignored. This means that the values given are the "apparent" partial molar volumes, except at infinite dilution when ionization becomes complete. This procedure is justified on the ground that the objective of this study is to analyse the effect of pressure on solubility, and it is the net volume change that concerns us. Consistent with the assumption of additivity of the ionic volumes, the value for the carbonate ion ("apparent") is the same for a given concentration, whatever the other ions present; it is the value to be used in any computation.

We might also have treated the partial molar volume of H_2O by regarding it as a sum of contributions from all existing solute ions. Since, however, the partial molar volume of H_2O in solution is nearly equal to that in the pure phase, such calculations are unnecessary for the present purposes.

DISCUSSION

The preceding data should be used with caution in actual situations. The need for precautions stems from the assumptions that have gone into the calculations.

In the first place, all the calculations refer strictly to the volumes at 1-atm pressure; while in many geological problems the pressure may be considerably higher. However, for most electrolytes the partial molar compressibilities, in particular the difference between these and the corresponding compressibilities of the solids, integrated over the pressure range, is certainly small. For example, using the data of ADAMS (1931, p. 3797) and BIRCH *et al.* (1942, p. 52), we find that for infinitely dilute solution of NaCl, the value of β is about 28×10^{-6}, whereas

Table 5.* Ionic partial molar volumes, in c.c./formula, at 25°C, using data of Table 1

N_2	CsCl	Cs^+	K^+	Na^+	H^+	Br^-	Cl^-	NO_3^-	Ca^{++}	Mg^{++}	SO_4^{--}	CO_3^{--}	N_2
0·00	39·26	17·00	4·13	−5·50	−4·56	28·79	22·26	34·05	−26·15	−28·88	24·95	5·02	0·00
0·0005	39·73	17·20	4·45	−5·32	−4·68	29·15	22·53	34·22	−25·67	−28·36	26·28	6·76	0·00025
0·001	39·93	17·29	4·58	−5·25	−4·73	29·30	22·64	34·29	−25·47	−28·14	26·83	7·48	0·0005
0·002	40·21	17·41	4·77	−5·15	−4·80	29·50	22·80	34·38	−25·19	−27·83	27·61	8·49	0·0010
0·003	40·42	17·50	4·92	−5·07	−4·85	29·67	22·92	34·46	−24·98	−27·59	28·21	9·28	0·0015
0·004	40·60	17·58	5·04	−5·00	−4·90	29·80	23·02	34·52	−24·80	−27·40	28·71	9·93	0·0020
0·005	40·75	17·64	5·15	−4·95	−4·94	29·92	23·11	34·58	−24·64	−27·22	29·15	10·52	0·0025
0·006	40·89	17·71	5·24	−4·89	−4·97	30·03	23·19	34·63	−24·49	−27·06	29·55	11·04	0·0030
0·007	41·02	17·76	5·33	−4·85	−5·01	30·12	23·26	34·67	−24·36	−26·91	29·92	11·52	0·0035
0·008	41·15	17·81	5·42	−4·80	−5·04	30·22	23·33	34·71	−24·24	−26·78	30·26	11·97	0·0040
0·009	41·26	17·86	5·49	−4·76	−5·07	30·30	23·40	34·75	−24·12	−26·65	30·58	12·39	0·0045
0·01	41·37	17·91	5·57	−4·72	−5·10	30·38	23·46	34·79	−24·01	−26·53	30·88	12·79	0·0050

* In this and the following tables, the bivalent ions are compared with the univalent ions at mole fractions equal to half of the latter's. This enables comparison at nearly equal normalities.

Table 6. Ionic partial molar volumes, in c.c./formula, at 20°C, using data of Table 2

N_2	CsCl	Cs^+	K^+	Na^+	H^+	Br^-	Cl^-	OH^-	NO_3^-	Ca^{++}	Mg^{++}	SO_4^{--}	CO_3^{--}	N_2
0·00	38·65	16·74	4·12	−5·78	−4·91	28·33	21·92	−0·58	33·19	−26·25	−28·30	23·54	3·96	0·00
0·0005	39·20	16·97	4·41	−5·59	−4·95	28·72	22·23	+0·02	33·51	−25·79	−27·89	25·06	5·83	0·00025
0·001	39·42	17·07	4·53	−5·51	−4·96	28·88	22·35	0·27	33·63	−25·60	−27·72	25·70	6·60	0·0005
0·002	39·74	17·21	4·70	−5·40	−4·98	29·11	22·54	0·62	33·82	−25·33	−27·48	26·59	7·69	0·0010
0·003	39·98	17·31	4·83	−5·31	−5·00	29·28	22·67	0·89	33·96	−25·13	−27·30	27·28	8·53	0·0015
0·004	40·19	17·40	4·94	−5·24	−5·01	29·43	22·79	1·12	34·08	−24·95	−27·14	27·85	9·24	0·0020
0·005	40·37	17·48	5·04	−5·18	−5·02	29·56	22·89	1·32	34·18	−24·80	−27·01	28·36	9·86	0·0025
0·006	40·53	17·55	5·13	−5·12	−5·03	29·68	22·98	1·50	34·28	−24·66	−26·88	28·82	10·42	0·0030
0·007	40·68	17·61	5·21	−5·07	−5·04	29·78	23·07	1·67	34·37	−24·53	−26·77	29·24	10·94	0·0035
0·008	40·82	17·67	5·28	−5·02	−5·05	29·88	23·15	1·82	34·45	−24·41	−26·66	29·63	11·42	0·0040
0·009	40·95	17·73	5·35	−4·97	−5·06	29·98	23·22	1·97	34·52	−24·30	−26·56	30·00	11·88	0·0045
0·01	41·08	17·78	5·42	−4·93	−5·07	30·07	23·29	2·10	34·59	−24·20	−26·47	30·35	12·30	0·0050

Table 7. Ionic partial molar volumes, in c.c./formula, at 10°C, using data of Table 3

N_2	CsCl	Cs^+	K^+	Na^+	H^+	Br^-	Cl^-	OH^-	NO_3^-	Ca^{++}	Mg^{++}	SO_4^{--}	CO_3^{--}	N_2
0·00	37·34	16·17	3·80	−6·49	−3·93	27·50	21·18	−2·59	31·55	−26·64	−27·79	21·08	2·88	0·00
0·0005	37·95	16·43	4·10	−6·26	−4·06	27·91	21·52	−1·60	31·97	−26·12	−27·41	22·79	4·78	0·00025
0·001	38·20	16·54	4·22	−6·16	−4·12	28·08	21·66	−1·20	32·15	−25·90	−27·25	23·50	5·57	0·0005
0·002	38·56	16·69	4·40	−6·03	−4·19	28·32	21·86	−0·62	32·40	−25·59	−27·03	24·50	6·68	0·0010
0·003	38·83	16·81	4·54	−5·92	−4·25	28·51	22·02	−0·18	32·59	−25·36	−26·86	25·27	7·53	0·0015
0·004	39·06	16·91	4·65	−5·84	−4·30	28·66	22·15	+0·19	32·75	−25·16	−26·71	25·92	8·25	0·0020
0·005	39·26	17·00	4·75	−5·76	−4·34	28·80	22·26	0·52	32·89	−24·98	−26·58	26·49	8·88	0·0025
0·006	39·44	17·08	4·84	−5·69	−4·38	28·92	22·37	0·81	33·02	−24·83	−26·47	27·00	9·46	0·0030
0·007	39·61	17·15	4·93	−5·62	−4·42	29·04	22·46	1·08	33·13	−24·68	−26·36	27·48	9·98	0·0035
0·008	39·76	17·22	5·00	−5·57	−4·45	29·14	22·55	1·33	33·24	−24·54	−26·26	27·92	10·47	0·0040
0·009	39·91	17·28	5·08	−5·51	−4·48	29·24	22·63	1·57	33·34	−24·42	−26·17	28·33	10·93	0·0045
0·01	40·05	17·34	5·14	−5·46	−4·51	29·34	22·71	1·79	33·44	−24·30	−26·08	28·72	11·36	0·0050

Table 8. Ionic partial molar volumes, in c.c./formula, at 0°C, using data of Table 4

N_2	CsCl	Cs^+	K^+	Na^+	H^+	Br^-	Cl^-	OH^-	NO_3^-	Ca^{++}	Mg^{++}	SO_4^{--}	CO_3^{--}	N_2
0·00	35·66	15·44	3·20	−7·17	−3·76	26·23	20·22	−5·76	29·29	−26·70	−27·76	17·76	−0·81	0·00
0·0005	36·36	15·74	3·49	−6·92	−3·96	26·75	20·62	−4·31	29·96	−26·29	−27·39	19·75	+1·45	0·00025
0·001	36·65	15·87	3·61	−6·82	−4·04	26·96	20·78	−3·72	30·23	−26·12	−27·23	20·57	2·38	0·0005
0·002	37·06	16·05	3·77	−6·68	−4·15	27·26	21·02	−2·87	30·63	−25·88	−27·01	21·73	3·70	0·0010
0·003	37·38	16·18	3·90	−6·57	−4·24	27·49	21·19	−2·22	30·93	−25·70	−26·84	22·63	4·66	0·0015
0·004	37·64	16·30	4·01	−6·48	−4·32	27·69	21·34	−1·68	31·18	−25·55	−26·70	23·38	5·57	0·0020
0·005	37·87	16·40	4·10	−6·40	−4·38	27·86	21·48	−1·20	31·40	−25·41	−26·57	24·04	6·32	0·0025
0·006	38·08	16·49	4·19	−6·33	−4·44	28·01	21·60	−0·76	31·60	−25·29	−26·46	24·64	7·00	0·0030
0·007	38·28	16·57	4·26	−6·26	−4·49	28·15	21·70	−0·36	31·79	−25·17	−26·35	25·19	7·62	0·0035
0·008	38·45	16·65	4·34	−6·20	−4·54	28·29	21·81	+0·01	31·96	−25·07	−26·25	25·70	8·20	0·0040
0·009	38·62	16·72	4·40	−6·14	−4·59	28·41	21·90	0·36	32·12	−24·97	−26·16	26·18	8·74	0·0045
0·01	38·78	16·79	4·47	−6·08	−4·63	28·53	21·99	0·68	32·27	−24·87	−26·07	26·63	9·26	0·0050

Table 9. Comparison of calculated (C) and measured (M) partial molar volumes, and the relative errors (%), for selected salts at 25°C

N_2	NaBr			HNO_3			Na_2SO_4			K_2CO_3			N_2
	C	M	%	C	M	%	C	M	%	C	M	%	
0·00	23·30	23·43	0·6	29·49	29·03	1·6	13·96	10·92	27·8	13·27	12·17	9·0	0·00
0·0005	23·83	23·86	0·1	29·54	29·25	1·0	15·64	13·18	18·6	15·66	14·12	10·9	0·00025
0·001	24·05	24·03	0·1	29·56	29·34	0·8	16·33	14·11	15·7	16·64	14·92	11·6	0·0005
0·002	24·36	24·28	0·3	29·58	29·47	0·4	17·31	15·43	12·2	18·04	16·07	12·2	0·0010
0·003	24·59	24·47	0·5	29·61	29·57	0·1	18·07	16·45	9·8	19·11	16·94	12·8	0·0015
0·004	24·80	24·63	0·7	29·62	29·66	0·1	18·70	17·30	8·1	20·01	17·68	13·2	0·0020
0·005	24·97	24·77	0·8	29·64	29·73	0·3	19·26	18·05	6·7	20·81	18·33	13·5	0·0025
0·006	25·13	24·90	0·9	29·65	29·80	0·5	19·76	18·73	5·2	21·53	18·91	13·8	0·0030
0·007	25·28	25·01	1·1	29·67	29·86	0·6	20·22	19·36	4·6	22·19	19·45	14·0	0·0035
0·008	25·41	25·12	1·2	29·68	29·92	0·8	20·66	19·94	3·6	22·80	19·95	14·2	0·0040
0·009	25·54	25·22	1·3	29·69	29·97	0·9	21·06	20·49	2·8	23·38	20·43	14·5	0·0045
0·01	25·66	25·32	1·3	29·70	30·02	1·1	21·44	21·00	2·1	23·92	20·87	15·1	0·0050

for solid NaCl it is 4×10^{-6}. Since the molar volume of solid NaCl is about 27 c.c., we have, initially,

$$\frac{\Delta V(P = 0) - \Delta V(P)}{\Delta V(P = 0)} = \frac{\Delta(V\beta)_{P=0}}{\Delta V(P = 0)} \approx -3 \times 10^{-5} \tag{21}$$

the correction is only about 3% per thousand atmospheres of pressure change.

A second point to remember is that the partial molar volumes have been calculated for binary systems. When, then, the system, such as sea-water, is polycomponent, the possibility of interference among the ionic species arises. Experimental data on this subject is scanty. However, the work of Wirth (1937, 1940b) on the partial molar volumes of a number of ternary systems shows that the volumes of the salts in solution are virtually independent of one another, provided that the partial molar volume of each electrolyte is reckoned in terms of a fictitious concentration whose ionic strength equals the overall ionic strength of the actual complex solution. Although Wirth finds that a small additional correction term improves the agreement with empirical density data, the difference is definitely of higher order and is not significant for our purposes.

Indications on Geologic Applications of the Data

Many geological applications of the data presented above could be made. A few of the possible areas of application follow, and one numerical example is given.

The first area of application, first pointed out by Wirth (1940a), takes advantage of the fact that for waters of open oceans the *relative* amounts of the various salts remain virtually constant. Thus, from a knowledge of the partial molar volumes of the individual ions and of water, as a function of concentration, we could compute the detailed composition of the water from the bulk-density data alone, for known values of the temperature. Such data may greatly simplify the preliminary work for the study of certain aspects of physical oceanography, such as the balance of the salts.

A second type of application deals with the calculation of solubility of salts in water as a function of pressure:

$$\left(\frac{\partial N_i}{\partial P}\right)_T = \frac{V_i^{\alpha} - \bar{V}_i^{\beta}}{(\partial \mu_i / \partial N_i)^{\beta}_{T,P}} \tag{2}$$

In order to evaluate this effect numerically, we notice, first of all, that

$$\frac{\partial \mu_i}{\partial N_i} = \frac{RT}{N_i}\left(1 + \frac{\partial \ln \gamma_i}{\partial \ln N_i}\right) \tag{22}$$

where γ_i is the activity coefficient of component i in the solution. The term $(\partial \ln \gamma_i / \partial \ln N_i)$ can be evaluated explicitly only by adapting some equation of state for the solution. The Debye-Hückel theory is the only self-consistent theory in existence, although by the very nature of the theory the results are valid only for very dilute solutions. We will therefore consider the effect of pressure on the solubility of calcite in the binary system, $CaCO_3$—H_2O, at 20°C.

According to the Debye-Hückel theory (Fowler and Guggenheim, 1952, p. 401),

$$\log \gamma_i \approx \frac{-0{\cdot}50 z_+ |z_-| I^{1/2}}{1 + \frac{a}{3 \times 10^{-8}} I^{1/2}} \tag{23}$$

where I, the ionic strength, is defined by

$$I = \tfrac{1}{2} \sum_i c_i z_i^2; \tag{24}$$

$$c_i = N_i / \tilde{V} \tag{11}$$

and z is the ionic charge. Since the quantity a is commonly of the order of 3×10^{-8} cm (Fowler and Guggenheim, 1952, p. 402), equation (23) becomes, very nearly, and in terms of the natural logarithm,

$$\ln \gamma_i = \frac{-1{\cdot}16 z_+ |z_-| I^{1/2}}{1 + I^{1/2}} \tag{25}$$

Differentiating the above expression with respect to $\ln N_i$ and substituting in the value $z = 2$, we get

$$\frac{\partial \ln \gamma_i}{\partial \ln N_i} = -1{\cdot}16 \times 4 \frac{\bar{V}_1}{\tilde{V}} \left(\frac{N_2}{\tilde{V}}\right)^{1/2} \left\{\frac{1 - 8(N_2/\tilde{V})^{3/2}}{[1 - 4(N_2/\tilde{V})][1 + 2(N_2/\tilde{V})^{1/2}]}\right\} \tag{26}$$

According to Sverdrup *et al.* (1942, p. 205), the measured solubility product of calcite at 20°C is 5×10^{-9}; hence, taking $\tilde{V} = 0{\cdot}018$ litre, $\bar{V}_1 \approx \tilde{V}$, and

$$N_2 = 0{\cdot}018 \times \sqrt{5 \times 10^{-9}} \approx 1{\cdot}3 \times 10^{-6}$$

we have

$$\frac{\partial \ln \gamma_i}{\partial \ln N_i} \approx -0{\cdot}038$$

and $\partial \mu_i / \partial N_i \approx 1{\cdot}8 \times 10^{10}$ c.c.-atm.

Using the data of Table 6 for $N_2 = 0$, we have $\bar{V}_2 \approx -22$ c.c. Since the molar volume of solid calcite is about 37 c.c., we have

$$\left(\frac{dN}{dP}\right)_T \approx \frac{59}{1{\cdot}8 \times 10^{10}} = 3{\cdot}3 \times 10^{-9} \text{ atm}^{-1}$$

or

$$\Delta N / N \approx 3 \times 10^{-3}$$

The increase in the solubility of calcite in a saturated solution, in the absence of other salts, is about 0·3% per atmosphere pressure, provided that the temperature and the chemical potential of carbon dioxide in the system are held constant. Gibson (1938, p. 65) arrives at an estimate of 0·1% for the same coefficient for altogether different reasons; the figures are in qualitative agreement.

For evaporites in contact with their own brine, the course of crystallization is dependent on the temperature, pressure, and bulk composition. Changing total pressure could conceivably affect the course of crystallization, and, if fractionation occurs, the nature of the resulting solid phases. A knowledge of the volume relationships will clearly contribute towards a more thorough understanding of the petrology of the evaporites.

A third type of application of the volume data deals with simple dehydration

reactions of hydrous minerals, a typical example of which, between anhydrite and gypsum, has been considered by MacDonald (1953). Reactions of this sort not only enter any consideration of processes of precipitation from aqueous solutions, but also bear upon consideration of changes subsequent to deposition.

Finally, pressure may also affect the composition of the precipitated phase, if such a phase is capable of solid solution. Consider, for example, the mineral halite, NaCl, forming solid solution with KCl. What is the effect of pressure (i.e. depth) on the composition of this halite in equilibrium with a brine of constant composition? We will be able to solve this problem if we know the partial molar volumes of sodium and potassium ions in solution, the *partial* molar volumes of NaCl and KCl in the halite crystal, as well as $(\partial\mu/\partial N)_{T,P}$. Studies of this sort, when systematically carried out, may eventually enable us to fix closely the particular temperature and pressure of deposition of specific evaporite beds.

Summary and Conclusions

A large class of geochemical processes in the accessible part of the earth's crust involves equilibria between solids and an aqueous solution. This includes not only processes in standing bodies of water such as lakes and seas, but also such processes as ground-water circulation, weathering, and diagenesis, to mention but a few salient examples. Equilibria in chemical processes that take place below the earth's immediate surface will generally be displaced as a result of the pressure effect. Since the amount of such a displacement is measured quantitatively by the volume change in the reaction, a knowledge of the volumes of the substances involved is required in understanding the process of interest.

For this reason the partial molar volumes of a number of salts have been computed for different temperatures and salt concentrations. A practical difficulty that arises in this undertaking is the choice of a method to extrapolate the data to infinite dilutions. Since partial molar volumes involve derivatives to measured quantities, they are sensitive to small errors in curve fitting. One might hope eventually to overcome this problem by numerical differentiation; but most of the existing data do not as yet justify such an attempt.

Fortunately, empirically the range of linear relationship between volume and concentration is sufficiently wide to encompass most problems of geologic interest, thus rendering the differentiation process relatively simple. Moreover, we have found that the volumes of the individual ions are additive to a satisfactory order of approximation, and the individual values of the ionic partial molar volumes have been computed with reference to CsCl. It is thus possible to estimate the partial molar volumes in aqueous solutions, of any salt composed of the studied ions, even though no direct data for these salts exist.

Comparison of our data with others in the literature by and large shows good agreement. At the same time, however, the differences among the methods and results obtained do indicate both the need for extremely accurate data, especially in the high-dilution range; and the limitations imposed by the lack of a reliable theory of solutions of electrolytes at appreciable concentrations.

Many areas of application to the volume data are open; a few of these have been indicated.

Acknowledgements—I wish to thank Professors J. B. Thompson Jr. and R. M. Garrels, both of Harvard University, for reading the manuscript and making critical comments. Professor Thompson suggested the series-expansion approach to derive equation (13), which I previously obtained by a more restrictive method. Professor J. P. Miller kindly left at my disposal a desk calculator, indispensable in the present work.

References

Adams L. H. (1931) Equilibrium in binary systems under pressure. I. An experimental and thermodynamic investigation of the system NaCl—H_2O, at 25°. *J. Amer. Chem. Soc.* **53,** 3769–3813.

Akerlöf G. and Teare J. (1938) A note on the density of aqueous solutions of hydrochloric acid. *J. Amer. Chem. Soc.* **60,** 1226–1228.

Akerlöf G. and Kegeles G. (1939) The density of aqueous solutions of sodium hydroxide. *J. Amer. Chem. Soc.* **61,** 1027–1032.

Akerlöf G. and Bender P. (1941) The density of aqueous solutions of potassium hydroxide. *J. Amer. Chem. Soc.* **63,** 1085–1088.

Batuecas T. (1946) Partial molecular volumes, at 0°, of water, sodium chloride, and potassium chloride in solutions of these halides. *An. Fis. Quim.* (Madrid) **42,** 713–722.

Bernal J. D. and Fowler R. H. (1933) A theory of water and ionic solution, with particular reference to hydrogen and hydroxyl ions. *J. Chem. Phys.* **1,** 515–548.

Birch F. (ed.) (1942) *Handbook of Physical Constants* 325 pp. Special Papers No. 36. Geol. Soc. Amer.

Darmois E. (1941) Qu'est-ce qu'un ion electrolytique? *J. Phys. Radium* **2,** 2–11.

Domke J. and Bein W. (1905) Ueber Dichte und Ausdehnung der Schwefelsäure in Wässeriger Lösung—Ein Beitrag zu Ihrem Physikalisch-chemischen Verhalten. *Z. Anorg. Chemie* **43,** 125–181.

Drucker C. (1941) Partial specific volumes in binary and ternary solutions. *Arkiv Kemi Min. Geol.* **14A,** no. 15, 1–48.

Fajaňs K. and Johnson O. (1942) Apparent volumes of individual ions in aqueous solution. *J. Amer. Chem. Soc.* **64,** 668–678.

Fowler R. H. and Guggenheim E. A. (1952) *Statistical Thermodynamics* 701 pp. University Press, Cambridge.

Geffcken W. (1931) Ueber die Scheinbaren Molvolumina Gelöster Elektrolyte. I. *Z. Phys. Chem.* **155A,** 1–28.

Geffcken W. and Price D. (1934) Zur Frage der Konzentrations-abhängigkeit des Scheinbaren Molvolumens und der Scheinbaren Molfraktion in Verdünnten Lösungen. *Z. Phys. Chem.* **B26,** 81–99.

Gibbs J. W. (1878) *On the Equilibruim of Heterogeneous Substances, in Collected Works* Vol. I. pp. 55–353. Yale University Press, New Haven.

Gibson R. E. (1938) On the effect of pressure on the solubility of solids in liquids. *Amer. J. Sci.* **35A,** 49–69.

Gucker F. T. Jr. (1934) The calculation of partial molal solute quantities as functions of the volume concentration, with special reference to the apparent molal volume. *J. Phys. Chem.* **38,** 307–317.

Guggenheim E. A. (1950) *Thermodynamics* 412 pp. Interscience Publishers, New York.

Hall R. E. (1924) The densities and specific volumes of sodium chloride solution at 25°. *J. Wash. Acad. Sci.* **14,** 167–172.

International Critical Tables Vol. III (1928) McGraw-Hill, New York.

Klotz I. M. and Eckert C. F. (1942) The apparent molal volumes of aqueous solutions of sulphuric acid at 25°. *J. Amer. Chem. Soc.* **64,** 1878–1880.

Lewis G. N. and Randall M. (1923) *Thermodynamics* 653 pp. McGraw-Hill, New York.

MacDonald G. J. F. (1953) Anhydrite-gypsum equilibrium relations. *Amer. J. Sci.* **251,** 884–898.

MASSON D. O. (1929) Solute molecular volumes in relation to solvation and ionization. *Phil. Mag.* (7), **8**, 218–235.

OWEN B. B. and BRINKLEY S. R. JR. (1941) Calculation of the effect of pressure upon ionic equilibria in pure water and in salt solutions. *Chem. Rev.* **29**, 461–474.

OWEN B. B. and BRINKLEY S. R. JR. (1949) Extrapolation of apparent molal properties of strong electrolytes. *Ann. N. Y. Acad. Sci.* **51**, 753–764.

PRIGOGINE I. and DEFAY R. (1954) *Chemical Thermodynamics* (Translated by D. H. Everett) 543 pp. Longmans Green, London.

REDLICH O. and BIGELEISEN J. (1942) Molal volumes of solutes. VI. Potassium chlorate and hydrochloric acid. *J. Amer. Chem. Soc.* **64**, 758–760.

SCOTT A. F. (1931) The apparent volumes of salts in solution. I. A Test of the empirical rule of Masson. *J. Phys. Chem.* **35**, 2315–2329.

SVERDRUP H. U., JOHNSON M. W., and FLEMING R. H. (1942) *The Oceans* 1087 pp. Prentice-Hall, New York.

WIRTH H. E. (1937) The partial molal volumes of potassium chloride, potassium bromide and potassium sulfate in sodium chloride solutions. *J. Amer. Chem. Soc.* **59**, 2549–2554.

WIRTH H. E. (1940a) The problem of the density of sea water. *J. Mar. Res.* **3**, 230–247.

WIRTH H. E. (1940b) Apparent and partial molal volumes of sodium chloride and hydrochloric acid in mixed solutions. *J. Amer. Chem. Soc.* **62**, 1128–1134.

Geochimica et Cosmochimica Acta, 1957, Vol. 12, pp. 123 to 132. Pergamon Press Ltd., London

Properties of silica in water

Go Okamoto, Takeshi Okura, and Katsumi Goto
Faculty of Engineering, Hokkaido University, Sapporo, Japan

(*Received* 2 *July* 1956)

Abstract—In view of the discordant theories for the mechanism of sedimentation of silica in natural waters, chemical properties of silica have been studied further. The solubility of amorphous silica has been measured over a wide range of pH and temperature. The study on the depolymerization of colloidal silica indicated that sea-water is not saturated with respect to molecularly dispersed silica. The presence of a small amount of aluminium greatly influences the state of silica in water. Thus colloidal silica can be precipitated even by a trace amount of aluminium, while a larger amount of the latter is required for the precipitation of molecularly dispersed silica. The optimum pH for the precipitation of colloidal silica is about 4·5 in contrast to that of about 8 for molecularly dispersed silica.

Introduction

Sedimentation of silica from solution is one of the most common geochemical processes. It has been reviewed in some detail by Twenhofel (1950), according to whom some silica is used in constructing micro-organisms in sea-water, while most of it is precipitated inorganically. Thus it is accepted in general that silica in river-water is in colloidal state and therefore flocculated or precipitated by electrolytes on mixing with sea-water. Stress is also laid by Murray and Gravenor (1953), in the discussion of the mechanism for the formation of marine sediments, on the chemical precipitation of silica.

On the other hand, it was concluded by Roy (1945) that silica in natural waters is in the ionic and not colloidal state. It has been shown by Aoki (1951) that solutions in equilibrium with solid amorphous silica should contain as much as 120 mg/l. of molecularly dispersed silica. The fact has been established more clearly by Goto *et al.* (1953) and also by other workers (Alexander *et al.*, 1954; Iwasaki *et al.*, 1954). Thus the solubility of silica seems to be high enough to allow silica to form a true solution in which its concentration corresponds to that of ordinary river-water. Bruevich (1953) has also discussed this point, and stated that sea-water is unsaturated with respect to silica, and it is precipitated for the most part by marine micro-organisms.

In view of the above two different opinions, it may be of some importance for the investigators of sedimentation to study the chemical properties of silica in water in more detail.

Experimental

1. *Determination of silica in water*

Silica dissolves in water in two possible forms, i.e. both molecularly dispersed and colloidal silica may exist in natural waters.

The determination of molecularly dispersed silica is based on the well-known reaction of silica with molybdic acid which forms yellow silicomolybdate complex (Aoki, 1950). In the presence of a large quantity of colloidal silica, however, the colour developed by this method sometimes deepens gradually and does

not reach a definite intensity even after a long period of time, as has been shown in our previous paper (Goto and Okura, 1955) and is also shown in Fig. 1. The slow rise in colour intensity with time may be, as discussed previously, due to the depolymerization of colloidal silica. The completion of the reaction of molecularly dispersed silica with molybdic acid requires 2 or 3 min or more, and during

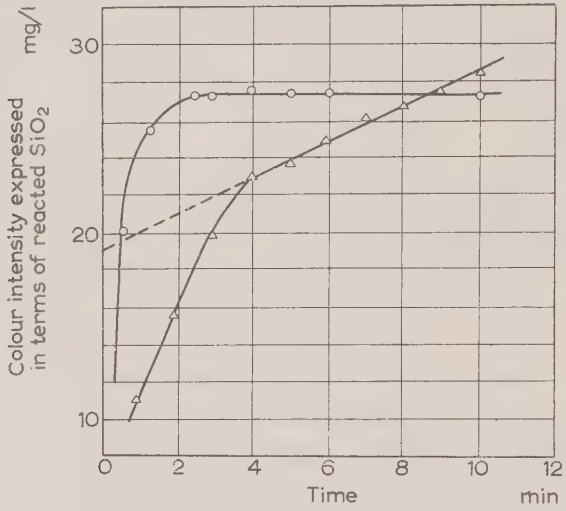

Fig. 1. Varying colour intensity with time.
—○—○— for sodium metasilicate,
—△—△— for solution containing colloidal silica.

the course of this reaction, colloidal silica seems to depolymerize and react with molybdic acid to a considerable extent. Molecularly dispersed silica must therefore be determined in such a case by extrapolating the plot of colour intensities versus time to the point where $t = 0$, as shown by the broken line in Fig. 1.

Tourky and Bangham (1936) have claimed that molybdic acid does not react with molecularly dispersed silica but with colloidal silica. When the depolymerizing character of colloidal silica is taken into account, however, it may be easily understood that such a conclusion cannot be drawn from their experiments.

The concentration of colloidal silica can be calculated from the difference in concentrations between total and molecularly dispersed silica, the former being determined by applying the silicomolybdate test after destroying colloidal silica by heating with a small amount of Na_2CO_3 in a small platinum crucible.

2. *Solubility of silica*

It has been suggested first by Aoki (1951) that silica dissolves in water, forming a true solution up to a certain concentration, which is now called the "solubility of amorphous silica," and that the remaining silica tends to polymerize to form a colloidal solution. Thus, molecularly dispersed silica never polymerizes as long as its concentration is lower than this solubility, in which case colloidal silica depolymerizes into molecularly dispersed state.

The measurements of the solubility of amorphous silica recently carried out at various pH values by Goto *et al.* (1953) and also by other workers (Alexander

et al., 1954; Iwasaki *et al.*, 1954) reveal that it increases rapidly as the pH rises above 9.

Thus, there is a considerable literature which deals with the effect of pH upon the solubility of silica, but little is known about the effect of temperature. It is the object of this section to present the solubility data over a wider range of pH and temperature.

A series of solutions of silica with various pH values were prepared by mixing

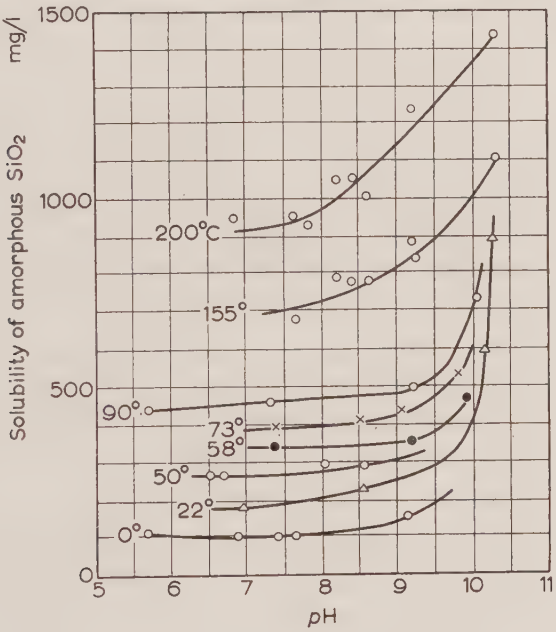

Fig 2. Solubility of amorphous silica.

the solutions of sodium silicate and of silicic acid in different proportions. The solution of silicic acid was prepared by means of ion-exchange from the solution of sodium silicate (Goto *et al.*, 1953).

After being equilibrated in a thermostat at various temperatures, the solutions were analysed for molecularly dispersed silica.

Above 100°C, where it is impossible to carry out this procedure, the measurements were made in the following manner: The solution of silica was equilibrated by heating in an autoclave for several hours. After this, the solution was bled into a 0·01 N H_2SO_4 solution, in which both polymerization and depolymerization proceed very slowly (Goto, 1955). The sulphuric acid phase was then analysed for molecularly dispersed silica. A small quantity of NaCl was previously added to the solution of silica so that the volume of the solution could be determined by measuring the concentration of Cl^- ion in the sulphuric acid phase.

The results are illustrated in Fig. 2, showing the increasing solubility of amorphous silica with temperature and pH.

This is somewhat different from the results obtained by Correns (1940), who determined silica gravimetrically after ultrafiltering the suspensions of powdered

silica gel. His results, however, seem to be not very accurate, presumably because the solubility equilibrium is not completely established owing to slow dissolution of silica gel, and also because the silica dissolved partly in colloidal form, which cannot be removed from solution even by ultrafiltration (Goto *et al.*, 1953).

3. *The effect of pH on the polymerization of silicic acid*

When the concentration of molecularly dispersed silica exceeds the solubility of amorphous silica described above, silica undergoes polymerization to form a colloidal solution. This change may be regarded as the first step towards the sedimentation of silica in natural waters.

Many workers have reported the effect of pH on the polymerization of silicic acid, but their conclusions are not identical. Iwasaki *et al.* (1954), measuring the change in concentration of molecularly dispersed silica with time, have recently stated that the polymerization is most rapid at the neutral point. Similar conclusions have been drawn from the measurements of gelation time (Merrill and Spencer, 1950; Heald *et al.*, 1955). On the other hand, Brady *et al.* (1953) have concluded from the light-scattering measurement that the optimum pH for rapid polymerization is about 8, while Greenberg and Sinclair (1955), on the basis of similar experiments, have reported a maximum rate of polymerization observed at pH about 8·6. A lower pH value was reported more recently by Bechtold (1955).

It is our belief that the above disagreement arises from the tacit assumption in each case that the polymerization proceeds to the same equilibrium state regardless of pH. This assumption seems to be incorrect when it is considered that the solubility of amorphous silica changes with pH, as has been shown in the above section.

Silicic acid dissolves in water, forming a true solution until its solubility is reached, and this solubility increases very rapidly as pH rises above about 9, where silicic acid never polymerizes or gels unless its concentration is high. It is thus apparent that gelation time cannot be used as a measure of polymerization rate, though it has been hitherto made use of by many workers.

In the present investigation, the rate of polymerization at various pH values in the range from 7 to 10 was calculated from the rate of disappearance of molecularly dispersed silica, on the assumption that the polymerization reaction is of third order with respect to molecularly dispersed silica; namely, the following equation was assumed to be applicable to the polymerization of silicic acid:

$$-\frac{dC}{dt} = k(C-S)^3$$

where C is the concentration of molecularly dispersed silica at time t, S the solubility of amorphous silica, and k, a constant.

Polymerization of silicic acid may presumably be a reaction too complex to be fully dealt with by such a simple assumption. However, the equation for third-order reaction fairly fits the experimental results since the plot of $\frac{1}{(C-S)^2}$ versus time becomes a straight line, as is shown in Fig. 3.

The calculated values of k are shown on logarithmic scale in Fig. 4, which shows clearly that the polymerization is catalysed by OH^- ions.

4. *Effect of pH on the depolymerization of colloidal silica*

When a solution containing colloidal silica becomes unsaturated, for any reason, with respect to molecularly dispersed silica, the colloidal silica depolymerizes into molecularly dispersed state to resaturate the solution.

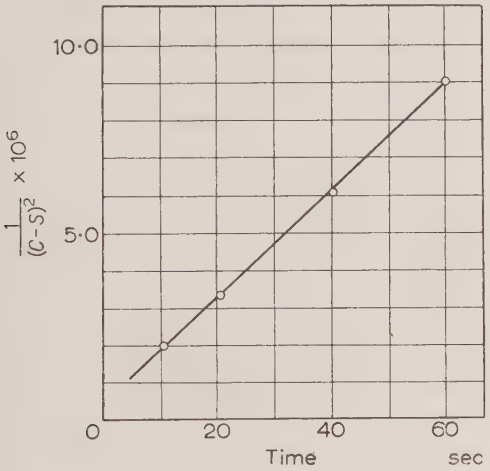

Fig. 3. Linear relationship between $1/(C - S)^2$ and time.

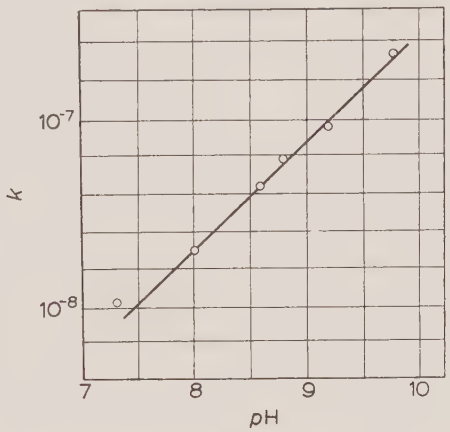

Fig. 4. k at various pH values (22·3°C)

Some workers (Lovering, 1923; Gibb and Ritchie, 1954) have reported on the solution rate of silicate rocks in solutions of various electrolytes, but little attention has been called to the effect of pH.

Two millilitres of the solution of colloidal silica containing 2 g/l. of SiO_2, prepared by ageing for several months, were diluted with 200 ml of water. The pH was controlled by dissolving Na_2CO_3 and $NaHCO_3$ in different ratios and the ionic strength was kept constant at 0·05. The change in the concentration of molecularly dispersed silica was then measured.

The following equations can be derived for the dissolution of fine spherical particles in a monodisperse system (Suito *et al.*, 1951), on the assumption that the dissolution rate is proportional to the surface area of the particles.

$$M^{\frac{1}{3}} = K(\tau - t)$$

$$\tau = b\gamma_0$$

where M is the total weight of particles in the system at time t, τ the time required for complete dissolution, r_0 the initial radius of particles, and K and b are constants.

These equations seem to be applicable also to the depolymerization of colloidal silica, since the plot of cubic roots of the concentration of colloidal silica versus time t becomes a straight line, as illustrated in Fig. 5.

By extrapolating this straight line to the point where $M^{\frac{1}{3}} = 0$, values of τ can be obtained for the depolymerization of colloidal silica at various pH values. The results are shown in Fig. 6, from which it may be concluded that not only

the polymerization but also the depolymerization is promoted by OH^- ions. However, since the slope of the straight line in Fig. 6 is 0·27, it appears that the depolymerization reaction is rather complicated.

5. *Depolymerization in sea-water*

In view of the rather large solubility of silica in water shown above, it is very doubtful, as discussed by Bruevich (1953), whether sea-water is saturated with respect to silica, because sea-water contains only a trace amount of silica.

In order to solve the above question, a small volume of the solution of colloidal

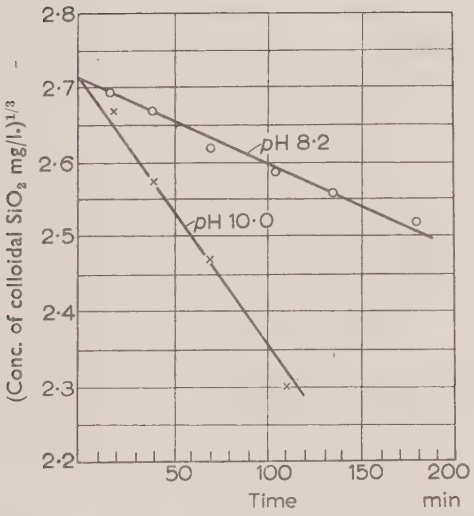

Fig. 5. Depolymerization of colloidal silica.

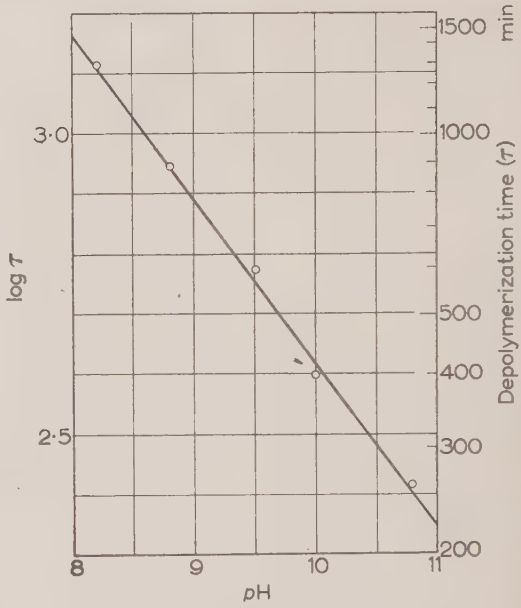

Fig. 6. Depolymerization time at various pH values.

silica was added to a large body of sea-water, and the change in concentration of molecularly dispersed silica with time was measured. The result is shown in Fig. 7, which indicates that sea-water is a good depolymerizer for colloidal silica. This may be evidence for the fact that sea-water is not saturated with respect to silica. It is very interesting, too, to point out that sea-water becomes turbid on adding the concentrated solution of silica, but the precipitate once formed soon disappears on stirring.

6. *Effect of aluminium on the depolymerization*

Several workers (Jephcott and Johnston, 1950; Godbert and Halpin, 1955) have studied, as part of the general study of silicosis, the effect of aluminium on the dissolution of silica and silicate rocks in water.

This problem is of considerable importance also from a geochemical point of view.

One millilitre of the solution of colloidal silica was diluted with 200 ml of

0·01 N NaOH solution, to which a very small amount of aluminium sulphate was previously added.

The increasing concentration of molecularly dispersed silica with time at

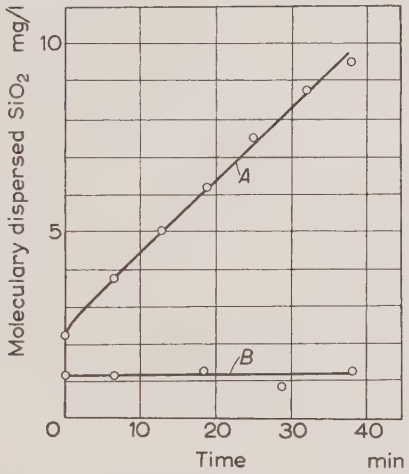

Fig. 7. Depolymerization of colloidal silica.
A in sea-water.
B in distilled water.

various aluminium concentrations is shown in Table 1, which is understood to indicate that aluminium greatly reduces the rate of depolymerization or the rate of dissolution of colloidal silica in an alkaline medium, where aluminium is supposed to be in the form of aluminate ion.

Table 1. Effect of aluminium on the depolymerization of colloidal silica in 0·01 N NaOH (total SiO_2 120 mg/l.)

Time (min)	Concentration of molecularly dispersed silica varying with time (mg/l.)			
	Conc. of Al			
	0	2·5	5·0	7·5
4	8·0	5·2	5·0	4·0
50	23·0	9·5	8·7	6·7
120	49	13	9·3	8·0

7. *Precipitation of silica by aluminium*

From the foregoing evidence it is clear that the mechanism of sedimentation of silica in natural waters is much more complicated than has been expected. On the other hand, silica is coprecipitated with aluminium hydroxide, a well-known fact often employed to remove silica from boiler-feed water (Betz *et al.*,

1940; Okamoto *et al.*, 1951). But little has been reported on the effect of aluminium on colloidal silica. The following experiments were carried out in order to realize the effect of aluminium on colloidal silica as well as on molecularly dispersed silica.

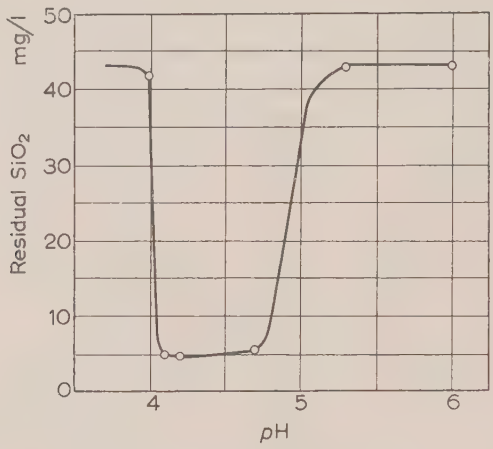

Fig. 8. Precipitation of colloidal silica.
SiO_2 45 mg/l., Al 1 mg/l.

An appropriate amount of aluminium sulphate was added to the solution of silica. After adjusting the pH of the solutions in the range of 4 to 10 with NaOH, and allowing to stand for about 30 min, they were filtered and analysed for residual silica concentration.

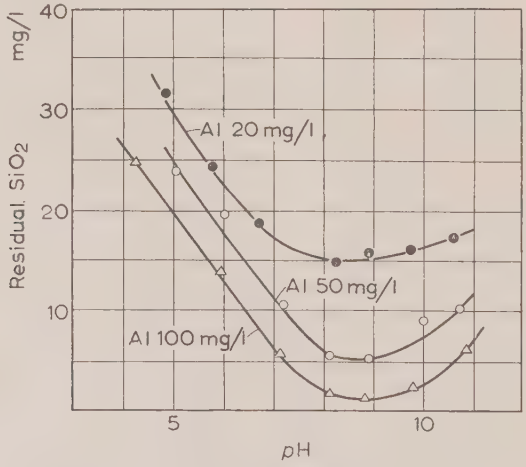

Fig. 9. Precipitation of molecularly dispersed silica.
SiO_2 35 mg/l.

The results are shown in Figs. 8 and 9. It is apparently shown in these figures that the optimum pH for the precipitation of colloidal silica is different from that for molecularly dispersed silica, and that only a trace amount of aluminium is sufficient for precipitating colloidal silica, while a larger amount is required

to precipitate molecularly dispersed silica. One milligram of aluminium was found to precipitate about 40 mg of colloidal silica.

It must be pointed out, however, that colloidal silica cannot be precipitated by aluminium in such a case, where the ratio of silica to aluminium added exceeds

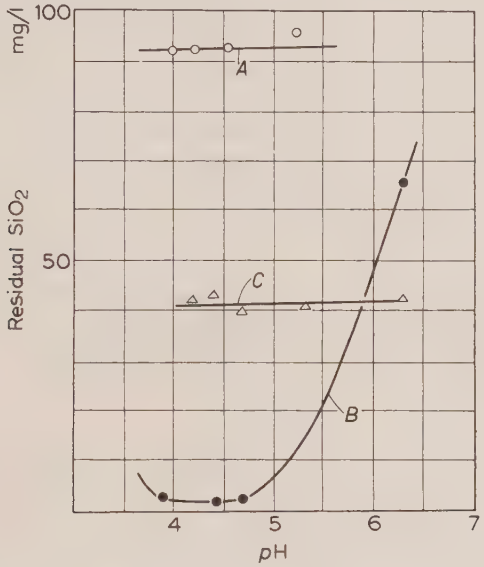

Fig. 10. Precipitation of colloidal silica at various Al concentrations.
A. SiO_2 92 mg/l., Al 1 mg/l.
B. SiO_2 92 mg/l., Al 2 mg/l.
C. SiO_2 43 mg/l., Al 0·5 mg/l.

a certain value, as is shown in Fig. 10. Neither aluminium nor colloidal silica is precipitated in this case.

Discussion

It is well known that the gelation of silicic acid does not take place in alkaline solution. Nevertheless the polymerization is catalysed by OH^- ions, as has been shown above. Earlier workers have failed to show this because they used the gelation time as a measure of polymerization rate, which does not work in alkaline medium. Silicic acid never gels at high pH owing to the different equilibrium state. It is very interesting to point out that ions which promote the polymerization of silicic acid also promote the depolymerization. Thus hydroxyl ions, hydrofluoric acid, and molybdic acid catalyse both polymerization and depolymerization (Goto, 1955).

Aluminium has a remarkable effect on the behaviour of silica, especially when the latter exists in the colloidal state, which can be precipitated by a mere trace of aluminium. This may explain the sedimentation of silica in natural waters, e.g. thermal spring-water, which usually contains a large quantity of silica. On cooling or on changing the pH, the water becomes supersaturated with respect to silica and it polymerizes into colloidal form, in which case it may be precipitated by quite a small amount of aluminium or other trivalent cations, forming a precipitate consisting of very pure amorphous silica.

Since aluminium reduces the depolymerization rate of colloidal silica, it may be assumed that the silica once precipitated by aluminium is resistant to the attack of water even at higher pH values.

Sea-water is a good depolymerizer for colloidal silica. This indicates, as already pointed out by Bruevich (1953), that it is unsaturated with respect to silica. Thus it may be reasonable to assume that the inorganic precipitation of silica plays a minor role in the sedimentation in sea-water, where most silica is considered to be precipitated by living organisms.

It is true that sea- and river-waters contain aluminium (Ishibashi and Kawai, 1952; Ishibashi and Motojima, 1952). However, the amount seems to be too small to precipitate molecularly dispersed silica, the predominating form of silica in natural waters.

Acknowledgement—The authors are indebted to Professor Y. Uzumasa and Professor I. Kayama for their interest and encouragement. Thanks are also due to Mr. T. Ogawa for his help in carrying out the experiments.

References

Alexander G. B., Heston W. M., and Iler R. K. (1954) *J. Phys. Chem.* **58,** 453.
Aoki F. (1950) *J. Chem. Soc. Japan, Pure Chem. Sect.* **71,** 634.
Aoki F. (1951) *J. Chem. Soc. Japan, Pure Chem. Sect.* **72,** 17.
Bechtold M. F. (1955) *J. Phys. Chem.* **59,** 532.
Betz L. D., Noll C. A., and Maguire J. J. (1940) *Industr. Engng. Chem.* **32,** 1320.
Brady A. P., Brown A. G., and Huff H. (1953) *J. Colloid Sci.* **8,** 252.
Bruevich S. V. (1953) *Izv. Akad. Nauk. SSSR, Ser. Geol.* No. 4, 67, *Chem. Abstr.* **48,** 4894 (1954).
Correns C. W. (1940) *Chemie der Erde* **13,** 92.
Gibb J. G. and Ritchie, P. D. (1954) *J. Appl. Chem.* **4,** 473.
Godbert A. L. and Halpin R. K. (1955) *Ministry Fuel and Power (Brit.), Safety in Mines Research Estab., Research Rept.* No. 116, 18, *Chem. Abstr.* **49,** 14232.
Goto K. (1955) *J. Chem. Soc. Japan, Pure Chem. Sect.* **76,** 729.
Goto K. and Okura T. (1955) *Japan Analyst* **4,** 175.
Goto K., Okura T., and Kayama I. (1953) *Kagaku* **23,** 428.
Greenberg S. A. and Sinclair D. (1955) *J. Phys. Chem.* **59,** 435.
Heald I. A., Coates K. B., and Edwards J. E. (1955) *J. Appl. Chem.* **5,** 425.
Ishibashi M. and Kawai T. (1952) *J. Chem. Soc. Japan, Pure Chem. Sect.* **73,** 380.
Ishibashi M. and Motojima K. (1952) *J. Chem. Soc. Japan, Pure Chem. Sect.* **73,** 491.
Iwasaki I., Tarutani T., Katsura T., and Arino H. (1954) *J. Chem. Soc. Japan, Pure Chem. Sect.* **75,** 857.
Jephcott C. M. and Johnston J. H. (1950) *Arch. Ind. Hyg. Occupational Med.* **1,** 323.
Lovering T. S. (1923) *Econ. Geol.* **18,** 523.
Merrill R. C. and Spencer R. W. (1950) *J. Phys. Chem.* **54,** 806.
Murray H. H. and Gravenor C. P. (1953) *Science* **118,** 25.
Okamoto G., Okura T., and Sudo N. (1951) *J. Electrochem. Soc. Jap.* **19,** 289.
Roy C. J. (1945) *Amer. J. Sci.* **243,** 393.
Suito E., Hirai N., and Taki K. (1951) *J. Chem. Soc. Japan, Pure Chem. Sect.* **72,** 713.
Tourky A. R., and Bangham, D. H. (1936) *Nature, Lond.* **138,** 587.
Twenhofel W. H. (1950) *Principles of Sedimentation* p. 398. McGraw-Hill.

Geochimica et Cosmochimica Acta, 1957, Vol. 12, pp. 133 to 149. Pergamon Press Ltd., London

Isotopic standards for carbon and oxygen and correction factors for mass-spectrometric analysis of carbon dioxide

Harmon Craig*
Enrico Fermi Institute for Nuclear Studies, University of Chicago

Abstract—Seventy-four mass spectrometric analyses have been made on eight isotopic standards for carbon and oxygen. The standards reported on are the National Bureau of Standards limestone, water, and graphite reference samples, the Solenhofen standard used by Nier for absolute measurements, and the carbonate standards used by the Stockholm, Basel, Wellington, and Chicago laboratories. The basic measurements are reported as δ values relative to the Chicago PDB standard and as absolute isotope ratios. The absolute ratios are based on new figures for Nier's standard, derived from a re-evaluation of his data and new measurements on atmospheric oxygen.

The correction factors for instrumental effects and for the nature of the mass spectra have been studied. Simple but precise equations for the mass spectra effects have been derived, which give the correction factors as functions of the measured differences between sample and standard. The oxygen isotopic composition of carbon dioxide produced by combustion of carbon has been studied, and the derived correction factors for carbon measurements were checked experimentally by varying the oxygen-18 content of carbon dioxide.

1. Introduction

Mass spectrometric measurement of natural isotopic variations began with the work of Nier and Gulbransen (1939) on carbon isotopes. In 1950, McKinney *et al.* described a modification of the Nier mass spectrometer designed to increase the precision in the measurement of relative abundances by an order of magnitude; at the present writing fourteen spectrometers of this type have been constructed at various geochemical laboratories, and with these, and other instruments, a great mass of precise isotopic data has been accumulated. Craig and Boato (1955) recently reviewed the present status of stable isotope geochemistry. Some thirty laboratories are or soon will be active in this field, reflecting the present-day emphasis on the quantitative aspects of geology.

This paper has been prompted by the recent availability of isotopic standards prepared and distributed by the National Bureau of Standards (Mohler, 1955). It is based on the accumulated data and analytical experience of the past five years at the Chicago laboratory of H. C. Urey and on recent measurements on the NBS standards, and represents an attempt to obtain the most precise values possible for the various isotopic standards in use. These values should be useful in establishing the relations between the sets of data from the various different laboratories. For the most precise comparison of the various standards, a careful evaluation of the systematic errors inherent in the mass spectrometric analysis is necessary. Therefore, we first consider the mass spectrometer and the correction factors for the analysis of carbon dioxide, and then the relative and absolute isotopic values for the standards analysed in this study.

2. The McKinney-Nier Mass Spectrometer

The high precision of the McKinney-Nier spectrometer is chiefly the result of two factors: (1) replacing the electrometer tube and amplifier, or second feed-back amplifier, for the smaller

*Present address: Scripps Institution of Oceanography, University of California, La Jolla, California.

ion beam in the null-reading double-collector balancing circuit devised by Nier, Ney, and Inghram (1947) by a vibrating-reed electrometer; and (2) the introduction of a dual gas-feed system, originally designed by Ney, for rapid comparison of the voltages, tapped off from the balancing potentiometer, required to produce null readings for a sample and a standard gas. In addition, the electronic components used by Nier (1947) were redesigned for very high stability. With the introduction of the vibrating-reed electrometer, the ion-beam currents reported by McKinney *et al.* (1950) were reduced by a factor of 3, and have been maintained as such ever since. In the analysis of carbon dioxide, the potential drop across the $1{\cdot}5 \times 10^{10}$-ohm resistor of the mass-44 collector is maintained at 19·2 V, resulting in a mass-44 ion current of $1{\cdot}3 \times 10^{-9}$ amperes for both sample and standard. The second collector, for mass-45 or -46, has a $1{\cdot}5 \times 10^{11}$-ohm resistor in the balancing circuit, and the observed parameters for carbon and oxygen analysis are as follows:

Mass-45	Mass-46
$i_{45} = 1{\cdot}5 \times 10^{-11}$ A	$i_{46} = 5{\cdot}3 \times 10^{-12}$ A
$E_{45} = 2{\cdot}25$ V	$E_{46} = 0{\cdot}78$ V
BP ~ 1300 ohms	BP ~ 450 ohms
$\beta = 0{\cdot}117$	$\beta = 0{\cdot}0405$

The currents and voltages listed are the ion-beam currents and potential drops across the small-collector resistor; BP is the balancing panel resistance tapped off from the 11,111-ohm decade resistor potentiometer, and β (= BP/11,111) is the ratio of the potential drops across the respective resistors for mass-45 or mass-46 to mass-44.

For the comparison of ratios on the spectrometer, the mass-44 ion-beam intensities are adjusted by means of the manifold mercury pistons to identical values for sample and standard gas. The reason for this adjustment is the effect of the squared term in the mass-44 tail contribution to the smaller ion beam, which causes a dependence of the recorded ratio on ion-beam intensity (see below). Thus the input pressures of the two gases are different, and inversely proportional to the mass-44 mole fractions. In the initial adjustment of the instrument, and at periodic intervals, the sample and standard manifolds are interconnected, and a gas sample is thoroughly mixed into both reservoirs. The two reservoirs are then closed off from each other, the gas is fed through the twin leaks, and the capillary leaks are manually adjusted to produce equal isotope ratios at equal mass-44 ion-beam intensities ($E_{44} = 19{\cdot}2$ V), but generally different input pressures. This adjustment is necessary because there is a small but real fractionation in the leaks caused by back mixing, the differential effect of which must be eliminated. Mixing of the sample and standard gases in the source, due to imperfect closure of the ground-glass ball-joints in the double inlet valve, is corrected for by direct measurement of the leakage through each valve. This is done by analysing a sample gas some 3–4% different in composition from the standard, and noting the shift of the trace of the null point on the recording potentiometer when the sample and standard are alternately pumped away; from the measured difference in isotopic composition, the leakage through each valve is computed. For the instrument on which the present work was done, the correction factor for this effect has maintained a constant value of 1·007 for the past several years.

Shortly after the McKinney-Nier spectrometer was put into operation, the "pressure effect," i.e. the variation of the recorded ratio with ion-beam intensity, was discovered. Although the effect was small, it was found that it could be eliminated by setting a small potential bias on the vibrating-reed amplifier, with a polarity such as to increase the voltage drop of the smaller ion-beam current across the small-collector balancing circuit resistor, and, correspondingly, across the vibrating-reed resistor when the system is switched off balance. The biasing potential required to eliminate this effect is some 5 mV for mass-46, and 10 mV for mass-45. This procedure was followed in the Chicago laboratory for several years, but when the writer investigated the nature of the effect, the practice was then abandoned except for special circumstances. Since the voltage drop of the smaller ion current across its resistor is increased by the amount of the biasing voltage, the measured isotope ratio for a null reading is also increased, and the smaller ion-beam current is augmented by the ratio of the biasing voltage to the small-collector resistor. Thus the recorded 46/44 and 45/44 ratios are increased by an additive term in the

numerator which does not cancel when the ratio of the isotope ratios is taken. To correct for this, the measured δ value (defined below) for a sample must be multiplied by the factor $(1 + E_r/E_i)$, where E_r is the bias voltage set on the reed, and E_i is the smaller ion-beam potential drop, with values for carbon and oxygen as listed above.

The "pressure effect" cited above appears to be due to a squared dependence of the mass-44 tail contribution to the less abundant ion beams, since the isotope ratio would not increase with ion-beam intensity, nor with the applied reed bias, as is observed, unless the dependence were higher than first-order. The 44 tail contribution most probably goes as the square of the 44 ion-beam intensity, representing a coulombic effect. Thus we write the current added to the less abundant ion-beam current by the spreading of the mass-44 beam, as $i_t = k_1 I^2 + k_2 I$, where I is the mass-44 ion current. If i_{46} and i_r are then respectively the normal mass-46 ion current, reflecting only the mass-46 abundance, and the current across the small-collector resistor produced by the vibrating-reed bias voltage, the measured ratio will be $(i_{46} + i_r + i_t)/I$, or:

$$R_m = (R + k_2) + (i_r/I) + k_1 I$$

where we have written $R = i_{46}/I$ = the mass ratio in the impinging ion beams. Thus we see that the squared-term assumption predicts the elimination of the "pressure effect" by means of the reed-bias voltage, because of the addition of a term which goes as $1/I$ in the measured ratio. This expression predicts that, for small I, R_m should decrease with increasing I with a slope of $-i_r/I^2$, then go through a minimum, and finally increase linearly with a slope of k_1. For a reed bias of opposite polarity, R_m should increase continuously before attaining a linear dependence. After derivation of the above expression, measurements were made on R_m as a function of I, and these predictions were verified completely except that at very high values of I ($E_{44} > 25$ V), R_m again begins to increase rapidly because of saturation of the D.C. amplifier.

Setting $dR_m/dI = 0$ for the minimum where the ratio does not vary with I, we have: $i_r/I_{\min} = k_1 I_{\min}$, the I dependent terms are equal in the above expression, and their variation with I is equal and of opposite sign, explaining the minimum. The constant k_1, evaluated from the data for the minima as E_r was varied from $-1{\cdot}5$ to $+6$ mV, and from the slope of the linear dependence, was found to be 25,000 A^{-1}, with an error of about 20%. However, k_2 cannot be determined from these data, because, although R can be estimated by applying a square-root-of-mass correction for source fractionation to the absolute value, derived in a later section, for the standard gas, its value, so estimated, differs from R_m by much less than the uncertainty imposed by the tolerances assigned to the values of the resistors used in the balancing circuit. Since the sign of k_2 is not known, we make no correction for the tail effect as such, but data taken before the use of the reed-bias voltage was eliminated have been corrected for the applied voltage (which was recorded), because of the fact that it was variable from time to time and caused significant departures from our estimated analytical precision for samples quite different in composition from the standard.

However, the most interesting result of this effect is the quick and easy method it offers for evaluating the contribution of the H_3^+ ion to the HD beam in the mass spectrometric analysis of hydrogen. For, since the H_3^+ ion abundance varies with the square of the H_2 ion-beam abundance, and since with the use of double collectors there is no tail effect because of the wide beam separation, at the minimum ratio dependence on I produced at the working H_2 beam intensity by an empirically determined reed voltage, the equivalent reed current i_r is equal to the ion current contributed by the H_3^+ ions. k_1 above then becomes the proportionality constant for the H_3^+ dependence on I^2, and k_2 will be 0

Notation and Symbols

We continue to report our data as δ values relative to our standard. The Chicago carbon dioxide standard is CO_2 produced from PDB calcium carbonate by reaction with 100% H_3PO_4 at 25·2°C. PDB is a Cretaceous belemnite, *Belemnitella americana*, from the Peedee formation of South Carolina; the carbonate has undergone no treatment prior to the acid reaction other than crushing

and grinding. δ is the per mil isotopic ratio enrichment in a sample relative to the standard, i.e.:

$$\delta(‰) = \left[\frac{R_{\text{sample}}}{R_{\text{std}}} - 1\right] \times 1000$$

Throughout this paper we shall distinguish two δ functions, both of which refer always to the PDB standard, as follows:

δ_m = measured enrichment, calculated from the recorded ratios of the molecular masses collected. It is corrected for instrumental effects, i.e. for gas leakage through the inlet valves and vibrating-reed bias (if used), but for nothing else.

δ_c = the true enrichment of the sample relative to the standard, i.e. the measured δ corrected by the factors derived in section 4.

We have considered publishing data in the future as δ values relative to the new NBS standard, but after consultation with other laboratories have decided to continue using the Chicago standard as a reference. The paleotemperature scale is defined in terms of this standard, and a great deal of data on carbon and oxygen variations has been published relative to it; it is currently used as a reference standard by four laboratories. In addition, its oxygen value is very close to the average value for ocean water (as measured by the equilibration technique), and its carbon value is close to that of average limestone, which makes it a convenient reference standard for geochemical calculations.

In the following sections we derive the absolute and relative abundance values of the various standards, and the correction factors to be applied to the raw mass spectrometric data. The symbol R is used throughout both for isotope ratios and for the molecular mass ratios measured in the mass spectrometer. Oxygen isotope ratios are uniformly molecular, i.e. R refers always to $O^{16}O^{18}/O^{16}O^{16}$ rather than to O^{18}/O^{16}. With R we associate two sets of subscripts, denoting first the particular ratio, and second the material to which the ratio refers. The ratio denoting subscripts are:

$$R_{13} = C^{13}/C^{12}$$

$$R_{17} = O^{16}O^{17}/O^{16}O^{16}$$

$$R_{18} = O^{16}O^{18}/O^{16}O^{16}$$

$$R_{45} = \frac{\text{Number of mass-45 ions collected}}{\text{Number of mass-44 ions collected}}$$

$$R_{46} = \frac{\text{Number of mass-46 ions collected}}{\text{Number of mass-44 + mass-45 ions collected}}$$

As material-denoting subscripts we shall use (std) for the Chicago PDB carbon dioxide standard described above, (air) for atmospheric oxygen, and (x) for any sample of carbon dioxide being analysed. In addition, we distinguish the following:

(Solen) = carbon dioxide from the Solenhofen Jurassic limestone, Bavaria, analysed for carbon and oxygen isotopic ratios by NIER (1950). CO_2 was produced by treatment with an unspecified acid. This subscript refers specifically to NIER's values for his sample of CO_2.

(Solen-H_3PO_4) = carbon dioxide produced from NIER's Solenhofen limestone sample by reaction with 100% H_3PO_4 at 25·2°C in our laboratory. The limestone sample has undergone no treatment other than crushing and grinding.

It should be noted that, for the case of oxygen ratios, the (std) and the two Solenhofen subscripts refer specifically to the carbon dioxide rather than to the carbonate, since it is known that in the production of carbon dioxide by acid treatment of carbonate, the oxygen isotopes are fractionated. The two Solenhofen subscripts, referring to the same carbonate sample treated with different acids, are distinguished because it is also known that the oxygen ratio in the carbon dioxide varies with the acid used, and probably also with the isotopic composition of the water, if water is present. (See MCCREA, 1950, for data on the variation with type of acid.) According to NIER (personal communication), the acid used on his sample was probably HCl.

3. Derivation of the Absolute Abundance Ratios

Eleven isotopic abundance ratios are needed for the derivation of the mass spectrometric correction factors discussed in the next section; the three basic data are NIER's measurements of R_{18} and R_{17} in atmospheric oxygen and R_{13} in the Solenhofen limestone. In this section we discuss NIER's data, from which we obtain six ratios, and then derive the remaining five ratios from our relative abundance data.

Evaluation of NIER's *data on atmospheric oxygen and Solenhofen limestone*

NIER (1950) obtained the most precise isotopic abundance ratios for carbon and oxygen, by using synthetic mixtures of argon isotopes for calibration of the mass discrimination effects in his spectrometers. The analyses were made on two mass spectrometers, and after correction for mass discrimination effects, a weighted grand mean of data was obtained from six measurements of each isotopic ratio. NIER's absolute ratios for atmospheric and tank oxygen are shown in Table 1, which gives the 34/32 and 33/32 ratios (R_{18} and R_{17} respectively) obtained on each spectrometer. Each figure is the average of three measurements, and the bottom row gives NIER's weighted average from the two sets of data.

Table 1. Mass spectrometric analyses of atmospheric and tank oxygen
A. O. NIER (1950)

	$34/32 \times 10^5$			$33/32 \times 10^6$		
	Tank	Air	Δ(‰) tank/air	Tank	Air	Δ(‰) tank/air
MS-2	410·7	408·2	6·1	752·8	757·5	−6·2
MS-1	410·3	408·8	3·7	755·1	741·1	+18·9
Weighted average	410·3	408·8	3·7	755	749*	+8·0

* Unweighted value, as data from two instruments were assumed to be inconsistent.

The values of R_{18} for tank and air oxygen are in very good internal agreement, and we adopt immediately from NIER's data

$$R_{18(\text{air})} = 408{\cdot}8 \times 10^{-5} \qquad (1)$$

In Table 1 we have also calculated the per mil enrichment in O^{18} and O^{17} of tank oxygen with respect to atmospheric oxygen, termed Δ. TUDGE's data (Table 2) show that tank oxygen

is enriched from 4–6‰ in O^{18} with respect to atmospheric oxygen, in exact agreement with NIER's measurements; this agreement, though probably fortuitous in its exactitude, nevertheless testifies to the precision of NIER's data.* (Probable errors are given in NIER's original paper.)

NIER chose the unweighted average value of 749×10^{-6} for $R_{17(air)}$, noting that the two sets of data were inconsistent. Comparison of the enrichment factors for O^{17} in tank oxygen compared with air oxygen (Table 1) shows that the data are also inconsistent with the enrichment factors expected from consideration of the O^{18} enrichment in tank oxygen over air oxygen, for which the data are quite consistent. For systems in thermodynamic equilibrium, consideration of the vibrational frequency decrease for the addition of one and of two neutrons to a nucleus indicates that the fractionation factor for the distribution of O^{18} between two compounds should be the square of the fractionation factor for O^{17} (cf. CRAIG, 1954, p. 133). (Since these factors are close to 1, the enrichments should differ by about a factor of 2.) BIGELEISEN's reaction-rate theory predicts the same relationship for kinetic effects (BIGELEISEN, 1952). Such a relationship has been observed for sulphur in natural compounds and experimental systems (THODE *et al.*, 1949, p. 368 369), and in numerous instances for carbon (e.g. YANKWICH *et al.*, 1954). NIER's data for R_{17} in air oxygen are thus not only internally inconsistent, but are also inconsistent with the expected enrichment with respect to tank oxygen, based on the O^{18} data. The two sets of data give O^{17} enrichments which differ in both sign and magnitude, and there is thus no indication of a systematic deviation from the expected relationship. The measurements on atmospheric oxygen were made on air without removal of the nitrogen, which may account for the large deviations in the 33/32 ratios.

Since the R_{17} values for tank oxygen are quite consistent, we here assume that the 33/32 ratio in air oxygen is 2‰ less than in tank oxygen (based on the O^{18} difference.) Then, using NIER's value of 755×10^{-6} for R_{17} of tank oxygen, we obtain and adopt the value:

$$R_{17(air)} = 753{\cdot}5 \times 10^{-6} \tag{2}$$

We need next the ratio C^{13}/C^{12} in NIER's Solenhofen limestone sample. NIER's measured value of the 45/44 ratio is $R_{45} = 1199 \pm 2 \times 10^{-5}$. Now, since the measured ratio $R_{45} = R_{13} + R_{17}$, the value of R_{17} in the carbon dioxide which was analysed for the carbon ratio must be known in order to obtain the C^{13}/C^{12} ratio. NIER used his value of $R_{17(air)}$ for this figure and thus obtained $R_{13(Solen)} = 1124 \times 10^{-5}$. However, the value of $R_{17(Solen)}$ may be obtained from comparison of his data on $R_{18(Solen)}$ and $R_{18(air)}$, by assuming the relationship:

$$\left[\frac{R_{18(Solen)}}{R_{18(air)}}\right]^{\frac{1}{2}} = \frac{R_{17(Solen)}}{R_{17(air)}}$$

(cf. discussion on $R_{17(air)}$ above). Then, using NIER's value $R_{18(Solen)} = 415 \times 10^{-3}$, and the values of $R_{18(air)}$ and $R_{17(air)}$ given in (1) and (2) above, we obtain:

$$R_{17(Solen)} = 759{\cdot}2 \times 10^{-6} \tag{3}$$

this value referring to the O^{17} content of the CO_2 sample analysed by NIER. Then, from NIER's value for R_{45} given above, we obtain by direct subtraction:

$$R_{13(Solen)} = 1123 \times 10^{-5} \tag{4}$$

From NIER's final probable-error assignment we have an uncertainty corresponding to $1123 \pm 3 \times 10^{-5}$. Now, for much of the relative abundance work currently being done we are working one decimal beyond NIER's figure. We thus adopt arbitrarily the value $R_{13(Solen)} = 1123{\cdot}00 \times 10^{-5}$ as the C^{13}/C^{12} ratio in NIER's Solenhofen limestone sample, in order to present absolute ratios for other standards with the precision corresponding to that obtainable when relative, rather than absolute, measurements are being made. This corresponds to a C^{12}/C^{13} ratio of 89·05.

Evaluation of the abundance ratios in PDB standard

Having obtained the values of $R_{18(air)}$, $R_{17(air)}$, and $R_{13(Solen)}$ from NIER's data, we next proceed to derive $R_{18(std)}$, $R_{17(std)}$, $R_{13(std)}$, and $R_{45(std)}$ from direct measurement of the isotopic

* According to NIER (*op. cit.*), THODE has also found a difference of almost exactly the same magnitude.

differences between PDB standard carbon dioxide, atmospheric oxygen, and NIER's sample of Solenhofen limestone with which he kindly supplied the writer.

The measurements on atmospheric oxygen were made by A. TUDGE in the course of his work on the phosphate paleotemperature scale. Table 2 shows TUDGE's data on two brands of tank oxygen and air oxygen, given as δ values relative to PDB standard. The tank-oxygen samples were measured relative to each other as molecular oxygen. Atmospheric and Linde tank oxygen were then converted quantitatively to CO_2 by heating over spectroscopic graphite and condensing the CO_2 in liquid nitrogen. Details of the procedure will be published by TUDGE; the error in the present data is less than $\pm 0{\cdot}2‰$. The values in the table are corrected by the factors given in section 4; δC^{13} of the carbon dioxide was taken as $-28‰$, based on analyses of other samples of such graphite.

Table 2. Mass spectrometric analyses of oxygen from various sources (A. TUDGE)

Source	δ_c (O^{18})‰
Tank—National Cylinder oxygen	−10·8
Tank—Linde oxygen	−12·7
Air	−16·73

From NIER's value of $R_{18(air)}$ and TUDGE's analysis, we obtain:

$$R_{18(std)} = 415{\cdot}8 \pm 0{\cdot}5 \times 10^{-5} \tag{5}$$

the uncertainty being that assigned by NIER to his value for $R_{18(air)}$.

An independent check on TUDGE's analysis of atmospheric oxygen is obtained from analyses in our laboratory on samples of water produced from atmospheric oxygen which were given to us by M. DOLE. Analyses of two of these samples are as follows:

1. Dole sample No. 4, analysis published by EPSTEIN and MAYEDA (1953).* Analysed May 1952. $\delta_c(O^{18}) = +22{\cdot}66‰$
2. Dole sample No. 1. Analysed February 1953. $\delta_c(O^{18}) = +22{\cdot}81‰$

Average $+22{\cdot}73‰$

The δ value of $+22{\cdot}73‰$ is the analysis of CO_2 equilibrated with the water at 25·2°C, measured vs. the PDB standard. Taking the fractionation factor for O^{18} exchange between water and carbon dioxide as 1·039 at 25°C, the direct value for atmospheric oxygen vs. PDB standard is $\delta = -15{\cdot}66‰$, to be compared with TUDGE's value of $-16{\cdot}73‰$. Considering the possibility of some fractionation in the conversion of oxygen to water, the fact that the water samples were stored for years in small flasks sealed with rubber stoppers, and the considerable uncertainty in the fractionation factor between water and carbon dioxide, the agreement is considered excellent. Using the value obtained from DOLE's water samples, we would obtain $R_{18(std)} = 415{\cdot}3 \times 10^{-5}$, which is within the uncertainty assigned in (5) above.

In order to obtain the value of $R_{17(std)}$ we assume a similar relationship to that given above (3), namely:

$$\left[\frac{R_{18(air)}}{R_{18(std)}}\right]^{\frac{1}{2}} = \frac{R_{17(air)}}{R_{17(std)}}$$

and using the values given above by (1), (2), and (5), we obtain:

$$R_{17(std)} = 759{\cdot}9 \times 10^{-6} \tag{6}$$

* This value differs from their published value of +22·10 in having been here corrected for instrumental effects, C^{13} and O^{17} effects, and a 20 ml-size sample, using the factors derived in this paper. See footnote in Section 4.

We now need the value of $R_{17\ (\text{Solen-}H_3PO_4)}$ which differs from R_{17} in NIER's sample because of the different acid used in our analytical technique. NIER's Solenhofen limestone gives an analysis of $\delta_c\ (O^{18}) = -4{\cdot}40‰$ relative to PDB (see section 5). We therefore take the O^{17} enrichment (of the CO_2 produced by reaction with H_3PO_4) relative to PDB as $-2{\cdot}2‰$, and from (6) we obtain $R_{17(\text{Solen-}H_3PO_4)} = 758{\cdot}2 \times 10^{-6}$.

We may now derive $R_{13(\text{std})}$ from the following relationship:

$$\frac{R_{13(\text{Solen})} + R_{17(\text{Solen-}H_3PO_4)}}{R_{13(\text{std})} + R_{17(\text{std})}} = 1 + \Delta\left(\frac{45}{44}\right)$$

where $\Delta(45/44)$ is the measured difference in mass 45/44 ratio between Solenhofen limestone and PDB standard carbon dioxide, both produced by reaction with H_3PO_4, the value being corrected only for valve leakage in the spectrometer. The value of Δ is $-0{\cdot}74‰$ (see section 5), and using the ratio values given in (4), (6), and above, we calculate:

$$R_{13(\text{std})} = 1123{\cdot}72 \times 10^{-5} \tag{7}$$

based on the adopted value of $1123{\cdot}00 \times 10^{-5}$ for the C^{13}/C^{12} ratio of NIER's Solenhofen limestone. By direct addition, $R_{45(\text{std})} = R_{13(\text{std})} + R_{17(\text{std})} = 1199{\cdot}71 \times 10^{-5}$ for carbon dioxide prepared with H_3PO_4.

The basic isotopic ratios adopted in this paper for the two standards and for atmospheric oxygen are given in Table 3.

Table 3. Isotopic ratios adopted in this paper

	$R_{18} \times 10^5$	$R_{17} \times 10^6$	$R_{45} \times 10^5$	$R_{13} \times 10^5$
Atmospheric oxygen	408·8	753·5	—	—
Solenhofen carbon dioxide as analysed by NIER	415	759·2	1199	1123·00
PDB standard carbon dioxide prepared with H_3PO_4	415·8	759·9	1199·71	1123·72

4. CORRECTION FACTORS FOR MASS SPECTROMETRIC ANALYSIS OF CO_2

In this section we derive the correction factors to be applied to δ_m in order to convert the molecular mass ratio differences to specific isotope ratio differences (δ_c). It is assumed that δ_m is the recorded δ value, corrected for the instrumental effects described in section 2. Finally, we give the correction factor for the isotopic analysis of water by means of equilibration with carbon dioxide.

Carbon-13 analysis

In the analysis of carbon we collect simultaneously masses 44 and 45, and the ratio is given by:

$$R_{45} = \frac{C^{13}O^{16}O^{16} + C^{12}O^{16}O^{17}}{C^{12}O^{16}O^{16}}$$

The $C^{12}O^{16}O^{17}$ component constitutes about 7% of $C^{13}O^{16}O^{16}$ and about 6·5% of the total mass-45 beam. The delta functions are:

$$1 + \delta_m = R_{45(x)}/R_{45(\text{std})}$$
$$1 + \delta_c = R_{13(x)}/R_{13(\text{std})}$$

where (x) denotes, as always, the ratio in the sample gas. From the relationship $R_{45} = R_{13} + R_{17}$, we substitute for $R_{13(x)}$ in the second delta function, and after manipulation obtain:

$$\delta_c = \frac{R_{45(\text{std})}\delta_m + R_{17(\text{std})} - R_{17(x)}}{R_{13(\text{std})}}$$

The unknown term is $R_{17(x)}$, which we obtain from measurement of the O^{18} enrichment of the sample gas with respect to the standard gas. From the considerations discussed in section 3, equation (2), we write:

$$\frac{R_{17(x)}}{R_{17(\text{std})}} = \left[\frac{R_{18(x)}}{R_{18(\text{std})}}\right]^{\frac{1}{2}} = (1 + \delta\, O^{18})^{\frac{1}{2}} \sim 1 + \frac{\delta\, O^{18}}{2}$$

where $\delta\, O^{18}$ is the (corrected) oxygen-18 enrichment. Substituting for $R_{17(x)}$ in the previous expression gives:

$$\delta_c C^{13} = \delta_m \left[\frac{R_{45(\text{std})}}{R_{13(\text{std})}}\right] - \left[\frac{R_{17(\text{std})}}{2R_{13(\text{std})}}\right] \delta\, O^{18} \qquad (1)$$

in which all the ratio terms are known from section 3. Substitution of numerical values for the ratio terms gives:

$$\delta_c C^{13} = 1{\cdot}0676\delta_m - 0{\cdot}0338\ \delta\, O^{18} \qquad (2)$$

which is the correction factor to be applied to analyses made against the PDB standard. Equation (1) is, of course, perfectly general, and the ratio terms for any standard may be found by comparison of the standard with PDB (see Section 5).

The correction factor for carbon analyses thus contains a constant term, reflecting the O^{17} content of the standard, and a variable term, reflecting the difference in the O^{17} content of the sample and the standard. The latter correction is obtainable directly from an oxygen-18 analysis of the gas being analysed for C^{13}.

In previous papers (Craig, 1953, 1954a,b) it was assumed that the difference in O^{17} content of sample and standard was negligible, and only the first term of the correction factor given above was applied (δ_m was multiplied by 1·067). Since then the oxygen-18 content of carbon dioxide produced by combustion of carbon with tank oxygen and copper oxide (Craig, 1953) has been investigated. As might be expected, the oxygen-18 content of the CO_2 fluctuates between the general limits of tank and air oxygen (see Table 2), varying probably as a function of the degree of exchange between the hot CuO and atmospheric oxygen during the time the combustion tube is open, and also as a function of the proportions of oxygen in CuO to tank oxygen bled into the line for the combustion. Oxygen-18 analyses of CO_2 resulting from the combustion procedure range from $\delta = -11{\cdot}4$ to $-18{\cdot}4$‰, averaging about -15‰ relative to PDB. (The lightest values probably reflect a dominance of an isotopic effect in distillation of oxygen from liquid oxygen in the guard trap of the oxygen purification system.)

Using a value of $-15 \pm 3{\cdot}5$‰ for the O^{18} content of combusted gas samples, the second term in equation (2) is $+0{\cdot}5$‰ $\pm$ 0·1, the uncertainty here being about the same as the analytical precision. We use this value for general correction of combusted samples except where high precision is desired, in which case the samples are analysed for O^{18} as well as for C^{13}. Thus, all the analyses of combusted carbonaceous material given in the papers cited above should be corrected further by the addition of $+0{\cdot}5$‰; the differences between such samples remain the same, but their differences from carbonate samples will be altered. Corrected values for noncombusted samples will be published in a future paper dealing with the isotopic geochemistry of carbon and oxygen in carbonates and the carbon paleotemperature scale.

A direct check on the derived correction factor was made by cycling CO_2, extracted from carbonates by phosphoric acid, over hot copper oxide with oxygen gas in the system, thus duplicating the combustion technique using samples of known C^{13} content. From equation (2), equating the δ_c values before and after the experiment, since they must be the same, we may write the change in δ_m as a function of the O^{18} content before and after the experiment, and compare the measured and calculated change. A sample of PDB gas was "combusted" in this fashion, and on measuring the new C^{13} and O^{18} concentrations, the measured and calculated change in δ_m differed by only 0·02‰.

At this point fourteen more CO_2 samples, derived from carbonates of varying known composition, were run through the mock combustion procedure. These samples ranged in C^{13} content from $\delta = +3$ to -30‰, and in original O^{18} content from $\delta = 0$ to -25‰, relative to PDB. The samples were run under varying conditions, such as presence or absence of oxygen, and using different times and temperatures. The change in δ_m C^{13} was then calculated, assuming an O^{18} content, after "combustion," of -15‰, and compared with the measured change. The calculated changes in δ_m ranged from $+0·33$ to $-0·46$‰, a spread of about eight times the precision of an individual analysis. For the total series of fifteen samples, the differences between the measured and calculated changes in δ_m ranged from $+0·16$ to $-0·17$‰, with only four differences exceeding 0·10‰. The average difference, taken by algebraic summation, was just zero, i.e. there was no systematic direction of difference. The average deviation, taken without regard to sign, was 0·07‰, and the experiments thus gave a decided confirmation to the derived correction factor. Nine of these "combusted" gases were then put through the mock combustion procedure a second time, which should not have produced any change in C^{13} content; for this series the algebraic average change in δ_m was $+0·04$‰, and the average change, taken without regard to sign was 0·06‰.

It was found that for combustion temperatures from 800–1000°C, there was no relationship between temperature and oxygen isotopic composition of the product CO_2; however, at a temperature of 550°C, the product CO_2 has a δ O^{18} of only -9‰. Assuming the oxygen to have δ $O^{18} = -15$‰, the CO_2 is thus about 6‰ heavier than the oxygen at the lower temperature, the difference vanishing at about 800°. This relationship is in good agreement with the calculations of UREY (1947), which indicate that CO_2 should be 11‰ heavier than oxygen at 327°C, with a fractionation factor approaching unity with increasing temperature.*

It should be noted that δ O^{18} may vary over a range of 30‰ in carbonates alone; this variation would give a false spread in δ C^{13} of 1‰ if the variable correction term were not applied, corresponding to about ten times the analytical error of the McKinney-Nier spectrometer. Alternatively, the samples and standard could all be equilibrated against a common water, but this is not practical, as, except for combusted samples, we wish to have the O^{18} analysis of the material also, and it is easier to make an oxygen-18 analysis directly after the carbon analysis, than to remove the sample, equilibrate it, and rerun it.

Oxygen-18 *analysis*

For the analysis of oxygen we measure the mass-46 ion beam vs. the combined mass-44 + mass-45 ion beam, and the ratio in terms of isotopic molecules is thus:

$$R_{46} = \frac{C^{12}O^{16}O^{18} + C^{13}O^{16}O^{17} + C^{12}O^{17}O^{17}}{C^{12}O^{16}O^{16} + C^{13}O^{16}O^{16} + C^{12}O^{16}O^{17}}$$

whereas the desired ratio, assuming the distribution to be purely statistical, is:

$$R_{18} = \frac{C^{12}O^{16}O^{18} + C^{13}O^{16}O^{18}}{C^{12}O^{16}O^{16} + C^{13}O^{16}O^{16}} = \frac{C^{12}O^{16}O^{18}}{C^{12}O^{16}O^{16}}$$

* In one experiment it was found that CO_2 exchanges directly with CuO at 550°C, with no oxygen having been put into the system. It thus appears that the technique used by KEITH *et al.* (1950, 1952) of oxidizing CO over CuO at 455°C, in order to measure the O^{18}/O^{16} ratio in quartz, cannot give correct results. These authors state that the reaction involves a 50% dilution of the oxygen from the quartz sample, but since the original oxygen in the CO can exchange with the CuO, the oxygen isotopic record is lost completely. TITANI, NAKATA, and KANOME (1942) have shown that the isotopic exchange reaction between CO_2 and CuO begins at about 400°C.

In the expression for R_{46}, reading from left to right, the isotopic species have the following relative abundances (McCrea, 1950): (numerator) 0·004, 9×10^{-6}, and $1{\cdot}5 \times 10^{-7}$; (denominator) 0·984, 0·011, and 8×10^{-4}. The species $C^{12}O^{17}O^{17}$ is thus two orders of magnitude lower than the next most abundant molecule and of no importance; it is neglected in the following derivation. The delta functions are:

$$1 + \delta_m = R_{46(x)}/R_{46(\text{std})}$$
$$1 + \delta_c = R_{18(x)}/R_{18(\text{std})}$$

Taking the first delta function (for δ_m), and substituting for each R_{46} the isotopic ratio given above, we now divide the numerator and denominator of $R_{46(x)}$ by $(C^{12}O^{16}O^{16})_{(x)}$, and the numerator and denominator of $R_{46(\text{std})}$ by $(C^{12}O^{16}O^{16})_{(\text{std})}$ and then write:

$$1 + \delta_m = \frac{R_{18(x)} + [C^{13}O^{16}O^{17}/C^{12}O^{16}O^{16}]_{(x)}}{1 + (1 + \delta\, C^{13})\, R_{13(\text{std})} + \left(1 + \frac{\delta_c}{2}\right) R_{17(\text{std})}} \Big/ \frac{R_{18(\text{std})} + [C^{13}O^{16}O^{17}/C^{12}O^{16}O^{16}]_{(\text{std})}}{1 + R_{13(\text{std})} + R_{17(\text{std})}}$$

In this expression we have made the obvious substitutions of R_{18}, R_{17}, and R_{13} for their isotopic equivalents, and in addition, have substituted in the denominator of $R_{46(x)}$ the following:

$$R_{13(x)} = (1 + \delta\, C^{13})\, R_{13(\text{std})}$$
$$R_{17(x)} = \left(1 + \frac{\delta_c}{2}\right) R_{17(\text{std})}$$

the latter equation having been derived for equation (1) of this section (see above), where δ_c is the oxygen delta.

We next perform the substitution:

$$\left[\frac{C^{13}O^{16}O^{17}}{C^{12}O^{16}O^{16}}\right] = R_{13}R_{17}$$

for both sample and standard terms, substituting again for $R_{13(x)}$ and $R_{17(x)}$ the expressions just given, and finally divide the entire numerator and entire denominator by $R_{18(\text{std})}$, substituting $(1 + \delta_c)$ for $R_{18(x)}/R_{18(\text{std})}$, and after rearranging, we have:

$$1 + \delta_m = \frac{\left[(1 + \delta_c) + \dfrac{(1 + \delta\, C^{13})\, R_{13(\text{std})}\left(1 + \dfrac{\delta_c}{2}\right) R_{17(\text{std})}}{R_{18(\text{std})}}\right]}{\left[1 + \dfrac{R_{13(\text{std})}\, R_{17(\text{std})}}{R_{18(\text{std})}}\right]} \times \frac{[1 + R_{13(\text{std})} + R_{17(\text{std})}]}{\left[1 + (1 + \delta\, C^{13})\, R_{13(\text{std})} + \left(1 + \frac{\delta_c}{2}\right) R_{17(\text{std})}\right]} \qquad (3)$$

which is the general expression relating δ_c and δ_m in terms of known ratios evaluated for the PDB standard in section 3, and the difference in C^{13} content of the sample and standard, $\delta\ C^{13}$. As with equation (1), the ratio terms for any standard may be found by analysis of the standard vs. PDB.

Equation (3) is evaluated numerically by substituting for the known ratios and neglecting all products of deltas, and yields:

$$\delta_c O^{18} = 1{\cdot}0014\delta_m + 0{\cdot}009\delta C^{13} \tag{4}$$

which is the correction factor for oxygen analysis made against the PDB standard. Thus 1% of the C^{13} difference enters into the oxygen correction factor; since natural carbonates show a range in C^{13} content of some 60‰, the C^{13} difference can cause a false spread in $\delta\ O^{18}$ of 0·6‰, or six times the analytical error, unless corrected for.

Correction of oxygen-18 analyses on water samples

The analysis of water for oxygen-18 content is commonly done by equilibrating CO_2 against the water samples and then analysing the CO_2 samples (e.g. EPSTEIN and MAYEDA, 1953). In this case the data must also be corrected for the amount and isotopic composition of the oxygen in the CO_2 used for the equilibration. From an equation derived in a previous paper (CRAIG, 1953, p. 87) for the material balance in a two-component isotopic system, we write out the material balance expressions before and after the equilibration and readily obtain:

$$\delta = \delta' \frac{(\rho + \alpha)}{\rho} - \frac{\alpha}{\rho} (\delta\ O^{18})_{(\text{tank } CO_2)} \tag{5}$$

In this expression α is the fractionation factor $R_{18(CO_2)}/R_{18(H_2O)}$, here taken as 1·039 at 25°C; δ' is the measured enrichment of the equilibrated CO_2 relative to the standard, this CO_2 being in equilibrium with a water whose O^{18} content has been slightly changed by the added CO_2; while δ is the corrected value, namely the delta of CO_2 in equilibrium with the original water. $\delta\ (O^{18})_{(\text{tank } CO_2)}$ is the oxygen-18 analysis of the tank CO_2 used for the equilibration, and ρ is the ratio of gram atoms of oxygen in the water sample to gram atoms of oxygen in the CO_2 introduced into the flask.

The correction factor thus consists of two terms, the first being a function only of the relative proportions of H_2O and CO_2, while the second term reflects the O^{18} content of the tank CO_2. In our case (EPSTEIN and MAYEDA, 1953; CRAIG and MAYEDA, in press) with 25 ml of water in a 200 cm^3 flask filled to a CO_2 pressure of 74 cm, ρ is about 90, ranging from 83 to 92 for distilled water depending on the amount of CO_2 which dissolves in the water before the flask is cut off from the gas. The uncertainty in ρ is negligible. The composition of the tank carbon dioxide (Liquid Carbonic Corporation, Chicago) is very constant, $\delta\ O^{18}$ having ranged from −12·8 to −15·9‰ for three large tanks used over a period of two years, with an average value of −14·9‰. (δC^{13} averages −29·2‰ having shown a total variation of only 0·3‰ during the same period.) Thus the correction factor for the Epstein-Mayeda technique becomes:

$$\delta = 1{\cdot}0113\delta' + 0{\cdot}17‰ \tag{6}$$

Combining this expression with the correction factor for O^{18} analyses given by equation (4), putting in the C^{13} value for the tank CO_2, we obtain:

$$\delta_c = 1{\cdot}013\delta_m - 0{\cdot}09‰ \quad (7)$$

which is the total correction to be applied to oxygen-18 analyses of water samples relative to PDB, using the Chicago technique, assuming that the instrumental corrections mentioned in section 2 have already been made.§

Table 4. Isotopic analyses of National Bureau of Standards reference samples relative to PDB standard (Chicago)

		δ_c (C^{13}) ‰	δ_c (O^{18}) ‰
Isotope reference sample No. 20:			
$CaCO_3$ (Solenhofen limestone) *		−1·05	−4·14
		−1·11	−4·24
		−1·01	−4·03
	Average	−1·06	−4·14
Isotope reference sample No. 21:			
Spectroscopic graphite†		−27·80	
		−27·76	
		−27·80	
	Average	−27·79	
Isotope reference sample No. 1:			
Water (steam condensate from			−8·05
Potomac River water)‡			−8·09
	Average		−8·07

* No treatment other than reaction with 100% H_3PO_4 at 25·2°C to produce CO_2; analytical procedure described by McCrea J. M. (1950) *J. Chem. Phys.* **18,** 849.

† Combusted at 1000°C; procedure described by Craig H. (1953) *Geochim. et Cosmochim. Acta* **3,** 53. The oxygen-18 analyses of the CO_2 produced by combustion were respectively: δ_c O^{18} = −15·58, −11·39, and −17·25‰.

‡ Analyses of CO_2 equilibrated with the water at 25·2°C as described by Epstein S. and Mayeda T. (1953) *Geochim. et Cosmochim. Acta* **4,** 213. Each figure represents an individual equilibration in which two aliquots of equilibrated CO_2 were analysed and found to differ by less than 0·2‰. The oxygen-18 content of the CO_2 used for the equilibration was δ = −15·74‰.

5. Comparison of Isotopic Standards

The isotopic reference sample programme of the National Bureau of Standards has been described by Mohler (1955). Since publication of that list of reference samples, a new carbon standard has been added to the list; the addition is a sample of spectroscopic graphite, some 3% lower in C^{13} than the limestone

§ The O^{18} analyses of natural waters given by Epstein and Mayeda (1953) are raw data uncorrected for any of the effects discussed in this paper. Including valve leakage and reed bias, their values should be corrected by $\delta_c = 1{\cdot}025\ \delta_{(EM)} - 0{\cdot}09‰$, where $\delta_{(EM)}$ signifies their published data. Most of their data are for ocean waters with small δ values, and the multiplying factor is negligible except for their nonmarine samples; however, all values should also be 0·1‰ lighter, and thus their value for average ocean water, relative to PDB standard, becomes −0·1‰ rather than O.

standard, adopted in order to permit intercalibration on a *difference* between two samples and thus allow comparative estimates of systematic errors in measurement. It should be noted that the Bureau of Standards is not analysing these reference samples, but is distributing them together with the analytical data provided by workers in the field.

In Table 4 we give the results of the mass spectrometric analyses of the NBS isotope reference samples relative to the PDB standard. Table 5 then shows

Table 5. Isotopic composition of various carbon and oxygen isotope standards. Carbonates untreated except for H_3PO_4 reaction.

Standard	Isotopic composition		Number of analyses and std. deviation			
			Carbon		Oxygen	
	δ_c (C^{13} ‰	δ_c (O^{18}) ‰	N	σ	N	σ
PDB-Chicago	0	0	—			—
Nier-Solenhofen limestone [*Phys. Rev.* **77**, 789(1950)]	−0·64	−4·40	13	0·10	8	0·14
NBS-Solenhofen limestone Reference sample No. 20	−1·06	−4·14	3	0·04	3	0·09
Basel (BAERTSCHI) Ticino marble	+2·77	−1·62	9	0·03	21	0·07
Wellington (RAFTER) Te Kuiti limestone	−1·67	−4·17	3	0·04	3	0·02
Stockholm (WICKMAN) $BaCO_3$	−10·32	−15·38	3	0·02	3	0·03
NBS-Graphite Reference sample No. 21	−27·79	—	3	0·02	—	—
NBS-Water Reference sample No. 1	—	−8·07	—	—	2	0·02

the analyses of the various standards for carbon and oxygen, together with the number of samples analysed and the standard deviations; a total of seventy-four analyses of these standards was made. The Nier, Basel, and Stockholm standard analyses were made at intervals during the past several years, the NBS and Wellington standard (RAFTER, 1955) carbonate analyses were spaced fairly equally over a three-month period in 1955, during which some five-hundred mass spectrometric analyses were made, and the two water analyses were spaced six weeks apart.

It should be noted that the Nier and NBS Solenhofen standards represent different samples of this limestone; the NBS sample was recently acquired from the U.S. Geological Survey. The values required for the derivations in section 3 were the $\delta_m(C^{13})$ (which was −0·74‰) and δ_c (O^{18}) of NIER's Solenhofen standard. The calculation of the correction factors was done by successive approximation, beginning with the raw data and running until no values changed. The figures given in Tables 4 and 5 are the final delta values, corrected according to the procedure described in the previous sections of this paper; the δ_m values may be

derived from the equations relating δ_m and δ_c and the values in the tables. Footnote 1 of Table 4 applies also to all carbonates in Table 5.*

Isotopic analyses reported relative to the various standards other than PDB may be converted to δ values relative to PDB by the equation:

$$\delta_{(x\text{-PDB})} = \delta_{(x\text{-}B)} + \delta_{(B\text{-PDB})} + 10^{-3}\, \delta_{(x\text{-}B)}\, \delta_{(B\text{-PDB})}$$

in which (x-B) and (x-PDB) refer to analyses of a sample (x) relative to some standard (B) and relative to PDB, and (B-PDB) is the analysis of the standard (B) relative to PDB, these values being given in Table 5. All δ's in this equation are expressed directly in per mil. In this form, which is exact, comparisons are easily made, and the relationship of course simplifies to the direct algebraic sum when the delta values are small.

The standard deviations shown in Table 5 are well in accord with the limit of error of $\pm 0{\cdot}1‰$ for both carbon and oxygen, generally given by the Chicago laboratory. In general, the precision for carbon is better than for oxygen because of the three-times-larger ion beam, and is probably about $\pm 0{\cdot}05‰$ for samples ranging up to about 10‰ different from the standard; at differences of the order of 30‰ the reproducibility for both carbon and oxygen drops off to about $\pm 0{\cdot}2‰$, all factors considered. The Nier standard analyses showed a spread of 0·3‰ for both carbon and oxygen and were thus considerably less reproducible than analyses of the other standards; this material was finely ground and there was some indication that isotopic exchange with atmospheric CO_2 and water over several years might account for the deviations, but this was not certain. On the other hand, the Basel standard, which was the coarsest of the carbonates, gave highly reproducible analyses over three years; in fact, the reproducibility was so high that this sample was used as a check on oxygen-18 fractionation of the standard in the machine with time. Thus the oxygen variance shown in Table 5 includes analyses in which the standard was slightly off, and the real reproducibility of this sample was much better than shown. The desirability of storing finely powdered carbonate samples under vacuum or in a dry gas should be emphasized. The Basel standard also shows no change of C^{13} and O^{18} composition upon roasting in helium to char organic matter, as described by Epstein *et al.* (1953): carbon and oxygen analyses made on two roasted samples were identical with analyses of the untreated material.

Table 6 gives the absolute C^{13}/C^{12} and the R_{18} ratios deduced for the various standards. The C^{13}/C^{12} ratios are based on the value $1123{\cdot}00 \times 10^{-5}$ for the Nier Solenhofen standard, adopted in (4) of section 3, the other ratios being derived from the PDB ratio and the delta measurements. The oxygen ratios for carbonate standards refer specifically to CO_2 derived by reaction of 100% H_3PO_4 at 25°C with the untreated (i.e. unroasted) carbonate material. The standard ratio is based on Nier's value of $408{\cdot}8 \times 10^{-5}$ for $R_{18(\text{air})}$ and Tudge's analysis of CO_2

* Dansgaard (1953) reported analyses of the Nier, Stockholm, and Chicago standards. His values, stated in terms of δ relative to PDB, are $\delta\, C^{13} = -1{\cdot}42‰$, and $-10{\cdot}22‰$, $\delta\, O^{18} = -5{\cdot}33‰$ and $-22{\cdot}47‰$, for the Nier and Stockholm standards respectively. With the exception of the C^{13} value for the Stockholm standard, these values do not agree at all with those given in Table 5. The reason for the discrepancy is not known. He records his values as absolute ratio differences, i.e. $R - R_{(\text{std})}$, rather than percentage differences, and thus the systematic errors, which cancel when ratios of the recorded ratios are made, are not eliminated from his data.

prepared from atmospheric oxygen, as described in section 3; the other ratios are derived directly from the measured deltas. The relative and absolute values for the NBS water standard refer of course to CO_2 in isotopic equilibrium with the water at 25·2°C. The direct values for water are obtained by dividing by

Table 6. C^{13}/C^{12} and oxygen ratios in isotopic standards for carbon and oxygen. Oxygen values for carbonates refer to CO_2 produced by reaction with 100% H_3PO_4, for water to CO_2 in equilibrium with the water at 25°C. All carbon ratios are based on the adopted value for the Nier Solenhofen limestone standard

Standard	$C^{13}/C^{12} \times 10^5$	$O^{16}O^{18}/O^{16}O^{16} \times 10^5$
PDB-Chicago	1123·72	415·80
Nier-Solenhofen l.s.	1123·00	413·97
NBS-Solenhofen l.s. (No. 20)	1122·53	414·08
Basel (Baertschi)	1126·83	415·13
Wellington (Rafter)	1121·84	414·07
Stockholm (Wickman)	1112·12	409·40
NBS-Graphite (No. 21)	1092·49	—
NBS-Water (No. 1)	—	412·44

the fractionation factor, which is approximately 1·039 for O^{18} concentration in CO_2 with respect to liquid water; this value has not as yet been measured precisely.

Acknowledgements—This report would not be complete without an expression of thanks to Vernon Dibeler and Fred Mohler of the Mass Spectrometry Section, National Bureau of Standards, for their efforts in setting up an isotope reference sample programme of such fundamental importance for isotopic geochemical studies; all workers in the field are greatly indebted to them; and to Irving Friedman of the U.S.G.S., who did much to get the programme initiated. Moreover, it is also appropriate to express here an appreciation to Charles McKinney and the other members of Harold Urey's first Chicago group, whose painstaking work on the Nier mass spectrometer made possible the precision required for such studies; and to A. O. Nier for his continued interest and his ever-ready counsel and advice. The writer is greatly indebted to Mrs. Toshiko Mayeda for her assistance in the laboratory, and to Dr. Harold C. Urey, in whose laboratories these measurements were made. Financial support was given by the Office of Naval Research, the Atomic Energy Commission, and the National Science Foundation over the period during which this work was done.

References

Bigeleisen J. (1952) *J. Phys. Chem.* **56,** 823.
Craig H. (1953) *Geochim. et Cosmochim. Acta* **3,** 53.
Craig H. (1954a) *Science* **119,** 141.
Craig H. (1954b) *J. Geology* **62,** 115.
Craig H. and Boato G. (1955) *Ann. Rev. Phys. Chem.* **6,** 403.

Dansgaard W. (1953) *Geochim. et Cosmochim. Acta* **3,** 253.
Epstein S. and Mayeda T. (1953) *Geochim. et Cosmochim. Acta* **4,** 213.
Epstein S., Buchsbaum R., Lowenstam H. A., and Urey H. C. (1953) *Bull. Geol. Soc. Amer.* **64,** 1315.
Keith M. *et al.* (1950) *Carnegie Inst. Washington Yearbook* No. 49, 36.
Keith M. *et al.* (1952) *Bull. Geol. Soc. Amer.* **63,** 1270 (Abstract).
McCrea J. M. (1950) *J. Chem. Phys.* **18,** 849.
McKinney C. R., McCrea J. M., Epstein S., Allen H. A., and Urey H. C. (1950) *Rev. Sci. Instum.* **21,** 724.
Mohler F. L. (1955) *Science* **122,** 334.
Nier A. O. (1947) *Rev. Sci. Instum.* **18,** 398.
Nier A. O. (1950) *Phys. Rev.* **77,** 789.
Nier A. O. and Gulbransen E. A. (1939) *J. Amer. Chem. Soc.* **61,** 697.
Nier A. O., Ney E. P., and Inghram M. G. (1947) *Rev. Sci. Instum.* **18,** 294.
Rafter T. A. (1955) *New Zealand J. Sci. Tech.* (*B*) **37,** 20.
Thode H. G., Macnamara J., and Collins C. B. (1949) *Canad. J. Res.* **27B,** 361.
Titani T., Nakata S., and Kanome A. (1942) *Bull. Chem. Soc. Japan* **17,** 288.
Urey H. C. (1947) *J. Chem. Soc.* 562.
Yankwich P. E., Promislow A. L., and Nystrom R. F. (1954) *J. Amer. Chem. Soc.* **76,** 5893.

Geochimica et Cosmochimica Acta, 1957, Vol. 12, pp. 150 to 169. Pergamon Press Ltd., London

Fractionation of sulphur isotopes in nature

HITOSHI SAKAI
Department of Chemistry, Faculty of Science, The University of Tokyo, Hongo, Tokyo, Japan

(*Received* 23 *November* 1956)

Abstract—The S^{34}/S^{32} ratios in various sulphur compounds of igneous origin were determined. The present results on the distribution of S^{34} in them are in good agreement with those found by earlier workers.

The light and heavy sulphate were discriminated from their isotopic composition of sulphur. The former (S^{34}/S^{32}: 0·04406–0·04521) consists of secondary sulphates formed by the oxidation of sulphides on the ground surface, and the latter (S^{34}/S^{32}: 0·04542–0·04638) of igneous sulphates as well as oceanic sulphates. Some processes, which brought about the observed isotopic fractionation during magmatic and volcanic activity, were discussed. Possible formation temperatures of sulphates and sulphur dioxide of magmatic and exhalative origin were estimated; they are 75°C to 140°C for sulphates in hot springs, 140°C and 900°C for sulphur dioxide in volcanic fumaroles, and 120°C to 360°C for sulphates in the epithermal ore deposits of Japan.

It was also shown that the present isotopic composition of oceanic sulphates could be interpreted by volcanic sulphur dioxide.

INTRODUCTION

RECENT advances in the field of the "isotope geology" have demonstrated a wide variation in the isotopic composition of the lighter elements in nature. Detailed investigation of the isotopic fractionation of an element will provide valuable information on the geochemical cycle of the element. In respect of sulphur, THODE and his co-workers (1953a, 1953b) in Canada found an extensive variation of the isotopic composition of sulphur compounds of igneous and biogenic origin. According to them, the heavy isotope S^{34} is generally enriched in sulphate minerals as well as in sulphate ions in sea and in fresh water. They derived an interesting conclusion that bacterial activity was the most effective agency in the concentration of the heavy isotope in oceanic sulphate. Their results also suggested a significant fractionation of the sulphur isotopes during igneous activity.

TUDGE and THODE (1950) calculated the partition function ratios for some isotopic molecules of sulphur and the fractionation factors for some exchange reactions at 0°C and 25°C. It is, however, more desirable to know the fractionation factors at the higher temperatures often involved in the earth's crust, or during igneous activity. The ratios of partition functions at higher temperatures were calculated by the present author for some sulphur compounds and are shown in Table 1 together with those calculated by TUDGE and THODE at 25°C. From Table 1, the variation of the fractionation factor with temperature was evaluated for some exchange reactions, and is shown in Fig. 1. It was pointed out by earlier workers (TUDGE and THODE, 1950; UREY, 1947) that the heavy isotope is enriched in the compounds of the higher oxidation state, and that the fractionation factor becomes greater as the difference of the oxidation state between the two compounds becomes more pronounced. It is further seen from Fig. 1 that the temperature dependence of a fractionation factor is also more notable in a reaction with a greater fractionation factor. Thus, as the temperature becomes higher, the isotopic effect in almost all reactions rapidly decreases into a narrow range. At temperatures above 500°C, a fractionation factor more than 1·010 is only to be

expected for the exchange reaction of sulphide ions, or hydrogen sulphide, with sulphate and sulphite ions.

Sulphide ions as well as hydrosulphide ions failed experimentally to exchange their sulphur with the oxy-acids of sulphur with an appreciable rate at a lower temperature than 100°C (Voge and Libby, 1937; Voge, 1939). These exchange

Table 1. The ratios of the partition function of sulphur compounds*

Molecular species	Temperature °C				
	25	50	100	500	1000
$S^{34}O_4^=/S^{32}O_4^=$	1·082 (1·088)†	1·072	1·058	1·016	1·006
$S^{34}O_3^=/S^{32}O_3^=$	1·074	1·066	1·052	1·013	1·006
$S^{34}O_2/S^{32}O_2$	1·053 (1·045)†	1·047	1·037	1·010	1·003
H_2S^{34}/H_2S^{32}	1·013 (1·013)†	1·012	1·010	1·004	1·001
$S^{34}=/S^{32}=$	1·000	1·000	1·000	1·000	1·000

* These calculations were based on the table given by Biegeleisen J. and Mayer M. G. (1947) in *J. Chem. Phys.* **15**, 261.

† The values given by Tudge and Thode (1950).

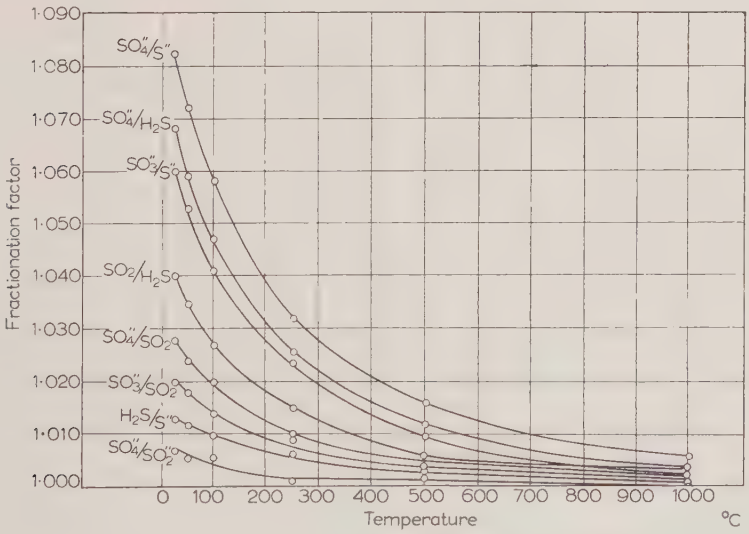

Fig. 1. Variation of the fractionation factors of sulphur compounds with temperature.

reactions would be slow, even in a high-temperature magma, because the collision probability of sulphur compounds would be considerably decreased in such a silicate melt. On the other hand, if two sulphur compounds in a different state of oxidation could reversibly change to each other, through a catalytic action of both a reducing and an oxidizing agent (see reaction 8), isotopic equilibrium could be

attained between them. Therefore, some isotopic exchange may take place among sulphur compounds in nature at an elevated temperature and in the presence of catalysts, even if they cannot directly exchange their sulphur at a lower temperature.

The main purpose of this paper is to determine the distribution of sulphur isotopes in various sources of igneous origin and to estimate the reaction or process which brought about the observed isotopic fractionation.

EXPERIMENTAL

Sulphur dioxide was prepared from various sulphur compounds* by the same procedure as described by THODE *et al.* (1953a), and the S^{34}/S^{32} ratio determined by the mass spectrometer CEC-21-103A of a single collector type. This mass spectrometer has four galvanometers, relative sensitivities of which are approximately 1, 1/3, 1/10, and 1/30. In the measurement of the isotopic ratio,† the two galvanometers, *G*-30 and *G*-3, of the relative sensitivities, 1/30 and 1/3, were used. Because of the difficulties in correcting the galvanometers with a high precision, the isotopic ratio was relatively determined by the following method:

The absolute intensities, i_{64} of $S^{32}O_2$ and i_{66} of $S^{34}O_2$, are related to the peak heights of mass numbers (m/e) 64 and 66, by the equation (1):

$$\begin{aligned} i_{64} &= a_{30}p_{64} \\ i_{66} &= a_3 p_{66} - 2\alpha a_{30} p_{64}, \end{aligned} \tag{1}$$

where a_{30} and a_3 represent the relative sensitivities of the galvanometers, *G*-30 and *G*-3, respectively; p_{64} and p_{66} stand for the peak heights of the mass numbers, 64 and 66, measured by the galvanometers *G*-30 and *G*-3, respectively; α stands for the O^{18}/O^{16} ratio in the tank oxygen. Then the isotopic ratio is related to the peak ratio by the following equation:

$$S^{34}/S^{32} = a_3 p_{66}/a_{30}p_{64} - 2\alpha \tag{2}$$

When the standard sample is measured as soon as possible before and after the measurement of an unknown sample, the correction factor for the latter is assumed to be equal to the mean in the two measurements of the former. Then the per-cent difference of the isotopic ratio, δ, between the unknown and the standard sample is written as follows:

$$\delta = \frac{(S^{34}/S^{32})_{\text{stand}} - (S^{34}/S^{32})_{\text{unknown}}}{(S^{34}/S^{32})_{\text{stand}}} \times 100 = \frac{(p_{66}/p_{64})_{\text{stand}} - (p_{66}/p_{64})_{\text{unknown}}}{(p_{66}/p_{64})_{\text{stand}}} \times \gamma \times 100 \tag{3}$$

where γ represents $[(S^{34}/S^{32})_{\text{stand}} + 2\alpha]/(S^{34}/S^{32})_{\text{stand}}$, and $(p_{66}/p_{64})_{\text{stand}}$ stands for the mean peak ratio in the two measurements of the standard.

Troilite sulphur from Tanogami meteorite in Japan was chosen as the standard sulphur and the isotopic ratio assumed to be 0·04500, the mean ratio of the eight troilite sulphurs measured by MACNAMARA and THODE (1950). According to them, the isotopic ratio in the troilite phase remains constant within experimental error and can be reasonably adopted as the international standard.

In the actual determination, a galena from the Hosokura mine in Miyagi Prefecture was used as the secondary substandard, the S^{34}/S^{32} ratio being carefully determined to be 0·04493 against the troilite sulphur. The isotopic ratio O^{18}/O^{16}, α, was assumed to be equal to Thode *et al.*'s value (1953a) and to remain constant throughout the experiment. The final expression for the per cent difference of the isotopic ratio between the unknown and the standard sample is shown in the equation (4):

$$\delta = \frac{(p_{66}/p_{64})_{\text{stand}} - (p_{66}/p_{64})_{\text{unknown}}}{(p_{66}/p_{64})_{\text{stand}}} \times 1{\cdot}092 \times 100 \tag{4}$$

* Volcanic sulphur dioxide was converted into sulphate ions by passing through iodine-potassium iodide solution and separated as barium sulphate. Hydrogen sulphide was similarly oxidized into free sulphur.

† In what follows, the "isotopic/ratio" means the S^{34}/S^{32} ratio, unless otherwise stated.

The time taken for three measurements was about 30 min, with ten runs for each measurement. The memory effect of the previous samples was negligible when a part of the successive sample was filled in and exhausted out of the gas inlet system of the instrument three or four times before the measurement.

By this method, the standard error was controlled not to exceed $\pm 0{\cdot}1\%$ of the final ratio, when the uncertainties in the absolute isotopic ratio of the standard sulphur and of the tank oxygen are kept out of consideration.

Result and Discussion

The isotopic ratios in about ninety samples from various sources were measured, and the results are shown in Fig. 2 and Tables 2–8. In Fig. 2 are also shown some of the results obtained by Thode *et al.* (1953a, 1953b). The present results are in good agreement with those of the earlier workers, except for the

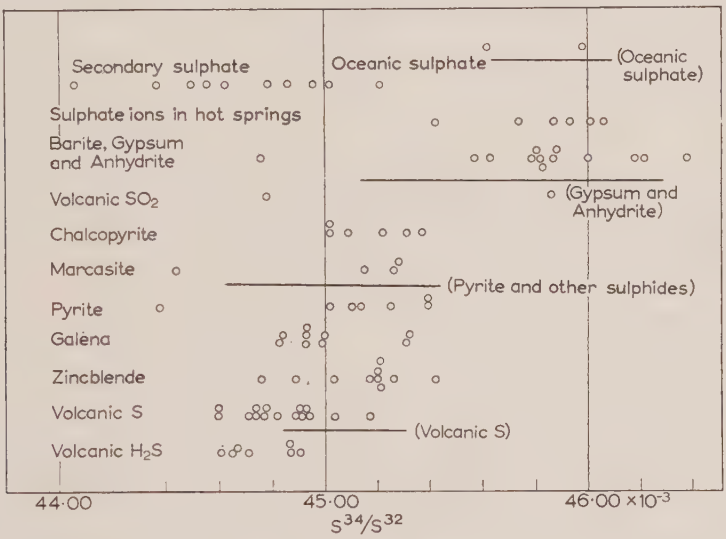

Fig. 2. Distribution of S^{34} in nature. ○ = the present author's results (standard error is $\pm 0.04 \times 10^{-3}$ unit). —— = the Canadian group's on the sulphur compound indicated in the bracket.

sulphate sulphur. The agreement between the present data on the sea-water sulphate and the Canadian group's, shows that the above-mentioned assumptions are fairly legitimate.

Fig. 2 shows that the sulphate is clearly discriminated into two groups, the heavy and the light sulphate. The former group consists of the sulphate of igneous origin and the sea-water sulphate, whilst the secondary sulphate, formed by the oxidation of sulphide minerals on the earth's surface, belongs to the second group.

The range of the isotopic ratio in sulphur dioxide in volcanic gases appears to cover the range both of the light and the heavy sulphate. Native sulphur, hydrogen sulphide, and sulphide minerals of igneous origin, on the other hand, are depleted in the heavy sulphur by some 1 to 3% as compared with the heavy sulphate.

Table 2. The isotopic ratio in igneous sulphide minerals

No.	Sample	Location	S^{34}/S^{32}*
1	Galena	Hosokura mine, Miyagi Prefecture (ep. V.)†	0·04493
2	Galena associated with barite (77)‡	Hanaoka mine, Akita Prefecture (B).	0·04531
3	Galena associated with barite (79)	Daira mine, Akita Prefecture (ep. V).	0·04532
4	Galena associated with barite (80)	Osaruzawa mine, Akita Prefecture (ep. V)	0·04499
5	Galena associated with anglesite (40)	Mikawa mine, Niigata Prefecture (ep. V.)	0·04493
6	Galena associated with anglesite (41)	Oharamura, Miyagi Prefecture	0·04493
7	Galena associated with anglesite (42)	Nakamaru mine, Gumma Prefecture	0·04483
8	Galena	unknown	0·04484
9	Pyrite	Ikuno mine, Hyōgo Prefecture (ep. V.)	0·04514
10	Pyrite associated with barite (78) and zincblende (16)	Hanaoka mine, Akita Prefecture (B.)	0·04511
11	Pyrite associated with barite (82)	Edate mine, Akita Prefecture (B. and ep. V.)	0·04525
12	Pyrite	unknown	0·04539
13	Pyrite associated with barite (86) and ferrous sulphate (38)	Zaō mine, Yamagata Prefecture (ep. V.)	0·04438
14	Pyrite	Sazare mine, Ehime Prefecture§	0·04502
15	Pyrite associated with zincblende (20)	Minakami mine, Gumma Prefecture (ep. V.)	0·04539
16	Zincblende associated with barite (78) and pyrite (10)	Hanaoka mine, Akita Prefecture (B.)	0·04489
17	Zincblende	Sasagatani mine, Shimane Prefecture (ep. V.)	0·04476
18	Zincblende	Takahi mine, Yamagata Prefecture (ep. V.)	0·04521
19	Zincblende	Budō mine, Niigata Prefecture (c. V.)	0·04520
20	Zincblende	Minakami mine, Gumma Prefecture	0·04542
21	Zincblende associated with barite (81)	Edate mine, Akita Prefecture (B. and ep. V.)	0·04503
22	Zincblende associated with pyrite (15)	Minakami mine, Gumma Prefecture	0·04526
23	Marcasite associated with ferrous sulphate (37)	Kaneuchi mine, Kyoto Prefecture‖	0·04444

* Standard error = ± 0.00004
† ep.V.—epithermal vein type deposits; B.—Black Ore Deposits; c.V.—contact vein deposits.
‡ Reference number of the associated sample.
§ The bedded cupriferrous pyritic deposits (so-called Kieslager deposits).
‖ Hypothermal vein deposits (wolframite-scheelite-quartz vein).

Table 3. The isotopic ratio in sulphide minerals from the Yoichi mine* in Hokkaido

No.	Name or No. of the ore deposits	No. of the ore vein	Depth above or under the surface	Sample	S^{34}/S^{32}
24	Koganeyama	–	+30 m	Galena	0·04500
25	Koganeyama	–	+30	Zincblende	0·04520
26	Yoichi-1	3	−165	Chalcopyrite	0·04509
27	Yoichi-1	3	−165	Marcasite	0·04515
28	Yoichi-1	5	−90	Marcasite	0·04528
29	Yoichi-1	5	−90	Chalcopyrite	0·04502
30	Yoichi-1	5	−205	Marcasite	0·04526
31	Yoichi-1	5	−205	Chalcopyrite	0·04522
32	Yoichi-1	9	−205	Zincblende	0·04521
33	Yoichi-1	9	−205	Chalcopyrite	0·04502
34	Yoichi-2	4	−40	Chalcopyrite	0·04531
35	Yoichi-2	4	0	Chalcopyrite	0·04533
36	Yoichi-2	4	0	Zincblende	0·04517

* Epithermal vein deposits.

Table 4. The enrichment factor between different species of sulphides of magmatic origin†

Location	Sample A (No.)	Sample B (No.)	Enrich. factor‡
Edate mine	Zincblende (21)	Pyrite (11)	1·005
Hanaoka mine	Zincblende (16)	Pyrite (10)	1·005
Minakami mine	Zincblende (20)	Pyrite (15)	1·003
Yoichi mine	Galena (24)	Zincblende (25)	1·004
Yoichi mine	Chalcopyrite (33)	Zincblende (32)	1·004
Yoichi mine	Chalcopyrite (26)	Marcasite (27)	1·001
Yoichi mine	Chalcopyrite (29)	Marcasite (28)	1·006
Yoichi mine	Chalcopyrite (31)	Marcasite (30)	1·001
Yoichi mine	Zincblende (36)	Chalcopyrite (35)	1·004

† Enrich. factor = (S^{34}/S^{32})in B/(S^{34}/S^{32})in A.
‡ Standard error: ±0·002.

The Isotopic Ratio in Igneous Sulphide Minerals

In Table 2 are shown the isotopic ratios in various species of igneous sulphide minerals, which were collected mainly from the Black Ore Deposits§ and the epithermal ore deposits. Table 2 as well as Fig. 2 shows that sulphide sulphur

§ The Black Ore Deposits or "Kuroko" are the characteristic ore deposits of mixed sulphides. They are composed of zincblende, galena, pyrite, tetrahedrite, and chalcopyrite, with varying amounts of barite, gypsum, and chalcedonic quartz. "Kuroko" deposits are widely scattered in the terrain of late Tertiary volcanic rocks throughout Japan, especially in north-eastern Japan. This terrain coincides with that of epithermal veins. They are epithermal replacement deposits, which were found in liparitic and andesitic rocks as well as in associated tuffs and even in the Tertiary shaly rocks.

The typical "Kuroko" deposits are generally accompanied by the other two types of ores, "Keiko" (Silicified Ore) and "Oko" (Yellos Ore) which were formed in the different stages of deposition. The "Keiko" is characterized by silica impregnated with variable amounts of pyrite and, in some cases, with small amounts of chalcopyrite. The "Oko" is mainly composed of chalcopyrite and pyrite.

The geological evidence shows that the "Keiko" was formed at the first stage of mineralization, the "Oko" followed it, and, at the last stage, the deposition of the "Kuroko" took place. When one refers to the Black Ore Deposits or "Kuroko" deposits, these three types of ores are included.

in these districts has rather a narrow range of the isotopic composition. SAKAI, HONDA, and MINAMI (1955) previously measured the isotopic composition of lead in twelve galenas collected in these localities and found that they are normal and uniform in their isotopic composition. These observations suggest that these sulphide deposits came from a uniform source, probably deep-seated in the earth's crust.

KULP and his co-workers (1956) found that the Pb^{206}/Pb^{207} and the S^{34}/S^{32} ratio in the sulphide deposits in the South-east Missouri district in U.S.A. systematically varied inversely to each other. According to them, such a systematic variation cannot be attributed to the isotopic fractionation of the

Table 5. The isotopic ratio in the secondary sulphate and the enrichment factor between the secondary sulphate and the original sulphide

Secondary sulphate				Original sulphide			Enrich. factor*
No.	Location	Sample	S^{34}/S^{32}	No.	Sample	S^{34}/S^{32}	
37	Kaneuchi mine	Ferrous sulphate‡	0.04450	23	Marcasite	0·04444	1·001
38	Zaō mine	Ferrous sulphate‡	0·04406	13	Pyrite	0·04438	0·993
39	Yoichi mine	Mine-water sulphate	0·04496	Average sulphide from the mine		0·04516	0·996
40	Mikawa mine	Anglesite§	0·04521	5	Galena	0·04493	1·006
41	Oharamura mine	Anglesite§	0·04502	6	Galena	0·04493	1·002
42	Nakamura mine	Anglesite§	0·04456	7	Galena	0·04483	0·994
43	Tamagawa Hot Springs, Akita Prefecture	Halotrichite‖	0·04479	Average hydrogen sulphide in the Springs		0·04472†	1·002
44	Mt. Yakeyama, Akita Prefecture	Halotrichite‖	0·04437	51	Hydrogen sulphide	0·04487†	0·9822
45	Mt. Sōunzan, Shizuoka Prefecture	Gypsum¶	0·04463				
46	Mt. Mihara, Tokyo	Anhydrite¶	0·04486				

* Enrich. factor: $\dfrac{(S^{34}/S^{32}) \text{ in secondary sulphate}}{(S^{34}/S^{32}) \text{ in original sulphide}}$.

† See Table 6.

‡ Ferrous sulphate has been formed on the surface of the sulphide samples since they were exposed to air in the laboratory.

§ Anglesite from the Oharamura mine and the Nakamaru mine was found on the surface of the galena samples No. 6 and 7. Anglesite from the Mikawa mine was found in a separate region where no sulphide vein can be found.

‖ Halotrichite was found on the silicified rocks in the springs and the volcano.

¶ Gypsum and anhydrite were deposited on the surface of lavas in the volcanoes.

two elements during the migration of the source materials, but is due to the variation of the uranium-sulphate ratio in the source. They also found a sulphide group in which the isotopic ratio of sulphur and lead varied randomly. These significant fluctuations of the isotopic ratio were attributed to the inhomogeneity of the source. The exceptionally low content of the heavy isotope in marcasite from the Kaneuchi mine and marcasite-pyrite mixture from the Zaō mine cannot be clearly interpreted by these two processes. It could be derived from an accidental contamination near the ground surface by sedimentary sulphide of low isotopic ratio.

Table 6. The isotopic ratio in sulphur compounds from volcanoes and hot springs

No.	Location	S^{34}/S^{32}
	Hydrogen sulphide	
47	Fumarole 1, Tamagawa Hot Springs, Akita Prefecture	0·04461
48	Fumarole 2, Tamagawa Hot Springs	0·04471
49	Fumarole 3, Tamagawa Hot Springs	0·04491
50	Fumarole 4, Tamagawa Hot Springs	0·04484
51	Fumarole 5, Mt. Yakeyama, Akita Prefecture	0·04487
52	Fumarole 6, Mt. Shirane, Gumma Prefecture	0·04465
53	Fumarole 7, Okumanaza Hot Springs, Gumma Prefecture	0·04487
	Native sulphur	
54	Fumarole 1, Tamagawa Hot Springs	0·04493
55	Fumarole 2, Tamagawa Hot Springs	0·04474
56	Fumarole 3, Tamagawa Hot Springs	0·04491
57	Fumarole 5, Mt. Yakeyama	0·04491
58	Mt. Yakeyama (deposited in the river water)	0·04471
59	Fumarole 6, Mt. Shirane	0·04478
60	"Yugama," the crater lake of Mt. Shirane	0·04489
61	Yonago mine,	0·04477
62	Mt. Asama, Nagano Prefecture (from the central crater)	0·04517
63	Shōzingawa mine, Hokkaido	0·04504
64	Shōzingawa mine, Hokkaido	0·04494
65	Atosanupuri mine, Hokkaido	0·04460
66	Manza mine, Gumma Prefecture	0·04482
67	Ōwakudani, Hakone, Shizuoka Prefecture	0·04460
68	Zaō mine, Yamagata Prefecture	0·04474
	Sulphur dioxide	
69	Fumaroles No. 9101 and 9081*, Mt. Shōwashinzan, Hokkaido	0·04478
70	Fumarole 6, Mt. Shirane	0·04586
	Sulphate ions	
71	Tamagawa Hot Springs	0·04574
72	Tamagawa Hot Springs	0·04606
73	"Yugama," Mt. Shirane	0·04601
74	Okumanza Hot Springs	0·04542
75	Hokutolite† deposited from the spring water of Tamagawa	0·04593
76	Hokutolite† deposited from the spring water of Tamagawa	0·04587

* The outlet temperatures of the fumaroles No. 9101 and 9081 are *c.* 800°C and 760°C (Oana S. and Matsuo S., private communication). Samples from the two fumaroles were very small and they were measured together as a mixed sample.

† Mixed crystal of lead and barium sulphate.

Table 7. The enrichment factor among sulphur compounds of exhalative origin

Sample species A–B	Location	Ref. No. of Sample A–B	Enrich.* factor
Native sulphur –hydrogen sulphide	Fumarole 1, Tamagawa	54–47	1·007
	Fumarole 2, Tamagawa	55–48	1·001
	Fumarole 3, Tamagawa	56–49	0·999
	Fumarole 5, Mt. Yakeyama	57–51	1·002
	Fumarole 6, Mt. Shirane	59–52	1·003
Hydrogen sulphide –sulphur dioxide	Fumarole 6, Mt. Shirane	52–70	1·023
	Fumaroles 9101 and 9081 of Mt. Shōwashinzan	Average hydrogen sulphide-69	1·002
Hydrogen sulphide –sulphate ions	Fumarole 2, Tamagawa	48–71	1·023
	Fumarole 4, Tamagawa	50–72	1·031
	Fumarole 3, Tamagawa	49–71	1·025
	Fumarole 6 and "Yugama," Mt. Shirane	52–73	1·026
	Okumanza Hot Springs	53–74	1·012
Sulphur dioxide –sulphate ions	Fumarole 6 and "Yugama," Mt. Shirane	70–73	1·003

* Enrich. factor: $\frac{(S^{34}/S^{32}) \text{ in B}}{(S^{34}/S^{32}) \text{ in A}}$.

Table 8. The isotopic ratio in sulphates of magmatic origin and the enrichment factor between the associated sulphate and sulphide

Sulphate of magmatic origin				Associated sulphide			Enrich. factor*
No.	Location	Sample	S^{34}/S^{32}	No.	Sample	S^{34}/S^{32}	
77	Hanoka mine (B.)	Barite	0·04581	2	Galena	0·04531	1·011
78	Hanaoka mine (B.)	Barite	0·04600	16	Zincblende	0·04489	1·025
78	Hanaoka mine (B.)	Barite	0·04600	10	Pyrite	0·04511	1·020
79	Daira mine	Barite	0·04579	3	Galena	0·04532	1·010
80	Osaruzawa mine (ep.V.)	Barite	0·04563	4	Galena	0·04499	1·014
81	Edate mine (B. and ep.V.	Barite	0·04587	21	Zincblende	0·04503	1·018
82	Edate mine (B. and ep.V.)	Barite	0·04583	11	Pyrite	0·04525	1·014
83	Kosaka mine (B.)	Barite	0·04588				
84	Kawarage Hot Springs, Akita Prefecture	Hokutlite	0·04557				
85	Akaiwa mine (ep.V.)	Barite	0·04618				
86	Zaō mine	Barite	0·04638	13	Pyrite	0·04438	1·045
87	Tsubaki mine (ep.V.)	Barite	0·04476				
88	Yonaihata mine (B.)	Gypsum	0·04582				
89	Hanaoka mine (B).	Anhydrite	0·04622				

* Enrich. factor $\frac{(S^{34}/S^{32}) \text{ in sulphate}}{(S^{34}/S^{32}) \text{ in sulphide}}$.

Small variation in the isotopic ratio is always observed in these sulphide minerals, a considerable part of which is presumably attributed to the same causes described above. During successive deposition of sulphide minerals, however, the isotopic ratio in the source liquid could have been continuously varied, and a slight variation could have resulted in the deposited sulphide, depending on the stage of their formation. To examine this, the isotopic ratio in some thirteen sulphide samples from the Yoichi mine in Hokkaido were determined, the results being summarized in Table 3. No systematic variation with their depth and the ore vein is observed.

The isotopic fractionation between different species of sulphides would also bring about a slight variation of the isotopic ratio during their deposition. Table 4 represents enrichment factors evaluated from Tables 2 and 3 for some species of sulphide minerals found together. In three mixtures of pyrite and zincblende, the heavy isotope is enriched in pyrite by some 0·5% more than in zincblende. Chalcopyrite from the Yoichi mine appears to contain the heavy isotope slightly less than the associated marcasite. It can be seen from Fig. 2 that the isotopic ratio in pyrite, marcasite, and chalcopyrite is apparently concentrated into the heavier part within the range of the isotopic ratio of igneous sulphides. But these effects are so small that nothing conclusive could be stated, when the limit of detection in the present research is taken into account. To obtain conclusive information on these variations, more precise determinations are required with selected samples.

The Variation of the Isotopic Ratio during Oxidative Weathering of Sulphide Minerals

Some parts of sulphide minerals exposed on the ground surface are converted into sulphides by an oxidation process.

In Table 5 are shown the isotopic ratios in some secondary sulphates as well as those in the original sulphides. The enrichment factors between these sulphide-sulphate pairs were also evaluated, and are shown in the last column of the table.

The present results appear to indicate a slight enrichment of the light isotope into the secondary sulphate during its formation. An anglesite ($PbSO_4$) -galena pair from the Mikawa mine could be an exception, because they were separately found in the mine. As oxidation proceeds on the solid surface of sulphides, almost all sulphur near the surface being successively converted into sulphates, the observed isotopic effect would be smaller than the theoretical one.

In their isotopic ratio, these secondary sulphates are clearly distinguished from sulphates of igneous origin, and from the sulphate ions in sea-water. In Tamagawa Hot Springs, the isotopic ratio in the sulphate ions is 2 or 3% larger than that in the hydrogen sulphide, as shown in the following section. The isotopic ratio in halotrichite ($FeAl_2(SO_4)_4 \cdot 22H_2O$) in the Springs is nearly equal to that in the hydrogen sulphide and to the average of igneous sulphide minerals. Therefore, its sulphate sulphur was derived from the sulphide mineral or hydrogen sulphide in the Springs; few heavy sulphide ions in the spring water were added to the secondary sulphate. The same can be said for halotrichite from Mt. Yakeyama.

As described in the later section, however, the light sulphate may be formed through a different process, that is, from sulphur dioxide of a high-temperature origin. On the origin of gypsum in Mt. Mihara and anhydrite in Mt. Sōunzan, nothing conclusive can be stated as to whether their sulphates were formed by oxidation of sulphides or came from exhalated sulphur dioxide.

They present very interesting material for the consideration of the origin of the oceanic sulphate, as discussed in the later section.

The Isotopic Ratio in Sulphur Compounds of Exhalative Origin

The most vigorous reactions of sulphur take place in volcanoes and in hot springs. The isotopic ratio in sulphur compounds from such a district reflects that of sulphur in the source magna as well as its change during the reaction or process occurring near the ground surface.

The isotopic ratios in hydrogen sulphide, sulphur dioxide, native sulphur and sulphate ions in volcanoes and in hot springs are summarized in Fig. 2 and Table 6. The isotopic ratios in hydrogen sulphide and native sulphur are nearly equal to each other, while their content of the heavy isotope appears to be slightly lower than that of sulphide minerals of magmatic origin. The fractionation factors between hydrogen sulphide and deposited sulphur from the same fumaroles are presented in Table 7. As expected from Fig. 2, no appreciable isotopic fractionation is observed during the deposition of native sulphur in volcanoes and in hot springs.

On the other hand, in sulphur dioxide in Mt. Shirane, the heavy isotope is enriched by some 2·7‰ more than in hydrogen sulphide from the fumarole. In volcanic fumaroles, native sulphur is believed to have deposited through the following reaction:

$$2H_2S + SO_2 = 2H_2O + 3S \text{ (solid)} \qquad (5)$$

According to this equation, two parts of the deposited sulphur come from hydrogen sulphide and one part from sulphur dioxide. Hence, the isotopic ratio in the deposited sulphur must be the weighted mean of those found in the two gases. Using a radioactive tracer technique, van der Heijde and Aten (1953) found the radioactivity on the deposited sulphur, formed by the reaction, similar to that expected from the reaction formula. In the fumarole of Mt. Shirane, however, the observed isotopic ratio is 0·04478, some 0·9‰ lower than the calculated one, 0·04518.

This contradictory result probably resulted from other chemical reactions that occurred in the fumarole. The isotopic exchange reaction between native sulphur and hydrogen sulphide is considered to be the most probable of these reactions:

$$H_2S^{32} + \tfrac{1}{2}S_2^{34} \rightleftarrows H_2S^{34} + \tfrac{1}{2}S_2^{32} \qquad (6)$$

According to Trudge and Thode (1950), the fractionation factor of this reaction is equal to unity at 25°C. The exchange rate will be increased at a high temperature.

Further, a certain fraction of the deposited sulphur may be formed by the dissociation and the oxidation of hydrogen sulphide. Sulphur thus deposited

would be nearly of the same isotopic composition as the original hydrogen sulphide.

The content of the heavy isotope in hydrogen sulphide is slightly lower than that in sulphides of magmatic origin. This is attributed to the enrichment of the light isotope in the gaseous hydrogen sulphide during the crystallization of sulphide minerals from the source magma.

In Table 7 are also evaluated the enrichment factors among hydrogen sulphide, sulphur dioxide, and sulphate ions from the same fumaroles or the same hot springs. A remarkable difference in the isotopic ratio is found between sulphur dioxide from Mt. Shirane and that from Mt. Shōwashinzan. The enrichment factor or the content of the heavy isotope in sulphur dioxide is apparently dependent on the temperature of the gases from the fumarole.

In hot-spring waters, sulphate ions contain 2 or 3% more S^{34} than hydrogen sulphide, and they can be distinctively discriminated from the light sulphate group as previously mentioned. These heavy sulphate ions are, therefore, considered not to have been formed by the direct oxidation of sulphide minerals or hydrogen sulphide, but to have come from exhalated sulphur dioxide.

"Yugama" in Mt. Shirane is a crater lake in the central crater of the volcano, and the temperature of the lake water is about 28°C. The fumarole No. 6 is vigorously spurting on the crater rim. The similarity of the isotopic ratio in sulphate ions in the lake water and in sulphur dioxide from the fumarole also suggests that they have come from a common origin.

The slightly higher content of the heavy isotope in the lake-water sulphate than in the sulphur dioxide is probably due to the following exchange reactions:

$$S^{34}O_2 + S^{32}O_3^{=} \rightleftarrows S^{32}O_2 + S^{34}O_3^{=}$$
$$S^{34}O_3^{=} + S^{32}O_4^{=} \rightleftarrows S^{32}O_3^{=} + S^{34}O_4^{=} \qquad (7)$$

In addition, some isotopic effects during the oxidation of sulphur dioxide may take place, resulting in a slight enrichment of the heavy isotope into the sulphate.

The isotopic ratio in sulphur dioxide as well as in the heavy sulphate will be more closely discussed in later sections.

The Isotopic Ratio in Sulphate Minerals of Magmatic Origin

The isotopic ratios in barite, gypsum, and anhydrite in the Black Ore Deposits as well as in the other epithermal ore deposits are summarized in Table 8. In this table, the isotopic ratios in the sulphide minerals associated with the sulphates are also presented together with the enrichment factors between these sulphides and sulphates.

The range of the isotopic ratios of these sulphates overlaps that of sulphate ions in hot springs and volcanoes. The enrichment factors for the sulphide-sulphate pairs in the ore deposits of magmatic origin are nearly equal to those found for the hydrogen sulphide-sulphur dioxide or sulphide-sulphate ion pairs of exhalative origin. These observations strongly support a common origin of these sulphur compounds. Sulphates are certainly derived from exhalated sulphur dioxide near the ground surface. If the reaction of their formation could

be known in some detail, the formation temperature could be estimated from the observed enrichment factor.

Origin of the Heavy Sulphur in Sulphates of Igneous Origin and Possible Estimation of Their Formation Temperature

The heavy isotope is enriched in sulphates of igneous origin, possibly through the isotopic exchange of sulphur between sulphate and sulphide ions in the magma reservoir. As seen from Fig. 1, the observed enrichment factors, 1·010 to 1·030, between sulphates and sulphides in these epithermal ore deposits correspond to the formation temperatures approximately from 700°C to 300°C. Similar but somewhat lower, temperatures are also estimated on the assumption of the isotopic exchange between sulphate ions and hydrogen sulphide. For sulphate ions in hot springs, a similar temperature is also obtained on the two assumptions. On the other hand, the sulphur dioxide-hydrogen sulphide exchange reaction indicates that volcanic sulphur dioxide in Mt. Shirane was formed at as low a temperature as 100°C.

The temperature of the eipthermal solution is believed, however, not to exceed such a high temperature as 400°C. At a final stage of deposition, the residual solution would have as low a temperature as the boiling-point of water under 1 atm pressure. Rather high temperatures estimated for these ore deposits could be understood, if the isotopic equilibrium in a high-temperature source had been kept frozen.

L. Ricciardi (1886) suggested the occurrence of sulphur dioxide in a volcano by the action of sulphate minerals with silica at a high temperature. He observed evolution of sulphur dioxide, by heating a mixture of granite and calcium or magnesium sulphate. The discrepancy between the formation temperature of sulphur dioxide and that of sulphate ions in Mt. Shirane could be interpreted, if the sulphur dioxide could be derived from the sulphate in the source.

As pointed out previously, there is considerable difficulty in assuming these exchange reactions. The discrepant result in Mt. Shirane could be negative evidence for them. A further study is, however, required with reference to the possibility of the occurrence of exchange reactions involving sulphur at a high temperature, especially in the presence of such a catalyst as silica.

Oana and Matsuo (1955) gave a more interesting theory on the occurrence of sulphur dioxide in the high-temperature fumaroles of Mt. Shōwashinzan. They assumed that hydrogen sulphide, sulphur dioxide, hydrogen, and water vapour in a volcanic fumarole are in a fictive equilibrium state as given in the equation (8):

$$H_2S + 2H_2O \rightleftarrows SO_2 + 3H_2 \qquad (8)$$

Table 9 shows the composition of the fumarolic gases of Mt. Shōwashinzan as well as the outlet temperature found by Oana and Matsuo. From a thermodynamic consideration of the gas equilibrium, they estimated the fictive equilibrium temperature of the fumaroles No. 9081 and 9063. The results are also represented in Table 9. They concluded that a source at a temperature as high as 1100°C was located very near to the ground surface.

As previously mentioned, the rate of sulphur exchange between sulphur dioxide and hydrogen sulphide is probably very small, even at a high temperature. In a reversible reaction, as shown in the equation (8), however, the isotopic equilibrium is certainly attained through the catalysing action of hydrogen and water vapour. Thus, the same isotopic fractionation could be obtained, as if these two sulphur compounds directly exchanged their sulphur with each other.

It is shown in Fig. 1 that the fractionation factor between sulphur dioxide and hydrogen sulphide is, within the limit of detection, nearly unity at a higher temperature than 900°C. No significant enrichment of the heavy isotope is observed in sulphur dioxide in Mt. Shōwashinzan as compared with the average isotopic ratio of volcanic hydrogen sulphide. This shows that the sulphur dioxide was formed at a higher temperature than 900°C, which is in good agreement with the observed temperature of the fumaroles as well as the estimated one of the source (Oana and Matsuo).

Table 9. The composition of the fumarolic gases in Mt. Shōwashinzan and their observed and estimated temperature. (Oana and Matsuo, 1955)

Vapour	No. of fumarole 9081	9063
	l./1000 l.	
H_2O	981	993
SO_2	0·426	0·203
H_2S	0·0042	0·575
CO_2	12·1	5·36
H_2	6·25	0·18
N^3	0·571	0·89
Outlet temp. observed	760°C	220°C
Estimated temp. from the gas equil.(8)	1200	470

The outlet temperature of the fumarole No. 6 in Mt. Shirane, on the other hand, is as low as 100°C. The inner temperature may be also lower than that of Mt. Shōwashinzan. This low temperature is clearly reflected in the isotopic ratio in the sulphur dioxide and hydrogen sulphide. As shown in Table 7, the enrichment factor is 1·023, the calculated reaction temperature being about 140°C.

As pointed out in the foregoing section, sulphates of igneous origin can be considered to be derived from volcanic sulphur dioxide. If the isotopic ratio in these sulphates is nearly equal to that in the original sulphur dioxide, their formation temperature is estimated from the enrichment factor between the associated sulphate and sulphide or hydrogen sulphide. In Table 10 are summarized the formation temperatures for these sulphates and sulphur dioxide. In these estimations, a barite sample from the Zaō mine was not considered because the associated sulphide had an exceptionally low content of the light isotope.

It should be remembered that these temperatures only reflect some ambiguous

stage during the formation of sulphur dioxide or sulphates. Oxidation of sulphur dioxide is, however, probably accelerated by the presence of water near the ground surface. Thus, they generally represent the minimum formation temperature.

The formation temperature of sulphates of magmatic origin is generally estimated to be higher than that of the heavy sulphur in volcanic gases and hot springs. This does not immediately mean, however, a higher temperature of the source of these ore deposits than that of volcanic gases. The low temperature for the volcanic gases in Mt. Shirane and the sulphate ions in hot springs is

Table 10. The formation temperature of the heavy sulphur of magmatic and exhalative origin

Sample	Location	Observed temp. °C	Ref. No. of samples used for H_2S	SO_2	Temp. °C
Spring-water sulphate	Tamagawa Hot Springs	98	48	71	140
Spring-water sulphate	Tamagawa Hot Springs	98	49	71	120
Spring-water sulphate	Tamagawa Hot Springs	98	50	72	75
Spring-water sulphate	Okumanza Hot Springs	55	53	74	310
Sulphate in "Yugama"	Mt. Shirane	28	52	73	110
Volcanic sulphur dioxide	Mt. Shirane	100	52	70	140
Volcanic sulphur dioxide	Mt. Shōwashinzan	*c.* 800	Average H_2S	69	900
Black Ore Deposits	Hanaoka mine	—	G*2	B77	340
Black Ore Deposits	Hanaoka mine	—	Z16	B78	120
Black Ore Deposits	Hanaoka mine	—	P10	B79	180
Epithermal vein deposits	Osaruzawa mine	—	G4	B81	260
Epithermal vein deposits	Edate mine	—	Z21	B82	200
Epithermal vein deposits	Edate mine	—	P11	B83	260
Epithermal vein deposits	Daira mine	—	G3	B80	360

* G = galena, Z = zincblende, P = pyrite, B = barite

probably that of the volcanic gases near the ground surface. These gases, coming from a deep-seated source at a high temperature, can be markedly cooled during their ascendence through a long vent. In Mt. Shōwashinzan, on the other hand, a high-temperature source is thought to be present very near to the ground surface, as mentioned above. Gases in this volcano are not considerably cooled in passing through the conduit.

The Tsubaki mine in Akita Prefecture is one of the epithermal deposits. The exceptionally low content of the heavy isotope in a barite from this mine strongly supports a high formation temperature or a deep location of the ore.

The example of the lowest formation temperature in the Hanaoka mine was provided by a barite-zincblende pair. This is also associated with pyrite, and from the barite-pyrite pair a higher temperature, 180°C, was obtained, because of a slightly higher content of the heavy isotope in pyrite than in zincblende. The other factor, bringing about a lower estimation of the temperature, is the isotopic fractionation during the oxidation of sulphur dioxide. For sulphate ions

in Okumanza Hot Springs, an unusually high temperature was obtained. This may be ascribed to the contamination of the light sulphate into the spring water.

The formation of the heavy sulphate involves some uncertain factors, as seen at the beginning of this section and just above. These temperatures are, however, in good agreement with those generally believed to appear at the formation of such epithermal deposits as the Black Ores. The sulphur dioxide-hydrogen sulphide exchange reaction is the most probable process to interpret the isotopic ratio in hydrothermal deposits and sulphur compounds of exhalative origin.

From this process, the maximum enrichment of the heavy isotope in sulphates of igneous origin is expected not to exceed a value corresponding to the minimum temperature at which the reaction (8) can take place with a measurable rate in both directions. This minimum temperature is probably higher than the boiling-

Table 11. The isotopic ratio in the sea-water sulphate

No.	Location	S^{34}/S^{32}
90	Pacific Ocean*	0·04598
91	Katsu-ura Bay	0·04562
92	Average sea-water†	0·04588

* Japan standard sea-water.
† Thode *et al.*'s value (calculated from the values quoted by Rankama in *Isotope Geology*, p. 279).

point of water, and, hence, the maximum enrichment for the normal sulphates is about 1·030, as seen from Fig. 1. Further, if the mean isotopic ratio in sulphides of igneous origin is nearly equal to that of meteoritic sulphur, the maximum isotopic ratio in the sulphates is about 0·04635. No heavier sulphate than that expected has been found as yet. The unusually high enrichment factor, found for a sulphate-sulphide pair from the Zaō mine, is due to the exceptional depletion of the light isotope in the sulphide phase as shown in Table 2. This probably suggests a different stage of intrusion of the two mineral species.

A further study is in progress in this laboratory with reference to the isotopic ratio in sulphur compounds of igneous origin and their formation condition.

Origin of the Heavy Sulphate in the Ocean

The isotopic ratios were determined with two samples, from the Pacific Ocean and from Katsu-ura Bay of Japan. These results are shown in Table 11 together with the mean ratio obtained by Thode *et al.* (1953a) for the sulphate ions from the Pacific Ocean.

The Canadian group reported some evidence that the bacterial activity was the most effective agency in the concentration of the heavy isotope into the oceanic sulphate. Thode, Kleerekoper, and McElcheran (1951) found that hydrogen sulphide, produced by a sulphate reducing bacteria, contains less S^{34} than the sulphate media. Further, Macnamara and Thode (1951) reported that native sulphur deposited in a lake bottom by a bacterial reduction of the sulphate in the lake water, contains 3·2% less of the heavy isotope than does the sulphate.

They also found that the isotopic fractionation started about 800 million years ago, the spread of the isotopic ratio between sulphide and sulphate of marine origin rapidly increasing with goelogic time.

Oceanic sulphur is continuously being deposited as sulphides and sulphates. At the same time, however, sulphur is continuously being supplied by the erosion of igneous rocks. Volcanic exhalation is also supplying sulphur in various states of oxidation into the ocean. These continuous additions and removals of the oceanic sulphur must be also taken into account in the interpretation of the present isotopic ratio in the oceanic sulphate and its variation with geologic time.

As previously shown, the secondary sulphate has, in general, nearly the same isotopic ratio as that in the initial sulphide. This lowers the isotopic ratio in the oceanic sulphate, when this secondary sulphate is introduced into the ocean. The somewhat lower content of the heavy isotope in the sulphate ions from Katsu-ura Bay is probably due to this addition of the light isotope into the heavy oceanic sulphate.

According to Goldschmidt (1954), the amount of sulphate ions in the sea-water, in comparison with the content of sulphides in the average igneous rocks, is so markedly greater that a considerable amount of the oceanic sulphate must be derived from gaseous exhalation of the globe. Having revised his calculation, Rankama and Sahama (1945) estimated that only some 35% of the present oceanic sulphate has been supplied by the weathering of igneous rocks. A part of the remaining sulphur may be a relic from volatile sulphur compounds in the primordial atmosphere. The considerable part is, however, considered to be supplied by the degassing of the globe, throughout the geologic history of the ocean. These estimations indicate that hydrogen sulphide and sulphur dioxide exhalated during igneous activity have been playing an important part in bringing the sea-water sulphate to the present isotopic ratio.

The mean isotopic ratio in hydrogen sulphide degassed out of the globe must be similar to that of the meteoritic sulphur regardless of the degassing temperature. The range of the isotopic ratio in sulphur dioxide, on the other hand, might have undergone a significant variation, depending on the degassing temperature as well as escaping condition from the ground surface.

For the estimation of the effect of these two gases on the isotopic ratio in the oceanic sulphate, the following values are essential: (1) the ratio of hydrogen sulphide to that of sulphur dioxide that has been effectively converted into the oceanic sulphate, (2) the mean isotopic ratio of the sulphur dioxide exhalated out of the globe throughout the geologic time, and (3) the amount of juvenile sulphur and its mean isotopic composition.

At present, however, no conclusive data have been presented to estimate these amounts with a good approximation.

"Yugama," the crater lake of Mt. Shirane, can be an extreme model of the ocean in an earlier age. According to Minami *et al.* (1952), the lake-water is strongly acidic (pH as low as 0·8), and no living organisms could survive in it. The chemical composition of the lake-water found by them is shown in Table 12. As previously shown, the isotopic ratio in the sulphate ions in the lake-water is nearly equal to that in the present oceanic sulphate. These sulphate ions have

been evidently formed from the sulphur dioxide evolved through the volcanic exhalation, and the present amount of the combined and free sulphuric acid in the water amounts to some 3000 t, according to them. If the isotopic ratio in the degassed sulphur dioxide and that in the secondary sulphate were respectively equal to that of the sulphate ions in "Yugama" and that of the meteoritic sulphur, the isotopic ratio in the oceanic sulphate could be calculated to be 0·04567, corrected for the estimated effect of the secondary sulphate, as suggested by

Table 12. Chemical composition of the water in "Yugama" (Minami *et al.*, 1952)

Evaporation residue	10320 mg/l.
Mg^{++}	57·6
K^{+}	21·8
Ca^{++}	255
Fe^{++}	320
Cl^{-}	5010
$SO_4^{=}$	5349
Free sulphuric acid	3760
Free hydrochloric acid	4650

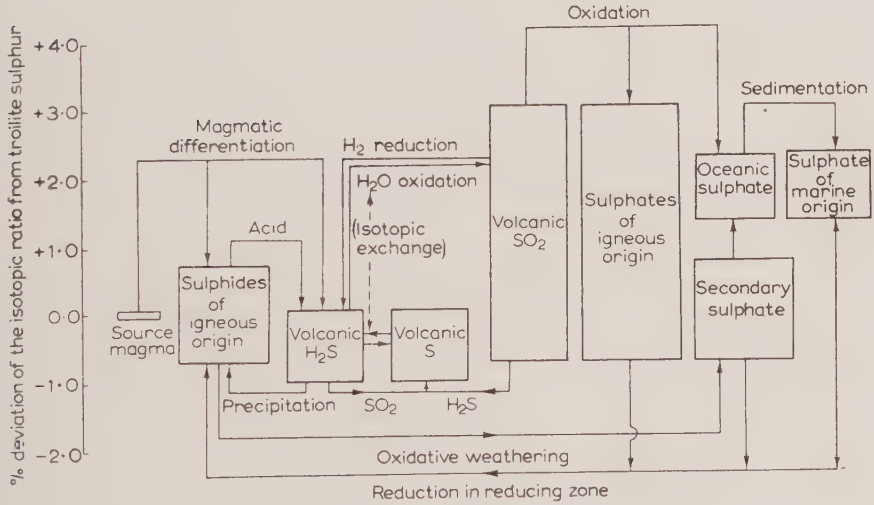

Fig. 3. The cycle of sulphur isotopes in nature.

Rankama and Sahama. This isotopic ratio of the sulphate ions in the hypothetical sea-water is in an approximate agreement with that in the real one. The heavy sulphate in the present ocean could be satisfactorily interpreted as a contribution of exhalated sulphur dioxide as well as secondary sulphate.

On the other hand, the other extremity can be assumed, where the degassing has occurred at such a high temperature as found in Mt. Shōwashinzan, or where the amount of exhalated sulphur dioxide has been much smaller than the hydrogen sulphide. In this case, the isotopic ratio of the continuously supplied sulphur

may be nearly equal to that of meteoritic sulphur, and the isotopic ratio in the sulphate ions in the present ocean must have come through some other process such as the bacterial activity given by the Canadian group. Vinogradov *et al.* (1956) failed to correlate the isotopic ratio in sedimentary sulphides with their geologic age. More essential is, however, the spread of the isotopic ratio between the associated sulphide and sulphate rather than their absolute isotopic ratio. At the present stage, it is rather reasonable to assume that these two processes have taken place side by side throughout the geologic history of the ocean, and the author cannot prefer the one to the other.

As a conclusion of this paper, the cycle of sulphur isotopes is schematically shown in Fig. 3. This diagram only shows the inorganic processes, and no biogenic activity is included. The range of the isotopic ratio in a sulphur compound can not be definitely determined at the present stage of research. In Fig. 3, the given ranges only indicate those of samples measured in this research, except for sulphur dioxide and sulphates of igneous origin. The ranges of the latter two compounds were estimated on the assumed mechanism of their formation. Further, the secondary sulphate was assumed to have the same isotopic ratio as that in sulphides of igneous origin. The cycle also involves many uncertain processes which should be investigated in future. The given diagram should be understood as a tentative one.

Acknowledgements—The author wishes to express his sincere thanks to the following researchers for their kind presentation of valuable mineral species: Professors E. Minami, and T. Watanabe, Dr. K. Sakurai, Assistant Professor H. Imai, Mr. J. Osaka, and Mr. A. Sasaki of the Univ. of Tokyo; Dr. I. Sunakawa, and Mr. K. Takahashi of Japan Geological Survey; Dr. M. Shima of Scientific Research Institute Ltd.; Mr. J. Ishida of Sumitomo Metal Mining Co.; and Assistant Professor N. Yamagata of Gumma University.

The author is also grateful to them and Professor N. Saito of this laboratory, Professor S. Oana, and Mr. S. Matsuo of Nagoya University for their kind advice and encouragement throughout the research. He is also greatly indebted to Assistant Professor S. Araki and his associates of the University of Tokyo for their kind help on the operation of the mass-spectrometer, and to Assistant Professor T. Shimanouchi, Dr. T. Miyazawa, and Mr. I. Nakagawa of the University of Tokyo, for their valuable suggestion in the course of the calculation of the normal vibration of isotopic sulphur compounds.

A part of this research was supported by a grant for Scientific Research given by the Ministry of Education of Japan.

References

Goldschmidt V. M. (1954) *Geochemistry* p. 526 Clarendon Press, Oxford. (Ed. A. Muir.)

Kulp J. L., Ault W. U., and Feely H. W. (1956) Sulphur isotope abundances in sulphide minerals. *Econ. Geol.* **51,** 139.

Macnamara J. and Thode H. G. (1950) Comparison of the isotopic constitution of terrestrial and meteoritic sulphur. *Phys. Rev.* **78,** 307.

Macnamara J. and Thode H. G. (1951) The distribution of S^{34} in nature and the origin of native sulphur deposits. *Research, Lond.* **4,** 582.

Minami E., Yamagata N., Shima M., and Saijyō Y. (1952) On crater lake "Yugama" of Volcano Kusatsu-Shirane. *Rikusui Gaku Zasshi* **16,** 64.

Oana S. and Matsuo S. (1955) Symposium on Geochemistry held in Tokyo (now preparing a complete paper).

Rankama K. and Sahama Th. G. (1947) *Geochemistry* p. 295. University of Chicago Press.

Ricciardi L. (1886) *Gazz. chim. Ital.* **16,** 38 (quoted in *A Comprehensive Treatise on Inorganic and Theoretical Chemistry*, Mellor W., Vol. X. p. 187).

Sakai H., Honda M., and Minami E. (1955) Isotopic composition of the common lead in Japan. *Bull. Chem. Soc. Japan* **28,** 533.

Thode H. G., Kleerekoper H., and McElcheran D. E. (1951) Isotopic fractionation in the bacterial reduction of sulphate. *Research, Lond.* **4,** 581.

Thode H. G., Macnamara J., and Fleming W. H. (1953a) Sulphur isotope fractionation in nature and geological and biological time scale. *Geochim. et Cosmochim. Acta* **3,** 235.

Thode H. G. and Macnamara J. (1953b) The distribution of S^{34} in nature. *Natl. Bur. Stand.* (U.S.) circ. No. 522, p. 235.

Tudge A. P. and Thode H. G. (1950) Thermodynamic properties of isotopic compounds of sulphur. *Canad. J. Research* **28B,** 567.

Urey H. C. (1947) The thermodynamic properties of isotopic substances. *J. Chem. Soc.* 562.

van der Heijde H. B. and Aten A. H. W. jr. (1953) Tracer studies on the formation of sulphur from hydrogen sulphide and sulphur dioxide in aqueous solution. *J. Amer. Chem. Soc.* **75,** 754.

Vinogradov A. P., Chupakhin M. S., Grinenko V. A., and Trofimov A. V. (1956) Sulphur isotope composition, in relation to age of sedimentary pyrites. *Geokhimia* **1,** 96.

Voge H. and Libby W. F. (1937) Exchange reactions with radiosulphur. *J. Amer. Chem. Soc.* **59,** 2474.

Voge H. (1939) Exchange reactions with radiosulphur. *Ibid.* **61,** 1032.

Geochimica et Cosmochimica Acta, 1957, Vol. 12, pp. 170 to 171. Pergamon Press Ltd., London

GEOCHEMICAL NOTE

Caesium in stony meteorites*

(*Received* 31 *December* 1956)

THE cosmic abundance of caesium is primarily based on its measured concentration in stony meteorites. I. NODDACK and W. NODDACK (1930 and 1934) have published two values, 0·1 and 1·1 p.p.m., of caesium relative to silicon in the stone meteorites. Recently (1956), SUESS and UREY interpolated a value of 0·4 p.p.m. from their curve of cosmic abundances versus mass number. The poverty of data in this mass region was pointed out to us by Professor UREY, and at his suggestion we have determined the caesium content of four stony meteorites, using a sensitive isotope dilution technique.

The total alkali content of 1-g samples of Holbrook, Beardsley, Pasamonte, and olivine from Finmarken meteorite was obtained by the distillation process of EDWARDS and UREY (1955a). An aliquot equivalent to 0·04 g of meteorite was first subjected to a preliminary ion exchange separation of caesium from the lower alkalies, using the method of HYDE (1952). Carrier-free Cs^{131} tracer was used to determine the yield of the separation. The Cs^{131} was prepared by neutron activation of natural barium carbonate in the Brookhaven reactor and subsequent chemical separation from the parent Ba^{131}. The tracer used in the ion exchange separation was held to 1% of the level used in the mass-spectrometer isotope dilution analyses.

A modified General Electric analytical mass spectrometer was used for these assays. The ions were produced from a double platinum filament surface ionization source and detected by an eight-stage secondary emission electron multiplier. Analyses were carried out on samples equivalent to 1 mg of meteorite with approximately 10^{-12} g of Cs^{131} as the calibrating isotope diluent. The Cs^{131} was independently assayed by counting in calibrated geometry with a sodium iodide crystal scintillation counter. The results are summarized in Table 1. Data of EDWARDS and UREY (1955b) were used to compute K/Cs ratios.

Table 1

Meteorite	% ($\times 10^5$)	K/Cs (by weight)	Atomic[1] ratio Cs/Si ($\times 10^6$)
Holbrook	4·84	1810	0·554
	4·94	1780	0·565
Beardsley	9·28	1120	1·06
	8·98	1160	1·03
Pasamonte	2·84	1830	0·324
Olivine from Finmarken	2·02	445	0·231

[1] Silicon in chondrites taken as 18·5% average used by SUESS and UREY.

* Research performed in part under the auspices of the U.S. Atomic Energy Commission.

The estimated accuracy of the absolute assay of Cs^{131} was $\pm 5\%$. The precision in mass spectrometer peak ratios was generally better than 5%, although occasional deviations from the mean of twenty or thirty ratios were larger than this because of variation in the rate of sample evaporation. The blank on the spectrometer and on the chemical separation of Cs^{133} from the meteorite solution is less than 3% of the Cs^{133} determined in the olivine sample. The blank on the original distillation of the alkali is less certain. Olivine from the Finmarken meteorite (a pallasite) is about ten times lower in potassium than average chondrite and its caesium value may be taken as the upper limit for contamination. Holbrook has typical values for sodium and potassium in chondrites. If all the alkalies are uniformly depleted in Finmarken with respect to the chondrites, the caesium in Finmarken would be approximately $0{\cdot}5 \times 10^{-5}\%$, indicating a contamination of about $1{\cdot}5 \times 10^{-5}\%$. (Total found, $2{\cdot}02 \times 10^{-5}\%$.) The uncorrected caesium concentration in Holbrook ($4{\cdot}90 \times 10^{-5}\%$) yields an atomic abundance for caesium with respect to silicon (taken as 18·5%) of $0{\cdot}560 \times 10^{-6}$ (Suess and Urey, $0{\cdot}456 \times 10^{-6}$). Deducting our estimated contamination of $1{\cdot}5 \times 10^{-5}\%$, Cs gives an atomic abundance Cs/Si of $0{\cdot}388 \times 10^{-6}$.

The Beardsley meteorite has an unusually high potassium content, and the present measurements indicate a similar enrichment in caesium. Pasamonte is an achondrite with potassium little more than half that in average chondrites, and this reduction is also reflected in the caesium concentration.

In general, the range of observed values agrees well with Suess and Urey's estimate and we believe helps establish their cosmic abundance curve in this mass region.

Brookhaven National Laboratory
Upton, Long Island, New York
B. M. Gordon
L. Friedman

Shell Development Company
Houston, Texas
G. Edwards

References

Edwards G. and Urey H. C. (1955a) *Geochim. et Cosmochim. Acta* **7,** 154.
Edwards G. and Urey H. C. (1955b) *Geochim. et Cosmochim. Acta* **8,** 285.
Hyde E. K. (1952) *J. Amer. Chem. Soc.* **74,** 4181.
Noddack I. and Noddack W. (1930) *Naturwissenschaften* **18,** 757.
Noddack I. and Noddack W. (1934) *Svensk Kem. Tidskr.* **46,** 173.
Suess H. E. and Urey H. C. (1956) *Rev. Mod. Phys.* **28,** 53.

Geochimica et Cosmochimica Acta, 1957, Vol. 12, pp. 172 to 175. Pergamon Press Ltd., London

SOME CURRENT PAPERS IN OTHER JOURNALS

A. P. Vinogradov and A. B. Ronov,* **Evolution of Chemical Composition of Clays of the Russian Platform.** From *Geokhimiya* (*Geochemistry*), No. 2, pp. 3–18, 1956.

Vinogradov and Ronov, who are considered among the best geochemists in the U.S.S.R., made a detailed study of the chemical composition of clays of the Russian Platform. Their results indicate that the chemical composition of clays was changing with time (Figs. 1, 2, 3, 4, 5). The results plotted in these figures are based on the analyses of 252 compound samples, representing 6804 single samples.

According to Vinogradov and Ronov, changes in the average contents of K and Na in the clays of the Russian platform (Fig. 1) are possibly due to a more intensive formation of

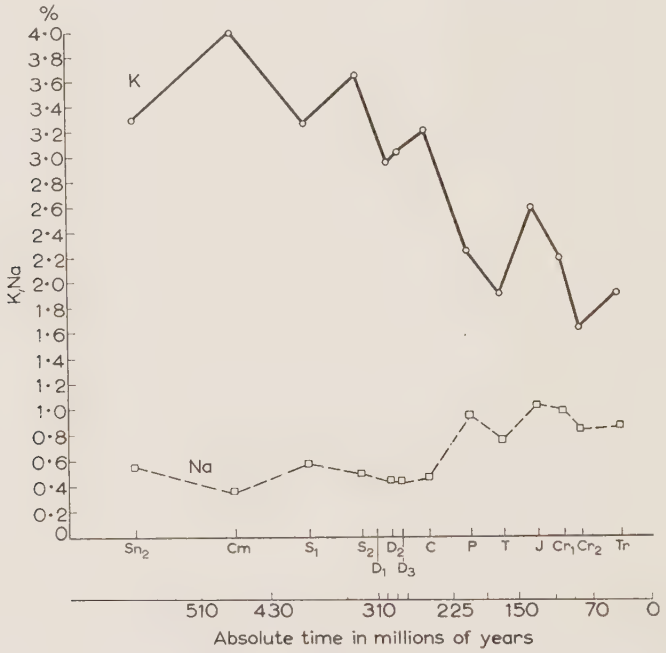

Fig. 1. Changes in average contents (%) of K and Na in clays of Russian platform with time (after Vinogradov and Ronov, 1956, p. 5).

the weathering products enriched in K on the ancient land. The weathering of micas and potassium feldspars gave rise to the hydromicas, which are enriched in K. This could explain the higher contents of K in the older clays.

Fig. 2 shows that there is a general increase in the average Ca/Mg ratio in going up the geologic column, with superimposed periodic fluctuations. Vinogradov and Ronov also mentioned that a similar evolution of Ca/Mg ratio has taken place in the carbonate rocks. The foregoing findings are of considerable interest, because the average Ca/Mg ratio of Canadian and United States carbonate rocks also increases in going up the geologic column, with superimposed periodic fluctuations (Chilingar, 1956, *Amer. Assoc. Petrol. Geol. Bull.*, Vol. 40, No. 9).

In Fig. 3, the curves showing the changes in the Ca and Mg contents (per cent) in clays

*Abstract prepared by George V. Chilingar

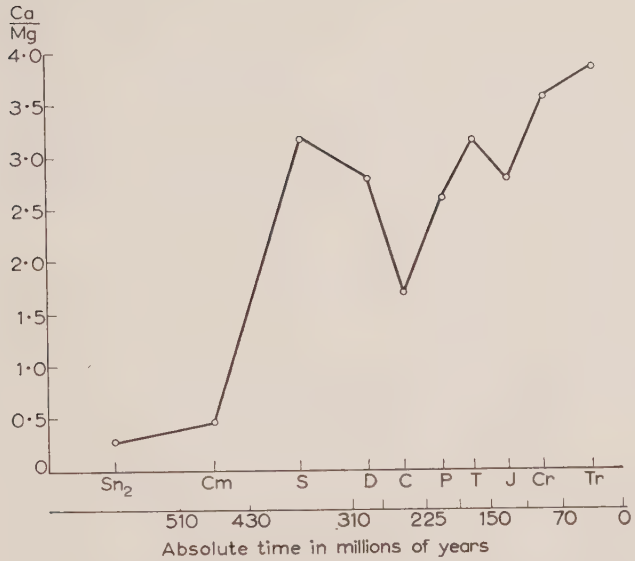

Fig. 2. Changes in Ca/Mg ratio of clays of Russian platform with time (after VINOGRADOV and RONOV, 1956, p. 12).

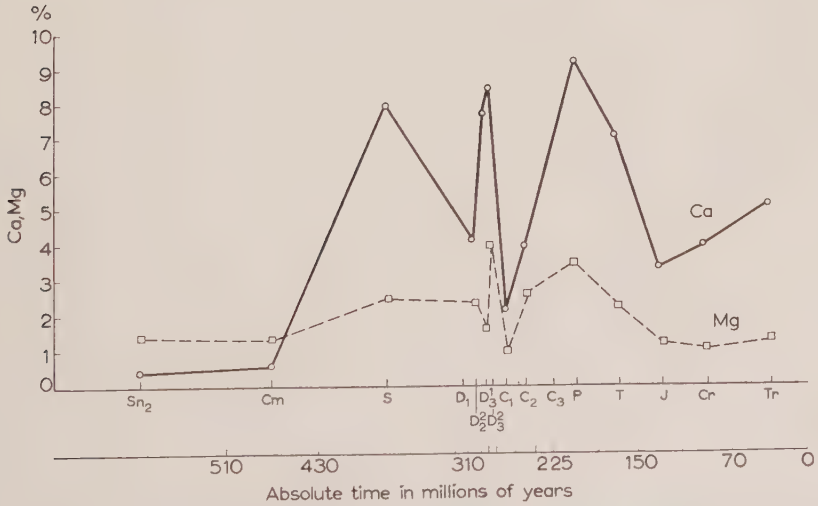

Fig. 3. Changes in average contents (%) of Ca and Mg in clays of Russian platform with time (after VINOGRADOV and RONOV, 1956, p. 13).

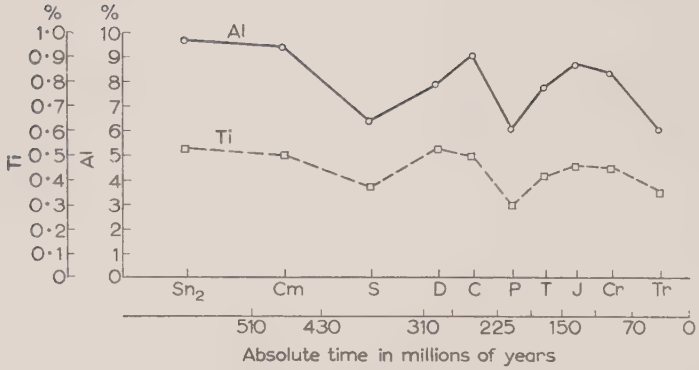

Fig. 4. Changes in average contents (%) of Al and Ti in clays of Russian platform with time (after VINOGRADOV and RONOV, 1956, p. 15).

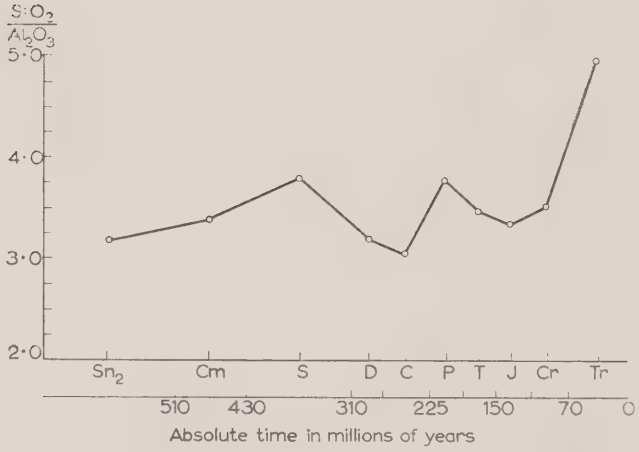

Fig. 5. Changes in SiO_2/Al_2O_3 ratio with time in clays of Russian platform (after VINOGRADOV and RONOV, 1956, p. 15).

with time have similar trends, which indicates that Ca and Mg have close paragenetic relationship in clays.

Fig. 4 shows a gradual decrease in the Al and Ti contents of clays with time, and their close paragenetic relationship.

According to VINOGRADOV and RONOV, as a rule the near-shore and continental clays are enriched in Al and Ti, and have low SiO_2/Al_2O_3 ratio. On the other hand, on approaching the central parts of the basins, the Al and Ti contents of clays decrease, whereas the SiO_2/Al_2O_3 ratio increases. The SiO_2/Al_2O_3 ratio has minimal values during the periods of accumulation of continental, near-shore, and coal-bearing facies.

The findings of VINOGRADOV and RONOV indicate that the evolution of the chemical composition of clays was possibly controlled by the general evolution of the environmental conditions in the biosphere with time.

Geokhimiya (Geochemistry)

No. 1. 1957

A. P. VINOGRADOV, L. S. TARASOV, and S. I. ZYKOV: Isotopic composition of the ore lead of the Altai and Kazakhstan.

V. I. BARANOV and L. A. KUZMINA: Content of radioactive elements in bottom deposits of the Pacific in the region of the Japanese Isles.

A. N. MURIN and I. A. UYTLANDOV: On the problem of cosmic age determination of meteorites.

V. L. BARSUKOV: On the geochemistry of tin.

O. G. KOZLOVA: Rare earths in fluor spars of various deposits of the USSR.

S. D. MALININ: Solubility of $PbCl_2$ in water in liquid and vapor phases.

V. V. IVANOV: The present hydrothermal activity of the volcano Ebeco on the isle of Paramushir.

V. A. KALYUZHNY: Results of the determination of pH in solutions of liquid inclusions.

S. V. ALBOV: On the problem of boron in underground waters of the Crimea.

YU. YU. BUGELSKY: Some peculiarities of zinc, lead and copper migration in groundwaters of lead-zinc ore deposits.

Chronicle

On the Conference of the Mineralogical Society of the USSR. V. V. Shcherbina.

BOOK REVIEW

H. W. HARVEY: **The Chemistry and Fertility of Sea Water.** Cambridge University Press, 1955. 224 pp., 65 tables–figs. 35s.

Two previous books by H. W. HARVEY have been, and still are, accepted references in the marine sciences. Both, however, have been out of print for some time. The present volume is a continuation of the earlier two books. It includes much material taken directly from the previous works, together with a summary of some of the more recent studies in the field.

This volume has many features that recommend it, and some that leave this reviewer rather dissatisfied. This is in contrast to the impression left upon first (and prolonged) contact with HARVEY's other works. These comments deserve an explanation.

There is a rather large body of information concerned with the chemistry, physics, and biology of the oceans that has become a more or less fixed and unchanging part of oceanography—the general features of the carbon dioxide system in the sea, certain aspects of oceanic circulation, aspects of the nutrient cycle in the sea, the rather predictable sequences in the seasonal changes of local flora and fauna, etc. These and many similar features of the science have been fairly well described or formulated for some time. Many such features were thoroughly and adequately presented in HARVEY's earlier books and have been retained in the present one with only minor modernizing modifications and additions. Most of these features, as now presented, represent the distillation of a great many interrelated studies, some of which were conducted during the late 1800's and early 1900's. They represent then generalizations based upon a large body of information accumulated from many laboratories over a considerable period of time.

In contrast to the above, there is a growing body of information that in a sense is as yet unclassified—it doesn't quite fit into any attempted generalizations. During the past ten years, and especially the last five, information of this kind has been accumulating at an accelerated pace. As an example, the analyses for trace substances in the sea and in marine organisms is continually being pushed to lower and lower concentration levels with corresponding improvements in precision and accuracy, and our knowledge concerning the distribution of these substances in the seas is increasing. Simultaneously, the results of biochemical studies have shown the importance of many of these substances in specific, essential metabolic functions. The obvious question, one that is now frequently asked, is, of what importance are these substances in regulating the reproduction, growth, and death of marine organisms? At present, the question cannot be answered, our information concerning the distributions of trace substance and the interrelations between them and the biota is sparse. The best that can be done is to tabulate the results of the analyses and to comment upon certain *in vitro* studies that point out the essentiality of the substances. In this specific case (trace substances), HARVEY has tabulated and commented.

It must be admitted that the dissatisfaction mentioned earlier probably is not with HARVEY the author, but stems rather from the lack of information available at present that prevents satisfactory answers to be given to questions, many of which are prompted by reading HARVEY. It must also be admitted that this probably is a desirable situation—it is just as important to generate questions as to answer them.

It is interesting to note that, at the date of writing, the first printing of this volume is already temporarily out of stock both in this country and in England.

DAYTON E. CARRITT

INFORMATION FOR CONTRIBUTORS

I. GENERAL

1. Papers on geochemistry should be submitted to the editors for the appropriate country or language (*Papers on cosmochemistry should be sent to Prof. F. A. Paneth, F.R.S.*). Papers submitted for publication will naturally be judged from the standpoint of scientific originality and novelty. Technical details of apparatus used in scientific investigation can, however, be presented in brief notes. Critical comments or preliminary results requiring early publication should be submitted as letters to the editors. Where possible, letters should be confined to 500 words. The preparation of progress reports and review articles will be invited by the editors from time to time. The journal appears as independent and complete numbers, which are combined into volumes of about 300 pages.

2. Only papers which have not been previously published can be accepted. Authors must agree not to publish elsewhere a paper submitted to and accepted by *Geochimica et Cosmochimica Acta*.

3. Fifty reprints of each paper are provided free. Additional copies can be purchased if ordered at the time the first proofs are returned. A reprint order form will accompany first proofs.

II. SCRIPT REQUIREMENTS

1. Scripts must be written in one of the three official languages—English, French, or German

2. The script should be typed (not a carbon copy). The text must be ready for printing and should be carefully checked for errors. Authors will receive proofs for correction.

3. Illustrations should accompany the script, mounted on separate sheets. Line diagrams that require to be redrawn should include all relevant details. Half-tone illustrations should be restricted to the minimum necessary. Photographs should be enlarged sufficiently to permit their clear reproduction, and if words or numbers appear on them, two copies should be sent, one clearly printed and the other without inscription. All illustrations should be provided with descriptive legends, which should be given on a separate sheet.

4. References in the text should be given by quoting the author's name and year of publication, i.e. AHRENS (1952). **Full references should be listed at the end of each paper, in alphabetical order, in the following manner:**

AHRENS L. H. (1952) *Geochim. et Cosmochim. Acta* **2**, 168.

and should include the standard abbreviated title of the journal, year, volume number, and page number.

5. The text of articles submitted should be concise and in a readily understandable style The technical description of the methods used should only be given in detail when such methods are new. The essential contents of each paper should be briefly recapitulated in an abstract in English. Such an abstract may, however, be submitted by the author in the language of the original typescript for translation into English by the editorial staff.

6. To conserve space, authors are requested to mark less important portions of the paper (such as description of methods, record of experimental results, etc.) for printing in smaller type.

Pergamon Press are also publishers of the following Journals

JOURNAL OF NUCLEAR ENERGY (*including* THE SOVIET JOURNAL OF ATOMIC ENERGY *on behalf of the Pergamon Press Institute, a nonprofit making foundation*)
JOURNAL OF INORGANIC AND NUCLEAR CHEMISTRY
TETRAHEDRON (*the International Journal of Organic Chemistry*)
INTERNATIONAL JOURNAL OF APPLIED RADIATION AND ISOTOPES
*BIOPHYSICS
*JOURNAL OF MICROBIOLOGY, EPIDEMIOLOGY AND IMMUNOBIOLOGY
*PROBLEMS OF HEMATOLOGY AND BLOOD TRANSFUSION
*PROBLEMS OF VIROLOGY
*PROBLEMS OF ONCOLOGY
*PHYSIOLOGICAL JOURNAL OF THE U.S.S.R. (SECHENOV)
CHEMICAL ENGINEERING SCIENCE
JOURNAL OF ATHMOSPHERIC AND TERRESTRIAL PHYSICS
SPECTROCHIMICA ACTA
JOURNAL OF THE MECHANICS AND PHYSICS OF SOLIDS
ACTA METALLURGICA (*for the Board of Governors of Acta Metallurgica*)
INTERNATIONAL JOURNAL OF THE PHYSICS AND CHEMISTRY OF SOLIDS
DEEP-SEA RESEARCH
JOURNAL OF NEUROCHEMISTRY
JOURNAL OF PSYCHOSOMATIC RESEARCH
JOURNAL OF INSECT PHYSIOLOGY
INTERNATIONAL ABSTRACTS OF BIOLOGICAL SCIENCES (*for Biological and Medical Abstracts Ltd.*)
JOURNAL OF EDUCATION

**Translations of Russian journals published on behalf of the Pergamon Institute, a non-profit-making foundation.*

OCT 23 Jun 610

20 Sep 63F
Mar 63
9 Jun 64F
8 Sep 64F

I. R. MAXWELL & CO LTD

SECOND-HAND & OUT-OF-PRINT DEPARTMENT

Scientists and Librarians

Please check this list of periodicals against your library. We urgently require these to fill orders for university and industrial libraries at home and abroad. We shall be most grateful for any you can offer, and will pay highest market prices. Please send us a list of your holdings of learned books and periodicals that you are willing to sell. We shall also be glad to receive a list of your wants of out-of-print books and journals to check against our extensive holdings. We shall send our quotations by return.

ACTA MATHEMATICA: Vol. 85–86, 88–89.

AMERICAN GEOPHYSICAL UNION, TRANSACTIONS: Vol. 1 to date.

AMERICAN JOURNAL OF PHYSICS: Vol. 1–7.

AMERICAN METEOROLOGICAL SOCIETY, BULLETIN: Vol. 1–22, 28 to date.

ANNALEN DER HYDROGRAPHIE UND MARITIMEN METEOROLOGIE: Vol. 1 to date.

ANNALEN DER METEOROLOGIE: Vol. 1 to date.

ANNALEN DER PHYSIK: Series II: Vol. 92, 106, 111. Series III: Vol. 2. Series V: Vol. 1–43, no. 8. Series VI: Vol. 1, 2, 12.

ANNALES D'ASTROPHYSIQUE: Series IX: Vol. 1–2, 4–20. Series X: Vol. 1–12. Series XI: Vol. 17. Series XII: Vol. 1–11.

ARCHIV FÜR HYDROBIOLOGIE: Vol. 38–43.

ASTROPHYSICAL JOURNAL: Vol. 1–116.

BIOGEOGRAPHICAL SOCIETY OF JAPAN, BULLETIN: Vol. 1–14, with BIOGRAPHICA: Vol. 1–3.

GEOFISICA PURA ED APPLICADA: Vol 1 to date.

GEOLOGICAL SOCIETY OF AMERICA, BULLETIN: Vol. 1 to date.

GEOLOGISCHES ZENTRALBLATT: Vol. 1 to date.

GEOLOGISTS' ASSOCIATION, LONDON. PROCEEDINGS: Vol. 1–48.

HONKONG OBSERVATORY. Meteorological Observations: Vol. 1 to date. Monthly Meteorological Bulletin: Vol. 1 to date.

JOURNAL OF GEOPHYSICAL RESEARCH: Vol. 1 to date.

JOURNAL OF METEOROLOGY: Vol. 1 to date.

JOURNAL OF THE AERONAUTICAL SCIENCES: Vol. 1–12, 17–23.

Single issues and duplicate volumes as well as complete or part sets welcomed.

Maxwell and Co. are the world's leading specialist booksellers aiding progress in science, medicine, industry and education. We offer the individual book buyer and professional librarian many up-to-date services, hitherto not available anywhere. We have the following service departments at your disposal:

New Book Department
Subscription to Periodicals and Serials Department
Out of Print and Difficult to Get Department
Micro films and micro cards Department
Technical Translating Department
Technical Writing Department
Information Department
Bookbinding Department
Library Valuation Department

For full details of services offered, please write to the address convenient for this free descriptive booklet.

I. R. MAXWELL & CO LTD ***International University and Industrial Booksellers***

LONDON: 4 & 5 FITZROY SQUARE, LONDON W.1
NEW YORK: 122 East 55th Street, New York 22, N.Y.
PARIS: 24 Rue des Écoles, Paris Ve